

Supersonic Laser Deposition and LaserForge: Process Mechanism Coating Characteristics



Laurent Michaux
Fitzwilliam College
University of Cambridge

This thesis is submitted for the degree of

Doctor of Philosophy

June 2019

Declaration

This thesis is the result of my own work and includes nothing which is the outcome of work done in collaboration except as declared in the Preface and specified in the text.

It is not substantially the same as any that I have submitted, or, is being concurrently submitted for a degree or diploma or other qualification at the University of Cambridge or any other University or similar institution except as declared in the Preface and specified in the text. I further state that no substantial part of my dissertation has already been submitted, or, is being concurrently submitted for any such degree, diploma or other qualification at the University of Cambridge or any other University or similar institution except as declared in the Preface and specified in the text

It does not exceed the prescribed word limit for the relevant Degree Committee.

Abstract

Supersonic Laser Deposition and LaserForge: Process Mechanism Coating Characteristics

Laurent Michaux

LaserForge is a commercial coating process, that uses a pulsed laser to deposit flat sided wire onto a substrate with minimal heat input. Supersonic Laser Deposition (SLD) is an emerging coating technology that can be used as an alternative to existing thermal spray processes. It has the benefit of low temperature, allowing the deposition of nanostructured and temperature sensitive coatings, which is not currently possible with existing thermal spray.

This main aim of this work was to undertake an experimental study aimed at identifying the process mechanism used in the LaserForge process. The understanding of the process mechanism could then be applied to process improvements for SLD coatings. As part of this study the bonding mechanisms of both LaserForge and SLD were studied.

Initially a laser system to enable the exploration of the LaserForge parameter space was specified and a system set up to enable investigation of LaserForge. The LaserForge process parameter space was characterised using a pulsed laser with Ti-64 on CP aluminium. Successful bonding was achieved with parameters of 10 ms pulse length, 1400 W per pulse and 0.8 mm spot diameter. The process was determined to be a form of welding-based laser cladding, a melt-based process.

Following discovery that LaserForge was a melt-based process, the direction of work was changed to focus on the SLD process mechanisms. Several WC-17Co coatings were deposited as a single layer (0.5 mm thick) on carbon steel. The coating cross section morphology was characterised using an optical microscope and scanning electron microscope. A tensile pull off test was used to measure the coating adhesion, and a four-point bend test with acoustic emission was used to monitor the failure of the coating. Plastic failure of the coating was identified, and a test limited adhesion strength in excess of 70 MPa measured. The coating was shown to have a stress-to fracture of approximately 550 MPa in tension, and a reinforcement effect of approximately 100 MPa when compared to the uncoated substrate. The problems with the deposition of the coatings with SLD were investigated and characterised, with the thermal effect from the laser during deposition found to be significant.

This work has characterised the mechanism behind the commercial LaserForge process and the deposition challenges of depositing WC-17Co using Supersonic Laser Deposition. The benefit of these advancements will provide guidance for the direction of future work into LaserForge, and Supersonic Laser Deposition of nanostructured and advanced materials.

Acknowledgements

I would like to thank my research group for their support during this work, in particular Dr Martin Sparks, Dr Andrew Cockburn and Prof. Bill O'Neill who provided helpful advice throughout.

I would like to thank the EPSRC for providing funding for this PhD.

Table of Contents

Declaration.....	3
Abstract.....	5
Acknowledgements.....	7
Table of Contents.....	9
Table of Figures.....	13
1 Chapter 1 - Introduction	17
1.1 Introduction	17
1.2 Background and Motivation	18
1.3 Structure of the Thesis.....	21
2 Chapter 2 - Review of Literature.....	23
2.1 Background	23
2.2 Literature Review Questions.....	23
2.3 Overview of Thermal Coating Technologies	23
2.3.1 Laser-Based Coatings	24
2.3.2 Thermal and Kinetic Spray	29
2.4 Overview of Selected Laser Surface Treatments	49
2.4.1 Laser Thermal Forming	52
2.4.2 Laser Glazing	54
2.4.3 Laser Fusion.....	54
2.4.4 Laser Shock Processing	55
2.4.5 Laser Welding.....	57
2.5 Discussion of Literature Review Questions.....	58
2.5.1 What is LaserForge and how does it relate to other coating deposition techniques? .	58
2.5.2 What are the advantages of using cold spray compared to other similar industrial surface coating treatments such as wire arc and HVOF?	59
2.5.3 What defines if a cold spray and supersonic laser deposition coating can be deposited successfully, and what are its issues?	60
2.5.4 Is cold spray a suitable technology for depositing advanced materials such as nickel-based alloys, WC-Co and HAP (Bio-Coating) for novel applications?	62
2.5.5 What new laser-based processes are there to modify and improve coating quality and performance?.....	63
2.6 Conclusions and Research Objectives.....	65
3 Chapter 3 – Materials and Methods	67
3.1 Bulk Materials	67
3.1.1 Titanium 6-4	67
3.1.2 Aluminium.....	67

3.1.3	Steel	67
3.1.4	Inconel.....	68
3.2	Powder Materials.....	68
3.2.1	WC-Co Spray Powder	68
3.2.2	316L Spray Powder	70
3.3	Experimental Methods.....	71
3.3.1	Optical Microscopy	71
3.3.2	SEM Imaging.....	71
3.3.3	Laser Processing System for LaserForge	71
3.3.4	Material Preparation.....	72
3.3.5	Etching.....	72
3.3.6	Hardness Testing.....	74
3.3.7	LaserForge Sample Mounting	74
3.3.8	Supersonic Laser Deposition (SLD).....	75
3.3.9	Pull-Off Testing.....	78
3.3.10	Bar Deflection Measurement.....	79
3.3.11	Bend Testing with Acoustic Emission Monitoring.....	80
3.3.12	Interferometer	81
3.4	Errors and Analysis Methods	81
3.4.1	Laser Setup and Positioning.....	81
3.4.2	Estimating Point of Failure.....	82
4	Chapter 4 – Experimental Investigation of LaserForge.....	83
4.1	Motivation for Investigation of LaserForge	83
4.2	Analysis of a LaserForge Sample	84
4.2.1	LaserForge Sample	84
4.2.2	LaserForge Surface	85
4.2.3	Cross-Sectioning of Sample.....	86
4.2.4	Etching of LaserForge Cross-section	88
4.2.5	Conclusions of Cross-Section Analysis	89
4.3	LaserForge Parameters	90
4.3.1	Process Parameter Space.....	90
4.3.2	LaserForge Process Claims	91
4.3.3	Conclusions for LaserForge Parameters	92
4.4	Setup of Laser System to Investigate LaserForge	92
4.4.1	Laser Processing System	93
4.4.2	Laser System Integration	93

4.5	Effect of Oxygen on Laser Processing in the Chosen Parameter Space.....	98
4.5.1	Comparison of Methods of Using Argon as a Processing Gas	98
4.5.2	Vickers Hardness Measurements.....	99
4.5.3	Conclusions from Effect of Oxygen on Processing.....	101
4.6	Parameter Space Investigation with Fixed Pulse Energy	101
4.6.1	Processing Parameters.....	102
4.6.2	Parameter Space Map.....	102
4.6.3	Conclusions from Fixed Pulse Energy Parameter Map	104
4.7	Improving Contact Between the Coating and Substrate	104
4.8	Investigation of Surface Interaction Spot Size	106
4.9	Parameter Space Investigation with Fixed Pulse Energy	108
4.9.1	Processing Parameters.....	108
4.9.2	Parameter Map	108
4.9.3	Conclusion from Parameter Space Investigation with Fixed Pulse Energy.....	112
4.10	Further Analysis of LaserForge Sample.....	113
4.11	Conclusions from LaserForge Investigation	114
4.11.1	Suggestions for Further Work.....	115
5	Chapter 5 - Failure Mechanisms in High Performance Nanostructured Cold Spray Coatings....	117
5.1	Motivation for Investigation of Failure Mechanisms in A Nanostructured Cold Spray Coating.....	117
5.2	Deposition of WC Supersonic Laser Deposition Coatings.....	118
5.2.1	Deposition of WC-17Co with Cold Spray.....	118
5.2.2	Deposition and Optimisation of Single Layer WC coatings.....	118
5.2.3	Effect of Laser Power on Deposition.....	119
5.3	Analysis of WC-17Co Supersonic Laser Deposition Coatings.....	120
5.3.1	Cross Sectioning of WC-17Co Coatings.....	121
5.3.2	Investigation of Coating Adhesion	124
5.3.3	Investigation of the Failure Mode of Coatings.....	126
5.4	Powder Size Effect on Coating Quality.....	135
5.4.1	Comparison of the Two Powders.....	135
5.4.2	Comparison of Coatings with Both Powders	138
5.4.3	Discussion.....	139
5.5	Discussion of Results.....	140
5.6	Conclusions	142
6	Chapter 6 – Thermal Stresses and Coating Modification	143
6.1	Motivation.....	143

6.2	Analysis of Thermal and Peening Effect on a Flat Substrate	143
6.2.1	Experimental Setup.....	143
6.2.2	Experimental Results.....	144
6.2.3	Discussion of Experimental Results	145
6.2.4	Theoretical Estimation of the Residual Stress from the Difference in Coefficient of Thermal Expansion (CTE)	146
6.3	Analysis of Sample Deformation with Multiple Coating Layers.....	148
6.3.1	Experimental Setup.....	148
6.3.2	Experimental Results.....	148
6.3.3	Failure of Multilayer Coatings	151
6.4	Coating Modification Techniques	151
6.4.1	Background	152
6.4.2	Deposition of an Interlayer to Modify Stress at the Interface.....	153
6.4.3	Welding of WC-17Co SLD Coatings	155
6.5	Discussion of Results.....	158
6.6	Conclusions	161
7	Chapter 7 - Conclusions and Further Work.....	163
7.1	Conclusions from Experimental Investigation of LaserForge	163
7.2	Conclusions from Failure Mechanisms in SLD	164
7.3	Conclusions from Thermal Stresses in SLD	165
7.4	Recommendations for Further Work.....	166
7.5	Bibliography	169
8	Chapter 8 - Appendix	181
8.1	Photo of the SLD Processing Chamber:.....	181
8.1.1	EDX Spectrum Graphs	181
8.1.2	Adhesion Testing Results	183
8.2	CTE Effects Data	186

Table of Figures

Figure 1: WC-17Co SLD coating on steel showing cracking.	20
Figure 2: Example of a LaserForge coating cross section [16].	27
Figure 3: Diagram of a cold spray system [53].	35
Figure 4: Figure showing the relative particle velocity and gas temperature space. High velocity and high temperature have not been investigated [43].	36
Figure 5: Graph of particle and gas velocities modelled through a cold spray nozzle [54].	37
Figure 6: Comparison of computational models for bonding of copper and aluminium for an incident particle velocity of 650 m/s at times of (a) 5 ns; (b) 20 ns; (c) 35 ns; and (d) 50 ns. Reproduced from [60].	38
Figure 7: A graph showing the optimal region for impact velocities for cold spray based on particle diameter [45].	39
Figure 8: A graph showing a comparison of available laser treatments in relation to absorbed intensity and interaction time [133].	51
Figure 9: Diagram showing the three mechanisms for laser forming, the temperature gradient mechanism, the buckling mechanism and the upsetting mechanism. Based on fig 6.2 from [138] ...	53
Figure 10: SEM image of an agglomerated spheres of powder containing particles of WC and Co.	69
Figure 11: Particle size distribution for Osprey 316L powder.	70
Figure 12: Diagram of the mount used to hold the sample under the laser.	74
Figure 13: Processing chamber with argon gas feed.	75
Figure 14: Diagram showing the key components of the supersonic laser deposition process. The components in the central rectangle are in an enclosed processing chamber.	76
Figure 15: Image of the spray nozzle spot, laser spot and pyrometer spot (red) during alignment of the system.	77
Figure 16: Example of a spraying pattern for three tracks on a flat substrate. The spraying occurs in one direction only and therefore the nozzle is returned to the start of the next track off the sample.	78
Figure 17: Diagram of the cross section of a sprayed track. The track is hill shaped and consists of the main bulk of the track bonded to the substrate with a think partially consolidated layer on the top.	78
Figure 18: Diagram of the pull off testing setup.	79
Figure 19: Image of the dial gauge being moved across the bend substrate being measured.	80
Figure 20: Diagram of the setup for the bend testing of the samples when the coating was in tension.	81
Figure 21: LaserForge sample of In625 on steel. The top edge has been sectioned off.	85
Figure 22: LaserForge sample surface under white light microscope. The larger circles are believed to correspond to individual laser pulses. This image is rotated by 90 degrees with respect to Figure 21.	86
Figure 23: White light microscope image of the cross section of the IN625 coating on a steel substrate in the X axis after polishing. The black layer at the top of the image is the mounting resin, the white material is the coating and the substrate is the darker grey material at the bottom. Black spots are porosity in the sample.	87
Figure 24: White light microscope image of the cross section in the Y axis after 30 seconds of etching with Kallings etchant. The microstructure is beginning to appear in the coating (centre) between the mounting resin (top) and the steel substrate (bottom) the sample is not etching at the same rate across the thickness of the coating. The steel is also etching much faster than the coating.	88
Figure 25: White light microscope image of the deformed interface showing pores and deformation.	89

Figure 26: Parameter space for laser processes, including the parameters for LaserForge from the patent for comparison.	91
Figure 27: Design of case (green) to cover power supply (grey) contacts.....	94
Figure 28: Power supply (top) connected to the laser (bottom).	94
Figure 29: Laser interlock circuit diagram that was designed and built.	95
Figure 30: Layout of processing chamber with YR30 processing head.....	96
Figure 31: Recorded laser pulse for 10 ms 10 Hz at 15 J.	98
Figure 32: Diagram of the cross-section line used to make the hardness measurements. The line of laser pulses is into the page. The measurement was only made in the titanium coating, as bonding to the aluminium layer did not occur.....	99
Figure 33: Graph of the Vickers hardness of the pulsed laser samples. A comparison is made between samples that were processed in an argon chamber or with a shield gas only.	100
Figure 34: Graph of the Vickers hardness across the three longest pulses 0.1 mm from the surface. Pulses are spaced 2 mm apart. The graph shows that the Vickers hardness does not remain constant across each of the laser tracks. Diagram of the cross-section line used to make the hardness measurements is overlaid for reference.....	101
Figure 35: Parameter space for a fixed pulse energy of 15 J. Rows are of equal power density and columns are of equal pulse length. The surrounding dark material is the mounting resin, the dark grey material is the Ti-64 and the lighter bottom material (missing on lower rows) is the aluminium substrate.	103
Figure 36: Interface between unpolished surfaces of aluminium (bottom) and Ti64 (Top). The variation at the interface is 5 μm	105
Figure 37: Interface between aluminium (top) and Ti-64 (bottom) after polishing surfaces that are in contact. The variation at the interface is 0.5 μm	106
Figure 38: Parameter map for a 1 mm laser spot to illustrate how a combination of laser power and interaction time can change the surface area affected by the laser. Numbers under the dark field images indicate measured diameter of spot. No hole was observed but the ripple feature was three dimensional.....	107
Figure 39: Diagram of the laser path on material from a top down view. Three overlapping tracks were made for each set of parameters.	108
Figure 40: Parameter space for a fixed laser spot size of 1 mm of 3 overlapping tracks showing a laser affected zone on the surface of the coating material. Rows are of equal power density and columns are of equal pulse length. The surrounding dark material is the mounting resin, the dark grey material is the Ti-64 and the bottom material (missing on lower rows) is the aluminium substrate.	109
Figure 41: Parameter space for a fixed 1 mm diameter spot of 3 overlapping tracks at higher pulse energies.....	110
Figure 42: Parameter space for a fixed 0.8 mm diameter spot with 3 overlapping tracks at higher pulse energies.	111
Figure 43: Examples of good bonding between the Ti-64 coating (top) and aluminium (bottom) with 3 overlapping tracks. The process parameters used were 0.8 mm laser spot, 6 ms pulse length, 1400 W (left), 10 ms pulse length, 1400 W (right).	112
Figure 44: White light dark field microscope image of the LaserForge sample of In625 (top) on steel (bottom) etched with Ralph's etchant. The microstructure is clear although the sample is not etching at the same rate across the thickness of the coating. The steel has etched much more than the coating and is out of focus.	113
Figure 45: Six tracks of deposited WC-17Co coating on mild steel, tracks were deposited right to left starting at the top and were of thickness 0.5 mm.....	119

Figure 46: Graph showing how the coating thickness of a WC-17Co coating changes with increasing laser power used during deposition. 120

Figure 47: WC-17Co coating (top) on mild steel (bottom) encased in mounting resin (black). The periodic dark vertical streaks in the image are an artefact of stitching multiple images together.... 121

Figure 48: A magnified view of the interface of the WC-17Co coating (top) on mild steel (bottom) showing a section where there is an unidentified dark area..... 121

Figure 49: SEM image of the interface of WC-17Co (top) coating on mild steel (bottom). This shows a clean edge to the interface between the materials. 122

Figure 50: SEM image of the interface of WC-17Co (top) coating on mild steel (bottom). The image shows that there is a region at the interface where the two materials appear to have been changed, and not formed a clean interface as expected in supersonic laser deposition. Within this region which was slightly recessed, cracks were visible. It was suspected that some mixing had occurred of the two materials..... 122

Figure 51: Image showing the location of EDX sampling. (a) within the steel substrate, (b) within the unidentified interface and (c) within the coating. 123

Figure 52: EDX spectrum from location (b) within the interface layer between substrate and coating. 124

Figure 53: Example of a typical result from the pull off test on the as deposited material. The pulled off test element is on the left and the corresponding remaining substrate is on the right. 124

Figure 54: Example of a typical result from the pull off test on a ground down coating. The image shows that the glue failed and remains stuck to both the test element (left) and the substrate (right). 125

Figure 55: Image of a sample bar placed in the bend tester prior to bending. The load was applied from the top and distributed into the sample using a conversion bar, resulting in four points of contact for bending..... 127

Figure 56: Graph of the AE events for a steel bar coated with WC-17Co undergoing a four-point bend test in tension. There are three phases to the signal, the first is pre-cracking where a random number of events occur. Subsequently the rate and maximum amplitude of events increases at the point of coating failure. A final increase in the peak amplitude shows the point at which complete failure occurred, this is usually accompanied by fragments of the coating being projected away. .. 127

Figure 57: Graph of AE events for uncoated steel bar undergoing a four-point bend test. The graph shows two phases: The first of pre-cracking where load is taken up by the bar, the second where the bar fails catastrophically almost instantly. 128

Figure 58: Plot modelling the deflection difference of the maximum displacement compared to displacement of the load points. A typical deflection at the point of failure was 3 mm. 129

Figure 59: SEM image of the fractured surface of a WC-17Co coating in tension. The cobalt matrix has been distorted indicating a plastic deformation during failure. 132

Figure 60: SEM image of a fractured WC-17Co coating under compression. The cobalt matrix has been distorted indicating a plastic deformation during failure..... 132

Figure 61: Fractured surface of a WC-17Co coating which was in contact with the substrate near the start of a deposited track. The image shows porosity where the coating is not in contact with the substrate, meaning there is limited surface area available for bonding to the substrate. 133

Figure 62: Graph showing the force vs. deflection profile for bending of a WC-17Co bar under compression. The increase in force is not linear indicating an amount of plastic deformation prior to complete failure at about 90 seconds. 134

Figure 63: Image of a WC-17Co coated steel bar bent using a vice. The coating is shown to stick well to the substrate and fractures within itself in preference to breaking off..... 134

Figure 64: Powder size distribution for both WC-17 Co powders as determined using a mastersizer 3000.	136
Figure 65: SEM images of the WC-17Co superfine powder used in the coatings. The images show the spherical geometry of the agglomerated particles (left) and the individual grains of WC and Co that make up the powder particles (right).	137
Figure 66: SEM images of the WC-17Co standard powder used in the coatings. The images show the spherical geometry of the agglomerated particles (left) and the individual grains of WC and Co that make up the powder particles (right).	137
Figure 67: Cross section of the agglomerated particles of WC-17Co. The superfine powder on the left and the standard is on the right.	138
Figure 68: Cross section of a multilayer WC-17Co coating using the standard powder on a mild steel substrate. A laser power of 2400 W was used to produce this best observed coating. Large porosity can be observed in this coating.	139
Figure 69: Graph showing the average bending of each of the sets of samples. Error bars are +/- 1 standard deviation. The samples that were coated with WC-17Co had a final deformation less than that of the uncoated samples. Samples that were processed with the laser only or with the laser and the powder for peening, were shown to have the same deformation.	145
Figure 70: Cross section of a two-layer WC-17Co coating using 2400 W power.....	149
Figure 71: Graph showing the average displacement for two and three layer coatings. The data for a single layer coating is included for reference from the previous chapter. The three layer coating deformed significantly more than the single or two layer coating. Error bars are 1 standard deviation in each direction.	150
Figure 72: Graph showing the average displacement for a single layer WC-17Co coating, 316L coating and WC-17Co on 316L on steel. The data for a single layer WC-17Co coating is included for reference from the previous chapter. The samples containing the interlayer bent much more than the single layer coatings of each material. Error bars are 1 standard deviation in each direction. ...	154
Figure 73: Illustration of the path of the laser for subsequent rows of pulses.	156
Figure 74: Results from the laser processing of a WC-17Co coating. The white streaks are artefacts of the image stitching.....	156
Figure 75: Results from Giacomantonio et al. showing laser fusing of a NI-based wear and corrosion coating. (Top left) As deposited FS coating, (top right) Laser fused coating with 2.5-3 kW of laser power, (bottom left) laser fused coating at 1 kW laser power with significant porosity [142].	157
Figure 76: SEM image of laser pulsed surface with 1 ms pulse width at 25% showing melting and increase of porosity in the surface.....	158
Figure 77: Image of the supersonic laser deposition chamber.....	181
Figure 78: EDX spectrum from location (a) within the steel substrate.	181
Figure 79:EDX spectrum from location (b) within the interface region.	182
Figure 80: EDX spectrum from location (c) within the WC-17Co coating.....	182
Figure 81: Images of the substrate after the test elements had been pulled off.....	184
Figure 82: WC-17Co coatings 149.3+4 after gluing the test elements and curing in a furnace.	184
Figure 83: Images of the substrate after the test elements had been pulled off.....	185
Figure 84: Mild steel sample after pull-off testing.	186

1 Chapter 1 - Introduction

1.1 Introduction

Corrosion and wear are estimated to cost the global economy hundreds of billions of dollars a year. Products and components that are not protected from their usage environment can degrade more rapidly than desired. This degradation leads to a shorter lifespan than could otherwise be achieved, resulting in the need to replace or repair components at a potentially significant cost.

One solution is to protect products and components with a wear and/or corrosion resistant coating. Common coating techniques that are widely used are paint, lacquer, anodising, electroplating or cladding; these common techniques are often sufficient for many applications.

In the early twentieth century thermal spray was invented as a method to metallize substrates with zinc for corrosion protection [1]. Thermal spray processes use heated or melted materials and spray them onto a surface to build up a coating. The advantages of this process over common coating techniques are that it can deposit temperature sensitive and materials such as ceramics, deposition rates are higher, thick coatings of several mm are possible, and therefore remanufacturing of the underlying component is possible. The ability to deposit materials that are highly wear resistant, heat resistant and corrosion resistant, makes thermal spray ideal to protect high value parts that require improved surface properties.

There are however barriers to greater uptake of thermal spray processes, such as a high initial cost and a lack of trust and process reliability, often due to a lack of full understanding about the science behind the processes. It is therefore important for the academic community to gain a greater understanding of the science behind these processes, to address reliability and quality issues, and to lead new advancements in the techniques that can deliver enhanced reliability and quality.

Cold spray is a thermal spray technology that is relatively young and less developed, compared to other thermal spray techniques such as wire-arc, high velocity oxy-fuel (HVOF) and plasma spraying. It was developed at the Institute of Theoretical and Applied Mechanics of the Russian Academy of Science in 1980's Soviet Russia and has only in the last 15 years been more widely accepted in industrial applications alongside techniques that have had decades more development [2]. A significant amount of the initial research and funding originated from military sources due to the high initial cost and associated risks, and only recently has industry and academia recognised the benefit from investment in R&D.

There are many advantages to researching cold spray as an alternative to existing thermal spray coating processes. Cold spray can deposit a wide variety of materials and composites, including temperature sensitive materials such as polymers, opening new possibilities for new types of coating. Due to the low temperature and solid-state deposition mechanism, the feedstock material does not recrystallise, enabling greater control of the final coating properties, especially when the coating is a mixture of materials with vastly different thermal properties. The process also works to bond coatings such as metals directly onto non-metal and temperature sensitive substrates such as glass and plastic.

Cold spray research is also being driven by increasing industrial demand for Maintenance, Repair and Overhaul (MRO). Cold spray can be used to deposit thick coatings of several mm and for additive manufacturing, something that other thermal spray processes are not capable of. This means that worn components, such as those found on aircraft, can be remanufactured and rebuilt. MRO can save material and energy by reusing the existing component to increase its lifespan. When spare parts are no longer available, this can lead to significant cost savings over a custom-made spare part. Due to the nature of cold spray these repairs can be performed in situ, saving on transportation and carbon footprint, and reducing the down time of expensive machinery. Cold spray is considered a green technology as it is free from the hazardous chemicals that are used to make other coatings such as Cr(VI), Dow17 or MIL-3171 [3].

There is currently poor knowledge of the relationship between process parameters and the quality of a given coating. In addition, the technical requirements necessary to achieve the required quality standards for many commercial coatings have not yet been met [3]. Looking at processes developed elsewhere in industry may help to better understand and improve this process.

The experiment-based research presented in this thesis is focused on understanding the LaserForge process and its potential benefit to cold spray and supersonic laser deposition (SLD). Supersonic laser deposition uses a high-power laser to modify the cold spray deposition conditions so that deposition of materials can occur at a lower impact velocity. This has many benefits, such as enabling the replacement of the helium process gas with nitrogen. Helium is a gas that is a finite resource and is therefore costly, and cold spray systems that use it often require a recapture and purification system.

1.2 Background and Motivation

This section will define the background and motivation for undertaking the research. This research is motivated by current observations and the potential to contribute to scientific knowledge and scientific novelty.

Currently cold spray is mainly used for coatings of materials and structural repairs [4], [5]. In future cold spray is expected to be used increasingly for nanostructured coatings and temperature sensitive materials.

Within the scientific community, it is generally accepted that there is a lack of knowledge linking the parameters of cold spray deposition to the associated coating quality. This lack of understanding means that whenever a new material is deposited, it is unknown whether it will generate a good coating. Before cold spray can be used in more applications, there needs to be an increase in the understanding of how deposition parameters affect coating structure. A modification to the deposition process may also be required for more complex coating materials.

A novel process called LaserForge was identified through discussion with a commercial partner. LaserForge is marketed as a non-melt based process that can easily deposit a coating wire on a substrate using a pulsed laser. Cold spray is also marketed as a low temperature non-melt based process for coating substrates. The similarities between the two processes warrants investigation.

Prior to the start of this work, two separate trials were performed by one of the group's postdoctoral researchers, Dr Cockburn. The first was a visual investigation of LaserForge. A sample from this commercial process was analysed. It showed good bonding between a hard-facing material and a steel substrate. It was understood that a high energy pulsed laser had been used to deform the coating and substrate to bond the coating. As this was a commercial process, there were very few details about the method, which claimed to be solid-state metallurgical bonding using pulsed laser energy. It appeared to be similar in function to the solid-state non-melt bonding of SLD but with additional interface deformation for improved adhesion. It was believed that the method was using a shock deposition technique. This technology warranted further scientific understanding as it could be of benefit for in or post processing coatings made using the supersonic laser deposition process to enhance their structure.

The second trial was the coating of teeth from an excavator bucket with a single layer of WC-17Co. This material was deposited with SLD, and tested by a commercial partner, but it was reported to crack off too easily in subjective tests. For hard facing materials such as this to be commercially viable with the SLD process, further investigation would be required to optimise deposition parameters and understand the failure mode of the coating. It was therefore desirable to undertake further work to understand the limitations for deposition of this material, and the issues associated with it, as it suffered from problems such as cracking.

The outcomes of these trials were positive but left many questions unanswered. It is upon these initial studies that this work was formulated.

The primary motivation of this work was therefore to investigate the LaserForge process and understand its process mechanisms. Such an understanding was thought to be beneficial to developing improvements to the CS and SLD process.

To investigate the primary aim of investigating LaserForge, an experimental approach was taken. There was no system available at the Centre for Industrial Photonics (CIP) to reproduce the results from literature, so a new laser system was specified and built.

The secondary motivation of the work was to identify the issues with the deposition of this hard material with LCS, with the hope that the LaserForge process understanding could be used to add an additional laser process step or system modification to improve deposited coatings.

This work will investigate the problem of depositing hard materials, that do not deform easily, with SLD. Hard materials such as titanium or nanostructured ceramic coatings have been observed to have porosity, cracking and delamination. Once LaserForge mechanisms are understood it may be possible to add an additional laser-based process to SLD to change the deposited coating structure, either in or post process.

This work on LaserForge and SLD takes an experimental approach using a new laser system for LaserForge investigation and the existing SLD system at the Centre for Industrial Photonics (CIP). The current supersonic laser deposition system is used to trial the deposition of new materials for applications such as low friction or hard-wearing coatings. With this system, coatings such as titanium, show porosity. Others, such as tungsten carbide cobalt, show cracking and delamination, as in Figure 1.



Figure 1: WC-17Co SLD coating on steel showing cracking.

Titanium and WC-17Co were selected as materials for this work as they had previously been trialled with the deposition system at the university and found to make coatings that required structural improvement. They are also good examples of hard materials, and WC-17Co is formed from a

nanostructured powder, enabling advancements in understanding the deposition characteristics of such nanostructured materials with the SLD system.

When selecting materials, it was also found that material supplied by one supplier may work, whereas material from another would not deposit. As cold spray is a relatively new process, and not widely used in industry, the powder used for coatings is designed for general thermal spray applications. As such its powder properties are not controlled for cold spray. The properties required for cold spray powder of a given material are also not well understood, making it hard to specify requirements in advance. Understanding why materials such as Ti or WC-Co do not deposit well was a question whose answer could help to speed up the development of these coatings.

The output from this work will contribute to scientific knowledge and would have a potential impact on industry by:

- Understanding the LaserForge process deposition mechanism.
- Determining if the LaserForge process mechanisms could be used to improve the supersonic laser deposition process.
- Identifying failure mechanisms in nanostructured coatings using supersonic laser deposition.
- Identify the deposition parameters which have the most significant influence on coating structure and properties.
- Understanding whether a given material is likely to deposit prior to experimental trials based on the powder properties and required processing conditions.

1.3 Structure of the Thesis

This section will outline the structure of the following chapters.

Initially a series of questions will be defined, to be answered by a review of relevant literature. These questions will be used as the basis for presenting the state of the art and outlining where there are benefits to undertaking further research. Following the literature review the research questions for this thesis will be defined.

A section on materials and methods used during the following work will be presented. This will outline the materials used and how they were prepared. It will also explain how the samples were analysed following experimentation.

The first results chapter investigates the novel commercial coating technique called LaserForge that uses a high energy pulsed laser to deposit flat-sided wire coatings onto a substrate using a solid-state process. This will be investigated with the aim of understanding the required laser-material interaction

to deform a coating material into a substrate. Understanding this commercial process will be beneficial as it will provide the understanding of the underlying physics, so that the supersonic laser deposition process can be improved using an additional high-powered laser either in or post process.

The second results chapter will present the deposition and characterisation of WC-17Co coatings using the supersonic laser deposition process. This aims to answer the questions of identifying key deposition parameters that are necessary to control for this nanostructured material. It will also answer the question of how this coating fails, and how it could be prevented from doing so. This is beneficial as it will provide guidance when determining deposition parameters of other hard nanostructured coatings. This chapter will use methods such as visual observation, adhesion testing, and 4-point bend testing to characterise WC-17Co coatings.

The third results chapter will investigate the effect of thermal and residual stresses in WC-17Co coatings produced with supersonic laser deposition. Existing cold spray development work has shown that thick coatings can deform the substrate, and at the start of this work it was not clear whether it was the origin or contribution of the stresses that were deforming the coatings. This chapter aims to provide answers to the source of deformations seen during deposition. The benefit of this investigation is that the sources of deformation and poor coating structure will be better understood. This knowledge can be used in future to improve the SLD deposition process, and mitigate the effects causing the poor coating structure. Additionally, this chapter investigates the use of a high-power pulsed laser to improve deposited coatings, like the use of the pulsed laser in LaserForge.

2 Chapter 2 - Review of Literature

2.1 Background

This chapter will define the review questions, provide an analysis of the state of the art, and define the research aims and objectives for the following work. The LaserForge process will be placed in the context of other technologies, in order to determine our current understanding of it. In addition to this the Supersonic Laser Deposition process will be analysed, as the LaserForge process may give understanding that will be beneficial to making improvements to this process.

2.2 Literature Review Questions

This section will define the initial review questions that will define the scope of the literature review in this chapter.

Based on the initial motivation for the work presented here it is necessary to understand the current research landscape that surrounds the area of interest of LaserForge and its potential benefit for improvement of Supersonic Laser Deposition. To define the scope of the review, a set of questions were defined.

- 1. What is LaserForge and how does it relate to other coating deposition techniques?**
- 2. What are the advantages of using cold spray over other similar surface coating processes such as wire arc and HVOF?**
- 3. What defines if a cold spray and supersonic laser deposition coating can be deposited successfully, and what are its issues?**
- 4. Is cold spray a suitable technology for depositing high value materials such as nickel-based alloys, WC-Co and HAP (Bio-Coating) for novel applications?**
- 5. What processes are there to modify and improve coating quality and performance?**

Following the literature review the thesis research questions and objectives will be presented.

2.3 Overview of Thermal Coating Technologies

This section will give an overview of the current landscape in thermal based coating technologies and outline where LaserForge and cold spray is situated within it. It will first discuss laser-based coatings, which includes LaserForge and then discuss thermal and kinetic spray, which includes cold spray and competing technologies to answer the first 4 questions defined above.

Coatings are used where it would not be possible or economical to use the desired coating material as the bulk material for the component. It enables the desired functional material, which may have

advantageous properties such as corrosion protection, to be exposed during use, but have the bulk made up of a more suitable material. For example, this could be a painted steel railing.

A large selection of coatings are available depending on the desired properties for the tool or machine part, and these coatings protect the underlying bulk material of the component during its lifetime [6]. With many machine parts and components costing significant sums of money, there has been an increase in recent years in the development and use of surface deposition processes to repair and increase the life of existing components due to its economic attractiveness. This review will be limited to the deposition of metallic based coatings on metallic substrates.

In this work we define thermal based metallic coatings to mean coatings where an element of thermal energy is required to deposit the coating material. The deposition technologies can be broadly categorised into three areas; Laser-based coatings, thermal spray and kinetic spray. Each of these will now be discussed in turn.

2.3.1 Laser-Based Coatings

LaserForge is believed to be a laser-based coating method. Laser based coatings are sometimes referred to as laser cladding. In this section a comparison will be made between traditional laser cladding and the novel commercial process called LaserForge. As the focus of this work is to understand the LaserForge process, it is important to understand other competing technologies. Gaining an understanding of laser-based coating methods, the current challenges and state of the art will be beneficial for development of SLD. These processes use a laser as the primary energy source, whereas in cold spray the kinetic energy is dominant. With SLD relying on the laser as an additional energy source there is an increased requirement to understand the challenges in laser dominated coating processes. The following sections will outline the key laser processes used to deposit metal-based coatings on a metal substrate.

2.3.1.1 Laser Cladding (Welding)

Laser cladding is any process that uses a laser heat source to clad one material onto another. In detail this has been defined by Jayakumar et al. as "a process which is used to fuse with a laser beam another material (called clad material) which has different metallurgical properties on a substrate (base metal) where by only a very thin layer of the substrate has to be melted in order to achieve metallurgical bonding with minimal dilution of added material and substrate in order to maintain the original properties of the coating material" [7].

Laser cladding requires a coating material, which can be in the form of wire feed, powder injection or pre-placed powder. The most common method used in industry is powder injection, due to its

advantages in flexibility and control. The laser cladding can be done as either a one or two step process. In a single step process a constant feed of the cladding material to the workpiece is required. In a two-step process the coating material can be preplaced on the workpiece, such as in paste form, prior to the laser scanning. To bond the coating to the substrate a high-powered laser is scanned over the workpiece, and the surface of the workpiece and deposition material absorbs the laser energy and begins to melt. The coating forms a metallurgical bond with the substrate as the coating and melt pool that reaches into the substrate solidifies forming a crack free and fully dense coating. Typical coating thicknesses are in the range of 50 μm to 2 mm in thickness [8][7].

In all cases of laser cladding there is a dilution zone which is necessary for the bond to form between the coating and substrate. Advancements in control of the heat input have minimised these dilution interface zones so that they are comparatively thinner than other techniques such as flame and plasma surface welding. This control also enables well controlled microstructures and coating properties. Laser cladding can be done over large areas. To do this overlapping tracks of approximately 50-60 % are laid down to produce large surface areas [8] [9].

Sometimes included in the category of laser cladding are processes such as laser re-melting, welding, shock hardening, transformation hardening and annealing. In these cases, no additional material is added but the surface is modified to have different properties. These will be considered as laser surface treatments in this document and will be discussed in more detail in a later section.

Laser cladding has many advantages. It is a process that can coat almost any shape with a high level of control. As the technology is advanced, it has become a compact technology and is now also being used for near-net-shape manufacturing. The process has high control over the total heat input and therefore produces minimal interface dilution between the coating and substrate, a small heat affected zone (HAZ) and thus low substrate deformation. The process can therefore be carried out on a small part of a large component for repair purposes. A strong bond is also formed at the interface with the ability to deposit a wide variety of materials.

Disadvantages of laser cladding are that it requires the creation of a melt pool and a thin dilution layer for the formation of a strong metallurgical bond, which requires higher heat input than other processes such as thermal spray. As the process requires melting and metallurgical bonding it cannot be used to coat non-metals such as plastics and glass. Microstructure of the original feedstock is also lost when the material is melted [10].

One area that is being actively researched is the use of laser cladding remanufacturing (LCR). There are still issues with the reliability and quality of repairs for high value-added components such as

compressor blades and aircraft. One way to improve this is with the use of in-situ monitoring and adaptive control (IMAC). According to Wei-Wei Liu et al. the key issues to overcome are in the repeatability and quality of subsequent layers which can generate accumulative error, good adaptive control of the process, and a reliable and a cheap post process inspection mechanism [11].

Possible control methods that are actively being researched are visual feedback of process geometry and defects, temperature feedback from cameras, thermocouples to control microstructural properties, spectrum feedback to monitor microstructure and finally acoustic monitoring to monitor crack formation [11].

Additional research is being done to look at microstructure, melt bead geometry and residual stress in remanufactured components [12] [13]. This is a key area of interest due to the modern demands of increased remanufacturing and manufacture of laser engineered net shaped components to prevent cracking and component failure.

Additional work is also now looking at using pulsed lasers for metal wire deposition. One such example is called Micro Laser Metal Wire Deposition (μ LMWD) and uses a Nd:YAG ms pulsed laser for the formation of thin walled structures. These thin walls can be built up to form thin walled 3D metal components [14].

Current trends appear to be working towards optimising the process for repair of components and development of better control and monitoring process to reduce the variability in the process. This should lead to a greater understanding of how the heat input affects residual stress and early failure of repaired components. The other key area that is expected to grow in future years is the use of laser cladding techniques for the formation of 3D printed metals due to its advanced stage of control and optimisation that results in better surface finish compared with other deposition techniques. This however will require more research into the process parameters on novel geometries [15].

2.3.1.2 LaserForge

One application of using pulsed lasers in laser cladding is a process called LaserForge or Precision Metal Deposition (PMD). Understanding this technology is of particular interest for this work and will be investigated experimentally in a later chapter. It is hoped that understanding the LaserForge process mechanism in this work will lead to advancements in future development of Supersonic Laser Deposition. This is a proprietary commercial coating technology that can be used to coat and repair materials, and as such publicly available literature is very limited.

It is a solid-state overlay process that “combines laser heat and shock waves (forging effect) to create extremely strong metallurgical bonds resistant to coating cracking and flaking-off” [16]. The company has been working with the Department of Defence (DoD) on the technology since 2003.

The public documentation claims that it can clad dissimilar materials that cannot be clad with conventional cladding technologies [16], because there is no substrate melting or intermixing. The process works by “forcing clad material into the parent material” and generating a wavy shaped interface, which increases the contact area and bond strength Figure 2. The process can deposit thick coatings compared to thermal chemical treatments. It can be used for applications such as protection and repair of components. Examples include repair of cylindrical shafts and turbine blades to extend their life [16]. The process is claimed to have an accuracy of ± 0.002 inches when depositing flat sided wire. Minimum porosity is achieved and a shielding gas is used such as argon or nitrogen. [17]



Figure 2: Example of a LaserForge coating cross section [16].

The technical details on the process are limited but at least five patents have been granted for the technology [18]–[23]. The work is based on an original patent by Frish et al. in 1987 which uses laser-induced heat and pressure to drive a pressure wave into the metal foil coating. This pressure wave is generated by the instantaneous surface vaporisation of the top layer of the coating material. This pressure wave then interacts with the coating/substrate interface to form a bond. Different laser intensity regimes produce different shockwaves, resulting in different bonding characteristics. For this original work lasers operating in the nanosecond regime were used to produce up to 500 J of energy into a spot of typically 300 by 700 microns. Coatings that bonded required a nominal flux of >20 MW/cm². A number of substrates and coatings were reported, with varying success of bonding.

The LaserForge technology originated in 1996 with the first patent from Rabinovich for a “Rapid prototyping system”. The system described uses a circularly polarised laser focused on a 0.25 mm thick and 0.5 mm wide flat sided wire to weld or fuse it onto the substrate under a shield gas. The

laser spot size is reported to be ~ 0.15 mm in diameter, for a 150 W CO₂ laser. This equates to ~ 0.85 MW/cm², significantly less than the previous work it was based upon. The patent describes a system capable of automating this deposition process based on CAD [22].

The next significant development was in the development of a Solid Feedstock Free-Form Deposition (SFFD) system in 2000. This claims to solve the previous issues of the original process, by having a system that can deposit fully dense metal feedstock without its prior liquification. This is in addition to more advanced automated control of the process that includes a feedstock preparation station and milling tools. The new laser process, it is claimed, requires less energy for deposition and increases the speed to up to 1 kg/hr. The key advancement is claimed to be the use of short laser interaction times. A 10 J laser is used at 4 ms pulse length at 10 Hz. This gives an average power of 100 W, but a peak pulse power of 2.5 kW, reducing the average energy required for the process, and therefore thermal build up into the substrate. This is known as low heat input laser welding. A later patent in 2004 introduced the use of a v shaped feedstock that can be used to fill v shaped groves for repair purposes [24].

A later patent from 2010 builds upon the previous work, and is called LaserForge or PMD elsewhere. The patent discloses a process of “solid-state welding on flat and curved surfaces with extremely strong wave shaped morphology”. It explains that previous work required very high energies to bond materials with preplaced foils, using thermal and pressure waves, due to small air gaps between the coating and the substrate. The automated deposition system gets around this by ensuring good thermal contact between the coating and substrate during pulsed laser deposition, increasing heat conduction at the interface, so that no melt pool is required. The top surface may be liquified, but the interface will not be. The good conduction is required for the coupling of the thermal wave, and subsequent shock wave that transports the wire particles. A laser of 300 W average power is claimed to be capable of bonding wires up to 500 μ m at rates of up to 300 mm/min. Examples of materials are Ti-64 on aluminium 6061, and Inconel on Cr42 steel [25].

The patent states that an impact force of 4466 N is generated for a nickel alloy wire, based on the stress produced in the top layer of the wire, which produces the stress wave. For a carbon steel substrate with the interface at 1150 °C, this is expected to produce 0.07 mm of deformation at the interface. This is because the modulus of elasticity of the steel decreases to 28 MPa at the high temperature compared to 550 MPa at room temperature. The impact force of the particles is therefore able to deform the two materials at the interface, as the required stress is now much lower for a given deformation. The patent claims that the experimental results match the theoretical

deformation in this case. Without the high temperature of the substrate, which is heated through the thermal wave, there would be no wave shaped interface [25].

LaserForge will be investigated in more detail experimentally in this work to better understand the true mechanism being used in this process, as from literature alone there is insufficient information.

2.3.2 Thermal and Kinetic Spray

Thermal spray techniques are coating processes in which melted, or heated, materials are sprayed onto a surface [26]. There are four main classification types of thermal spray: plasma arc, electric arc, flame and kinetic. Kinetic processes include those such as cold spray that do not require melting of the feedstock. Kinetic processes such as supersonic laser deposition combine an element of thermal energy into the kinetic process.

Thermal spray processes are currently a very common and widely used type of coating processes in industry. The significant investment in these technologies has enabled them to be qualified and used for demanding and novel applications in industries such as aerospace, biomedical, electronics and oil and gas [6].

The key principle of all thermal spray processes is the use of a feedstock, such as powder or wire that is heated or melted and accelerated towards a substrate using a processing gas or jet. This constant stream of successive 'splats' of material forms a bond with the substrate upon impact and is able to build up a fully dense solid coating ranging from microns to millimetres in thickness [26].

One of the key advantages of thermal spray coatings is the wide variety of materials that can be deposited. Notably, almost any metal-based coating can be used, so long as it does not decompose under the heat of the process being used. Thermal spray processes also impart minimal heat into the substrate as the thermal energy is used to melt/accelerate the feedstock rather than changing the surface properties of the target to enable the formation of the coating. This also means that repair of coatings and material is possible as the underlying substrate properties are unlikely to be changed during the process [27].

The disadvantages of thermal spray coatings are that they require a line of sight and access to the area to be coated. Such limitations limit the use of thermal spray coatings on complex geometries such as small cavities and internal structures [26].

Future developments in thermal spray are expected to be driven by areas such as improved control of feedstock and desired material properties, spray forming of 3D components, optimisation of lesser developed kinetic processes such as cold spray, and a greater ability to control processing through automation and sensor technology [26] [28].

A more detailed look at the technology and recent developments of key thermal spray technologies will be presented below. The following sections will discuss key thermal coating processes in addition to cold spray so that they can be more easily compared. This will enable the advantages of cold spray in the current industry to be more clearly defined.

2.3.2.1 Plasma Arc

Plasma spraying, a type of thermal spray, involves the use of a plasma, generated using radio frequency discharge or direct current discharge, to melt and accelerate a powdered feedstock. The powdered feedstock is injected into the plasma stream near the exit of the plasma gun. The melted or partially melted particles impact on a substrate and form a 'splat' on the surface whereupon they cool rapidly and solidify.

Conventional coatings use particles of about 10-120 μm in diameter and produce large splats enabling thick coatings to be built up quickly with a deposition rate of 2-10 kg/h. Newer finely structured or Nano-structured coatings use agglomerated particles in the 20 -30 μm range, formed of many smaller nano particles and deposited as a molten ball or in suspension. Such coatings are built up more slowly. Time scales for the process typically are < 5 μs for flattening of the splat and between 0.8 and 10 μs for solidification. To reduce oxidation during spraying, the process can be done in a controlled atmosphere chamber [29][30].

As the process can work with a plasma arc temperature at over 8000 K, there is very little limit to which materials can be deposited, assuming the material melting temperature is 300 K lower than the vaporisation temperature. Another key advantage of the process is that after many decades of development, the process can now be controlled as a closed loop system during spraying, and parameters adjusted in real time. Parameters that can be monitored include particle velocity, temperature and trajectory of spray pattern [31]. This has enabled rapid optimisation of the deposition parameters for many materials. For example, the substrate surface preparation, heating and oxide formation is tightly controlled to ensure optimal adhesion. Residual stresses of the coating are controlled through the control of the plasma gasses used for heating and spraying, the cooling system and positioning of the deposition gun. Plasma spray processes generally have very low porosity with deposited material density exceeding 99 % [29].

Disadvantages of this process are that the impact angle of the deposited material must be 90 degrees to the substrate for optimal deposition, which limits the geometries that can be coated. This is a common problem for all thermal spray technologies [32]. Angles smaller than 90 degrees can be used for deposition but with usually with reduced coating quality [33]. The initial capital expenditure needed to set up a plasma arc process is also considered very high. This is particularly the case when

a controlled atmosphere or vacuum chamber is required. Due to the nature of the process, robotic control of the spray gun is required.

The process is good for depositing materials such as iron, nickel and cobalt alloys in the transferred arc process variant. In the non-transferred arc variant high melting temperature materials such as stellite, chromium carbides, and stabilised YSZ can be deposited. The high temperature process is not ideal for temperature sensitive materials such as carbides or polymers. When specialist environments are not used, coatings often have greater oxidation or carbide decomposition due to the high temperature, leading to inferior coating properties when compared to HVOF coatings [34]. The latest developments are focusing on using plasma spraying to deposit novel materials such as LaCoO₃, MCrAlY bond coats, LaTi₂Al₉O₁₉ (LTA) and Y₂O₃-stabilized ZrO₂ (YSZ)/ Gd₂Zr₂O₇ double layer thermal barrier coatings with reduced oxidation and decomposition.

Ceramic-based thermal barrier coatings are currently a strong driver of plasma spray development. These new coatings combined with processing modifications can lead to new coating structures such as highly strain tolerant columnar structures. To enable deposition of these new coating materials and structures new variants of plasma arc are being developed, currently research is limited to ceramic based coatings but may have benefits for nanostructured metallic coatings in future. These include High Velocity Atmospheric Plasma Spraying (HV-APS), Suspension Plasma Spraying, Plasma Spray-Physical Vapour Deposition (PS-PVD) and Pressure Plasma Spraying-Thin Film (LPPS-TF) [35].

Developments in coating microstructure can deliver significant cost savings in industry, and one such development is the use of liquid feedstock for plasma spraying. Liquid feedstock plasma spraying (LFPS) offers the advantage of depositing nanostructured coatings with custom microstructural features such as columnar structure, vertical cracks or nano-sized pores [36]. In addition, computer modelling and control of in-process parameters means that coatings can be optimised during processing, reducing the need for significant post analysis of coatings and reduced likelihood of cracking and unwanted porosity. These developments also improve the process reliability and repeatability over time during scaled-up manufacturing [37] [38] [39]. Currently this research is limited to metal oxides and thermal barrier coatings. The key problems of LFPS are that coatings such as YSZ which decomposes above 1200 °C, are still subject to high temperatures. The process is also very difficult to control and optimise.

2.3.2.2 Electric Wire Arc

The electric arc process is over 100 years old, although it has developed significantly since its introduction. The process works by using two wires as electrodes. These two wires are the feedstock and are consumed by the process and are therefore continually fed into the system. A current is

passed between these two wires to form an electric arc. This arc heats the end of the wires into a molten state. A high velocity gas jet is used to blast the molten material off the ends of the wires and atomise them in the gas stream. The gas directs these particles towards the substrate where they impact, deform and solidify into a thick coating made up of splats [6].

The process generally makes coatings that are coarser in finish compared to other thermal spray processes. The deposited spherical particles are similar in size to those used in other processes but have a much larger size distribution ranging from submicron to 200 microns. The process uses a current source higher than 50 A DC but can be up to 1500 A DC for high deposition rate applications [26].

Due to the process only heating the feedstock wire directly, the process is very thermally efficient when compared with other thermal spray processes. This also has the advantage that there is less heat transferred to the substrate, as the thermal energy is all in the atomised coating. Coatings can therefore be deposited on materials such as metal, wood, glass, fiberglass, polymers and paper. Typical material feed rates are between 20.46 kg/hr for Tin and 1.38 kg/hr for Titanium, and on average these are higher than other thermal spray processes. Due to their rough finish, coatings are good for making non-skid coatings. Although the deposited particles are similar in size to other spray processes, it is possible to modify the deposited particle size and distribution by altering the process parameters. The same feedstock can therefore be used for different final coating finishes [26].

The atomised material begins to cool as soon as it leaves the nozzle, which means that standoff distances need to be very small. There is also the issue that higher oxidation is present in these types of coatings due to the oxidation of the molten particles. Increasing the air flow rate increases the oxidation due to increased breakup of droplets [40]. Another disadvantage is that high throughput systems require water cooling to prevent overheating of the gun [26]. Porosity is usually in the range of 5-10 % and coating adhesion is mediocre in the range of 28-41 MPa [6].

Current trends in wire arc are in the use of new materials, such as the use of composite wire with a core of a non-metal polymer with a lower melting point and the use of multiple materials sprayed simultaneously [41]. This includes combined processes and techniques, for example, deposition of a coating and subsequent vaporisation of one of the materials to leave a designer porous structure [42] [41].

As with other spray processes, it is possible to use the process with inert and controlled atmospheres to improve deposited coatings [6]. Continuous improvement is also looking to use higher power, better melting, and improved coating characteristics through optimisation of deposition parameters

and design of the technology [43]. A big driver is the need for nanostructured, metallic and ceramic coatings for new and repaired high value-added components in oil and gas and aerospace.

2.3.2.3 Flame (Wire/Powder/HVOF/D-gun)

Flame spraying technology is one of the oldest thermal spray processes and has a low barrier to implementation in terms of capital investment. Over the years, it has been developed and now encompasses several popular processes. These include wire, powder, rod, HVOF (high velocity oxy-fuel) and D-gun (detonation gun) [6].

The traditional processes of wire, powder and rod all use a flame which is created using a combustible gas to melt the coating material. The feedstock is usually powder but can also be wire or rod. The melted material is atomised and transported to the substrate in the gas stream and forms a splat in the same way as other thermal spray processes.

A more recent variation (1980s) on this process is HVOF. This uses rocket engine technology to spray metal powders. The process puts fuel, oxygen and the feedstock powder into a combustion chamber. The high temperature and pressure combustion flame melts the powder and generates a supersonic flow out of the nozzle due to expansion of gasses. Flame temperatures are in the region of 3000 K. Process parameters can be altered to change the degree of melting of the powder. In addition to standard flame spraying, the supersonic jet gives the molten particles significant kinetic energy that enables the coating to have improved deposition characteristics, such as lower porosity [6].

Typical spray rates are 0.5 to 9 kg/hr dependent on material and spray parameters. HVOF coatings have low oxide contents and are suited to high quality metallic and cermet coatings which have low porosity of < 0.5 %. This is especially true for materials such as tungsten carbide that require high kinetic energy and low thermal energy for deposition [6].

The weaknesses of this process are that it is very thermally inefficient, with only about 10% of the energy used going to melt the feedstock. In addition the substrate can become hot compared to a process such as electric wire arc due to the flame [26].

Current work in flame and HVOF is on the use of liquid feedstock for processes such as Liquid Flame Spray (LFS) and High Velocity Suspension Flame Spray (HVSFS). This enables either a suspension of suspended nanostructured particles to be deposited or the use of precursors that form the desired material during the deposition [44]. A low temperature version of HVOF, called warm spraying, mixes gasses differently and controls the temperature to lower than used as standard in HVOF to enable better deposition of temperature sensitive materials such as WC-Co [45]. Maximum particle temperatures were modelled to be between 600 to 1500 K depending on nitrogen flow rate. Current

and future work in flame spraying is focused on improving the liquid injection systems and understanding the process of material splats on the substrate that leads to improved coatings. Higher kinetic energy processes are also of interest, but modifications to existing technology to increase acceleration distances are necessary [46] [47].

2.3.2.4 Cold Spray (CS) and Supersonic Laser Deposition (SLD)

As work presented in later chapters will have some focus on cold spray and Supersonic Laser Deposition, a more detailed analysis will be presented than for other techniques.

2.3.2.4.1 Introduction to Cold Spray

In comparison to many of the coating technologies discussed so far, cold spray is relatively new and has not undergone as much development. The original technique was discovered in Russia in the 1980s and the technique and a coating device were first granted patents in Russia in 1991 and the US in 1994 [48] [49] [50]. It has been commercially available for under 20 years [51].

Cold spray is a kinetic-based deposition process. Unlike the other techniques discussed above it does not melt the feedstock powder. Instead it uses a carrier gas to accelerate the particles to supersonic velocities out of a nozzle towards a substrate. Due to their high kinetic energy, the particles impact and deform and are adhered to the substrate. Subsequent particles also plastically deform the lower layers of particles to form a fully dense coating.

A typical cold spray setup is shown in Figure 3. A high-pressure gas supply (10-60 bar) is input into the system [51]. The gas used to accelerate the particles can be helium, nitrogen or even air, depending on the required sonic velocity of the gas. The gas is heated prior to accelerating the particles, to between 400 and 1100 °C, to increase the sonic velocity of the gas [52]. Most of this gas is heated with the use of a gas heater. Simultaneously a small amount of the gas is combined with the powder in a powder feeder to make it fluid through the system. This controlled rate fluid powder/gas mixture is fed into a nozzle and combined with the heated carrier gas. The powder is accelerated through the De Laval nozzle that causes the gas to expand. Due to the expansion of the gas, temperatures at the exit of the system are typically in the range of 100 – 500 °C. The accelerated particles in the gas stream from the nozzle are directed towards the substrate. Particles that have attained a required critical velocity will then adhere to the substrate [53].

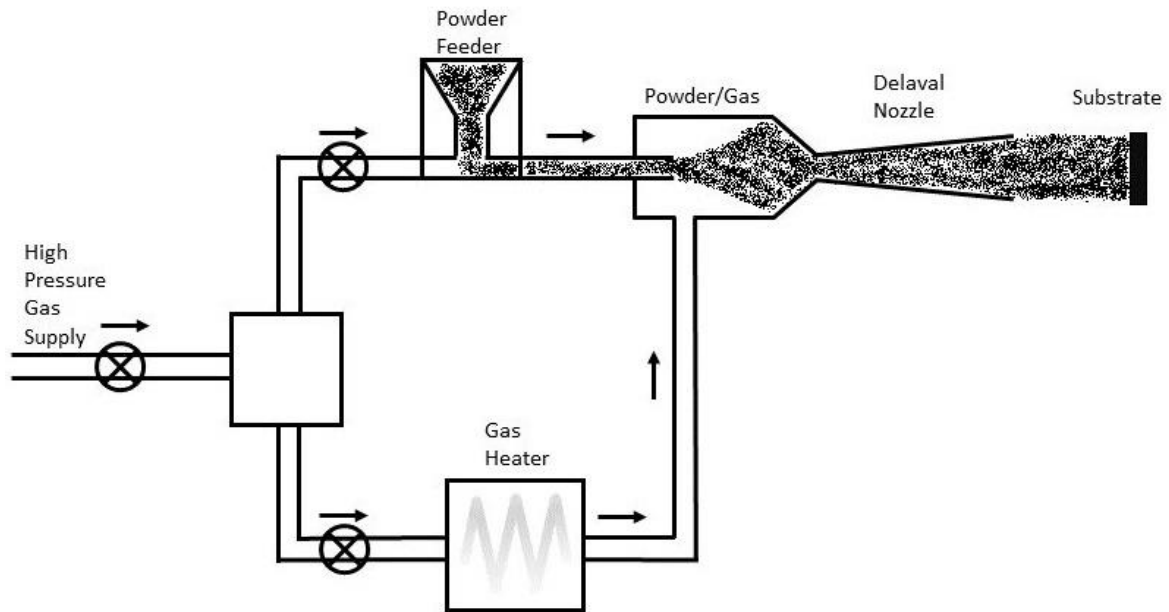


Figure 3: Diagram of a cold spray system [53].

The critical velocity is different for each material sprayed, however typical velocities are in the range of 500 to 800 m/s. In addition to the gas type mentioned above, the geometry of the particles plays an important role in determining the achieved velocity. Particles that have more angled surfaces have higher drag and so accelerate more rapidly to a higher velocity. The powder feedstock has a size distribution, and as such some of the particles will not reach critical velocity and not adhere to the substrate on impact. The critical velocity is also dependent on the particle size, with smaller particles having a larger critical velocity. As with all thermal spray processes, the deposition efficiency is defined by how much of the powder sticks to the substrate.

When compared to other thermal spray processes, the particle velocity of cold spray can be much greater, with a lower gas temperature. Only HVOF and D-gun come close to matching the particle velocity, but also involve melting of the coating particles. Warm spraying does not involve molten particles. A comparison of the techniques is shown in Figure 4.

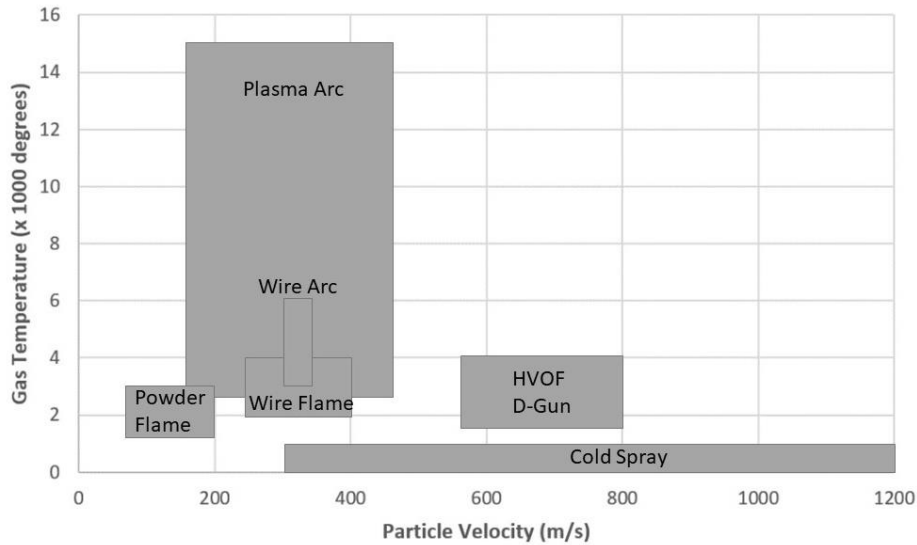


Figure 4: Figure showing the relative particle velocity and gas temperature space. High velocity and high temperature have not been investigated [43].

Research has been done to model the gas flow and particle velocities through a cold spray nozzle. Studies have been undertaken from both a theoretical and experimental perspective. 1D frictionless calculations have been done for various cold spray conditions, as in Figure 5 [54]. They show that particle velocity increases uniformly by the gas flow through the nozzle and particles are not affected by gas velocity variations at the nozzle exit due to their momentum [55]. CFD modelling has also been done to optimise nozzle geometry [56]. Additionally the theoretical models have been compared to experimental measurements of particle velocity at the nozzle exit [57] [58]. Models in 1D, 2D and CFD have differences to experimentally measured velocities, but it has been shown that these models are good enough to approximate results, and the US Army Research Laboratory Centre for Cold Spray (ARLCCS) therefore uses modelling to calculate feasibility and deposition efficiency for new materials [55]. More advanced modelling not based solely on mathematical methods but also taking into account the whole flow field is now underway [59].

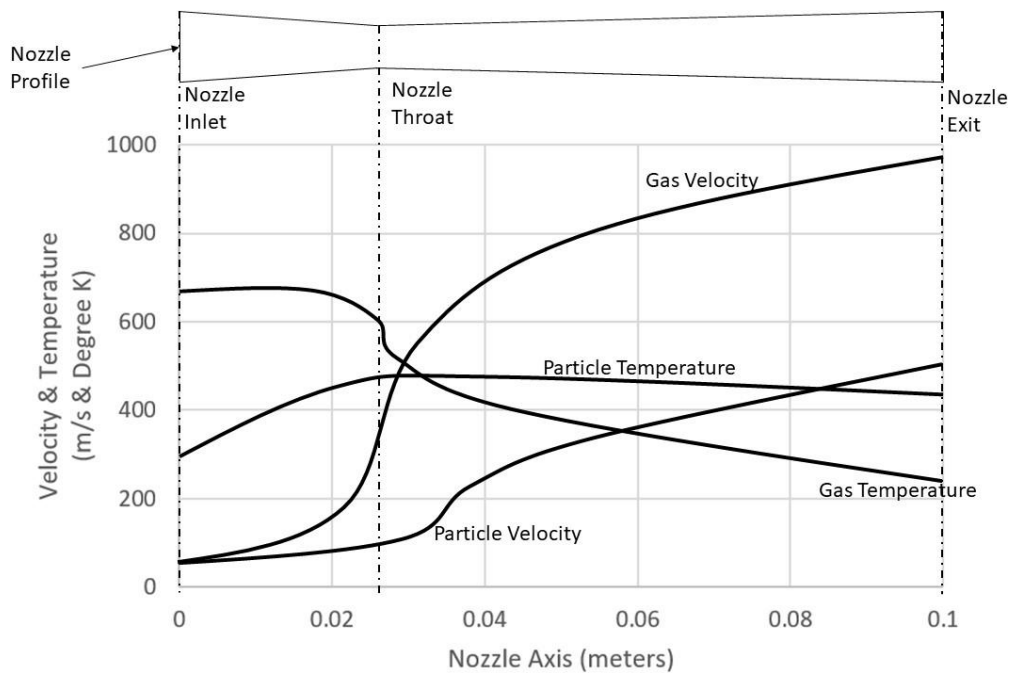


Figure 5: Graph of particle and gas velocities modelled through a cold spray nozzle [54].

The exact mechanism for the adhesion of the coating particle on the substrate is still an active area of research. According to Grujicic et al. the leading theory suggests that the incident high velocity particles plastically deform upon impact along with a thin layer of the substrate, which disrupts the thin oxide surface films to enable conformal contact of both surfaces. High strain rates locally heat the interface between the particle and substrate resulting in adiabatic shear instabilities. Bonding then occurs due to the conformal contact and high pressure [60] [46]. The process does result in bulk melting of either the coating particles or the substrate [61]. It should be noted that the initial thin layer of particles may have different bonding characteristics and deposition efficiencies compared to subsequent layers, due to the material change. For example, the first layer may be copper on steel, but subsequent layers should be treated as copper on copper.

Computational modelling has shown that a critical velocity for cold spray to occur is associated with the requirement for conditions that enable the formation of a particle/substrate interfacial jet composed of both materials. At sub-critical velocity the interfacial jet is only made up of one material. Higher kinetic energy contributes to greater contact pressures along with better developed interfacial jets and are the dominant factor in the strength of the interfacial bond and therefore the deposition efficiency. With two different materials that have different viscosities, an interfacial instability may occur resulting in roll-ups and vortices. This will lead to a greater surface area for bonding through nano/microscale material mixing and mechanical interlocking and can also have the effect of

mechanically interlocking the two materials together over the length of the particle [60]. Two mechanisms from computational simulation are presented in Figure 6. They show that the differences in the incident material can lead to different bonding of the particle and positioning of the interfacial jet.

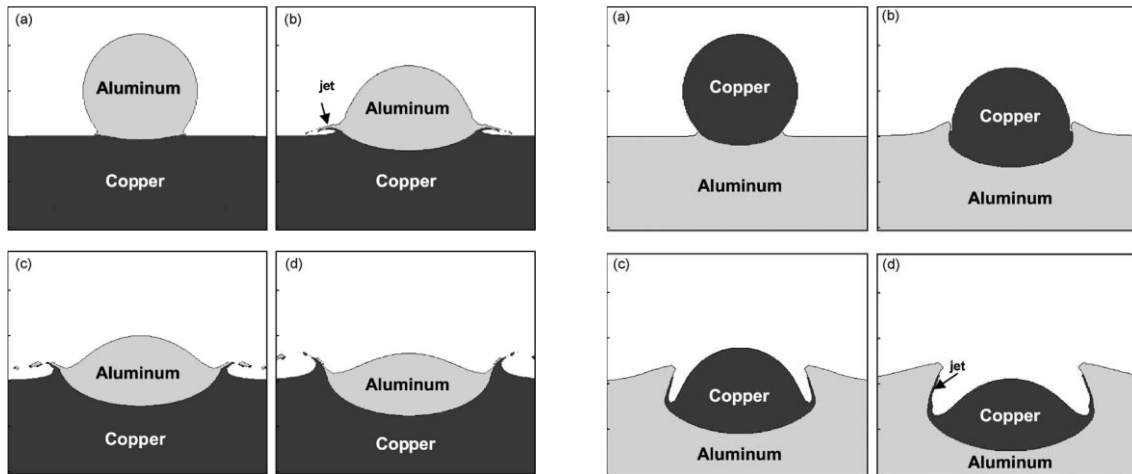


Figure 6: Comparison of computational models for bonding of copper and aluminium for an incident particle velocity of 650 m/s at times of (a) 5 ns; (b) 20 ns; (c) 35 ns; and (d) 50 ns. Reproduced from [60].

Having looked at a single particle impact, it is also important to understand the implication of two particles that impact simultaneously and the effect this has on building up bulk material. It has been shown through numerical modelling that the formation of holes in the surface can occur when two particles impact the substrate without any space between them. This can occur due to high powder feed rates. These holes cannot be subsequently be filled in if subsequent particles cannot reach the bottom of the hole, leading to hole growth in the coating [62].

As described, the role of particle velocity is important in the process: it is not just required to reach the minimum critical velocity for the coating and substrate, but also to achieve good bonding. There is an optimal region of particle impact velocity that is related to the particle diameter, Figure 7. Too low particle velocity will lead to erosion of the substrate. Increasing the particle velocity beyond the critical velocity will lead to super-deep penetration (SDP) of particles. At even greater velocities the process enters a range where the two materials act like liquids, as the kinetic energy is much greater than the yield point of the materials [45]. This is undesirable as material mixing at the interface can occur.

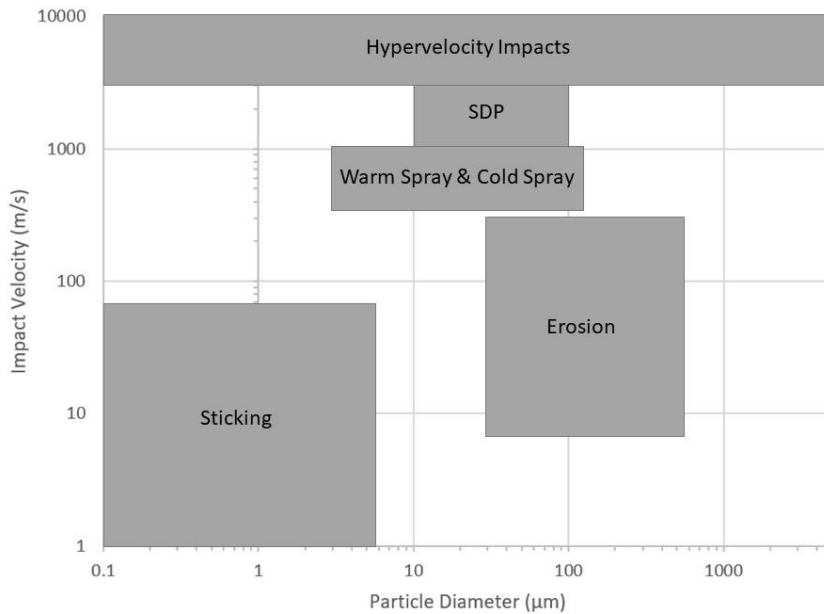


Figure 7: A graph showing the optimal region for impact velocities for cold spray based on particle diameter [45].

There are several key benefits to cold spray, the first of which is the non-melting nature of the deposition. This enables coatings to be deposited without re-crystallisation or modification of the coating crystal structure. A wide selection of materials can be deposited such as nano-crystalline and amorphous materials, e.g. metals, metal alloys, cermets, epoxy resins, polyurethane and thermoplastics [53] [63] [64]. Coating properties can therefore be designed directly into the feedstock powder without the need to tightly control cooling rates as would be necessary with many other thermal spray processes. The low temperature of the deposition also enables it to be deposited on temperature sensitive materials such as plastic.

Due to the relatively low temperature deposition the coating is free from thermally induced tensile stresses and usually has minimal or compressive residual stress (< 100 MPa) [65]. The coating is also not affected by residual stress from uncontrolled solidification of particles. Overall the deposited coatings have low porosity and usually have comparable properties to the unsprayed bulk form such as thermal conductivity, electrical conductivity and mechanical strength [66].

There are several weaknesses to the process, one of which is the cost of the gas. Many materials require a high critical velocity that necessitates the use of helium gas. Helium gas is very expensive and requires the use of helium recycling to make it cost effective, due to the large volume of gas required for processing. Many materials can be deposited by the process described above, but hard and brittle materials cannot be deposited without the use of a binder material that can be deformed in the deposition. Fouling and erosion of cold spray nozzles is also an issue.

Cold spray is less developed than many other thermal spray processes, and as such the control of deposition still has significant opportunity for improvement. The process has, however, been certified by the military for repair of components and is therefore seen to be a viable deposition option and is receiving funding for continued research in both academic and industrial settings.

2.3.2.4.2 Cold Spray Applications and Development

The main applications currently for cold spray are for coatings of materials and structural repairs. Coatings such as Al-Mg, Zinc, Tantalum and Ni-cu can be deposited for corrosion protection [4], [5], [5], [67], [68]. Wear protection can also be deposited, but due to the limitations of the process, a soft binder material is required. Materials such as WC-Co and W-Cu have been successfully deposited and show high Vickers hardness values. These materials benefit from the low process temperatures that do not cause the phase transformations or decarburisation that is seen with HVOF [69], [70]. For repairs, aerospace is the biggest beneficiary of this new technology enabling component repairs of parts that cannot be subject to the thermal stresses of other thermal spray processes [51].

One variant of cold spray that has been developed by the Inovati Corporation is called Kinetic Metallization. This process uses helium and nitrogen gas but at much lower pressure of 0.5 to 9 bar, yet still achieves particle velocities of up to 1000 m/s using a sonic nozzle to accelerate the gas. It can deposit antennae and electrical interconnects with copper coatings. The process is also able to deposit WC-Co and niobium. One of the key advancements Inovati claim is the advancements of the fine feedstock powders they make specially for the process and the system for feeding and fluidising the particles. Deposition rates are from 0.06 to 6 kg/hr [71]–[74].

Improved nozzles are already in development and use, including the move to more rectangular outlets that have a more even coating cross sectional thickness. To make such cold spray nozzle geometries it is necessary to use laser additive manufacturing [75] [76]. In addition, smaller and angled nozzles are being developed that can reach into small areas to deposit on the inside of more complex geometries. These developments are also combined with more advanced powder feed mechanisms to fluidise the powder in the nozzle gas stream [56].

Residual stress in coated cold sprayed components can become significant depending on deposition conditions and material and can be detrimental to coating integrity and can lead to delamination and cracking of the structure. This problem has been addressed by recent modelling of residual stresses both at the microscale and macroscale. At the microscopic scale, it was found that impact velocity, incident angle of impact, density and the materials yield strengths are the key factors that influence the residual stress formed. At the macroscopic scale it was found that residual stress could be

minimised by using a deposition strategy that uses successive layers of perpendicular relative orientation, resulting in up to 32 % less residual stress for aluminium on copper [77].

A further area of development is in powder feedstock for cold spray. As powder is mainly manufactured for melt-based processes, it is not designed for use in processes that retain its microscopic structure. As such, cold spray requires powder that has greater control over the microstructure as it is reflected directly in the coating. This also allows the formation of nanoscale powders that can be directly transferred to the coating. Nanoscale powders can be combined into larger agglomerates which can then be sprayed and result in coatings with a structure of the nanostructured particles upon deposition [78] [51].

As systems evolve there has been a drive towards higher particle velocities and the market demand to deposit harder less ductile materials. One direction has been to move to higher gas pressures and higher temperatures to achieve the required increase in particle velocities. The other significant problem with existing systems is the reliance on helium gas to give the higher required particle velocities. As helium is a finite and expensive gas, a helium recycling system would be required to make it commercially viable. An alternative route to using helium and increased gas pressure and temperature is supersonic laser deposition.

Numerous post treatments have been developed, but the most common are re-melting to improve density and adhesion, which can be achieved through spark plasma sintering for densification of porous coating [79], melting either in a low oxygen environment or in a vacuum [80] and laser-fused coatings.

There are two directions for improving the cold spray process. The first is improvement in the equipment and feedstock control of the cold spray process itself. The second is the use of pre-, in- or post- process assistants to modify the traditional cold spray process to achieve improved results.

2.3.2.4.3 Supersonic Laser Deposition

Supersonic laser deposition (SLD) is a novel process under development at the University of Cambridge. It has been demonstrated in studies that increasing the particle temperature in cold spray can result in an increase in deposition efficiency and a reduction in critical deposition velocity. Increasing particle temperature does however have its risks, as it makes low melting point materials more likely to clog the deposition nozzle. SLD is a process that means increasing the deposition particle temperature is not necessary [81], [82].

SLD uses a laser in combination with the cold spray process to heat the deposition site on the substrate. Heating the substrate to just below its melting point reduces the shear strength of the

material and softens the deposition site. This reduces the required critical velocity of the deposition material. Bonding has been shown to occur for impact velocities at around half of those required for cold spray (<500 m/s) [83].

A typical supersonic laser deposition system works in a similar way to traditional Cold Spray systems as shown in Figure 3, but also has the addition of an external laser focused at the deposition site that moves with the deposition nozzle. A pyrometer monitors the deposition site temperature to ensure constant heating through a feedback to the laser power. Typical laser powers used can vary from a few hundred W to several KW depending on the material being deposited. Materials that can be deposited are similar to those that are deposited with cold spray and include 316L stainless steel, copper, aluminium, titanium and Inconel 718 [83].

The laser in supersonic laser deposition has been investigated for use as a pre-treatment, a post-treatment and an in-situ treatment. In pre-treatment, the laser can anneal soften and ablate the substrate preparing it for optimal bonding to the substrate. Post-treatment enables annealing and ablation of deposited materials. In-situ treatment works to anneal, ablate and soften the material to reduce the critical velocities required. Each of these methods have been shown to have benefits over the original cold spray [84].

Several research institutes are now working on a variation of supersonic laser deposition called Coaxially Laser-Assisted Cold Spray (COLA) which places the laser inside the spray nozzle. This technology reduces the size of the system but limits the laser to being used in process only [85] [86].

Supersonic laser deposition has many benefits over both cold spray and other thermal spray technologies. It does not require expensive gas such as helium to deposit materials that are hard to deform, resulting in significant cost savings. The process also enables coatings that have reduced porosity due to greater deformation of the particles during deposition. Particle deformation similar to that seen in HVOF has been observed [87].

The major weakness in SLD is the thermal input into the substrate; this can be especially high for brittle and hard materials that do not deform easily and have a high SLD critical velocity. Under these high thermal input conditions, the substrate can heat up and incur residual stresses from the thermal effects. Upon cooling this can lead to cracking and delamination of the coating, making it unsuitable for industrial use.

Future trends in cold spray and supersonic laser deposition are heading towards smoother, more predictable deposits to reduce machining. In order to do this, there needs to be an improvement in the control of the process and its parameters, such as better estimation of deposition site

temperatures and tighter control of thermal input, smaller deposition spot size and more consistent powder delivery through improved powder feed systems.

Work to develop better nozzles that do not clog, and a miniaturisation of existing systems, is in progress. Portable and micro cold spray systems have already been demonstrated that are now able to print fine features such as micro-circuitry with tracks of under 500 um [88].

To enable a greater commercialisation of the technology a more integrated approach is necessary. This integrated approach will require teams specialising CAD, hardware, process optimisation, simulation and building to develop complete systems that are attractive to industry. Once industry has begun adopting this technology to a greater degree, it is expected that there will be a shift to better control of powder and more funding for process control and optimisation [89] [90].

2.3.2.4.4 Cold Spray Materials and Coatings

Cold spray is very good at depositing a range of materials. This section will discuss which materials are currently used with cold spray.

Metals were the first materials that were investigated with the cold spray process. The suitability of a metal for spraying can be attributed to its physical properties such as hardness, melting temperature and density [91]. Metals such as copper, zinc and aluminium have relatively low melting points and mechanical strength and are therefore ideal metals for deposition. Alloys of these metals have also widely been deposited. Thermal properties of the material are important for deposition, such as for aluminium which has a high heat capacity, affecting its shear instability properties which can make it harder to deposit. Iron and nickel-based materials have a higher strength, which requires increased energy to deposit with cold spray. Materials such as nickel alloys, titanium alloys, stainless steel and tantalum have all been reported in literature to work with the cold spray process [90]. In literature the properties of deposited metal coatings have been tested for hardness, oxidation, corrosion and bond strength and the results compare favourably to requirements for industrial usage. It is of interest to use CS for deposition of these materials as for example stainless steel currently has oxidation issues when deposited with HVOF for some applications [92].

Although fatigue accounts for 90% of mechanical failures, there are limited studies for cold spray, with many controversial results. The outcome of such work has led to a model to predict failure based upon residual stress, coating hardness and stress gradient of the coating [93]. Thermal barrier coatings have been widely studied, where cold spray is used for the bond coat (e.g. CoCrAlY) under a plasma sprayed top coat to promote bonding [94] [95]. Amorphous metal, otherwise known as metallic glass, is a solid metallic alloy material that has been deposited with cold spray. These form bulk metallic glass (BMG)

coatings with low critical cooling rates. Due to the unusual structure of this material the underlying deposition parameters that affect coating quality are still unknown.

Novel materials such as Hydroxyapatite (HAP), a biocompatible calcium phosphate, can be deposited with CS as the process retains the original material properties, ensuring that the final coating will be biocompatible. This has advantages over traditional thermal spray that can cause the material to change its chemical properties, due to the higher temperatures used in their processes. Cold spray has key advantages in the manufacture of the Al-Sn slide bearings that are used in ships and automobiles. When using other thermal spray processes such as HVOF, the process coarsens the Sn grains and reduces its effectiveness [96]. Another application that has been enabled by cold spray is the development of CuCrAl and NiCrAlY thermal and oxidation resistant coatings, for use as liners for rocket engines by NASA [97]. Mg alloys that are used in helicopter and aircraft gearboxes such as in the UH-60 Seahawk and MH-60S Seahawk, are highly susceptible to galvanic corrosion when coupled to other materials. Cold spray is used to repair these coatings and protect them with aluminium coatings as they are affected by processes such as HVOF due to their heat sensitive nature [98] [99].

Metal matrix composites (MMC) are a group of materials that can enable the deposition of brittle materials using cold spray. A metal matrix composite is defined as a material that contains a metal as a binder and another metal or material that is distributed in this binder. Brittle materials do not have significant ductility at high strain rate, and therefore cannot easily be directly deposited using cold spray. The key advantage to using CS for this type of coating is the lack of alloying, phase transformations or thermite reactions for the deposited materials. The materials that benefit most from being cold sprayed are those that require a low deposition temperature to reduce existing problems such as fracturing, decarburization and delamination [100].

Metal matrix compounds successfully deposited with cold spray where two or more metals are involved include Ti+Al, Al+Ni, Zn+(Al-Si), Zn+Al+Si, W+Cu, NdFeB+Al. The issues with metal-metal MMC deposition is that the deposition of the mixed powder depends on the method of mixing and can result in different coating structures, which may not be uniform throughout the coating. Metal-ceramic MMC coatings enable the deposition of non-deformable particles such as ceramics. Studies have been done on Al+Al₂O₃, Al+SiC, WC+Co, CrC+NiCr. In general, there is a lack of fundamental understanding on the impact of reinforcement particle ratio. Many experimental case studies have been done to prove the concept, however future work should target a systematic quantitative understanding of the process to lead towards a generalised theory. It is suggested that an increase in theoretical studies would help to advance understanding of MMC cold spray deposition [90].

As discussed, ceramic material is not suited to deposition with cold spray due to its lack of ductility at high strain rates. In some cases, it is possible for ceramics to form a thin coating layer. Ceramic cold sprayed coatings that have been studied in literature include WO_3 on silicon substrates and TiO_2 on Al, Cu and Ti substrates [101] [102]. The fact that ceramic on ceramic and ceramic on metal coatings are possible indicate that our limited understanding of CS bonding from metal on metal deposition is not complete, as it does not fit completely into the existing model. For the case of ceramic on ceramic the bonding mechanism was identified to be particle fragmentation to smaller particle size and mechanical interlocking. For ceramic on metal, the mechanism was embedding in the substrate. Ceramics have very different properties to metals on impact and there is scope for further studies to investigate the bonding mechanism and properties of ceramics during high energy impact on a substrate [101] [102].

Polymers can be used as both as a coating and substrate with cold spray. When polymers are used as a substrate, a metallisation coating can be directly applied to them. This can be useful as it protects the substrate and can provide different surface properties. Higher temperature processes such as plasma or HVOF are not well suited to deposition on polymers due to the molten state of the coating process. Examples of materials that have been deposited on polymers using CS are copper, aluminium, tin, lead, titanium and Hydroxyapatite (HAP) [103] [104] [105] [106]. It is possible to use a polymer as a coating with cold spray such as polythene, however the critical velocity is significantly lower. For example, polyolef CS on an aluminium substrate required a critical velocity of 100 m/s [107] [108]. Fundamental understanding of the bonding mechanisms between polymers and metals is still in early stages as this is still a relatively new field.

Cold spray is an attractive process for the deposition of nanostructured materials as it can retain the properties during deposition due to low thermal input, unlike processes such as HVOF [109]. Materials such as aluminium, its alloys (5083, 6061 and 2618) and Cu-Ni-Fe, have been successfully deposited and demonstrated increased hardness [110] [111]. In addition, nanostructured copper alumina, Fe/Al, WC-Co, $Cr_3C_2-25(Ni-20Cr)$, Si_3N_4 , silicon carbide, boron nitride and cerium oxide have also been cold sprayed [112] [113] [96]. The cold spray process retains the nanostructured aspect of the powder; however, it was observed that nanostructured coatings had increased porosity when compared to other thermal spray processes. Literature has not yet investigated the cause of this issue of increased porosity. Addressing the problem of increased porosity in these coatings should be an area for future research in cold spray [90].

2.3.2.4.5 *State of Cold Spray Research*

Cold spray materials research is already at the point of understanding metal on metal deposition from both an experimental and theoretical perspective. There is already significant research into deposition of metal matrix composites, however there is still a lack of theoretical understanding in literature to describe the fundamental mechanisms involved. Novel areas of cold spray such as with deposition of polymers or nanostructured materials is still at a very early stage and there exist large gaps in academic understanding of the bonding process.

There are numerous key problems with thermal spray coatings that are in the process of being addressed. These include insufficient process control, lack of options regarding non-destructive testing of deposited coatings, a lack of understanding of the cold spray process, difficulty in formation of net shape parts, feedstock production variation affecting processes, spraying of thick coatings, spraying onto non-flat geometries, spraying of composites and spraying of nanoscale materials. An example of ways these limitations are being overcome might be the increased research into integrated systems for cold spray to improve process control. Processes parameters that would benefit from increased control are gas temperature, gas pressure, gas flow rate, powder flow rate. An integrated system that could also provide feedback to maintain consistency of deposition over time. Novel methods for non-destructive testing such as infrared thermography and acoustic microscopy are being developed [114]. Thin coatings are being developed by using liquid suspensions to deposit finer particles such as nanoscale materials, and thicker coatings are limited by particle size and required thermal input to heat them [115].

Future trends in cold spray are expected falls into two categories, novel applications using coatings that are currently limited by thermal issues, and enhanced nanostructured coatings that can be made due to the low thermal input nature of cold spray [89]. Examples of this are in surface protection and remanufacture, and ability to embed sensors for real-time monitoring of structures.

The development of cold spray is behind technologies such as HVOF and plasma spray. It is necessary to better understand the fundamental deposition process of cold spray, so that the process control can be improved to the level currently seen in HVOF and plasma spray. Currently there is not always a good understanding of what deposition parameters will lead to a good coating. Based on the literature reviewed there are key areas that need further development. These are:

- Better understanding of the relationship between deposition parameters and quality of coating. This includes differences of depositing material A on B vs B on A and deposition behaviour of untried material combinations. Computational modelling and experimental testing of novel combinations are already being done.

- Development of specialist powders for cold spray. Most existing powder is designed for melt-based deposition processes, where powder properties are less critical to the coating properties, than the process deposition parameters. Specialist companies are already developing specialist powders, but much knowledge remains as undisclosed IP in industry.
- Surface preparation effects on coating quality. [116]
- Variants of cold-spray based on the fundamental principle but with additional advantages, such as supersonic laser deposition.

2.3.2.5 Comparison of Cold Spray to Other Thermal Spray Technologies

Now that each key type of coating has been introduced, this section will compare them to cold spray to determine where advancements in cold spray could be beneficial. A table comparing the numerical properties of each process is shown below, Table 1.

Table 1: Numerical comparison of thermal spray methods [27],[117], [118], [119],[120],[121],[122],[123].

		Plasma arc	Wire arc	Flame spray	HVOF	Cold spray
Particle velocity (m/s)		<450	150	<50	<700	300-1,200
Gas temp (°C)		14,000	4,000	3,000	3,000	600
Deposition rate (kg/h)		2-10	10-25	2-6	1-9	2-15
Adhesion (MPa)	Ferrous alloys	21-34	28-41	14-21	48-62	10-200
	N-ferrous alloys	14-48	14-48	7-34	48-62	
	Ceramics	21-41	-	14-34	-	
	Carbides	55-69	-	34-48	>83	
Coating thickness (mm)	Ferrous alloys	0.4-2.5	0.1-2.5	0.05-2.0	0.05-2.5	0.05-10.0+
	N-ferrous alloys	0.05-5	0.1-5	0.05-5.0	0.05-2.5	
	Ceramics	0.1-2.0	-	0.25-2.0	-	
	Carbides	0.15-0.8	-	0.15-0.8	0.05-5.0	
Porosity (%)	Ferrous alloys	2-5	3-10	3-10	<2	<1
	N-ferrous alloys	2-5	3-10	3-10	<2	
	Ceramics	1-2	-	5-15	-	
	Carbides	2-3	-	5-15	<1	
Oxides (%)		0.5-1	0.5-3	4-6	0.2	<1
Energy required to melt (kW/Kg)		13-22	0.2-0.4	11-22	22-200	(Non-melt process)
Typical coating materials		Ceramic coatings such as chrome oxide, aluminium oxide and titanium oxide.	Pure metals such as aluminium, zinc, copper. Alloys such as stain-less steel.	Pure metals such as zinc, chromium, and aluminium. Abradable coatings such as nickel graphite and nickel chrome.	Tungsten carbide, Inconel, chrome carbide and Stellite.	Metals and alloys such as aluminium, silver, copper, zinc, TiAlV, CuCrAl, CuAgCe. Ceramic based WC, SiC. Oxides Al ₂ O ₃ , TiO ₂ .

This table shows that cold spray is comparable in many ways to other thermal spray processes. It is very similar in many aspects to HVOF on paper, such as in porosity, adhesion and deposition rates (thermal efficiency). Cold spray stands out in three areas; gas temperature, adhesion and energy required to melt. The gas temperature in cold spray is lower due to the lack of a need to melt the feedstock. This therefore requires much less energy to deposit the same amount of material as HVOF, making it more cost effective and energy efficient. Adhesion is also comparable to or greater than HVOF. Coatings that are deposited with cold spray can exhibit the same properties as the bulk unsprayed material. HVOF has advantages of producing less carbide phases than arc or flame, however cold spray is better than HVOF in this respect with its lower thermal input. HVOF has limited powder size distribution capability of 5-60 μm , something that cold spray is not limited by.

Developments in HVOF research have moved on to being able to deposit finer nanostructured materials using sub-micron powders. These fine powders are required to form coatings that have enhanced properties for functionality such as low friction coatings (titanium oxide), wear protection and electrical insulators (aluminium oxide), and bioactive and biodegradable materials (HA, TCP, Bioglass). To deposit these fine powders, they are suspended in a liquid. Doing so enables molten drops that are one or two orders of magnitude smaller than previously. The issues with using a liquid suspension is that there is a limit to the possible combinations and final properties of the coating. Cold spray can solve this by forming the desired coating properties into a dry powder and depositing it without changing the chemical composition or material properties. HVOF is very sensitive to parameters, especially where a liquid suspension is used, and therefore the final coating properties are not guaranteed. Cold spray is more forgiving and does not generate carbide decomposition and excessive oxidation. Cold spray research should therefore focus on depositing these nanostructured materials that are hard or impossible to deposit with HVOF [124].

Plasma arc coatings are mainly limited by the high temperature of the process. It is the hottest of all the thermal spray processes by several factors. This causes problems with oxidation which have been solved by using a controlled atmosphere. Plasma arc is generally used to deposit materials with high melting points such as ceramics, although it is still able to deposit metals such as aluminium, stainless steel and zinc. It is not competing for deposition of pure metals and wire arc and flame spray are already preferred over plasma arc for deposition of metallic coatings. For metallic coatings, plasma arc requires significantly more energy than cold spray per kg of material. It also introduces more porosity and oxide content.

There is now a pull from industry to have coatings with properties, such as low friction and thermal barriers. These types of coatings, such as ZrO_2 , YSZ or graphite doped stainless steel (2% graphite),

require dense coatings with fine microstructures [125]. Recent plasma spray research has successfully produced some of these dense microstructure coatings using a liquid suspension for the powder [126]. Such suspensions have particles with a size of the order of 1 μm . Cold spray can have advantages over this process, by the lack of need for melting the feedstock. This means that with cold spray there are no issues with oxide formation, decomposition of carbides, and the need to suspend the powder in a liquid as the original chemistry is conserved during deposition. It would therefore make sense to research the use of cold spray which is already capable of depositing many of these coatings with fewer drawbacks [127], [27].

Electric wire arc can only easily deposit coatings that are electrically conductive. This is not a limitation of cold spray. Wire arc has tried to work around this limitation by using wire that has a core of non-conducting material. Wire arc produces coatings that are of a rougher finish and increased porosity when compared to plasma or HVOF, as they have a greater porosity and poor surface finish. This is not an issue when the coatings are sacrificial. One of the key advantages of wire arc over other thermal spray processes is its low transfer of thermal energy to the substrate, due to its very high efficiency when melting the feedstock. It can therefore be used to spray onto materials that are thermally sensitive such as paper or plastics. In areas such as aerospace, there is a demand to deposit high performance nanostructured coatings, where low thermal input is a desirable characteristic. Cold spray, like wire arc can deposit onto temperature sensitive materials, as it minimises the thermal energy required for the process and is therefore also capable of spraying onto plastic with limited thermal heat transfer. The coatings that are produced with cold spray are also of better quality with less porosity and greater adhesion, and therefore suitable for more demanding applications such as a thermal barrier bond coat or corrosion protection layer.

Although cold spray is competitive with other thermal spray processes, on their own its advantages are not enough to justify replacing HVOF or other thermal spray processes with cold spray. The real benefit of cold spray is in new applications and coatings where other thermal spray processes are reaching their limitations. The key advantages of cold spray over the other processes are: deposition of nanostructured coatings, coatings where less oxidation is required, spraying of thermal sensitive materials or where less heat input is required, where thermally sensitive substrates are used and when less decarburisation is required than the melt-based processes.

2.4 Overview of Selected Laser Surface Treatments

This section will discuss current understanding and trends in laser surface treatment. This will address the fifth research question defined in section 2.2, which looks to understand which surface modification techniques would be able to improve cold spray deposited coatings. Understanding these

processes will also aid in the understanding of LaserForge, which is itself a process that uses laser interaction with the surface, to deposit coatings. This section is limited to laser surface treatments as supersonic laser deposition already uses a laser, and it is desirable to understand how the findings from the work on LaserForge could use this existing available laser or an additional laser to improve the process.

The advantages of using a laser in materials processing are numerous. Amongst its advantages are its ability to provide localized thermal treatment, rapid heating and cooling rates and a large degree of control of thermal history for each part. For specific localised tasks such as laser cutting it can be advantageous to use lasers in high productivity environments where time productivity increases of up to 49 % are possible. Being a non-contact process means that tooling does not wear, and consistent production is maintained without the cost of replacing components. A reduction in processing costs of finishing operations can be achieved such as through the use of laser finishing, which is expected to reduce polishing costs by up to 75 % and time by up to 90 % [128] [129] [130].

Laser thermal treatments fall into two categories, heating without melting and heating with melting. In general, a laser is used to generate a targeted beam of energy at the workpiece. This energy can be in the form of a continuous-wave (CW) or pulsed beam. There are two key parameters that must be considered, the power density and the interaction time. The former is defined by the beam diameter and the laser power. The latter is the time for which the power density is incident on a point on the surface [131] [132]. A graph showing a comparison of techniques is presented in Figure 8.

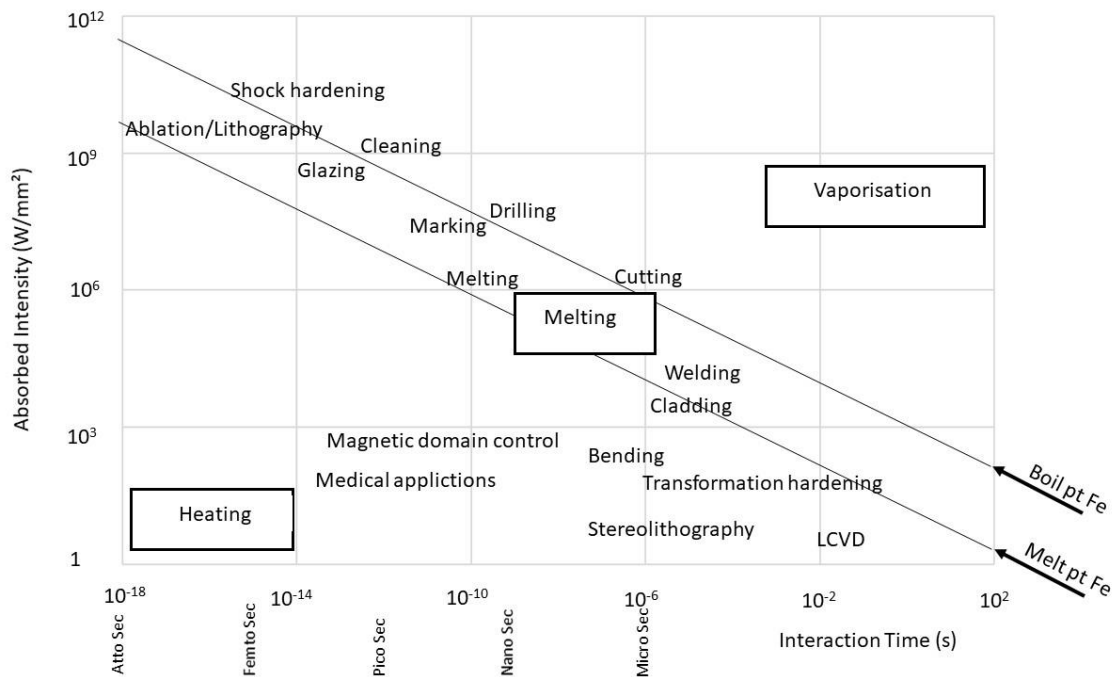


Figure 8: A graph showing a comparison of available laser treatments in relation to absorbed intensity and interaction time [133].

Processes that benefit from laser heating without melting are transformation hardening and annealing. Non-melt-based surface hardening processes on metals are often done to enhance wear characteristics or fatigue properties of parts. Hardened zones can range between 0.25 and 2.5 mm in depth. For carbon steel and iron deep hardening can reach depths of 0.5 to 1 mm with laser spot densities in the range of 500 to 5000 W/cm². To achieve this lasers of 3000 to 6000 W average power are used [134]–[136].

LaserForge is described as a process that uses a pulsed laser beam to generate a waved shaped interface to achieve good bonding. The exact mechanism is the object of study of this work, but in order to achieve deposition some element of heating from the laser is required.

Supersonic laser deposition is a low temperature thermal spray process. The use of a laser in the process introduces a local heat source as in LaserForge. Laser thermal forming is a process where a local laser beam is used to modify a substrate. In supersonic laser deposition the laser source is used to heat the local deposition site to aid with coating deposition. Further modification and forming of the surface are undesirable. For materials such as refractory materials that have a high melting temperature, a greater laser power is sometimes required for successful deposition, which begins to introduce side effects to the deposition process. Understanding these surface treatments along with LaserForge is therefore beneficial so that side effects can be mitigated in any potential solution to SLD.

As described above, some materials deposit with SLD more easily than others. To get some materials to deposit well extreme parameters may be required, such as very high laser temperature or very high critical velocity. One avenue of exploration considered here is the deposition of these materials with more regular deposition parameters to form a sub optimal coating, than can later be enhanced by an in or post deposition laser surface treatment to improve the coating properties. The problems of cold spray coatings that could be addressed with surface treatments are the adhesion at the interface, the residual stress in the coating, the consolidation of coatings that are not fully dense, and modification of the surface finish.

It is also important to understand existing laser surface treatments as in supersonic laser deposition the laser is used as a heat source, to soften the material during deposition. This introduces a thermal element of laser surface modification, such as seen in LaserForge that must be understood on its own before being combined with supersonic laser deposition.

The next sections will discuss a selection of laser surface treatments available to industry, to enable an understanding of potential similarities to the LaserForge process and improvements that can be made to metallic coatings. The use of lasers in surface treatments encompasses a large area, as such several areas have been selected for discussion as potential candidates for use in improving cold spray metal coatings. These are laser thermal forming, laser glazing, laser shock processing and laser welding.

2.4.1 Laser Thermal Forming

This section will describe the use of lasers for heating and bending of metals. Unlike traditional heating where the bulk of the material is thermally treated, lasers can target specific areas. The targeted approach enables minimal heat input and a greater control over the process to enable localised modification of microstructures. Traditional competing methods of heating include using a furnace, flame or induction coil.

Laser bending, a type of laser thermal forming, is the modification of sheet metal through the use of thermal stresses to control its shape [137]. There are two types of bend, out of plane bending and in plane bending. There are three main thermal mechanisms that have been identified for producing deformations with a laser. These are the thermal gradient mechanism, the buckling mechanism and the upsetting mechanism [138].

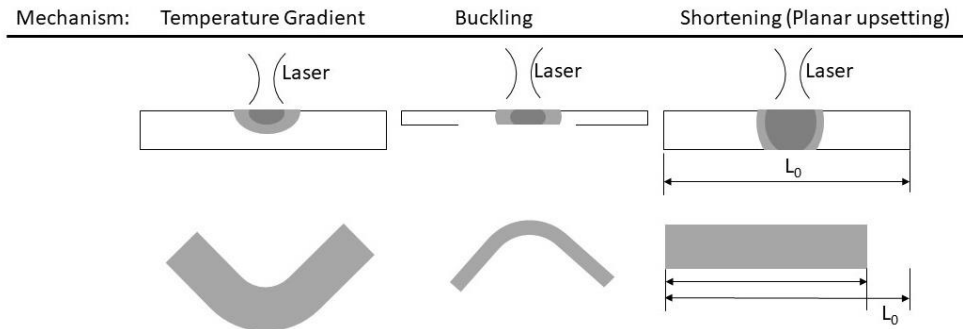


Figure 9: Diagram showing the three mechanisms for laser forming, the temperature gradient mechanism, the buckling mechanism and the upsetting mechanism. Based on fig 6.2 from [138].

Laser bending works by scanning a laser across a metal surface to induce a steep thermal gradient in the material. If the thickness of the thermal gradient produced in the material as the laser scans over it is small in comparison to the thickness of the workpiece, then the plastic deformation from plastic flow will not be recovered upon cooling and will be in tension in comparison to the surrounding material. Initially the heated material will expand, bending the workpiece slightly away from the laser, but upon cooling it contracts and pulls the surrounding material with it. This results in a final bend towards the laser.

If the thermal gradient passes through the thickness of the workpiece, the buckling mechanism is dominant. In this case a bulge is formed in the direction of initial stress in the sheet due to the expanding material. The centre bends plastically but the edges bend elastically. Upon cooling the bend is retained due to the plastic deformation [139].

The upsetting mechanism results in a shrinkage of the workpiece with a thicker section at the irradiated zone. This occurs when the surrounding material is constrained from bending. Plastic deformation occurs due to expansion upon heating. Upon cooling there is a shrinkage of the processed area in the plane of the sheet, inducing residual tensile stresses in the surrounding material [133].

Laser bending is done because it enables a cost-effective manner of producing highly accurate bends in an industrial setting, with a significant amount of flexibility in the process enabling components to be made that would be difficult or impossible to do on a conventional metal bending press [140].

The typical applications of metal bending are in the processing of thin metal sheets. Such techniques are often employed for use in ship building, microelectronics and automobile industries [139].

In principle any thickness of material can be bent, given enough time and appropriate heat source. One example of a study where a 0.5 mm thick sheet of 304 stainless steel was bent had parameters of 1.5 mm spot diameter, 2 ms pulse CO2 laser at 18 Hz, 4 mm/s scanning and energy from 1.4 to 10 J

or 0.7 to 5.6 kW to generate bending of 4 to 10 degrees [141]. In another study a 1.2 mm thick sheet of stainless steel was bent using 100 to 300 W from a focused diode laser, but using between two and six passes to generate bending on the same scale. These laser powers are not dissimilar from those used in supersonic laser deposition, but the effect of a given laser power on substrate bending is dependent on the thickness of the substrate [137].

When looking at thermal forming in relation to the supersonic laser deposition process which uses a multi kW high-energy laser to heat the surface of the workpiece, there are many similarities. Unlike thermal forming, the SLD process currently only considers the monitoring of the laser spot at the deposition site to keep it at a constant temperature. This can result in the whole workpiece heating up over time with thermal gradients across and through it as the laser scans over the surface. The workpiece geometry in relation to the heat input is not considered. The residual stresses that build up as the workpiece is heated and cooled at different rates during deposition has not been thoroughly investigated and is an area of investigation that should be treated to minimise the build-up of stresses that lead to cracking and delamination of coated surfaces.

2.4.2 Laser Glazing

Laser glazing involves the melting of a surface, while not imparting heat into the bulk of the material. It involves the scanning of a laser across a surface to induce a thin melt layer of about 25 to 100 microns. Because of the high cooling rates the surface layer can be made amorphous. Laser glazing helps to enhance the corrosion resistance and wear of the processed surface. Laser glazing has been shown to give a new surface morphology to existing sprayed porous coatings [25] [131]. As described above, the residual stress in laser glazing is likely to come from the temperature gradient mechanism.

Heating can be done in many ways with well-established existing technology, therefore the advantages of using a laser are key in these processes. Lasers provide a non-contact method of heating that can produce very high power densities, equivalent to temperatures of 20 000 °C [131]. The high thermal input along with minimal heating of surrounding areas enables a rapid process that can easily be integrated into workflows as no additional steps are required.

Disadvantages of the process are that in some applications a high degree of control of the heat input is required to control the residual stress. The high cooling rates in laser glazing and transformation hardening impart residual stresses in the surface of the workpiece, and as seen in laser bending these can cause bending of the substrate if it is thin enough or the stresses are large.

2.4.3 Laser Fusion

Laser fusion is a name given to a post processing of a coating using a CW or pulsed laser to anneal or remelt the thickness of the coating. Traditionally post-deposition heat treatment of thermally sprayed

coatings is done using a furnace or heat torch for annealing or remelting. These processes are inaccurate at delivering controlled targeted thermal input and therefore usually only used on simple geometries. A laser can provide a more controlled heating process than gas flame fusing enabling the technique to be used on temperature sensitive substrates, when a very narrow temperature range is required and on larger parts [142] [143]. Laser fusion can therefore target re melting of the metal matrix in a MMC while leaving the carbide reinforcement solid [144].

Deposited thermal spray coatings sometimes have higher than desired porosity or a rough finish, which is usually undesired. Laser fusion can remove surface roughness, seal coatings, decrease porosity and increase interface bonding. For example on flame spray and HVOF coatings it has been shown to produce a bond that has 10 times the original bond strength [142] [144].

Laser re-melted Ni coatings that include WC and Chromium have been successfully produced where carbide dissolution is undesired and needs to be minimised. This was done when using a CO₂ laser power of 2.5 kW, traverse speed of 500 mm/min, spot size of 3 mm, standoff 20 mm and 50 % overlapping passes. These gave a lower roughness appearance at the interface and decreased porosity [142]. These processes can also be used to improve the properties of the coating and reduce cracking at the surface from the deposition process to increase the coating lifetime [145], [146], [147]. At present the process has been shown to work for plasma and HVOF coatings, but not on cold spray coatings.

2.4.4 Laser Shock Processing

Having considered that there are residual stresses that exist in supersonic laser deposition coatings, one possible method of modifying residual stresses post-process is with the use of laser shock processing. Traditional peening also has similarities to the cold spray process. This section will describe the current situation surrounding shock processing of metals and the possibility to use this to modify residual stresses in a coating material.

Laser peening has appeared as an alternative to traditional shot peening that has been widely used for decades. Shot peening is used to introduce compressive residual stresses into the surface of a metal. This is used to improve fatigue performance and is commonly used in the aerospace industry. Depth of compressive stress of traditional shot peening is up to 0.25 mm in thickness for soft metals [148].

Laser shock processing is the process of using a high energy pulsed laser to introduce residual stress into a metal surface. This is done through enhancing the amplitude of stress waves and has enough energy to lead to plastic deformation in metals [149] [150] [151]. Laser shock waves are produced

using Q-switched lasers, which can produce pulses exceeding 100 joules with pulse lengths under 100 ns.

Originally target surfaces were processed in a vacuum, but nowadays an overlay can be used. An overlay such as water that is transparent to the laser, confines the expanding plasma that is produced from the laser material interaction. This directs more energy into the metal in the form of a high energy short duration pressure pulse. A sacrificial layer such as black paint can be used to increase the absorption of the laser energy [152]. When the shock pressure into the metal is greater than the dynamic yield of the metal, a transformation occurs in the surface changing its properties and microstructure. The plastic deformation that occurs during a shock reaches a depth defined as the point where the peak pressure is no longer greater than the metal's Hugoniot elastic limit [153] [148].

Residual compressive stresses in laser peening are caused by a stretching of a localised area due to the local plastic forming, resulting from the induced shockwave. These stretched areas are then under compression from the surrounding material once the initial pressure from the laser peening has dissipated [154].

Many of the applications of laser peening are to improve metal surface properties, control the growth of cracks and increase fatigue life and strength. Laser peening has been used in applications including brazed repairs, turbines and rotor blade components. The main pull for the technology is from the aerospace industry as it provides significant advantages over shot peening. It is expected that in future laser peening will progress into biomedical and other industrial applications [148].

The advantages of laser shock processing are that it provides a more consistent peening intensity than shot peening. In addition, the laser pulses can be monitored in real time, enabling poorly formed low energy pulses to be re-fired to ensure the desired specification of residual stress is met. Laser peening also enables a greater depth of residual stress modification than shot peening, and as the surface does not need to be removed a much greater final thickness of modified surface properties are available.

Disadvantages of laser peening are that it is only able to process a small area at a time, scaling up will require higher repetition rate lasers capable of producing higher energy pulses more rapidly.

Fundamental research into the material properties of peened metals is still ongoing. For example current research is investigating fatigue in laser peened samples, on full scale turbine blades [155] and modified material properties of peening on Nickel-200 [156]. There is also work looking at using regimes where confinement and sacrificial layers are not required, as these may not be suitable for the application. One solution to this is using femtosecond lasers, as has been demonstrated by Sano et al. on 2024 aluminium [157].

Research is also being done to investigate the thermal effect of laser peening both from a theoretical and experimental perspective. One interesting observation is that the temperature and exposure time of a material whilst undergoing laser peening affects the extent of residual stress relaxation, in part due to grain refinement [158]. It has also been shown that warm laser peened samples have improved fatigue life and it is expected that the thermal element in laser peening will be further investigated in future [159]. As technologies go there is still a significant lack of understanding within the research community for a technology that is being rapidly adopted by industry; Montross et al. are concerned that much of the fundamental research is hidden within individual companies and is buried within commercially sensitive industry-focused research [148].

The use of laser peening as a post-processing option in cold spray is an attractive proposition to alter existing residual stress and add surface work hardening. The cold spray process produces residual stresses, and being able to modify these with a laser peening process would be desirable [160]. Cold spray coatings have already been tested with mechanical shot peening and it was shown that residual stress modification and surface work hardening are possible to enhance the lifetime of the coating [160]. The understanding of laser peening on warm substrates, such as those produced in cold spray or supersonic laser deposition, is still at an early stage. The latest findings indicate that this is a potential area of interest, but combining this with the residual stresses in supersonic laser deposition which is itself already not fully understood yet may not be a good idea at present. As understanding in both SLD and warm laser peening matures this could be an ideal application for a combination of both technologies.

2.4.5 Laser Welding

Laser welding is the process that uses a laser as a heat source to join two metallic components together. It will be briefly discussed here as a potential additional step in cold spray. Laser welding also has similarities to laser cladding and LaserForge, techniques discussed earlier [7].

Welding can occur in two ways, keyhole welding or conduction welding. The type of welding is defined by the power densities used. The eventual shape of the weld defines its quality and as such it is important to understand the processes that create a weld [133].

In conduction welding the laser is used to heat the metal until it melts. The depth of the weld comes from the heat conducting down through the material from the surface. This can be achieved using a pulsed laser, with the pulse length used to control the interaction time for the heating and conduction into the material. Conduction welds are usually wide and shallow.

In keyhole welding the high-power density enables the material to vaporise. This means that a deep keyhole is made down from the surface into the material as the vaporised material expands outwards. The keyhole can be made with a CW or pulsed laser [161]. This keyhole can be continuously made as the laser is moved across the material. The weld is filled in behind the laser from the surrounding molten material. Keyhole welds are typically narrow and deep. Most joining welds are of the keyhole type.

The advantages of using a laser for welding are that it enables precise positioning and control of the energy input to the workpiece. This can result in minimal HAZ, minimal changes to the microstructure and therefore low thermal distortion. The process is also very flexible and possible to do on complex geometries.

The downside to laser welding is the initial capital required to set up the system. Additionally, some filler material may need to be used to replace vaporised or ejected material, which introduces complexity and cost to the operation.

Laser welding has many similarities to laser cladding. It has been proposed that laser welding could be used to solve some of the current problems with cold spray. Currently delamination is an issue with some coatings, and it is proposed that laser welding could be used to reinforce the joint between a bulk coating and substrate where there are large residual stresses present on the joint. As the cold spray joint is mechanical in nature, introducing a melt-based reinforcement at key locations could strengthen the overall workpiece without weakening the bulk of the material. This could be similar to a technique that uses friction stir welding to improve densification during plasma spraying [162]. In 1993 a patent was filed by General Electric Co to cover this idea of using a laser to post process a coating on a workpiece, such as a plasma sprayed TBC on a turbine blade [163].

2.5 Discussion of Literature Review Questions

This section will discuss the findings from the review of literature in the previous sections on thermal coatings and laser surface treatments, in relation to the review questions outlined at the start, the investigation of LaserForge and the Cold Spray process. Each section below will discuss the five research questions, stated at the start of the chapter that guided the review of literature.

2.5.1 What is LaserForge and how does it relate to other coating deposition techniques?

LaserForge is a commercial process that uses high-energy pulsed lasers to bond coating material onto a substrate. Public literature is limited for this process and most understanding is based on patent literature and the prior visual physical sample analysis. As much of the development of the

process has been done in partnership with the military, it is understandable that there are limited explanations of the process mechanism.

The LaserForge process has some similarities to the SLD process, in that it uses a high energy laser to deposit a coating on a substrate. It claims to be a solid-state process and as such many be used for coating similar materials to SLD. The process deforms the interface into a waved shaped interface to improve bond strength. As the process uses a high energy laser, like SLD, an understanding of the LaserForge process would be beneficial to understanding how to improve the SLD process.

The process has similarities to laser cladding and laser shock processing. It appears that the high energy pulsed laser is used as an energy source to soften the coating material, making it more deformable. A laser shock mechanism is used to deform the coating material into the substrate. Due to the lack of understanding of the exact mechanism for this process, investigating this will be the initial focus of this work.

2.5.2 What are the advantages of using cold spray compared to other similar industrial surface coating treatments such as wire arc and HVOF?

The cold spray coating technique has been described above. It is classified as a kinetic thermal spray process that uses a gas to accelerate particles towards a substrate at high velocity. Cold Spray has only been commercially available for about 20 years, and as such is a relatively young coating technology. Literature identified cold spray as being less developed than other coating techniques such as competing thermal spray techniques like wire arc and HVOF. These alternative technologies have been around for longer and received substantial investment and development over the past 50 years, cold spray has received significantly less industry adoption and development.

Each of the thermal coating technologies discussed was shown to have its advantages and uses. Most of the technologies are now widely used in industrial applications and accepted as mature technologies. The cold spray process has been established as a valid coating technology in industry and has been approved for use in coatings and repairs as a Department of Defence (DoD) manufacturing standard.

The traditional thermal spray technologies such as plasma spray and HVOF are already well established and not in need of replacement. They are however reaching their limits of capability in certain areas such as for nanostructured coatings. Cold spray technology is not being considered a replacement for the existing thermal spray technologies. Cold spray is rather viewed as an alternative technology that provides the capability to expand the range of applications of thermal spray processes, enabling new possibilities in coating, especially in new applications where limitations of

current thermal spray prevent them being used. With so much existing investment in tradition technologies, cold spray is facing an uphill struggle to become accepted. It can be considered from an economical perspective, as reducing manufacturing steps and cost, or from a novel application perspective where it enables the use of new coatings using advance materials.

In literature it has been generally accepted that this kinetic based, solid state coating technique can produce fully dense coatings. Good coatings have been shown to be equivalent to bulk material in some cases and the bonding mechanism is better understood than it was 10 years ago.

The key advantages of cold spray over existing thermal spray processes are in its low temperature solid state deposition of materials. One of cold spray's advantages is that it is capable of depositing materials that are temperature sensitive. The low deposition temperature also means that coatings can be deposited on temperature sensitive substrates. The solid-state nature of the deposition means that it is possible to deposit a coating with a designer microstructure, such as nanostructured coatings.

Cold spray is the least understood thermal spray process and has many unknowns that are limiting its adoption. Much of the current research into cold spray is being done at research institutions such as universities and the military. It is currently used in industry mainly for remanufacturing of unique low volume components as a method of cost saving, or where a low temperature process is required.

Future trends in thermal spray coatings are working towards deposition of nanostructured coatings, and cold spray is an ideal candidate to deposit them. The key areas for cold spray development are in nanostructured coatings such as WC-Co cermet, oxygen sensitive materials such as stainless steel that require an expensive vacuum environment for some applications, where a low deposition temperature is required such as for biocompatible materials like HAP and where temperature sensitive substrates are used [92] [164].

2.5.3 What defines if a cold spray and supersonic laser deposition coating can be deposited successfully, and what are its issues?

A successful coating can be defined as having low porosity (<5 %) and good adhesion (>50 MPa); the exact values will depend on the required application. The deposited coating must also have the desired coating and bulk properties, such as low friction. In cold spray the bulk properties are governed by the powder that is used, more than the deposition parameters, as the powder is not melted as in flame spray or HVOF.

The first aspect of a successful coating is good bonding between the substrate and the coating. The bonding mechanism explained earlier in the chapter describes the necessary deformation of the coating particles and thin layer of the substrate at a particle level. The mechanical deformation leads

to mechanical interlocking through conformal contact and high pressures. A requirement for good adhesion is therefore a coating and substrate that are capable of small deformations and the incoming particle having enough kinetic energy to initiate the deformations required for adhesion between the coating and substrate. For the case of supersonic laser deposition thermal energy is used to soften the lower layer to reduce the required kinetic energy to achieve bonding.

The second aspect of a successful coating is the building up of a dense bulk of coating material. This can be impacted by the particle feed rate, particle size and particle geometry. The second and subsequent layers are different to the first layer as the effective substrate material has changed, which may require different deposition parameters.

The geometry of the workpiece also determines whether a coating can be successfully deposited. Cold spray requires that the deposition nozzle be close to 90 degrees to the substrate. With complex geometries it may not be possible to meet this requirement, and hence a coating may not be possible.

For two materials to bond well with cold spray it is believed that there is a requirement for there to be an interfacial jet composed of both materials (coating and substrate) during particle impact. The minimum critical velocity for the incoming particles is required for this condition to be met. It is believed that the dominant factor to increase the strength of the bonding is the higher the contact pressure and better formation of the interfacial jets which may lead to mechanical interlocking over the length of the particle.

Materials that deposit well with cold spray are those that have a low melting points, low mechanical strength and low modulus of compression values. These materials such as copper, zinc and aluminium deform easily on impact. In contrast dense coatings are difficult to achieve for materials such as 316L that have been strained hardened. Materials such as Ti-64 change their strain hardening with temperature, and as such results in coating with cracks and high porosity at low temperatures [91]. As a general trend materials that have a high melting temperature, are resistant to deformation or are a body centered cubic Structure (bcc) metal, do not deposit or require unusual deposition parameters such as higher velocity or temperature.

Based on the current literature there is a lack of full understanding of the relationship between deposition parameters and coating quality. Although some effort has been made to model cold spray and predict required deposition conditions, no single model can predict material compatibility in cold spray and supersonic laser deposition. For example, spraying A on B does not indicate that B on A uses the same parameters or is even possible. Much of the existing research is experimentally based and requires trial and error. There is significant variability in the success of cold spraying a material as it

depends on spray parameters, powder geometry and production method, thermal effects and substrate surface preparation.

The main disadvantages to cold spray can be split into two areas. The first is to do with the understanding for the process and determining process parameters. Due to a lack of process understanding it is very hard to transfer processing parameters between systems and therefore scale the process across the industry. A lack of in process monitoring means their increased need for destructive testing of deposited coatings.

The second area of disadvantages is in the cost of the system. The initial cost of setup is high and processing gas costs mean if helium is used a gas recycling system is necessary. This means that the process is best suited to high value manufacturing.

There is some adoption of cold spray in industry but most of the systems are still used for research and not mass-market manufacturing. The main reason for their lower level of development is their relative newness into the established coatings industry. Any new technique requires time to be researched and mature. There is always a barrier to bringing new technologies into industry as it requires change. Unproven technologies have a high risk and are therefore less likely to be adopted over established techniques, unless they have key advantages. There is also the effect that technologies that have been already accepted will undergo more rapid development as it is commercially advantageous to do so, and there is more likely to be funding and pull from industry for gains and process optimisations.

2.5.4 Is cold spray a suitable technology for depositing advanced materials such as nickel-based alloys, WC-Co and HAP (Bio-Coating) for novel applications?

The key direction of development of cold spray-based technology is in applications, where existing thermal spray technologies have significant drawbacks or cannot be used. One key area where cold spray has an advantage is in deposition of advanced materials such as cermets, nanostructured coatings and temperature sensitive materials. Cold spray is suitable of depositing these materials as it is a low temperature technology and does not melt the feedstock. It can therefore retain the nanostructure and properties of the powder feedstock in the deposited coating.

Cold spray is thus the leading thermal spray candidate for depositing coatings that are made of mixed elements, and where low temperature is key to preventing the coating or substrate from changing due to a high temperature thermal deposition environment.

With supersonic laser deposition an additional thermal source is introduced. This thermal source can be controlled to ensure that the coating and substrate do not melt, however this may be at the impact

of reduced coating adhesion. Further testing on individual material combinations would be required to determine the impact of additional laser heating.

From a materials perspective, many established techniques are now looking at high performance materials for applications such as corrosion protection, hard facing or self-lubricating low friction coatings. These materials are, however, hard to work with and require a greater understanding of the deposition processes to successfully deposit them. One problem is that these materials are harder and more brittle. They are therefore deposited in a binder matrix, for example WC in a cobalt matrix. This is a combination of materials with different melting points and properties. Techniques that require melting need to ensure that the deposited coating has the required characteristics of both materials, which is harder than controlling the microstructure for a single material. Kinetic processes such as cold spray that do not melt the material have an advantage in that the desired material properties can be imparted in the powder prior to spraying. The downside is that there is not enough volume in the industry to manufacture large amounts of custom powder for cold spray applications.

2.5.5 What new laser-based processes are there to modify and improve coating quality and performance?

As discussed, some materials are harder to deposit than others. Such materials may require extreme parameters to deposit well. As an alternative to using extreme parameters for deposition, more regular parameters could be used in combination with a second laser-based process to improve the coating adhesion and density. Three potential techniques were identified to fulfil this idea.

The review above discussed three areas for laser surface processing, namely laser thermal forming, laser shock processing and laser welding. These each have their own advantages and uses to modify a coating. Laser shock processing could be used to modify any residual stresses in a coating, whereas laser thermal forming could be used to change the shape of a coated sample.

Laser cladding could be investigated for use in combination with supersonic laser deposition as a method of coating, where melting is an option. The cold spray nozzle could be used to feed the powder while the laser melts it and enables it to adhere. This could improve the interface bond strength as a mechanical bond could be formed between dissimilar materials with minimal interface mixing, with melting only required to give a fully dense bulk coating above the initial interface bonding layer. Controlling the path and integrity of the molten particles would require greater control of the gas jet.

As discussed in the first question, LaserForge is a technology of interest that is the initial focus of this work, it claims to be a solid-state coating process, which could be more compatible with supersonic laser deposition. It was developed in combination with the US DOD. This process uses preplaced wires and a high energy pulsed laser to deform the coating into the substrate, to give increased surface area

at the interface. LaserForge is a proprietary technology that is not widely used. This technology's benefits are very similar to those of cold spray, such as its use in deposition of dissimilar materials and repair of components. Unfortunately, this technology is not well documented in literature and a desire to gain an understanding of the process is one of the motivations for this work. As the technology uses a high energy pulsed laser to bond the coatings, it is of interest to supersonic laser deposition and therefore understanding the deposition mechanism used in the process could aid the design of an improved method of bonding in supersonic laser deposition.

2.6 Conclusions and Research Objectives

This chapter has presented a review of literature based on the review questions outlined at the start of this chapter and discussed in the previous section. This section will outline the identified gaps in literature and define the research objectives.

The main motivation for this project is to investigate the LaserForge process. The literature review identified that the process is a commercial process developed in partnership with the DoD, however most of the knowledge about the process comes from patent literature. Performing an investigation into LaserForge is therefore going to increase the knowledge of this process and highlight understanding and mechanisms that could be beneficial to the SLD process. The process also has similarities to laser shock processing and laser cladding.

It is therefore proposed in this work that the LaserForge process be investigated experimentally to understand how the bonding mechanism could be beneficial to the supersonic laser deposition process. The other two similar processes, laser shock processing and laser cladding, are also not easily explored experimentally in the current laboratory due to lack of availability of required equipment.

From the review of thermal spray processes, it was clear that cold spray was less developed than other thermal spray processes. There appeared to be a lack of literature able to explain the required parameters necessary to deposit a given material. Two approaches had been taken to understanding the deposition process, a theoretical modelling approach and an experimental approach. The experimental aspect has been to deposit materials using trial and error to optimise parameters and understand what works. Much of the work uses post deposition analysis of the deposited coating. There was a lack of literature for in process monitoring of the process to understand the deposition mechanisms. The theoretical analysis studies have tried to understand what properties of the materials makes them suitable for deposition and what the key physical properties are that affect the deposition quality. At present there is no unified theory that can explain all aspects of the deposition, but most studies have been able to explain the key deposition parameters and requirements to first order.

Supersonic laser deposition introduces an additional thermal element into the mixture. There is again less material on this than cold spray alone, but the target of supersonic laser deposition is split between experimental studies that look at finding optimal deposition parameters and proof of concepts, and theoretical studies that try and understand the thermal effects of adding a laser into the process.

Literature has demonstrated cold spray is a proven and capable technology that can be used to deposit metallic coatings. Supersonic laser deposition has also been demonstrated to be viable, however it is much less developed and requires further experimental and theoretical investigation. Literature points to the key areas for development and growth in cold spray as nanostructured coatings, as it can deposit materials without re-melting, and thermally sensitive coatings and substrates, as its deposition temperature is lower than competing technologies. In supersonic laser deposition the key issues identified in literature that need greater understanding are the thermal effects on the deposition due to the laser. For both cold spray and supersonic laser deposition the parameters for deposition are still considered system dependent and therefore any study of this technology will require some understanding of the effect of different parameters on the coatings.

It is proposed in this study of SLD that nanostructured coatings are investigated further as there is significant benefit to the academic community in gaining further understanding of how they can successfully be deposited with the cold-spray and supersonic laser deposition process. This would align with the future direction of cold spray research and its benefits to industry when compared to existing traditional thermal spray processes.

Following the discussion of literature, clear research objectives and questions to guide the research can be specified. Based on the motivation previously discussed, the main aim will be to understand the LaserForge process. The second aim will be to better understand the failings of the SLD process so that improvements can be correctly targeted. The objectives and questions were defined as follows:

Objective 1: What is the process mechanism used in LaserForge and could the understanding of this be used to resolve deposition issues in supersonic laser deposition coatings?

- **Q1:** What mechanism is used to bond LaserForge coatings?
- **Q2:** Is such a mechanism feasible for use to improve SLD?

Objective 2: What is the relationship between supersonic laser deposition conditions and the coating quality of a nanostructured coating?

- **Q1:** How do nanostructured coatings respond differently from traditional materials such as copper and aluminium in the SLD deposition process?
- **Q2:** What are the limiting factors to successfully depositing nanostructured coatings?
- **Q3:** Quantitatively how are coatings failing and what is contributing to coating failure in SLD nanostructured coatings?

These research objectives and questions will be refined and investigated throughout this work in subsequent chapters.

3 Chapter 3 – Materials and Methods

This chapter will describe the materials and experimental methods used in subsequent sections.

3.1 Bulk Materials

This section will detail the bulk materials used for experiments and why they were chosen for their purpose.

3.1.1 Titanium 6-4

Titanium is a commonly used material in industry. The 6Al-4V alloy is the most commonly used form of titanium in manufacturing. It is used because it is lightweight and strong for its weight. It has a melting point of 1677 °C and has good corrosion resistance due to a thin oxide layer that forms on its surface. This material was identified as having some issues when deposited using the SLD process, and therefore would benefit from enhancement post deposition. It was thus selected as a good candidate material to investigate in combination with LaserForge.

The sheet titanium used for experiments was sourced from Goodfellow, Cambridge. The manufactures specifications for the material used were as follows:

- Ti90/Al 6/V
- Thickness 0.52 mm
- Temper: Annealed
- Typical Analysis : (ppm) Al 6%, Fe 300, V 4%, C 220, H 100, N 100, O 650, Ti balance.

The material was used as received, using only ethanol to remove any grease build up prior to use. Any additional preparation is detailed in the relevant experimental section.

3.1.2 Aluminium

Aluminium alloys are commonly used in aerospace manufacturing. Aluminium alloys are lightweight and have good corrosion resistance.

Commercially pure aluminium (> 99 % aluminium content) was selected for use in this project based on its softness. A soft material was chosen as it was used for experiments where the previously mentioned Ti64 was deformed into it, and it therefore needed to deform easily. The aluminium used in this study was aluminium sheet of thickness 0.8 mm.

3.1.3 Steel

The standard substrate used in these experiments was black ungraded flat mild steel. For the steel bars a grade of S275JR was quoted by the supplier. The steel was 5 mm in thickness. The material was supplied from Mackay, Cambridge and had a dark oxide coating on arrival. The material was washed

in soap and water followed by ethanol to remove grease and other contaminants. It was then prepared as described in the experimental method section prior to being used. This substrate was chosen as it is a common material for tooling and used extensively in industry.

3.1.4 Inconel

Inconel is an austenite nickel-chromium based super alloy. The Inconel series of super alloys are widely used in demanding industrial applications as they provide good resistance to corrosion and oxidation. They also retain their high strength over a large temperature range. Typical applications include use in turbine blades and boilers.

There are over 20 types of Inconel that are made up of varying compositions. An example is Inconel 625 which is often used in aerospace applications. The composition of Inconel 625 is given in Table 2.

Table 2: Inconel 625 composition [165].

Chemical Composition Limits													
Weight %	Ni	Cr	Mo	Nb + Ta	Fe	Ti	C	Mn	Si	S	P	Al	Co
Alloy 625	58.0 min	20 - 23	8 - 10	3.15 - 4.15	5.0 max	0.40 max	0.10 max	0.50 max	0.50 max	0.15 max	0.15 max	0.40 max	1.0 max

3.2 Powder Materials

This section describes the spray powder used in the supersonic laser deposition process.

3.2.1 WC-Co Spray Powder

The spray powder used for the supersonic laser deposition coatings was a WC-17Co Inframat Infralloy™ S7400 Series powder. This powder was supplied from Inframat materials, USA. This powder is designed for wear, erosion and corrosion resistance. The manufacturer specifications for the superfine powder were as follows:

- WC : Co wt. ratio, 83 : 17
- Powder grain size, 50 to 500 nm
- Agglomerated powder size, $15 < \Phi < 45 \mu\text{m}$

When viewed under a SEM the powder shows an agglomerated spherical geometry. Each of the agglomerated spheres is made up of smaller grains of WC and Co. These superfine grains are what make this powder nanostructured.

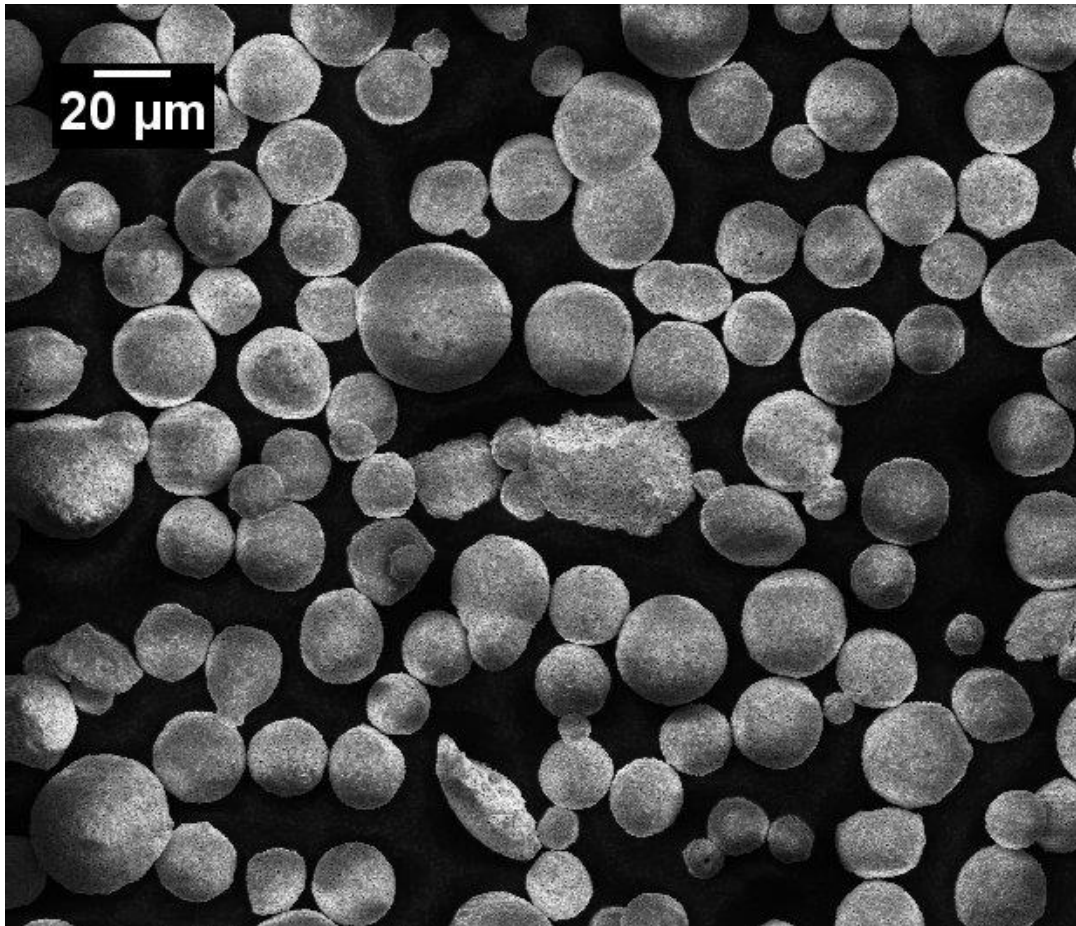


Figure 10: SEM image of an agglomerated spheres of powder containing particles of WC and Co.

A nanostructured powder was used for coating due to the enhanced tribological properties it exhibits when deposited with the supersonic laser deposition process [166]. As the supersonic laser deposition process is a non-melt-based process, these nanostructured coatings benefit from not being recrystallized as in traditional thermal spray techniques.

The advantages of a nanostructured WC-Co powder is that it has a smaller grain size giving improved mechanical properties such as hardness and strength [167] [168]. This is supported by previous work that compared the performance of a Stellite coating deposited using SLD and laser sintering. It concluded that the non-melt based SLD process retained the nanostructured properties and produced a lower coefficient of friction from the same powder [169]. A direct study of the benefits of the nanostructured WC-Co powder over a traditional cermet showed that in almost all cases the nanostructured coating has better properties than the cermet [170].

A second standard thermal spray powder also from Inframat materials, USA was used for some tests. The standard powder had the same product code but was described as standard with an agglomerated powder size of $15 < \Phi < 55 \mu\text{m}$. More details about the differences in these powders are presented in the results chapters.

3.2.2 316L Spray Powder

A 316L spray powder was used for some tests. It was selected as it is a commonly used material that is known to deposit well with the existing supersonic laser deposition system.

The powder was sourced from Osprey. The 316L powder particle size distribution used was measured using a mastersizer 3000, Figure 11. This was done as the manufacturer did not quote a lower bound for the size distribution.

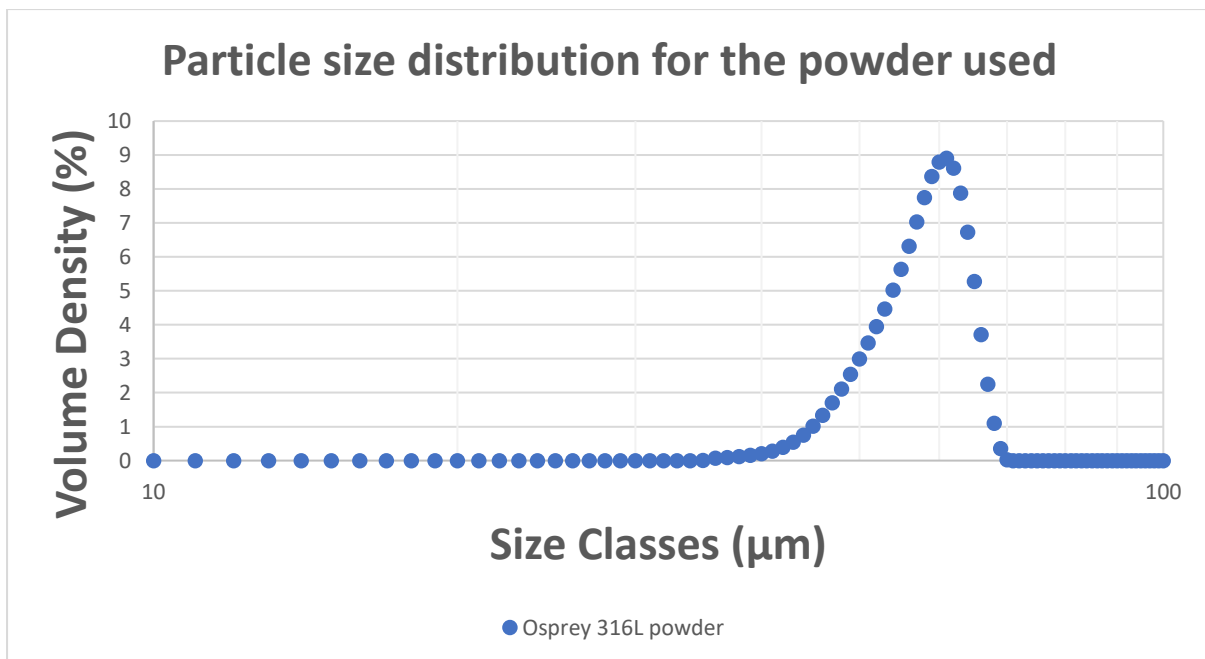


Figure 11: Particle size distribution for Osprey 316L powder.

3.3 Experimental Methods

This section will detail the standard methods and equipment used to obtain the results in this study. Any parameter changes or significant deviations from the methods described here will be described in the relevant results section. The following sections are presented in the order that they are used in the following chapters.

3.3.1 Optical Microscopy

For optical study of samples an Olympus BX51 microscope was used. This microscope is capable of optical magnification up to 100x. A dimmable light source was used to illuminate the sample through the microscope.

The microscope was capable of light field and dark field. Light field enabled white light observation of the sample. Dark field enabled the surface relief to be observed more clearly.

Images from the microscope were captured using a ProgRes C10 plus camera mounted on the microscope. This was controlled using dedicated computer software (A4I Docu). The software enabled stitching of images to create larger images covering larger regions than would be possible in a single frame. Measurements of the obtained images was also possible.

To obtain images, samples were placed under the objective and, the lighting level and focus were adjusted to optimise the image.

3.3.2 SEM Imaging

To obtain higher magnification images than an optical microscope, a scanning electron microscope (SEM) was used. A SEM uses beam of charged electrons to generate backscattered electrons, which are detected and used to build up a picture of the surface.

The system used was a Zeiss Crossbeam 1540 XB. This system is also capable of focused ion beam imaging (FIB), although this capability was not used for this work. An Oxford instruments X-Max EDS system was used for determining elemental composition.

To image samples in this system, they were mounted on a conductive substrate and inserted into the main chamber through the secondary vacuum chamber. An acceleration voltage of 5kV was used to obtain good images of coated surfaces.

3.3.3 Laser Processing System for LaserForge

A laser processing system was set up to investigate LaserForge. The full details of the equipment and specifications are detailed in the LaserForge results chapter.

3.3.4 Material Preparation

To prepare material for its desired use, it was sometimes necessary to cut, mount and polish it. This section will describe the standard procedures used.

Cutting was done using a Struers Secotom-10 cutter. A cooling lubricant of water and manufacturer additive was used for all cutting.

For sample mounting an Opal 400 hot mounting press was used. If the sample was to be used in an SEM a conductive mounting resin (Conducto-Mount) was used, otherwise a none conductive resin (BAKELITE) was used. The sample was placed on the mounting bed with the use of a plastic support if required. The resin was added, and the press closed and started. A pressure of 3 was set on the dial with a heating time of 14 minutes and a heating temperature of 200°C. The hydraulic mounter then completed the mounting operation automatically.

The polishing process was done using a Saphir 550 polisher. The machine consists of a rotating head and rotating table. The magnetic rotating table enables the desired abrasive disc to be attached magnetically. The sample is pressed against this abrasive disc along with a lubricant and/or a polishing solution to polish the sample surface. The disc and parameters are dependent on the material and desired finish.

The standard parameters used to polish WC-17Co cross sections were:

- 220 MD-plano, water lubricant, until smooth.
- 1200 MD-plano, water lubricant, 25N, 250 RPM 2 minutes
- Abracloth, 9µm diamond solution, 25N, 250 RPM, 8 minutes
- Planocloth, 1µm diamond solution, 25N, 100 RPM, 4 minutes
- Chemicloth, 0.04µm opus solution, 15N, 80 RPM, 4 minutes

In some cases, steps were repeated multiple times until the desired surface finish was achieved.

3.3.5 Etching

For cross sections that required etching a chemical etching was done. Once a sample was prepared, it was etched in a fume cupboard. Appropriate PPE was used depending on the etching solution used. The method used to etch all the samples was the swab method.

To etch a sample with the swab method, a small amount of the etching solution was placed in a beaker. The mounted sample was also placed in the beaker with the sample facing upwards. A small amount of cotton wool was used to soak up the etching solution and was placed on the sample and held using tweezers. The cotton wool was moved around on the sample but ensuring that it remained in contact

with the sample. A timer was used to time the swabbing. Once the elapsed time was up, the sample was removed from the swabbing beaker and immersed in a beaker of neutralising solution.

The sample was then rinsed under running cold water, deionised water and then ethanol. A hair drier was then used to dry the sample surface to avoid a residue forming. The sample was then looked at under an optical microscope to ensure the etching was successful.

Four key standard etchants were used. The composition of each of the etchants is detailed below.

Kalling's No. 2

Good for stainless steel and Ni-Cu alloys.

- CuCl_2 , 5 g
- Hydrochloric acid, 100 ml
- Ethanol, 100 ml

Kellers etch

Good for aluminium and titanium alloys.

- Distilled water, 190 ml
- Nitric acid, 5 ml
- Hydrochloric acid, 3 ml
- Hydrofluoric acid, 2 ml

Krolls reagent

Good for titanium alloys.

- Distilled water, 92 ml
- Nitric acid, 6 ml
- Hydrofluoric acid, 2 ml

Note: Stored in plastic bottle.

Ralp's etchant

Good for stainless steel and nickel-based alloys.

- Distilled water, 100 ml
- Methyl alcohol, 200 ml
- HCL, 5 ml
- CuCl_2 , 2 g
- FeCl_2 , 7 g

- Nitric acid, 5 ml

3.3.6 Hardness Testing

Samples that were tested for Vickers hardness were tested using a Mitutoyo HV-112 hardness tester. This system was set up in a room with minimal air disturbance. Prior to testing the system was calibrated using a standard sample.

To perform the testing a weight was selected. The weight used for testing titanium was 1KG. Initially the sample was brought into focus and the two black lines in the eyepiece were brought together by turning a dial to indicate a zero distance between them. The measuring system was then zeroed.

The sample was then loaded automatically for 15 seconds and the imprint of a diamond was left on the sample surface. The dimensions in both the x and y direction were measured using the black lines in the eyepiece and the hardness was calculated by the tester from this.

3.3.7 LaserForge Sample Mounting

As outlined in literature, a good contact between the coating and substrate is required to reduce the energy requirements of the laser. To ensure good contact the sample was held in a curved mount, Figure 12. The 2 mm thick base was formed into a bent shape, and the flat coating and substrate placed on this were forced into contact with each other on the curved surface when clamped down. A coating of 0.5 mm thick Ti-64 was used as it was outlined as the material that was successfully used in the patent.

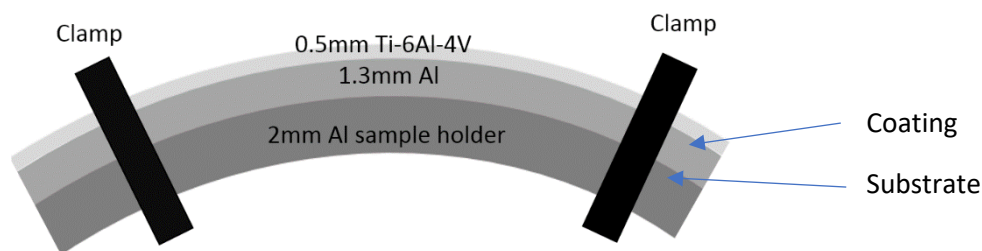


Figure 12: Diagram of the mount used to hold the sample under the laser.

The samples were processed in an argon chamber to reduce the oxygen content whilst processing, Figure 13. Some experiments used an argon shield gas during processing.



Figure 13: Processing chamber with argon gas feed.

3.3.8 Supersonic Laser Deposition (SLD)

This section will describe the components of the supersonic laser deposition system and the process for setting up and spraying a coating.

The supersonic laser deposition system is made up of several key components. A chamber that contains the cold spray nozzle, the laser head, a pyrometer and a CNC stage that moves the substrate. Separate to the chamber is a powder feeder, a manifold cylinder pallet (MCP) of nitrogen, a gas heater and a fibre laser. A diagram of the system layout and details of each key component of the system are shown in Figure 14 and Table 3. A photograph of the processing chamber is included in the appendix for reference.

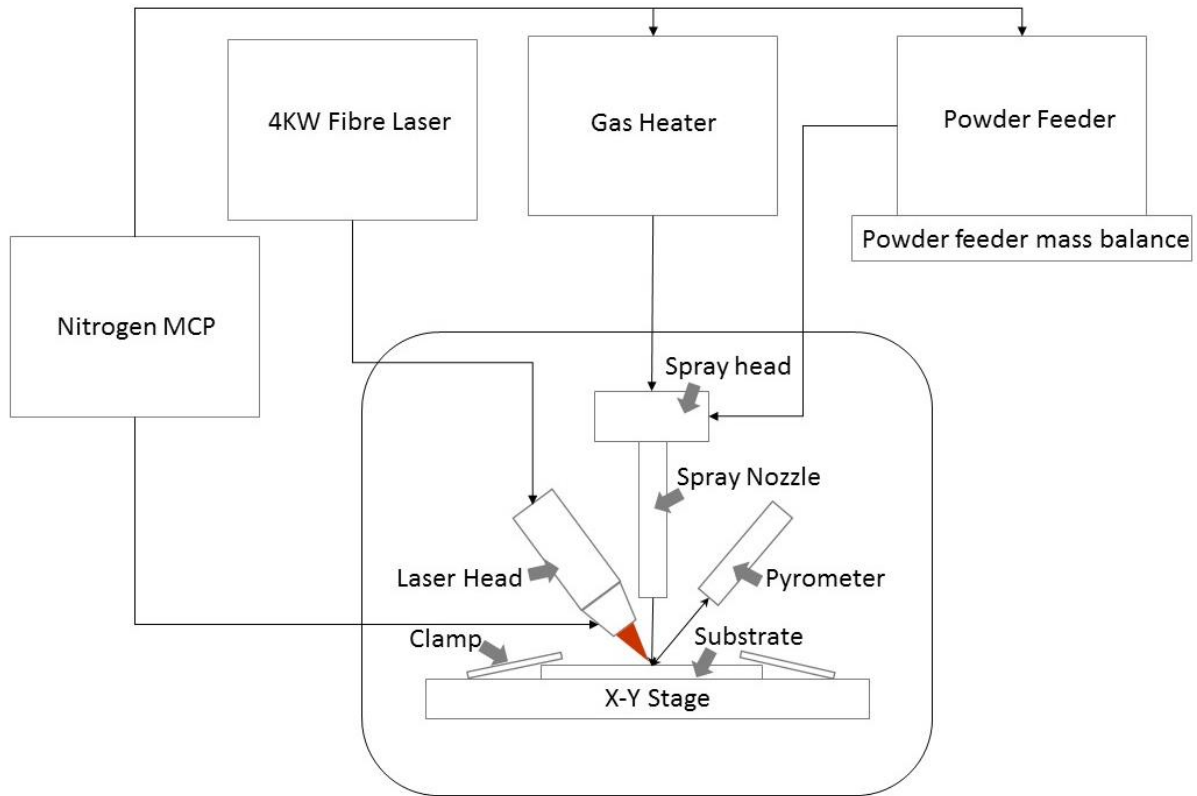


Figure 14: Diagram showing the key components of the supersonic laser deposition process. The components in the central rectangle are in an enclosed processing chamber.

Table 3: Table detailing the key components of the supersonic laser deposition system.

Component	Manufacturer	Model
Laser	IPG	YLS-4000
Laser head and optic	Precitec	120 mm head with optic
Cold spray nozzle	Custom	Custom
CNC stage	Aerotech	Pro 115
Powder feeder	PraxAir Surface Technology	1264
Gas heater	Linspray	Kinetic 3000 cold spray system

3.3.8.1 Setup

Setup for spraying requires loading the desired powder into the powder feeder and mounting the substrate to be sprayed into the chamber.

Powder is preheated to about 50 °C in advance to remove moisture from the fine powder ensuring it flows correctly into the system. The powder is placed in the heated cylindrical feeder and sealed.

The substrate to be sprayed is clamped down on the CNC stage under the nozzle. The substrate is positioned so that its top surface is flat with respect to the nozzle to ensure a constant working distance. The flatness of the clamped substrate was checked using a spirit level. The nozzle was positioned 40 mm above the substrate, as this has been found from previous work to give the best

results with this system. For a cylindrical sample, a rotary axis was attached to the surface of the CNC and the sample clamped securely in the rotary head.

Prior to spraying, the alignment of the cold spray head, the laser spot and the pyrometer were checked. For the experiments, unless otherwise stated, the laser spot was positioned in the centre of the cold spray deposition spot. The pyrometer was aligned with the centre of the laser spot to monitor the laser spot temperature, Figure 15.

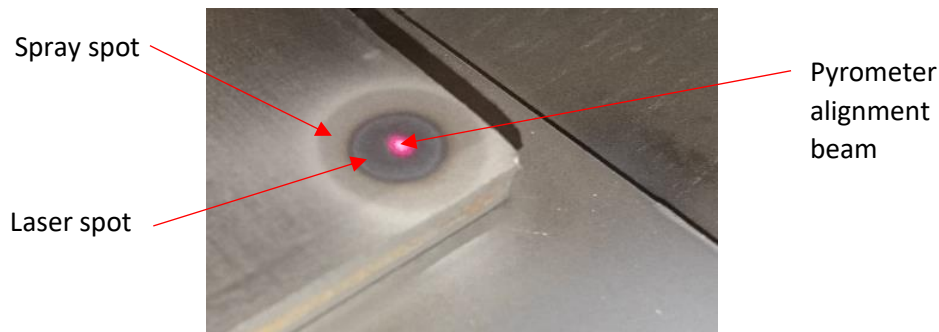


Figure 15: Image of the spray nozzle spot, laser spot and pyrometer spot (red) during alignment of the system.

3.3.8.2 Spraying

The spraying procedure is controlled from the operator workstation in the same room as the chamber. The movement of the sample and experimental parameters during spraying are programmed in to the computer in advance.

The first step of the spraying was to increase the gas pressure through the nozzle to 30 bar. The gas was then heated using the gas heater until the head reached 500 °C. Once the head had reached the desired temperature the powder feeder was enabled, releasing the powder into the gas flow. The pre-programmed movement of the substrate under the nozzle and laser was then run, Figure 16. Following the spraying, the powder feeder was stopped, and the system was left to cool down with the aid of the gas flow. Once the system had cooled the sample was removed from the chamber. With some rotary samples, the sample was swapped whilst the heated gas flow was still on. This was because only one sample can be mounted in the rotary stage at a time.

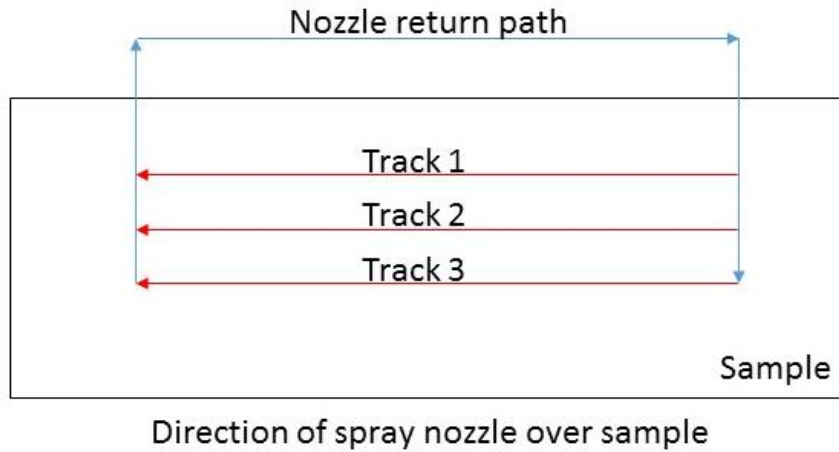


Figure 16: Example of a spraying pattern for three tracks on a flat substrate. The spraying occurs in one direction only and therefore the nozzle is returned to the start of the next track off the sample.

The track profile after spraying is “hill shaped”, Figure 17. Due to the deposition method of deposited particles compressing the lower layers, there is a thin layer on the top of each track that is sometimes machined away to reveal the bulk.

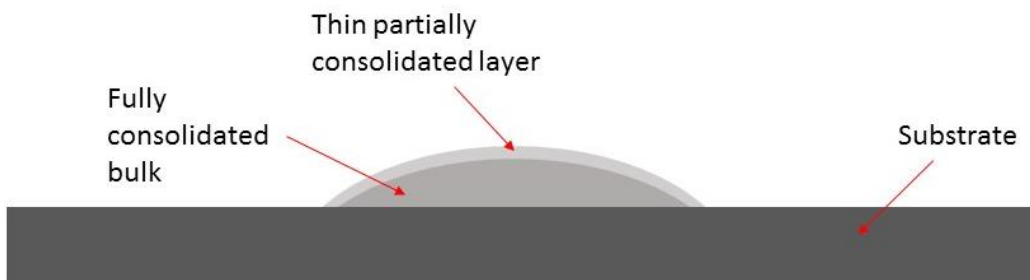


Figure 17: Diagram of the cross section of a sprayed track. The track is hill shaped and consists of the main bulk of the track bonded to the substrate with a thin partially consolidated layer on the top.

3.3.9 Pull-Off Testing

A DFD P.A.T. GM01 with a 6.3kN testing head was used to test the adhesion of coatings. This system can be used with different sizes of test elements. Test elements with the smallest surface area were used as the coating was expected to be at the limit of the tester, this means that the greatest force per unit area could be imparted on the coating. A circular test element with a diameter of 8.16 mm and surface area of 0.52 cm² was used.

The test elements were glued to the coating with the use of DFD E1100S Epoxy, this epoxy has a minimum rated tensile strength of 70 MPa according to the manufacturer. The epoxy was applied to a roughened surface, roughened using 180 SiC paper on both the test element and the coating, and

was cured in a furnace at 150 °C for at least 1.5 hours until the epoxy had hardened. The test elements were drilled around using a core drill to separate the glued coating from the surrounding material. This was to ensure the pull-off test was not influenced by surrounding coating material. Drilling was found to generate significant heat in the sample, to alleviate this the sample was immersed in cooling oil (Rhenus Nor SSL) during drilling to dissipate heat.

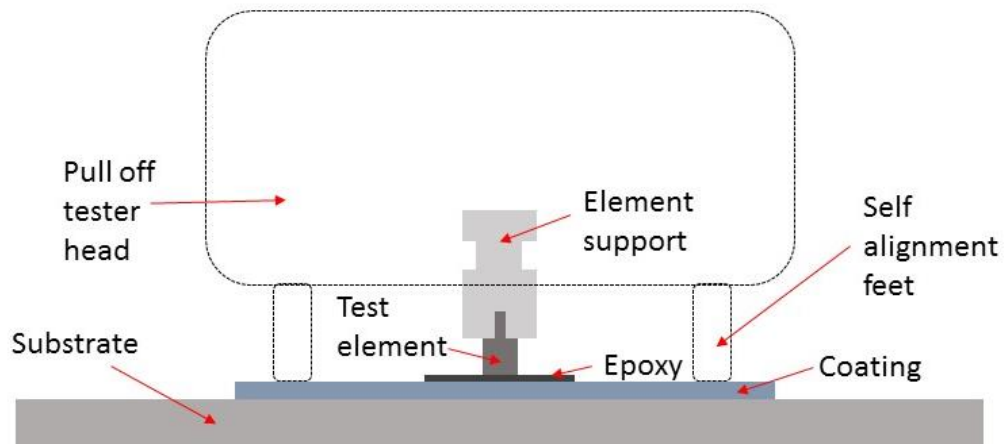


Figure 18: Diagram of the pull off testing setup.

The pull off test was performed by attaching the tester head to the test element support, Figure 18. The pressure was increased on the legs using the hand pump until they were comfortably on the substrate. The pull off was then done using one swift motion of the hand pump, at which point either the coating or glue failed.

The failure point was recorded on the dial gauge, with a red needle that was pushed around to the maximum value. This recorded value could then be converted into a tensile strength in MPa.

3.3.10 Bar Deflection Measurement

Samples were noted to have distorted during spraying. To measure this, samples were measured to determine their bend profile after being coated. The procedure for measuring this used a dial displacement gauge mounted on a CNC axis. The sample was placed on a flat surface and the dial gauge moved across the sample using the CNC stage, Figure 19. At several points along the sample the displacement was manually recorded from the gauge. The samples were measured on the reverse side to the coatings to produce a consistent measurement independent of the thickness of the coating.

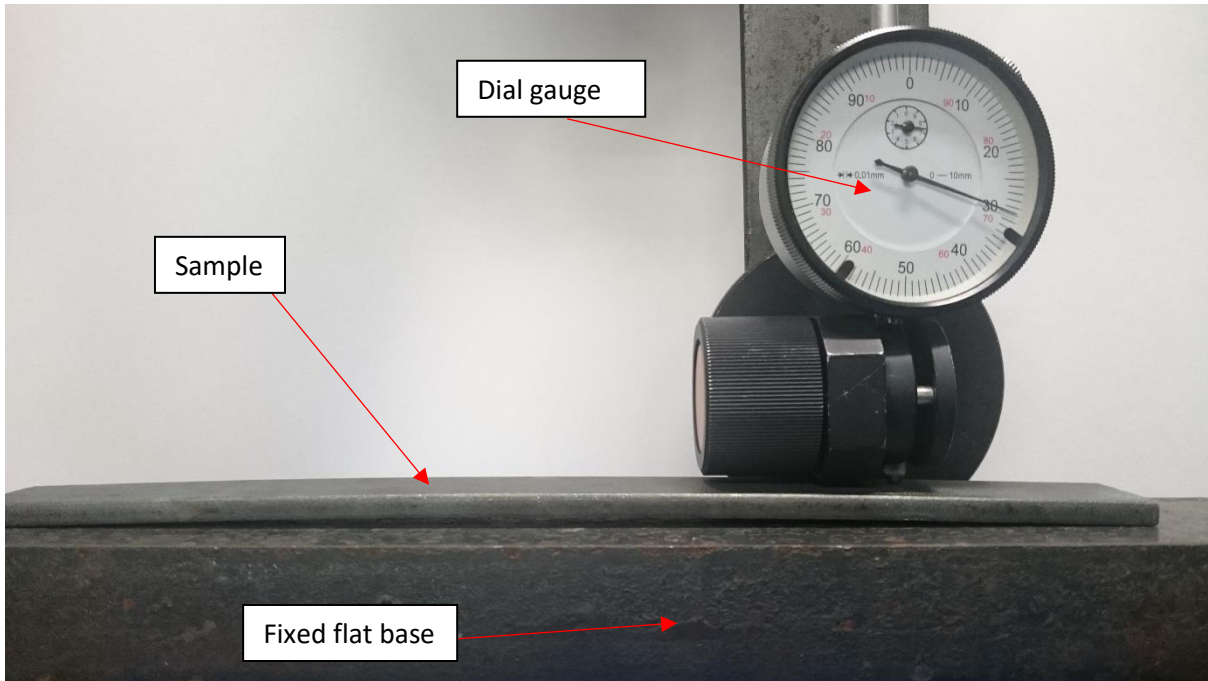


Figure 19: Image of the dial gauge being moved across the bend substrate being measured.

3.3.11 Bend Testing with Acoustic Emission Monitoring

Bend testing was done using a Hounsfield 5KN bend tester Model H5KS. The acoustic emission (AE) was recorded using a Physical Acoustics USB AE node coupled to a Pico wideband sensor with a response over the range 500-1850KHz.

The sensor was coupled to the sample using RS Pro Silicone Grease to ensure good acoustic contact between the sample and sensor. The sample was additionally taped down using electrical tape to prevent movement during experimentation as the sample was bent. Parametric outputs of force and displacement from the bend tester were output to the AE node for calibration between the two instruments. The bend tester was set up in the geometry shown in Figure 20.

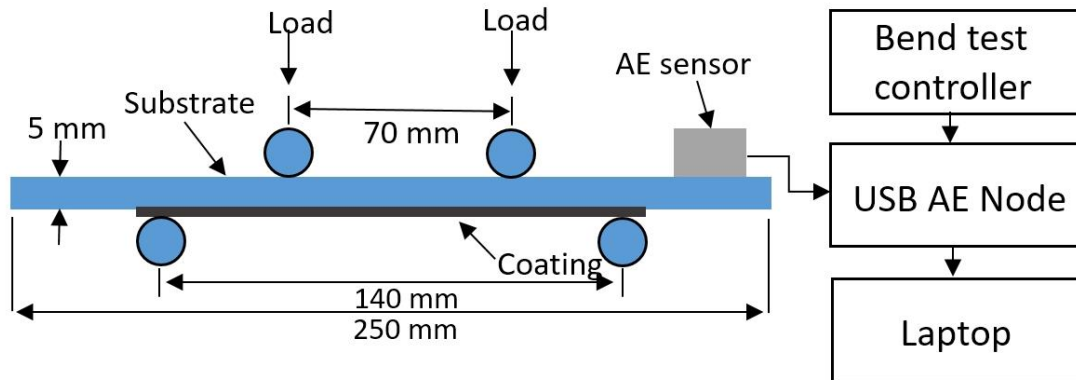


Figure 20: Diagram of the setup for the bend testing of the samples when the coating was in tension.

For measurement, the acoustic emission recording was started first. The bend tester was then set to increase force at a fixed rate of 7 mm/min until stopped by the operator. The acoustic emission software on the computer recorded each event of AE along with the values from the parametric inputs. Following the testing the data from the bend tester was matched up to the results from the AE using the parametric values for calibration.

3.3.12 Interferometer

A Veeco Wyky Non-contact Profilometer NT3300 was used for surface profiling measurements. It is a commercial non-contact optical profiler capable of measuring sub nanometre roughness features on a sample. The system uses Phase-shifting interferometry (PSI) and vertical scanning interferometry (VSI) to provide plots and data about surface roughness and features. In this work the system was used to determine surface roughness. This was done using the standard operating procedure for the system to output the desired roughness metrics.

3.4 Errors and Analysis Methods

This section describes the errors and analysis methods used in the results chapters.

3.4.1 Laser Setup and Positioning

Laser position control was provided using an Aerotech stage. The linear stages were rated accurate to $\pm 5 \mu\text{m}$. The position of the laser spot with relation to the cold spray nozzle was accurate to $\pm 0.5 \text{ mm}$. It was assumed that the laser and cold spray system remained aligned during the test and thermal cycling of the system.

3.4.2 Estimating Point of Failure

To determine the point of failure of the coatings, an analysis was performed on the raw data. Firstly, the output parametric from the bend tester recorded by the AE system was aligned to the recorded data from the bend tester. This was done by overlaying the two curves, to fix the timing offset between the two systems.

Once the two sets of data were aligned, the timing of each AE activity was aligned to a corresponding bend tester position and force. To determine the point at which there was increased activity, where the number of AE hits increased, a histogram was plotted to count the number of events measured at each force. The point of increased activity could then be found when the histogram increased the count activity above 50 events measured per 100 N. A value that was set to determine the point where there was rapid increase across many samples. The error on this was estimated to give a value of force to ± 10 N

4 Chapter 4 – Experimental Investigation of LaserForge

This first results chapter investigates a commercial laser cladding process called LaserForge. The primary aim of this work was to understand this process. A LaserForge sample was visually analysed, then a laser processing system was set up to be able to experimentally investigate the parameter space. With this new system the LaserForge process was investigated by experimentation to reproduce the coating deposition parameters, in order to better understand the process.

4.1 Motivation for Investigation of LaserForge

Based on discussion with a commercial partner and an initial analysis of a LaserForge Sample, the technology was identified as being of interest. LaserForge is marketed as a non-melt based process that uses a pulsed laser for deposition of flat sided wire. Cold spray is a low temperature non-melt based deposition process. Recent developments mean that a cold spray variant, Supersonic Laser Deposition, uses a high energy laser to soften the substrate to improve deposition. It is hoped that a better understanding of the LaserForge process deposition mechanisms using a high energy pulsed laser can lead to advancements to improve the SLD process. For example, by adding a new high energy pulsed laser to the system either through using the laser to compress existing coatings or to reinforce weak interfaces by increasing their surface area.

A preliminary study had previously been done within the research group to visually analyse a sample of LaserForge. The sample that was provided was identified as Inconel 625 bonded onto steel. Conclusions from this preliminary study indicated that the process provided a clean interface between the two materials with no mixing and that there were issues with porosity close to the interface between the deposited wire and substrate. Following this preliminary study, it was not clear how the process worked or the underlying laser-material interaction that generated the final sample structure.

LaserForge is described in patent literature as performing “solid-state metallurgical bonding of wires” [25]. It is also specified that the LaserForge process generates a wave-shaped interface between the coating and the underlying substrate [171]. It was believed that a laser shock mechanism was used to generate this interface bonding. Such a deformation would indicate enhanced bonding between the coating and substrate due to an increase of surface area. Due to the commercial nature of this technology, there is very little literature. Most available literature detailing the process is patent based, and as such there is no journal peer reviewed explanation of the technology used.

Understanding the mechanism in use in LaserForge was thought to be potentially useful to the SLD process, as the SLD process uses a high energy laser to aid deposition. Understanding any thermal effect of the Laser Forging process could then be used to resolve some of the issues with SLD. Currently

SLD does not control heat input with the laser beyond a simple feedback loop, for which there is limited control and understanding on its impact for processing different materials.

Understanding the mechanism in use in LaserForge was thought to be potentially useful to the development of the SLD process. If LaserForge works as claimed, it would indicate that it clads a coating wire to a substrate using the same bonding technique used in cold spray, but using a laser to input energy rather than kinetic energy gained from acceleration of particles with a gas. Understanding such a novel technology could be beneficial to the development and understanding of supersonic laser deposition and could even be used to aid deposition of coatings that are hard to currently deposit with the supersonic laser deposition process. Understanding the deformation and bonding at the interface could potentially be used in SLD to improve the consolidation and adhesion of the deposited layers to resolve the issues of delamination and cracking encountered when depositing some materials.

A detailed investigation to gain a thorough understanding of the LaserForge process was therefore undertaken and is described in this chapter, with the aim of understanding the underlying scientific principles and its potential benefits to supersonic laser deposition.

A laser system capable of exploring the parameter space of LaserForge was not initially available in the research group, therefore as part of the work it was necessary for such a system to be designed and set up and forms a significant part of this work.

4.2 Analysis of a LaserForge Sample

This section will detail an experimental analysis of a LaserForge sample to understand the results of the process. This was done to gain additional understanding from the physical LaserForge sample that was available.

4.2.1 LaserForge Sample

A sample made using the LaserForge process was obtained for this study. This is the same sample which was used for a previous preliminary study within the group. The sample was a block of steel with a deposited coating of In625, Figure 21. At one edge, there were bulges of coating hanging over the edge of the substrate. The coating does not cover the whole substrate, and the coating therefore appears as a raised area on top of the substrate.

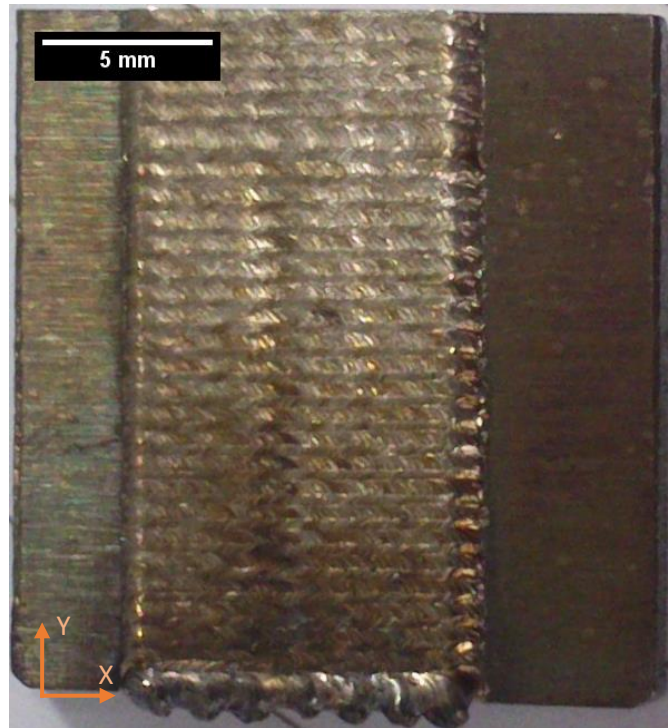


Figure 21: LaserForge sample of In625 on steel. The top edge has been sectioned off.

The sample was previously cut along the top edge shown at the top of Figure 21. This will be called direction X. The new cross section for analysis was taken vertically through Figure 21 and will be called direction Y.

4.2.2 LaserForge Surface

The sample coating surface was imaged under a white light microscope. The surface showed a regular pattern of overlapping circles that snaked back and forth across the surface. Each of these circles contained smaller concentric circles. It is believed that that each of the more defined circles corresponded to an individual laser pulse and the internal circles were ripples caused by the molten material at the surface, Figure 22.

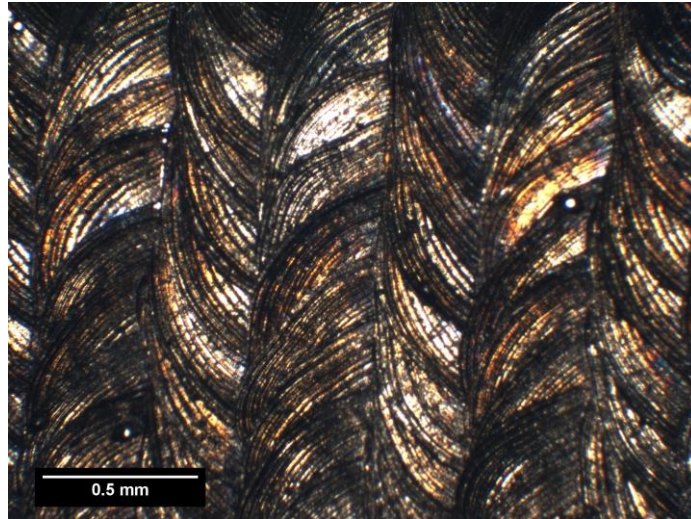


Figure 22: LaserForge sample surface under white light microscope. The larger circles are believed to correspond to individual laser pulses. This image is rotated by 90 degrees with respect to Figure 21.

Measurements of the surface estimate that each larger circle is approximately 1 mm in diameter, with an overlap of 0.6 mm between horizontal lines in Figure 22. This would indicate an overlap of 60% between lines of pulses.

At the macroscopic level, there were seven slight bulges along the length of the sample, corresponding with the seven bulges at the end of the substrate. It is believed these correspond to wires laid down on the surface, prior to laser forging with the fine snake pattern of laser pulses, which run at 90 degrees to the lengths of wire cladding.

4.2.3 Cross-Sectioning of Sample

A new cross section was taken from the LaserForge sample in the Y axis of Figure 21. This cross sectioning was performed using a rotating cut off blade. A cross section was taken in this direction to add to the existing cross section in the X axis to better understand the interface between the coating and substrate, and any differences there may be between the two axes.

The sectioned material was mounted in a conductive resin puck, to enable easier polishing and analysis. Samples from both axes were then polished using the following parameters:

- 240 SiC grit paper, water, 25 N, 150 rpm, until planar
- Planocloth H, 9 μm diamond solution, 25 N, 250 rpm, 4 minutes
- Planocloth, 3 μm diamond solution, 25 N, 250 rpm, 4 minutes

The samples were subsequently imaged under a white light microscope. An example of the coating cross section in direction X is shown in Figure 23. Some porosity was observed in the coating and at the interface. The coating thickness was approximately 0.6 mm.

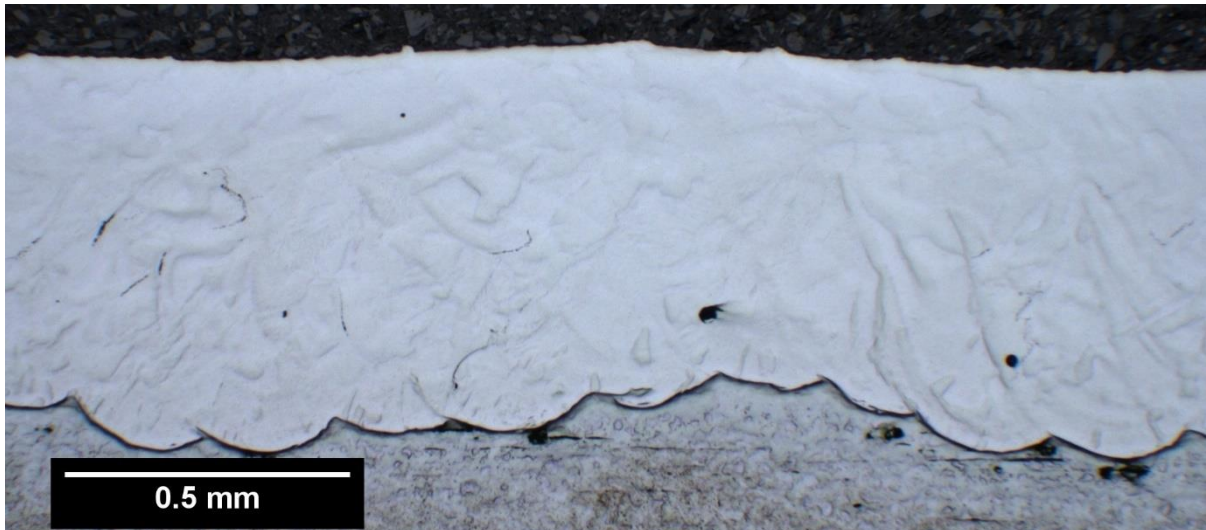


Figure 23: White light microscope image of the cross section of the IN625 coating on a steel substrate in the X axis after polishing. The black layer at the top of the image is the mounting resin, the white material is the coating and the substrate is the darker grey material at the bottom. Black spots are porosity in the sample.

In both axes a wave-shaped interface was observed between the coating and substrate. In the X direction, the deformation of the coating appeared more consistent in depth along the length of the sample. This is along the lines of laser pulses. In the Y direction, the deformation was less consistent in deformation along the length of the sample. This was at right angles to the laser pulse snake pattern. The difference in deformation profile can be explained by the direction of sectioning with respect to the direction of laser pulses. When looking at the cross section in X the cross section is following a continuous line of subsequent laser pulses. When looking at the Y cross section, the cross section is intersecting lines of laser pulses going into and out of the image. As the deformations will have a different origin for each line of pulses into and out of the image, the different apparent penetration is due to the different intersection of the deformed coating for adjacent lines of pulses. In the Y axis, there is a repeating pattern every three pulses (~1 mm) indicating a systematic and well controlled positioning of laser pulses in adjacent lines.

A correlation was observed between the number of overlapping circular spots on the surface on the LaserForge sample in one row of pulses and the number of deformations of the coating into the substrate. From this it could be theorised that the spots on the surface relate to the indents at the interface. A figure in the LaserForge patent supports this theory, showing the laser beam directly above an indentation [171].

Simply polishing the sample does not indicate anything about the microstructure beyond the existence of pores in the coating. To gain a greater understanding of the process, the microstructure must be revealed. This can be done through etching.

4.2.4 Etching of LaserForge Cross-section

The cross-section samples were etched in Kallings etchant. This etchant was chosen as it is recommended for Ni-Cr super alloys, and therefore ideal for revealing the microstructure of In625.

It was unknown how rapidly the sample would etch, so an initial time of 30 seconds was used. The grain structure became visible as seen below, but the coating did not etch evenly. One possibility for this was that the steel substrate was etching in preference to the coating, reducing the etchant's effectiveness near the steel substrate. Etching was repeated several more times up to a total time of 27 minutes, but the grain structure was not revealed any more clearly than in Figure 24, the top section of the coating only became darker. One option is that the structure near the interface region is amorphous, although a magnified view does produce a very faint microstructure.



Figure 24: White light microscope image of the cross section in the Y axis after 30 seconds of etching with Kallings etchant. The microstructure is beginning to appear in the coating (centre) between the mounting resin (top) and the steel substrate (bottom) the sample is not etching at the same rate across the thickness of the coating. The steel is also etching much faster than the coating.

A magnified view of the interface region shows the extent of the porosity and deformation of the coating material, Figure 25. Some larger holes were apparent in the coating with one large one measuring 1.8 mm in diameter and 40 microns deep.

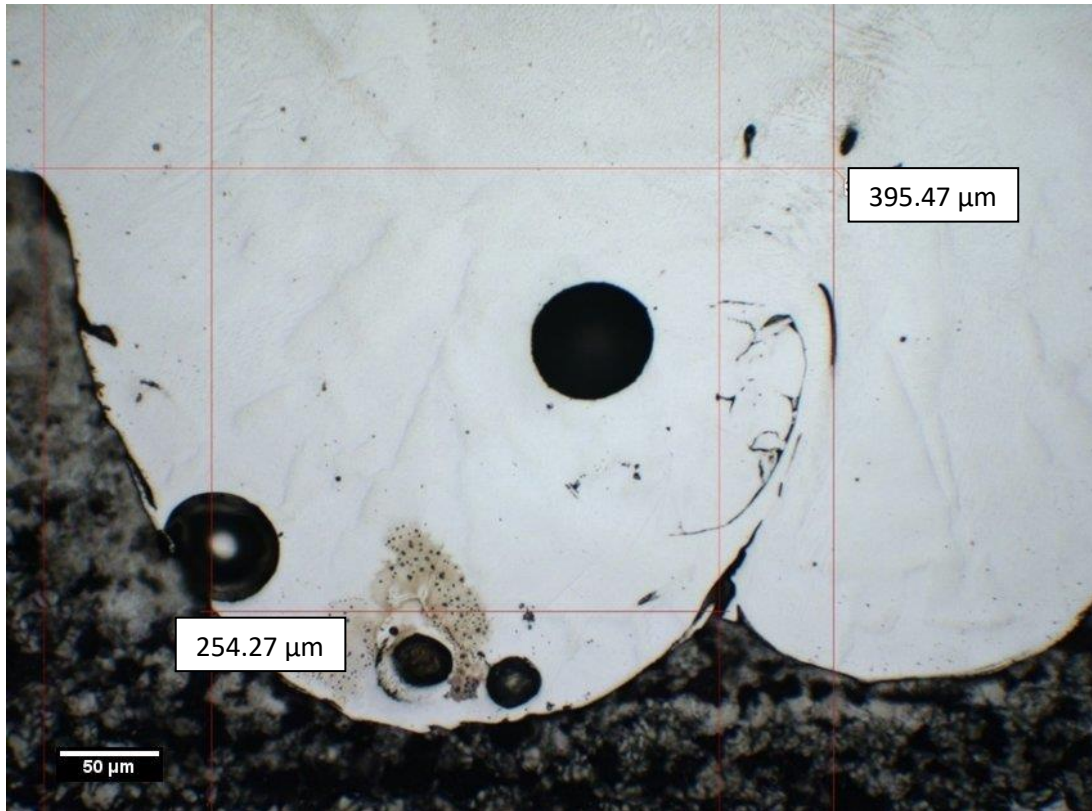


Figure 25: White light microscope image of the deformed interface showing pores and deformation.

4.2.5 Conclusions of Cross-Section Analysis

The LaserForge sample that was analysed was successfully imaged, sectioned and polished. Etching did not successfully reveal the microstructure.

Results indicate that the process does indeed deform a coating material into the substrate using a pulsed laser. The coating process involves the pre-placement of metal wires on the substrate. These wires are then impacted by a pulsed laser passing in overlapping lines at 90 degrees to the lengths of wire. The laser pulses deform the coating wire into the substrate, without mixing with the substrate material.

Achieving a good etch to reveal the microstructure was unsuccessful despite several attempts. From the grain structure that was visible, the grain structure did not appear to change through the material and pores were clearly visible as expected.

The sample analysed appeared to have a single layer of coating. According to literature a single layer is often sufficient although multiple layers are possible with this process.

Further experimental investigation into this process would be best achieved by reproducing the coating technique with materials that are easier to work with. Investigating the parameter space

would help to better understand where the bonding mechanism lies in relation to other laser-based processes.

4.3 LaserForge Parameters

This section will describe the parameter space that the LaserForge process occupies along with example parameters that are known to work. This will be beneficial to specifying the requirements for building a system to investigate LaserForge. Additionally, the currently understood physics of the process will be presented.

4.3.1 Process Parameter Space

The previous section illustrated the results of the LaserForge process. It is important to understand the parameters that can be used in the LaserForge process. In the patent “Process for energy beam solid-state metallurgical bonding of wires having two or more flat surfaces” parameters were provided for the deposition of Ti-64 on AL-6061 [25]. The values provided were:

- Wire 0.5 mm thick
- Power density 0.0785 MW/cm²
- Pulse time duration 10 ms
- 300 W average power YAG laser
- Argon atmosphere

These parameters can be plotted on an interaction time vs intensity graph, Figure 26, to observe where the process compares to other processes. The figure shows that it resides at the same intensity as welding or cladding processes, but at shorter interaction times. This would correlate to the description of the process using a minimal heat input and a lower specific energy.

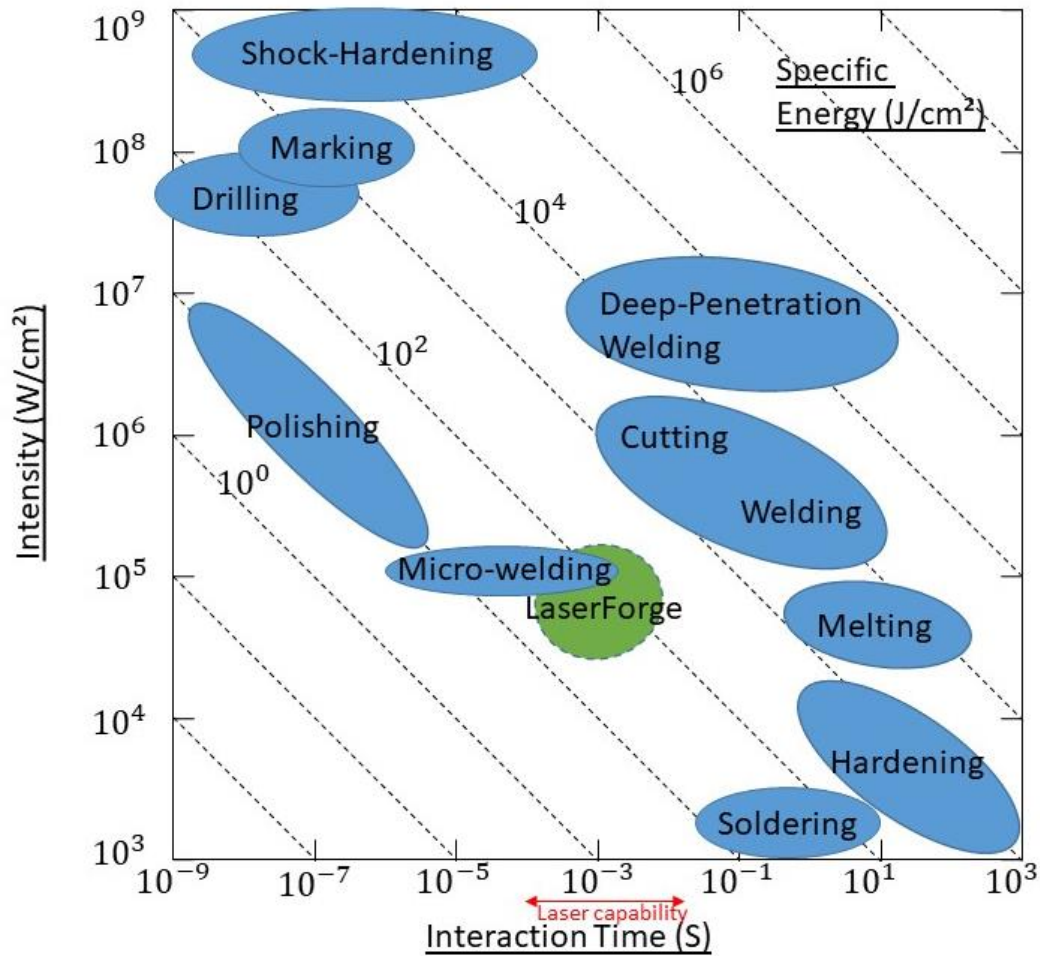


Figure 26: Parameter space for laser processes, including the parameters for LaserForge from the patent for comparison.

These key parameters that have been claimed to work for LaserForge were used as the starting point for the experimental investigation into the process mechanism. The QCW laser system described in the following section was specified to be capable over the desired range, to investigate LaserForge in the target area.

4.3.2 LaserForge Process Claims

The LaserForge process is described as a process that uses flat sided wire as a coating material; it uses a pulsed laser as an energy source to bond this thin wire to a substrate. The laser provides energy to the flat outer surface of the wire, causing the wire to heat with a thermal gradient through it and in the process generates compression stress waves that deform the coating material into the substrate resulting in metallurgical bonding [20].

The LaserForge process is based upon the Precision Metal Deposition process (PMD). It is understood that the PMD process was developed for the bonding of metallurgically similar materials, using a similar method of heating a flat-sided wire to liquefy it along with a thin surface layer of the substrate

to induce bonding. The process uses an Nd-YAG laser and with power densities of $< 0.1 \text{ MW/cm}^2$ over 10 ms, although CO_2 lasers were used in development. This itself is based upon original work from 1985 by Frish et al. on the theory and application of pulsed laser welding.

The original work by Frish et al. on pulsed laser welding, and others at a similar time, indicates that during the interaction of a pulsed laser with a surface a pressure wave can be generated. It is this pressure wave that interacts with the interface region to generate a thermal wave that aids the bonding of the two dissimilar materials. In the case of this work, the laser used was a CO_2 laser with up to 500 J per pulse over 30 ns which produced energy densities from 20 MW/cm^2 to 130 GW/cm^2 to achieve successful bonding of films of typical thickness of $25 \mu\text{m}$. There were however issues in minimising the gap between the coating and substrate for successful bonding [172][173][174][175]. Comparing these values to those above we see that a longer pulse time is used for LaserForge with a corresponding decrease in power density.

The key claim advancements of LaserForge over existing literature are therefore a high control of the coating wire application to minimise small gaps between the coating and substrate, moving to a longer pulse length to account for thicker wire coating and optimising the laser parameters to precisely control the thermal gradient through the wire.

4.3.3 Conclusions for LaserForge Parameters

In conclusion, the LaserForge process is not revolutionary, but rather an evolutionary step of pulsed laser welding building on previous work, but taking advantage of modern control methods and laser systems.

The subsequent sections of this chapter therefore investigate the claimed LaserForge process and attempt to generate bonding of two dissimilar materials using metallurgical bonding by use of a pulsed laser. The motivation behind this is that such a process could be a beneficial addition to the supersonic laser deposition process, which itself is used to bond dissimilar metals using metallurgical bonding, without mixing of the materials. The patent literature indicates parameters for the LaserForge process of titanium 6-4 on aluminium. These two materials were therefore selected as candidates for this study.

4.4 Setup of Laser System to Investigate LaserForge

Following the analysis of literature on LaserForge, a laser system was specified. No laser system existed in the research group that could explore the desired parameter range. A new laser system was therefore set up as part of this work.

4.4.1 Laser Processing System

A new laser was purchased to investigate the parameter space of LaserForge. A Quasi-CW fibre laser from IPG was selected, model IPG YLM-150-1500-QCW. This laser is an OEM unit designed for system integration, as such it required a system to be integrated into. This laser was selected as it could operate in the region that was believed to be used for LaserForge processing.

It is a Class 4 Ytterbium fibre laser capable of both CW and pulsed output. The laser wavelength is 1070 nm. It has a maximum rated maximum pulsed peak power of 1500W (1620 W measured) and a CW rated maximum power of 250 W (274 W measured). It has a minimum pulse duration of 0.2 ms. There is a 0.1 mW red guide laser that is useful to position the head in the correct position. The advantages of this type of laser is that it can generate a high peak power, that is $\sim 10x$ the average power. This QCW design of laser enables it to be more affordable and in a compact package.

The laser was supplied as an OEM laser unit with attached fibre. Integrating the laser into a processing system was necessary before it could be used, and was a significant amount of work. In order to set up the laser for use it required a suitable power source, communication system, processing chamber with safety system, processing head and laser positioning system. This following section details the setup of the system.

4.4.2 Laser System Integration

3.4.2.1 Power

The laser was supplied without power supplies. Two supplies were needed, one for the main diodes and another for powering the internal electronics of the laser.

A MeanWell supply was sourced with a specification of 1500 W, 48 V 32 A. This supply unfortunately had exposed electrical contacts, which needed to be enclosed to comply with additional university health and safety regulations. Due to the size of the supply it was decided that a custom enclosure for the rear of the supply would be built.

I learned how to use a 3D modelling package to produce a design for an enclosure over the electrical connections from sheet stainless. The package enabled the bends to be simulated and to generate technical drawings that could be used in the workshop. Several iterations of the model were designed before reaching the final design. The final design can be seen in Figure 27. The final part was then manufactured and assembled in the workshop by me, which required learning metal working techniques.

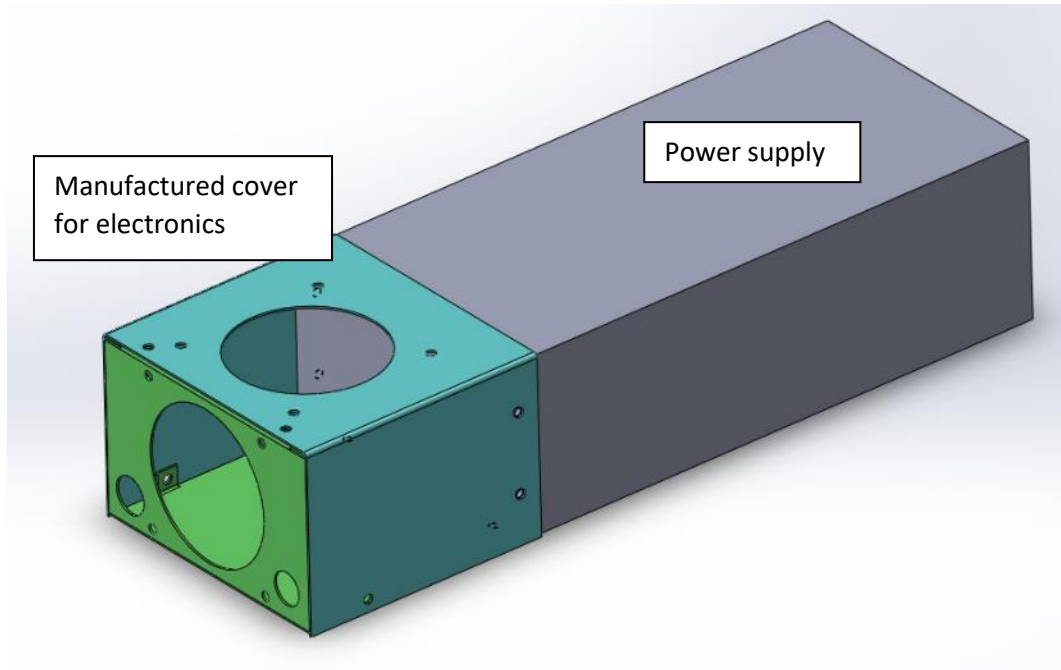


Figure 27: Design of case (green) to cover power supply (grey) contacts.

An image of the power supply connected to the laser can be seen in Figure 28, showing the case around the electrical contacts.

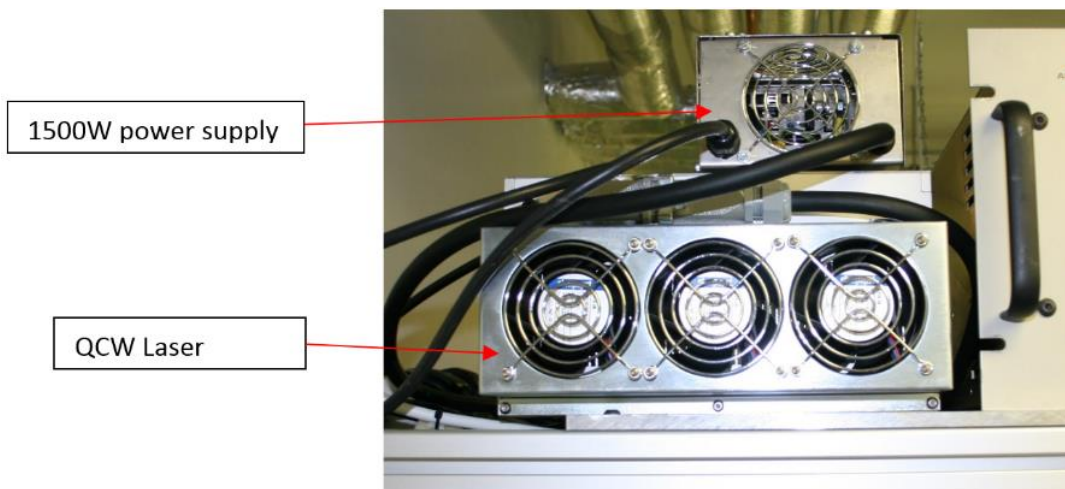


Figure 28: Power supply (top) connected to the laser (bottom).

The input for the supply is from a standard main plug with 13A fuse and the supply should not draw more than 8A@230VAC under full load. The output from the supply to the laser is via a 2m, 3 core cable which is rated at 25A and has a 4mm² conductor area per core.

The second source of power for the laser electronics was a 24V DV 500mA supply. This was connected to the laser via the communications port.

3.4.2.2 Safety

To correctly set up the laser, the manufactures instructions required that an electronic circuit be designed and built to safely discharge the laser diodes, to make the laser safe after use. It was decided to integrate the laser system into a Class 1 processing chamber. To comply with health and safety requirements, this chamber required an interlock circuit to be built, which would cut power to the laser diodes and discharge them safely should the chamber doors be opened.

An interlock system was therefore designed and built to prevent laser exposure to the user. As the laser can be operated using Ethernet, RS-232 and analogue controls, the interlock was set up to cut the laser diode power supply when the doors of the chamber were opened. If triggered, any power in the laser diode system is then discharged safely through a resistor. The designed interlock circuit is illustrated in Figure 29. The circuit uses an electrically controlled relay linked to the interlock switches on the doors to safely disconnect and discharge the power from the laser diodes when triggered. The specified components were integrated into an enclosure that I modified for purpose in the workshop. Once complete the interlock circuit was installed in the processing chamber.

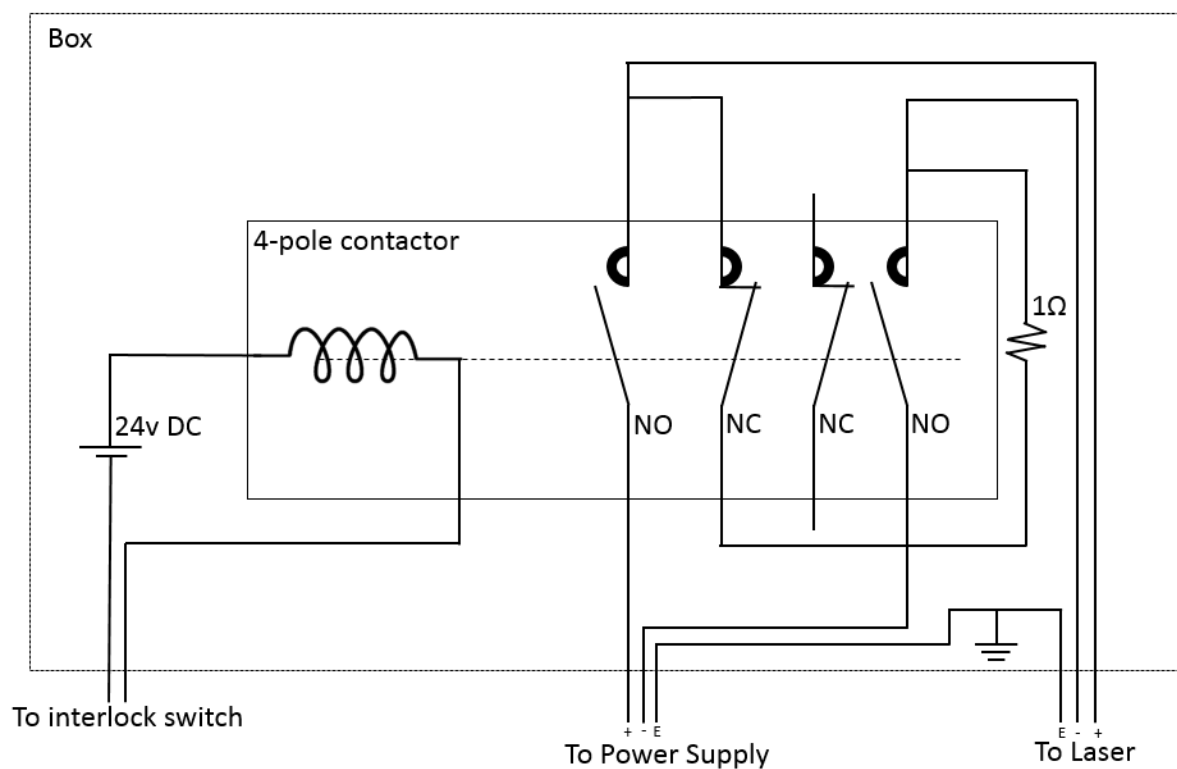


Figure 29: Laser interlock circuit diagram that was designed and built.

3.4.2.3 Processing Optical Head

The laser is coupled into an existing optical processing head that was repurposed for this work. The laser head is a Precitec YR30 cutting head coupled to a custom optical system with a collimator and camera, Figure 30. The head was connected to an air supply and recirculating water supply to cool the optics from the laser energy. Initially a nitrogen supply was used as the air supply for the head.

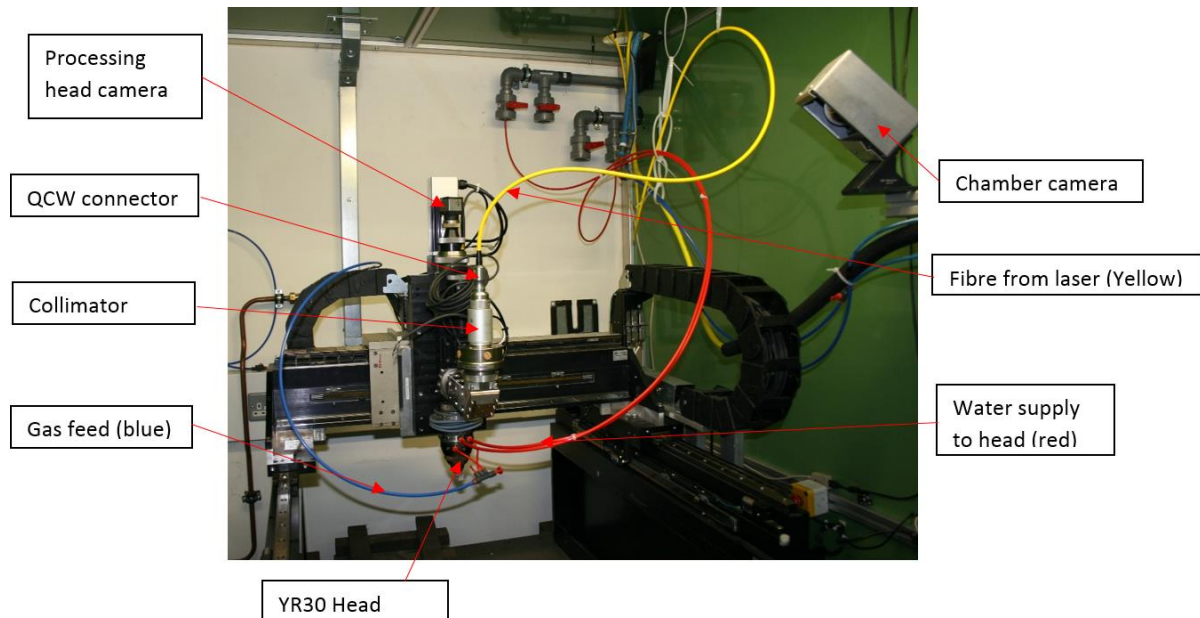


Figure 30: Layout of processing chamber with YR30 processing head.

The head contains an optic with a glass cover slide in the lower section to protect it. This cover slide was changed as necessary when it became contaminated with particles. A nozzle of diameter 1.2mm was used as the focused beam diameter at the nozzle was calculated to be ~ 1.1 mm based on a 73mm focal length lens.

3.4.2.4 Laser Position System

Two options were considered for positioning the laser beam on the workpiece, a laser galvanometer or a CNC stage. The advantages of using a galvanometer is that it reduces the size of the system and increases movement speed compared to a large CNC stage. It was decided against this as the material required for the galvanometer mirror was prohibitively expensive, as it would need to be able to deal with high intensity pulses from the laser. An existing 3 axis CNC stage was used to control the position of the laser on the workpiece.

The 3 axis CNC stage as seen in Figure 30 is controlled by an Aerotech controller. This is interfaced with a computer and could be programmed. The Aerotech controller is also capable of interfacing with the laser via analogue and digital inputs/outputs. The laser was therefore connected to the stage

controller so that both the laser and stage could be programmed together. The Aerotech controller has the capability to deliver precise timing of laser triggering that is synchronised with the position.

3.4.2.5 Communications

The laser has three methods of communication, Ethernet with a web interface, RS-232 and a 25 pin analogue connector.

The Ethernet connection provides a web interface that shows the status of the laser and enables manual control of most settings. This communication method is useful for debugging purposes and running simple experiments, however any rapid changing of setting and synchronisation to laser head movement is not possible.

The RS-232 interface was explored, initially using a USB to RS-232 adaptor, but this was found not to work due to the non-standard communications from the laser. After further investigation, it was found that the laser could be controlled by this interface, but the commands had to be sent as a complete command rather than a letter at a time as is standard practice. The time out for sending a complete command was found to be about 1 second.

The main way of controlling the laser is by the analogue inputs on the 25 pin connector. The electronic circuit for these new connections was designed and made. All the control electronics were then wired up and documented. This included connection to the Position Synchronized Output (PSO) output that enables precise scripted pulse timing control for the laser emission.

The Aerotech software used a programming language called G-Code. This scripting language was able to send commands to the laser via the analogue communication. Scripted experiments were therefore written in G-Code and run using this software.

All connections were tested, and the laser was found to operate successfully in both pulsed and CW mode up to maximum output power.

3.4.2.6 Laser Testing

To ensure the laser was performing as expected the pulse shape in time was measured. A photodiode detector (Thor Labs DET10A) was setup in the chamber close to a reflective steel surface upon which the laser was pulsed. The detector was connected to an oscilloscope and the data from the oscilloscope was downloaded onto a PC, Figure 31. The pulsed signal was recorded at 10% intervals of the laser set point. The rise and fall times of the pulse were also calculated and found to be of the order of 10 ms as expected for all set point powers. An exact value of the rise time could not be established due to noise in the signal. It was determined that the noise was due to the poor signal from the detector as the wavelength of the laser was at the very edge of sensor responsivity. In

conclusion, it was found that the laser was outputting the expected pulse shape and was therefore configured correctly.

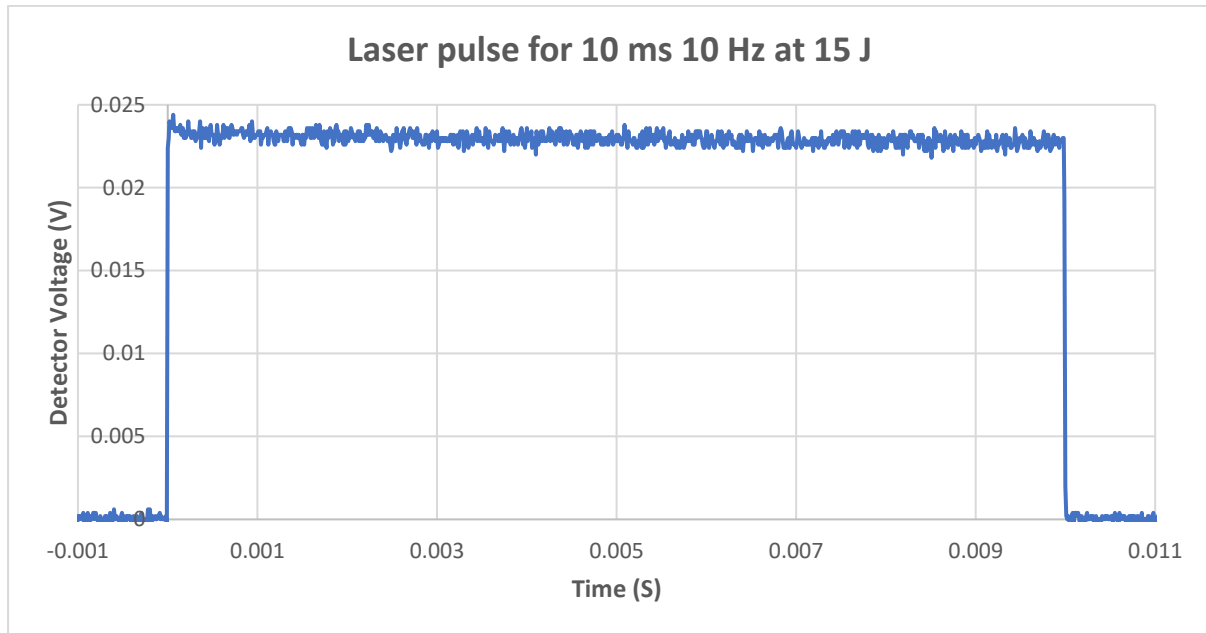


Figure 31: Recorded laser pulse for 10 ms 10 Hz at 15 J.

As part of the work, documentation was written to specify the correct setup and use of the system for other users. Following the successful setup of the laser system work was carried out to investigate the LaserForge process.

4.5 Effect of Oxygen on Laser Processing in the Chosen Parameter Space

In this section the effect of oxygen was evaluated on the laser processing of cp titanium on cp aluminium. The motivation for doing this was to evaluate the need for an argon processing chamber and to measure the effect of oxide formation on the Vickers hardness of the processed material.

4.5.1 Comparison of Methods of Using Argon as a Processing Gas

Here an experiment was performed to evaluate the effect of two different methods of using argon as a processing gas, and the effect they have on the final laser processed material. One method was to use gas coming out of the laser processing nozzle, and the other was to place the sample and laser nozzle in an argon filled chamber.

A sheet of 1 mm thick titanium was clamped onto a substrate of aluminium. Two configurations of argon gas shielding were compared. The first configuration placed the target under a nozzle emitting a nitrogen shield gas. The second configuration placed a chamber wall around the sample and the chamber was filled with argon both from under the sample and from the nozzle. The top of the

chamber was open to the atmosphere and the gas pressure was kept at < 2 bar. The argon chamber was measured to have < 0.1 % oxygen next to the sample.

In both environmental conditions the laser parameters were kept constant, except for the variable of pulse length. The full details on the experimental setup are detailed in the materials and methods section. The laser parameters used were as follows:

- Laser pulse energy 1580 J/s per pulse (100% laser setpoint)
- Spot size 1.56 mm (Power density 0.08 MW/cm², gaussian beam)
- Distance between pulses 0.5 mm (Pulse rate 10 Hz, 5 mm/s velocity)

Pulse length was varied between 1 and 10 ms in 1 ms increments. A lower power density than LaserForge was used to reduce the chance of mixing of the coating material into the substrate for this study.

Samples were sectioned at 90 degrees to the direction of processing and mounted in resin. The exposed cross sections were then polished.

4.5.2 Vickers Hardness Measurements

The Vickers hardness was measured through the thickness of the Ti-64 sample at the position in the centre of the laser processed track as shown in Figure 32. A control was taken where there was no pulse to ensure there was not a natural variation of the material hardness. A summary of the results is presented in Figure 33. The error in position of the Vickers hardness measurement was ± 0.025 mm.

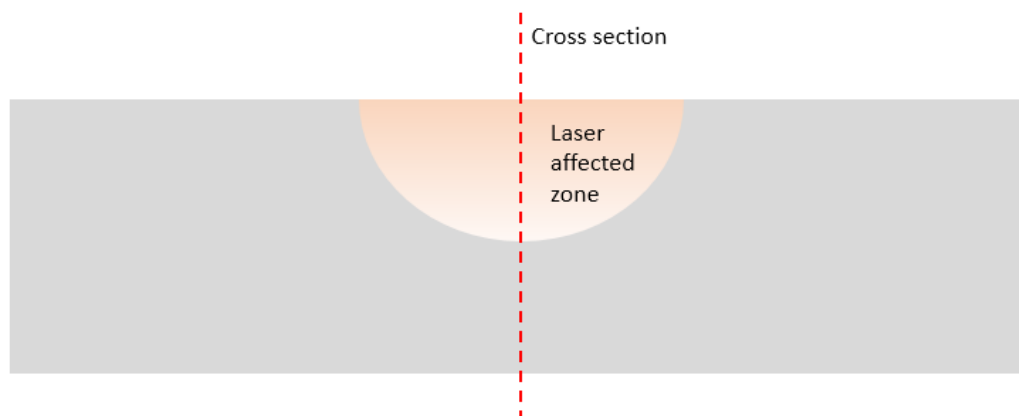


Figure 32: Diagram of the cross-section line used to make the hardness measurements. The line of laser pulses is into the page. The measurement was only made in the titanium coating, as bonding to the aluminium layer did not occur.

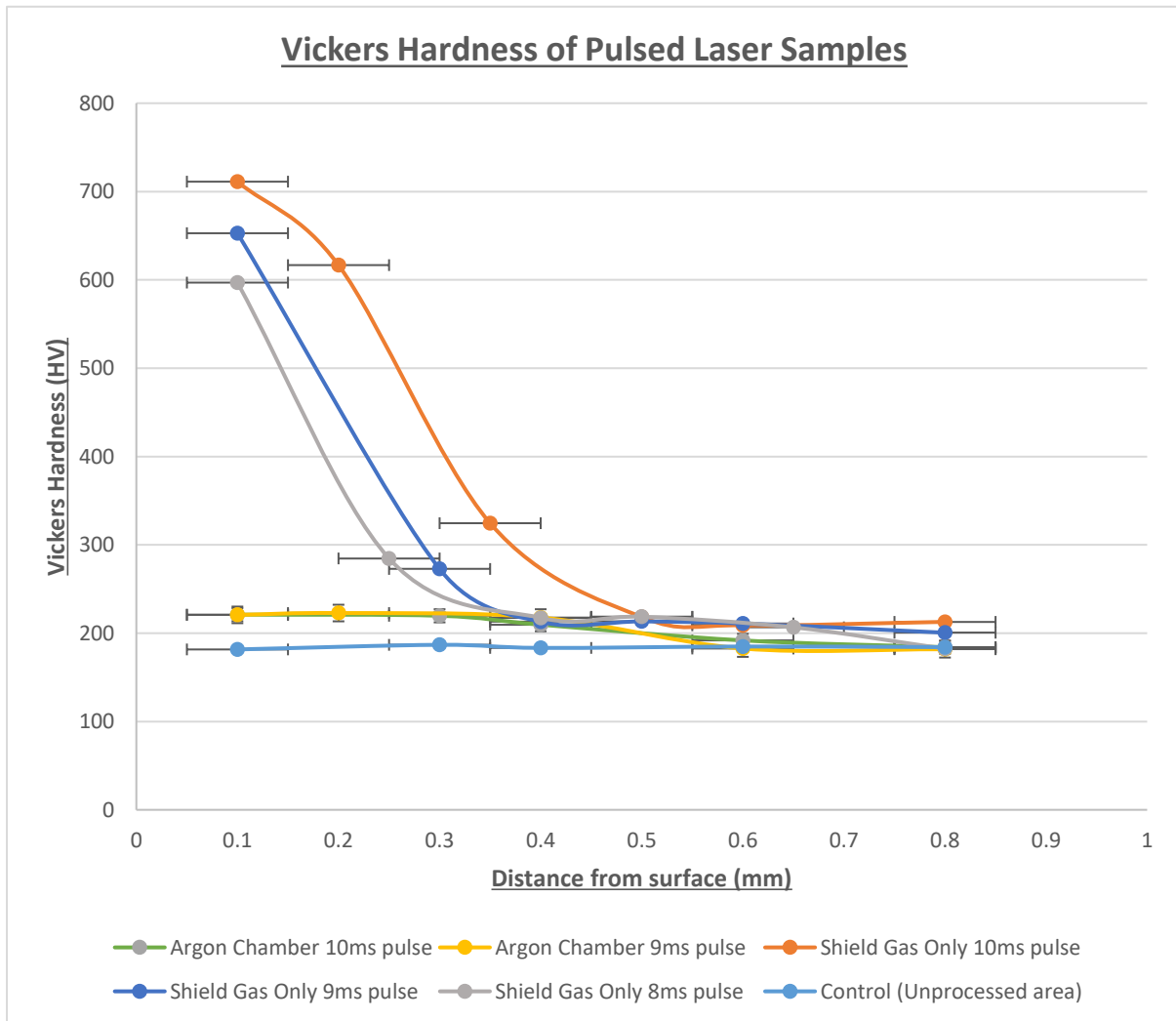


Figure 33: Graph of the Vickers hardness of the pulsed laser samples. A comparison is made between samples that were processed in an argon chamber or with a shield gas only.

The results show that the tracks that were pulsed in air with only a shield gas were significantly hardened by pulsing with the laser. The spots pulsed with the laser in argon were not significantly hardened. Pulses with a longer pulse length resulted in a greater hardness when pulsed in air.

The hardening of the titanium near the surface for samples exposed to higher oxygen content is consistent with literature. It is expected that oxidation of titanium yields higher hardness values [176]. It is also consistent that greater depths have less hardening due to lower exposure to oxygen during processing.

Measurements were also taken across the laser affected zone 0.1 mm below the surface, to compare the oxidation profile for different pulse lengths.

The results, Figure 34, indicate that there is some variation in hardness across each pulse line. This suggests along with visual inspection that there was some mixing which meant that the oxygen reacted material was not uniform across the pulse area. This accounts for the variation in hardness.

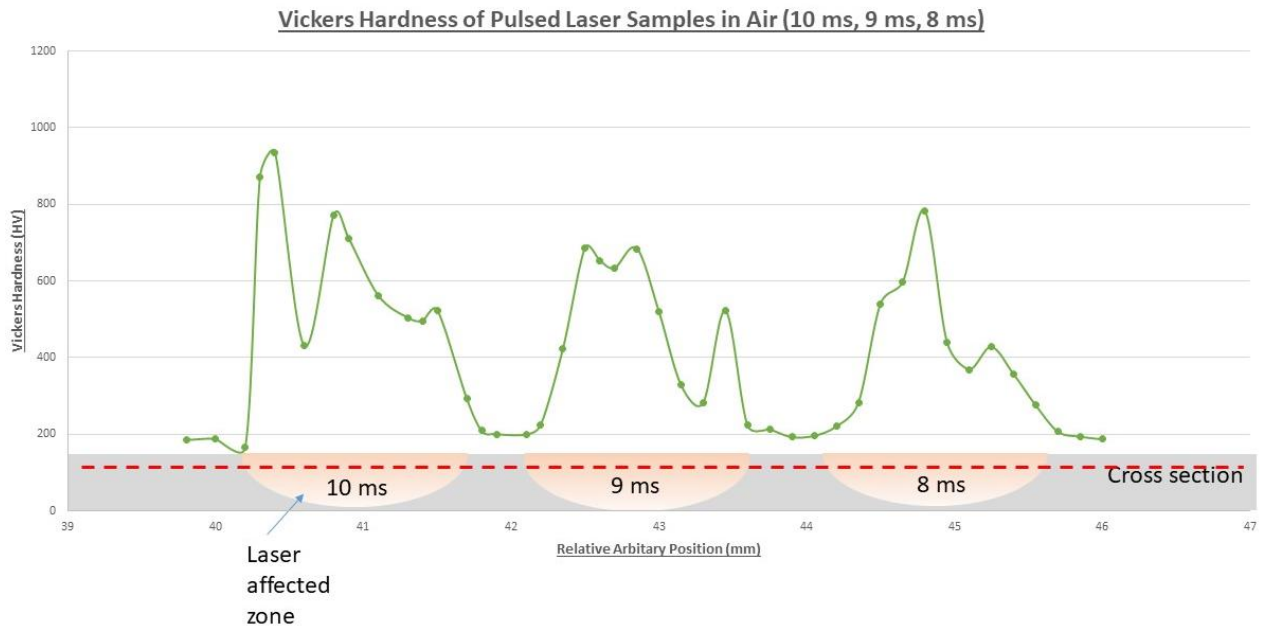


Figure 34: Graph of the Vickers hardness across the three longest pulses 0.1 mm from the surface. Pulses are spaced 2 mm apart. The graph shows that the Vickers hardness does not remain constant across each of the laser tracks. Diagram of the cross-section line used to make the hardness measurements is overlaid for reference.

4.5.3 Conclusions from Effect of Oxygen on Processing

The results from the experiments presented here indicate that oxidation is a problem if an argon processing chamber is not used. They show that the argon processing chamber used was successful at removing oxidation of titanium from the process.

They also suggest that under the laser processing conditions used, melting is occurring through a significant portion of the titanium along with material movement, so when processing in this parameter region oxygen needs to be removed.

As the LaserForge process displaces a larger amount of material a higher energy density is required, as expected. The next step is therefore to map the process parameter space.

4.6 Parameter Space Investigation with Fixed Pulse Energy

This section investigates the parameter space around the expected parameters for LaserForge. The aim was to determine if the expected material response occurred at the expected parameter location and to better understand the material response occurring in response to the laser.

4.6.1 Processing Parameters

The two materials used for the subsequent section were a coating Ti-64 of thickness 0.52 mm and a substrate cp aluminium of thickness 1.3 mm.

The initial parameter space investigation fixed the pulse energy at 15 J and modified the pulse length and power density (spot size). Pulse length was varied between 0.2 and 10 ms. 10 ms was the longest pulse length available at this energy for the laser used. Power density was varied between 10^4 and 10^6 W/cm². Pulses were overlapped by 0.2 mm.

Samples were processed in an argon chamber to minimise the effect of oxygen. Ti-64 of thickness 0.52 mm was used on a substrate of pure aluminium of thickness 1.3 mm.

4.6.2 Parameter Space Map

Once the samples had been processed with the laser they were sectioned, mounted in resin and polished. As some parameters did not result in joining of the two materials together, the aluminium substrate was not mounted along with the Ti-64 in all cases. The polished samples were then etched using in Krolls etchant. The results are shown in Figure 35.

Parameter Space for Fixed Pulse Energy

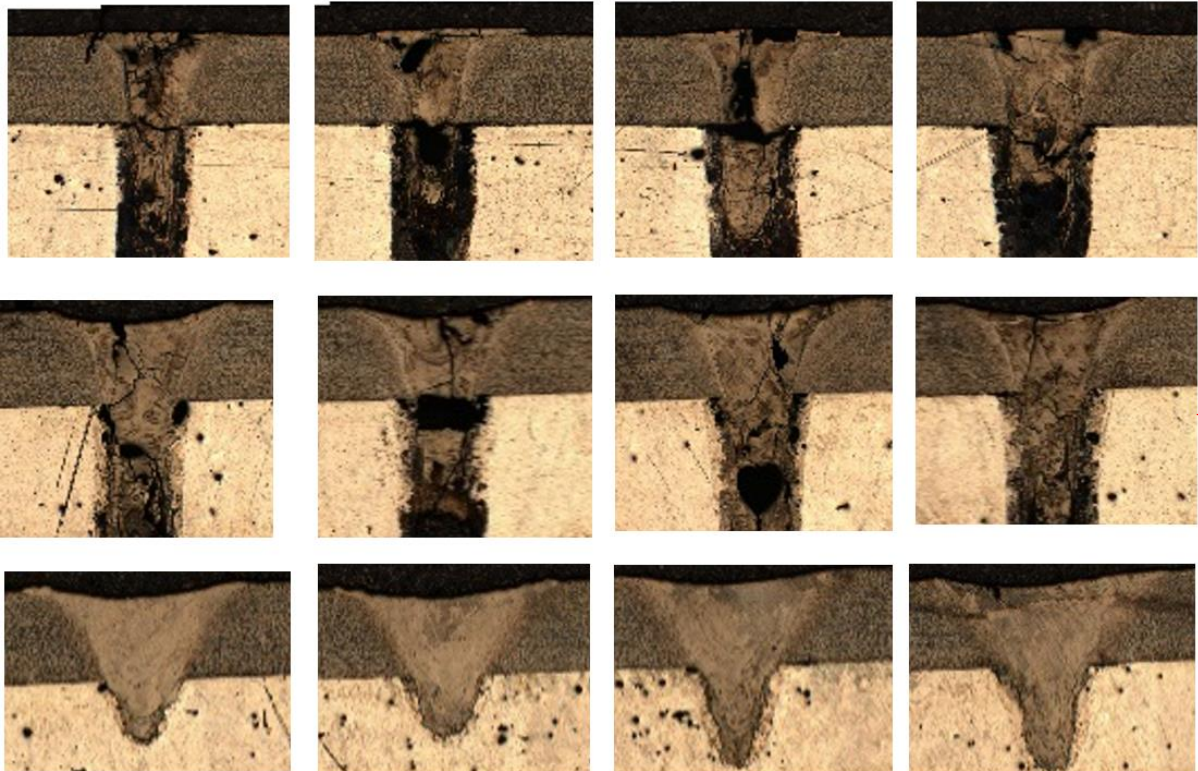
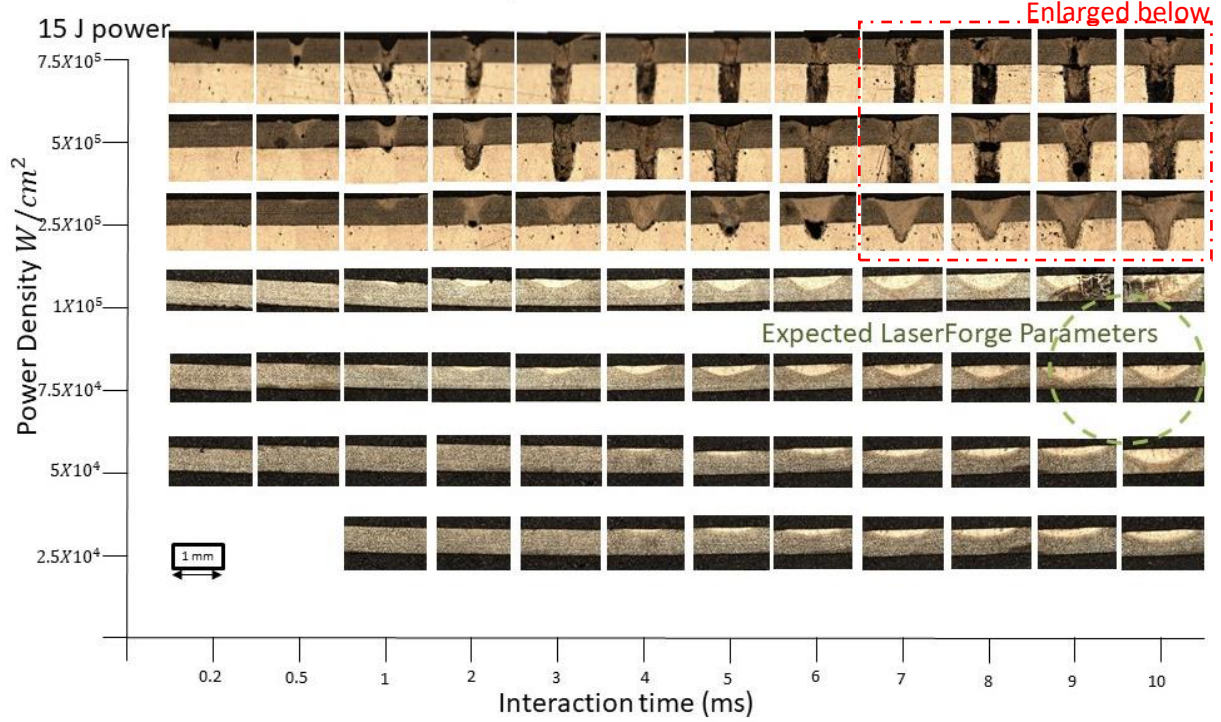


Figure 35: Parameter space for a fixed pulse energy of 15 J. Rows are of equal power density and columns are of equal pulse length. The surrounding dark material is the mounting resin, the dark grey material is the Ti-64 and the lighter bottom material (missing on lower rows) is the aluminium substrate.

As can be seen from the results, this parameter space covers the extremes from no interaction (bottom left) to deep welding (top right). Within this parameter space only welding was observed where the two materials were joined together, no evidence was seen for the deformation of the Ti-64 into the substrate using a mechanism that would not be considered a weld. Possible reasons for this could be lack of good contact between the Ti-64 and the aluminium for heat transfer, or a spot size that was too large increasing the required amount of mass to heat per pulse.

4.6.3 Conclusions from Fixed Pulse Energy Parameter Map

The results showed that within the expected parameter range, it was possible to bond the coating to the substrate. This was not at an order of magnitude larger power density and similar interaction time given in the patent, but the laser used meant that the spot size was twice the surface area of the theoretical one used for LaserForge. It is postulated therefore that the decreased power density could be achieved by optimising the processing conditions such as surface finish, pulse shaping and coating material geometry. From the surrounding interactions, it is clear to see that the process is in the parameter region of welding, and nothing more novel is occurring.

There are two avenues of exploration to ensure LaserForge is only welding. The first is to resolve the likelihood of poor contact, which would reduce the thermal contact at the interface. The second is to use a smaller spot size to reduce the volume of material that is heated to produce the bond to the substrate. It should be noted that these trials used a solid bulk of coating material, whereas the LaserForge process uses flat sided wire. The thermal mass and thermal dissipation characteristics will therefore be different, and potentially explain the need for lower energy in the LaserForge process. The Ti-64 has a much higher melting point (1604 °C) vs pure aluminium (660 °C), the differently coloured material in the laser affected region is therefore likely to be an intermetallic compound with a clearly defined interface with the aluminium due to the high temperatures involved.

4.7 Improving Contact Between the Coating and Substrate

The LaserForge patent makes clear that good thermal contact is required between the coating material and the substrate for the process to operate successfully. A sample mounting procedure that clamps the two materials together was already used, but the materials were used in their as received form. The roughness of these materials may therefore reduce conformal contact between the two materials. This section describes how polishing each of the materials improves the conformal contact.

To evaluate the existing contact between the coating and substrate, a section was imaged under a white light microscope. A typical example of a good contact between the coating and substrate is

shown in Figure 36. A key issue that can clearly be seen is the interface, which is not uniformly flat. There was also no specification on how flat the surface should be for successful processing. In the existing case, there is variation of the interface of about 5 μm . Taking the case of the LaserForge sample analysed above, deformation was about 0.3 mm into the substrate, so the deformation should clearly be seen here over the roughness of the interface, but it may require sub-micron interfacial contact.

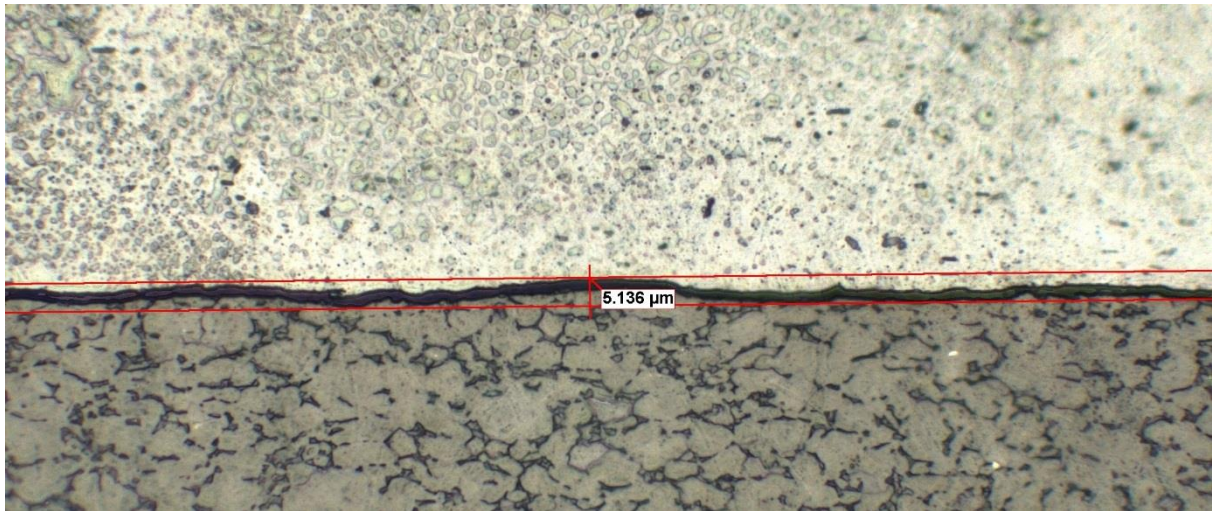


Figure 36: Interface between unpolished surfaces of aluminium (bottom) and Ti64 (Top). The variation at the interface is 5 μm .

One method of improving the interface would be to polish the materials prior to bonding. To investigate if this would have an effect, an interferogram was taken before and after polishing using a 3 μm diamond polishing solution. Polishing was performed until a mirror surface was achieved.

Prior to polishing the surfaces, the aluminium had 95 % of surface height within a 4 μm range. Following polishing, this reduced to 95 % of surface height within a 0.2 μm range. A similar improvement is seen for Ti-64. As can be seen from Figure 32 a variation of 0.5 μm was observed for bonded surfaces post polishing.

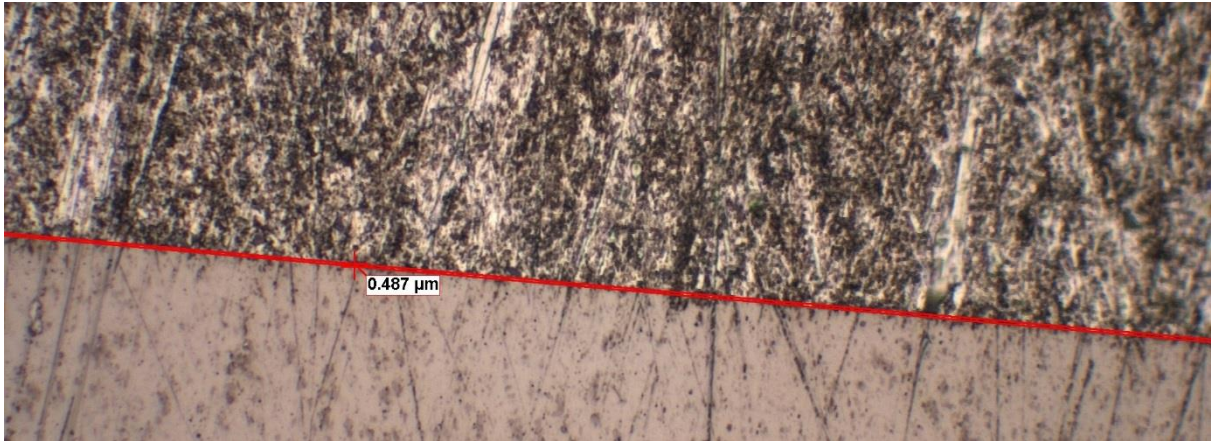


Figure 37: Interface between aluminium (top) and Ti-64 (bottom) after polishing surfaces that are in contact. The variation at the interface is $0.5 \mu\text{m}$.

In conclusion, the process of polishing the materials before bonding using the laser processing produces a significantly clearer interface that will clearly have good thermal contact and show if deformation has occurred.

4.8 Investigation of Surface Interaction Spot Size

Following on from the previous parameter map, it was theorised that the spot size plays an important role. To better understand this an experiment was devised to illustrate the effect of pulse energy and interaction time on the resultant laser-material spot size on Ti-64 in relation to the laser spot size.

Laser power from 500 W to 1500 W at intervals of 250 W were selected and mapped against interaction times of 0.5, 1, 5 and 10 ms. A fixed laser spot diameter of 1 mm was selected as it is believed to work for LaserForge. The resultant laser spots were imaged with a white light microscope and are presented in Figure 38.

Map of Surface Spot Size

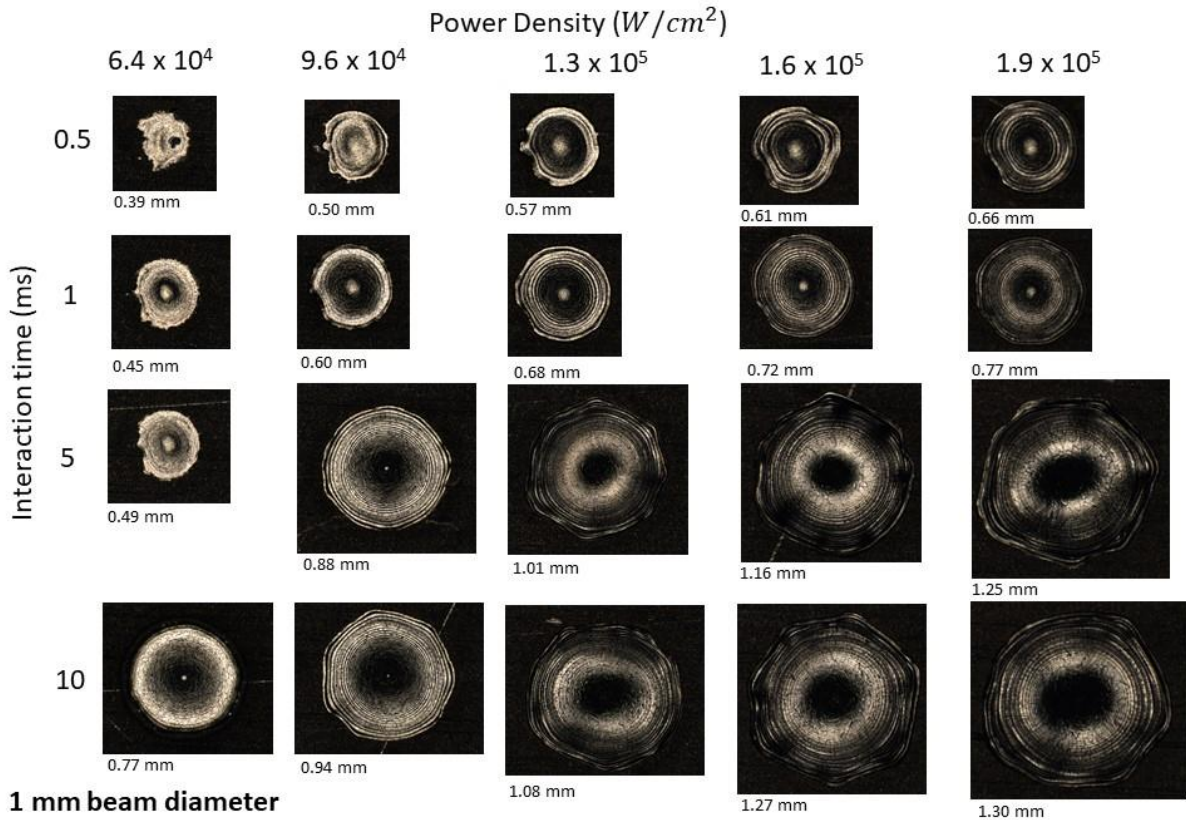


Figure 38: Parameter map for a 1 mm laser spot to illustrate how a combination of laser power and interaction time can change the surface area affected by the laser. Numbers under the dark field images indicate measured diameter of spot. No hole was observed but the ripple feature was three dimensional.

From the parameter map it can be observed that a variety of interaction spot sizes occurred. For the lower energies and shorter pulses material spot sizes were less than 1 mm. For longer pulses and higher energies spot sizes larger than 1 mm are observed. This illustrates that an area surrounding the laser beam is affected. In this case it is likely that significant melting is observed, and material is ejected from the central spot. This type of interaction where significant melting occurs is unwanted for the LaserForge process as it is desired for the material to be liquefied not melted and expelled from the spot. The rippling effect seen at larger power densities and interaction times are like those seen in the LaserForge sample. Interpolating the weld spot diameters for a LaserForge power density of $7.9 \times 10^4 W/cm^2$, would give a predicted spot diameter of approximately 0.85 mm, very similar to what was observed in the LaserForge sample above. This supports that experiments are being done in the correct parameter area.

4.9 Parameter Space Investigation with Fixed Pulse Energy

This section investigates the parameter space around the expected spot size parameter for LaserForge. A spot size of 1 mm was investigated. Additionally, a smaller spot size of 0.8 mm diameter was mapped to include the region with the power density equivalent to that used in LaserForge.

4.9.1 Processing Parameters

For the first experiment the laser spot size was fixed at 1 mm diameter. An additional experiment was done with a spot size of 0.8 mm diameter. Distance between pulses was 0.5 mm. The interaction time was varied, and the laser power was varied to change power density.

Unlike the previous parameter map, three lines of pulses were used, Figure 39 . The cross section of each therefore has three overlapping tracks for each parameter. The motivation for this is to evaluate if the wave shaped interface can be achieved from multiple overlapping pulses.

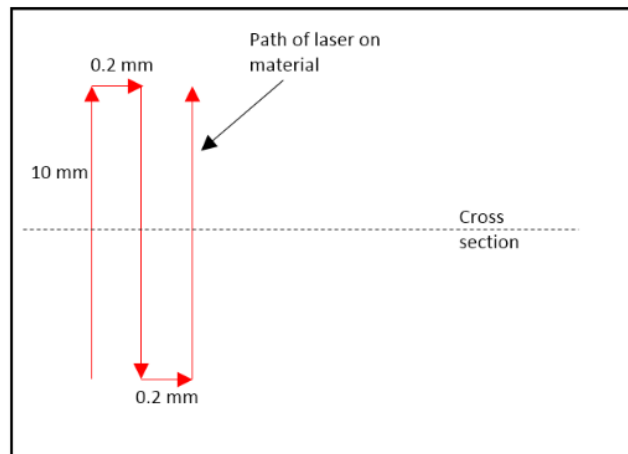


Figure 39: Diagram of the laser path on material from a top down view. Three overlapping tracks were made for each set of parameters.

4.9.2 Parameter Map

Each of the samples was sectioned, mounted in resin and polished before being etched with Krolls reagent. They were then imaged under a white light microscope.

The initial results for a fixed laser spot size of 1 mm are shown in Figure 40 and Figure 41. The expected result for LaserForge, calculated from the given intensity in the patent, was 616 W at 10 ms, however no deformation is seen for these parameters. Going to longer pulse lengths above 10 ms was not possible due to the constraints of the lasers operational range.

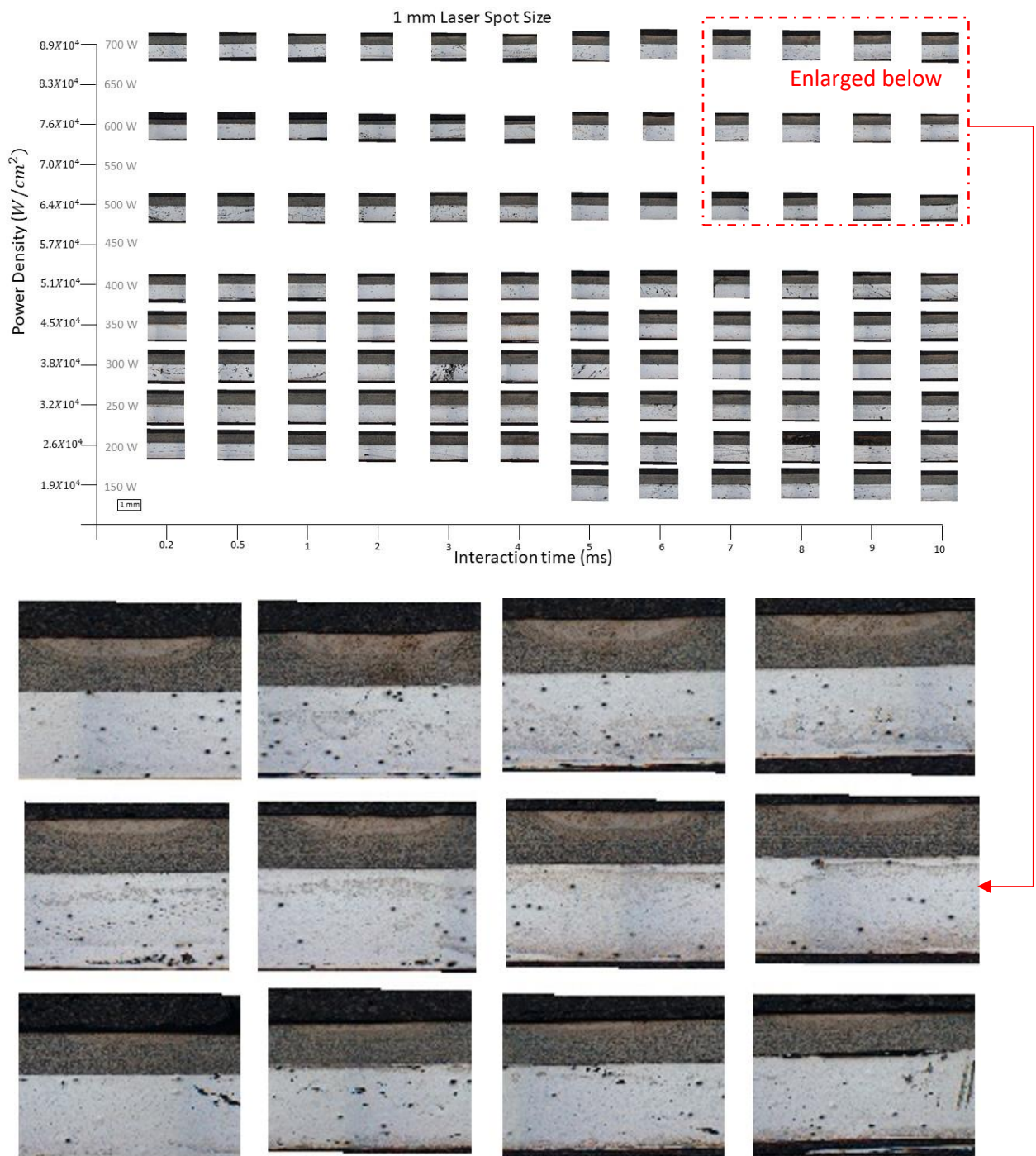


Figure 40: Parameter space for a fixed laser spot size of 1 mm of 3 overlapping tracks showing a laser affected zone on the surface of the coating material. Rows are of equal power density and columns are of equal pulse length. The surrounding dark material is the mounting resin, the dark grey material is the Ti-64 and the bottom material (missing on lower rows) is the aluminium substrate.

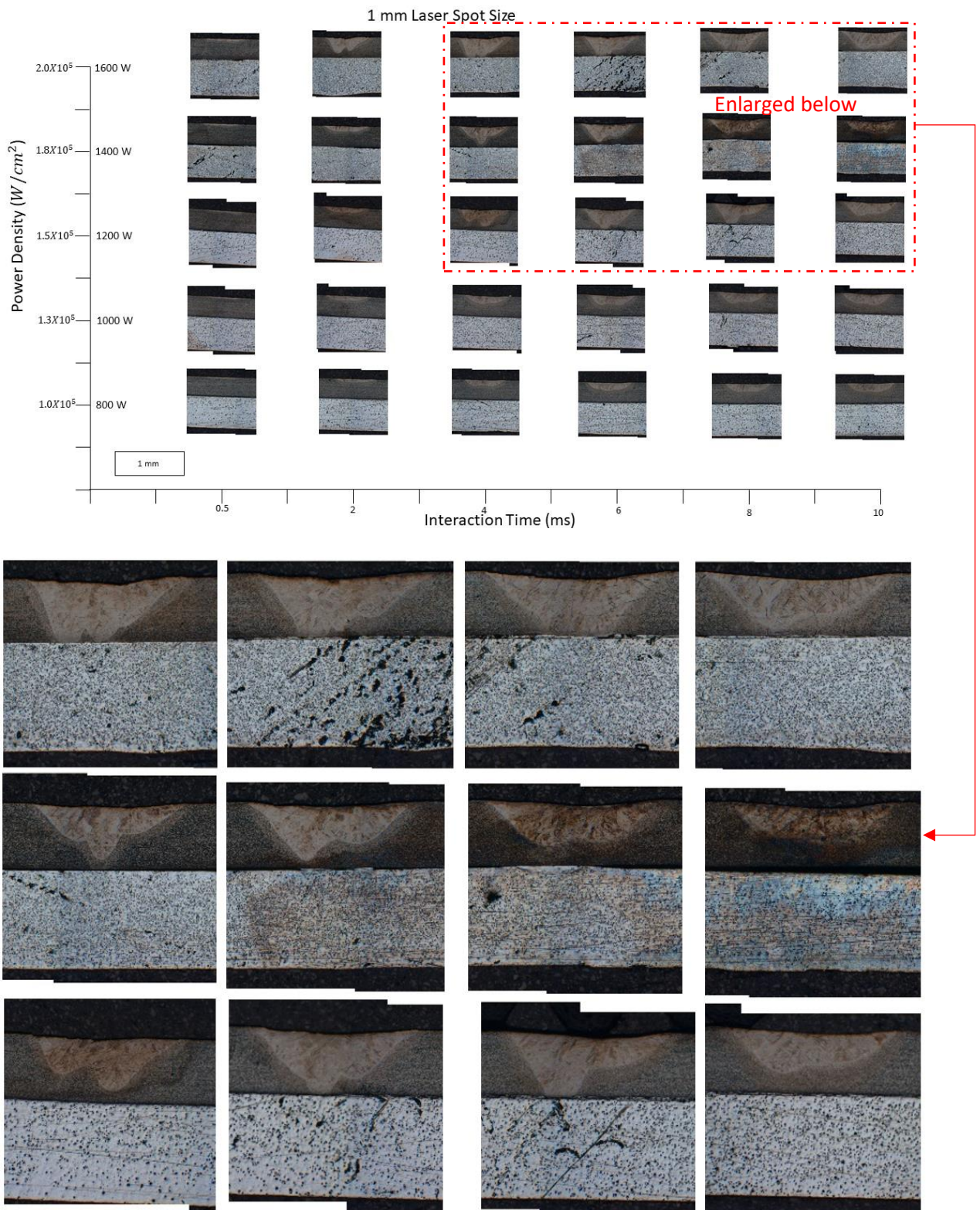


Figure 41: Parameter space for a fixed 1 mm diameter spot of 3 overlapping tracks at higher pulse energies.

As no bonding was observed here, an increase in power density was achieved by reducing the spot size to 0.8 mm diameter. Figure 42 shows the results from this reduced laser spot size.

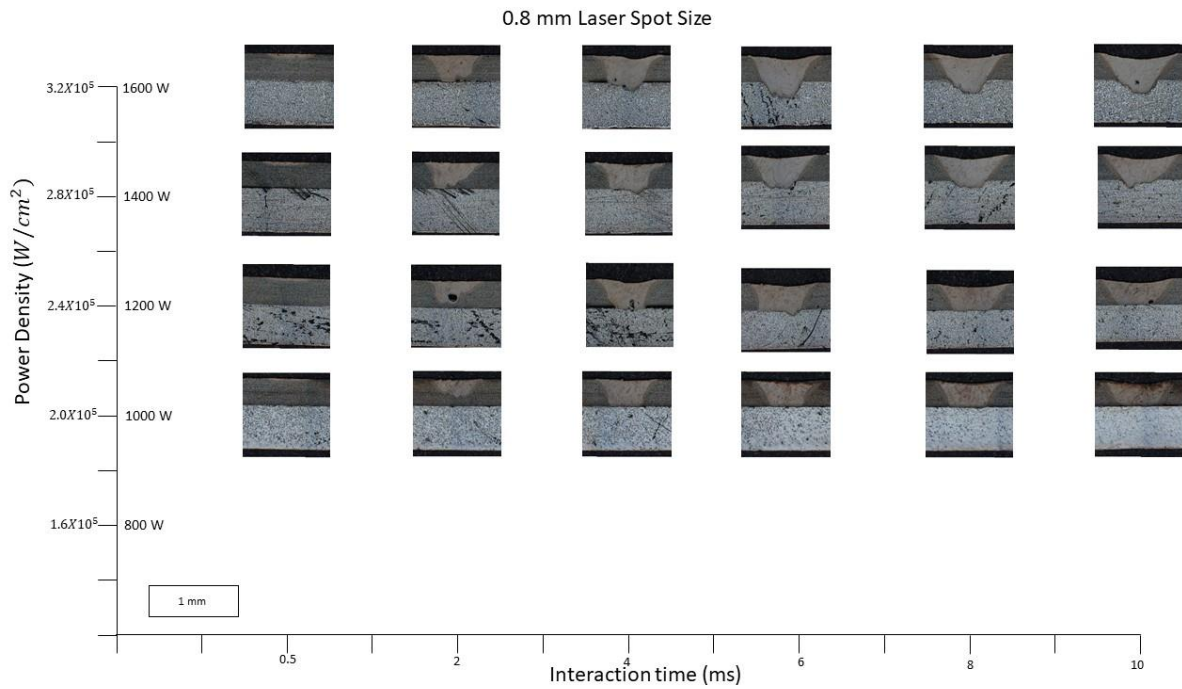


Figure 42: Parameter space for a fixed 0.8 mm diameter spot with 3 overlapping tracks at higher pulse energies.

At this reduced spot size, a power of 395 W would be expected to generate bonding at 10 ms pulse length. Results however show that bonding only occurs at over 1000 W of laser power. This bonding is similar in appearance to that seen for the previous parameter space map.

One potential reason for the need for higher power is that pulse shaping may be necessary to provide optimal heating of the coating material at these powers. Alternatively, longer interaction times than 10 ms may be necessary but not disclosed fully in the patent, but longer pulse lengths could not be explored using the current laser at higher powers.

Upon closer inspection of some of the bonding that has occurred in Figure 38, it can be clearly seen that a wave shaped interface is embedded into the aluminium as expected from the LaserForge Process, Figure 43. The optimal laser power appears to be 1400 W, this gives a power density of $2.8 \times 10^5 \text{ W/cm}^2$. This is approximately 3.5 times the expected power density.

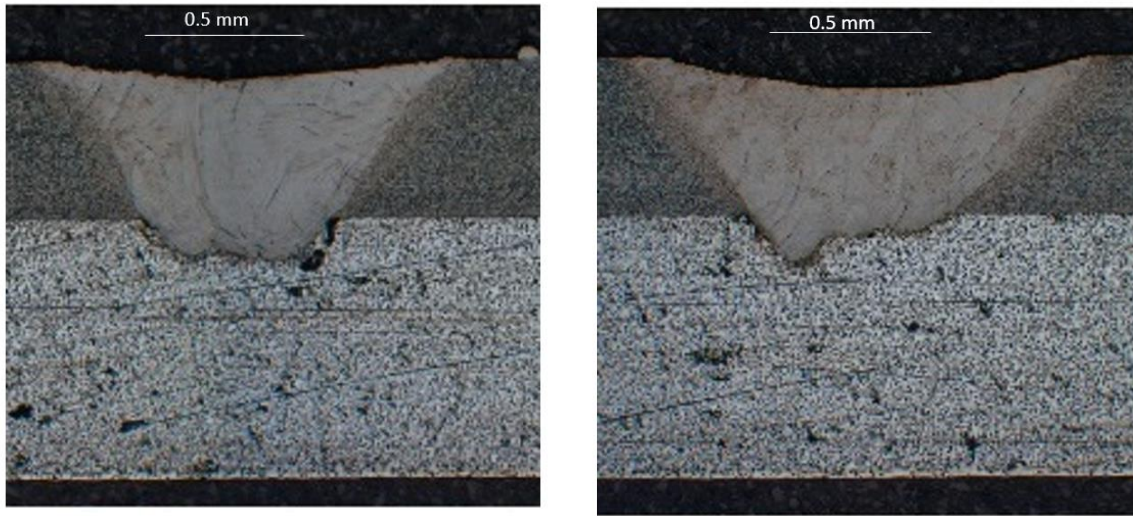


Figure 43: Examples of good bonding between the Ti-64 coating (top) and aluminium (bottom) with 3 overlapping tracks. The process parameters used were 0.8 mm laser spot, 6 ms pulse length, 1400 W (left), 10 ms pulse length, 1400 W (right).

This process that has been used to bond the coating the substrate would traditionally be described traditionally as a weld. However, it is exactly in the expected parameter space for LaserForge and visibly appears the same.

4.9.3 Conclusion from Parameter Space Investigation with Fixed Pulse Energy

This section has successfully reproduced the wave shaped interface of LaserForge, using parameters that are very similar to those expected for LaserForge.

Optimal parameters were found, although they were at a slightly higher energy density than expected. This may be because the process was not optimised, the laser used was different to that in literature, and pulse shaping was not investigated. Surface finish was also not investigated, which can affect the absorbed laser power. The as received finish was used which was visibly reflective, which may have reduced the absorbed energy. A longer pulse length may also be required to enable lower powers.

The cross section of Ti-64 coating appears very similar to that expected from literature on LaserForge, including the apparent material flow during the process. Based on the setup, good thermal contact between materials, parameters used and the response of the material, this should be classed as laser welding. The novel thing LaserForge appears to have done is optimise the process and heat input so that there is minimal mixing at the interface over large samples.

The only difference observed to what was expected in these samples was that we initially believed that LaserForge did not require re-melting of the whole coating. To investigate this discrepancy the LaserForge sample was re-etched below to understand if this was truly the case.

4.10 Further Analysis of LaserForge Sample

Following the exploration of parameters for LaserForge, the LaserForge sample was polished and re-etched with Ralph's etchant, which etches at a slower rate than HF based etchants. The etching was improved, and the microstructure was revealed more clearly, Figure 44. The microstructure appears to be continuous from the surface into the sample at the interface, making it unlikely that there is just a thin layer at the surface that was melted. It is also observed that the microstructure has formed radially outwards towards the bottom of the curved deformation.

Looking at the microstructure of this sample and comparing it to the results obtained using Ti-64 on aluminium above it appears that the LaserForge sample was likely formed using the same melt-based process.

The process can be optimised to minimise mixing at the interface, however it should not be described as a solid-state process as the material in the coating and at the interface has been melted.

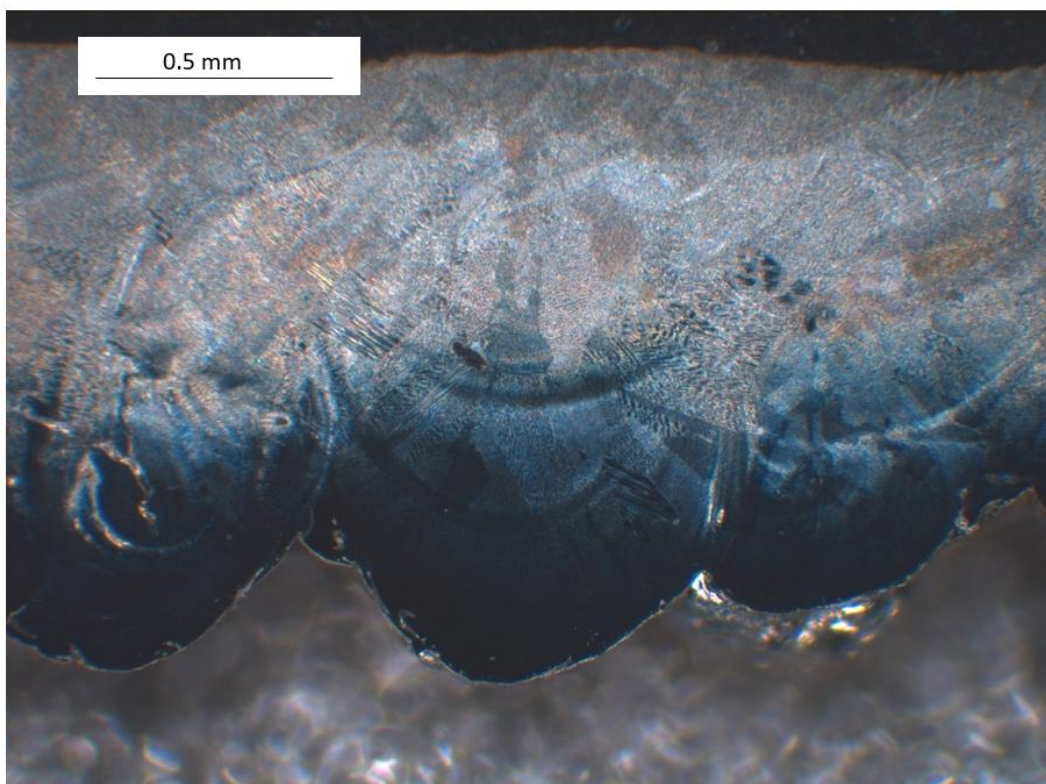


Figure 44: White light dark field microscope image of the LaserForge sample of In625 (top) on steel (bottom) etched with Ralph's etchant. The microstructure is clear although the sample is not etching at the same rate across the thickness of the coating. The steel has etched much more than the coating and is out of focus.

4.11 Conclusions from LaserForge Investigation

This chapter has investigated the LaserForge process which was the primary aim of this work. As part of this work a new laser system was set up to investigate LaserForge. This process was of interest due to the similarity to the cold spray process. The marketing claimed the process worked using solid-state metallurgical bonding, which would make it like cold spray. The potential knowledge gained from understanding the bonding mechanism was hoped to be beneficial to making future improvements in the cold spray and SLD process, which also coats materials using metallurgical bonding. A way of doing this could have been by adding a second pulsed high energy laser to the process to augment the existing coating technology, either through using the laser to compress existing coatings or reinforce weak interfaces by increasing their surface area.

Following analysis of the LaserForge process, it can be concluded that it is a mostly melt-based process. LaserForge can be described as pulsed laser welding of dissimilar materials, with a precisely controlled heat input to prevent material mixing at the interface. The coating material is completely melted, but the HAZ at the interface is negligible. Other coating technologies can have a large HAZ at the interface which causes a weakness in the coating structure.

As no novel bonding mechanism has been found, due to the mechanism having been identified as welding, the potential benefits from a novel technology are minimal. Adding a welding step into the SLD process is not attractive as the process requires the recrystallization of the coating material. The non-melting advantages of the cold spray process would be no longer advantageous, especially if the whole coating were to be reprocessed with a pulsed laser. However, there may still be some advantages to combining the two techniques. The investigation has shown that it is possible to precisely control the thermal energy when depositing a coating. This would suggest that the SLD process has significant potential for improvement in the area of thermal control from the laser.

The LaserForge welding process investigated here is capable of bonding two dissimilar materials together with minimal interface mixing. This means that both cold-spray and LaserForge have similar aims for bonding materials at the interface, even though the mechanisms are different. Using the benefits of LaserForge means that a high energy pulsed laser post process could improve the bonding and contact surface area at the interface and reduce delamination on difficult to deposit materials, so long as melting of the coating is acceptable. The cold spray part would therefore replace the wire placement control section of LaserForge. This proposition is less attractive due to the melt-based nature of the LaserForge mechanism.

An Alternative use for the LaserForge process could be to use a high energy pulsed laser in the laser assisted cold-spray process to deform the material immediately after the deposition site is at an

elevated temperature and may potentially be more mailable. This would be like existing pulsed laser deposition where a powder feedstock is used rather than a solid wire. This would have the benefit of requiring less laser power for deposition, and lead to reduced heat input into the substrate, therefore reducing the residual stress on the final part. The disadvantage would be that the coating material would be recrystallized, and for some materials such as WC-Co this would not be desirable. It would therefore only be desirable for materials that can be welded. It may also not be economically attractive when compared to laser cladding.

4.11.1 Suggestions for Further Work

Following the investigation into LaserForge, a new mechanism was not identified as hoped. This reduces the believed novelty of the LaserForge process. As the process uses already understood mechanisms and technology, there is nothing novel except the implementation into an optimised deposition system. The key value of LaserForge appears to be in the confidential IP of the deposition system design and deposition control algorithms. Some of the understanding from the LaserForge process, especially the deformation of the interface to improve bonding could be used to improve the SLD process. As the process is melt based this makes it less compatible with the solid-state deposition SLD process.

Recommendations for further work could be to implement one of the above described proposals. The issue, however, is that the residual stress of hard-to-deposit materials with supersonic laser deposition is not well understood and would require investigation prior to this.

Other laser processes could be investigated for their feasibility to be used with the cold-spray process. Three such processes have been identified. These were laser peening, laser heating and laser welding.

Much of this chapter has in some ways been looking at welding. This existing process could be adapted to reinforcing the SLD coatings, either in key locations to reduce delamination, or as a lower layer to reinforce the SLD boundary with the substrate. Such a layer could then be built up further with SLD on top.

Laser peening is a well-established industrial process. Its key benefit is to induce a residual stress into the surface of a material. Benefits to improving metallic coatings is that it is already proven and can improve the lifetime of components. It will however be generating additional residual stresses in an already stressed work piece. Experimental trials will be required to determine if adding additional stresses is beneficial to the process or would lead to a greater chance to failure and delamination of the coating. The effect of laser peening a potentially loose porous surface is also unclear at this stage. In addition, a water layer is often used, and this may be impractical for integration into the existing

system. This method also requires a very high energy pulsed laser which is not readily available in the current lab.

Laser heating has multiple possible avenues of exploration. The first is to remove the porous coating surface that results from SLD. This will have the benefit of reducing cracking and enhancing the corrosion resistance and lifetime of the surface. A second avenue of exploration would be the use of laser heating for the modification of residual stress. This could be done either in-process or post-process. If done in-process, laminated layers could be built up where residual stress has been released, rather than just releasing the residual stress on the surface.

Following the results of the LaserForge investigation presented in this chapter, it was decided to change the focus of work away from the LaserForge process. The new focus was to understand the main issues with the deposition of coatings in the SLD process. This change in direction was selected as it was the deposition technology that was targeted as potentially benefiting from LaserForge. Investigating its current issues with the aim to improve the process is therefore of benefit to furthering scientific knowledge.

5 Chapter 5 - Failure Mechanisms in High Performance Nanostructured Cold Spray Coatings

This chapter investigates the deposition and failure mode of a nanostructured coating deposited with supersonic laser deposition (SLD). The selected coating material for investigation was WC-17Co. The selected coating was deposited using the supersonic laser deposition process and analysed to determine its method of failure. This was done through investigation of the deposited interface, adhesion testing and four point-bend testing.

5.1 Motivation for Investigation of Failure Mechanisms in A Nanostructured Cold Spray Coating

Cold spray has been identified as an ideal candidate for use as a technology to deposit nanostructured coatings. Nanostructured coatings can provide benefits over other coatings by using a more complex material structure that can be used for demanding applications. It has been reported that these coatings can show improve wear resistance and toughness over conventional coatings [177]. SLD is a non-melt-based process that uses a low gas temperature, and therefore the material properties of the powder are retained once deposited, and the complex structure of the powder is retained.

This chapter looks at the deposition of an advanced material high-performance nanostructured coating deposited using the supersonic laser deposition process on a mild steel substrate. The material chosen was WC-17Co and the powder feedstock used is described in a previous chapter. This material was chosen as it is a representative nanostructured hard-wearing material that can be used as a coating in industrial applications but has typically been deposited using the melt based high velocity oxy-fuel (HVOF) process. This material has the potential for use in the hard facing of tooling, such as excavator bucket teeth. Hard facing components such as these teeth increases their lifetime and can result in a cost saving due to increased part lifetime. WC-Co is being marketed as a hard chrome replacement.

For this material the advantages of using supersonic laser deposition over the most commonly used HVOF process is that the low temperature nature of the cold-spray process removes the effect of decarburisation and reaction of WC and Co during spraying, preventing the formation of brittle phases [69]. There is very little work understanding the limitations of cold spray deposition of this material. The lack of ductility of the WC phase, makes it a challenging material to deposit, even though it contains a ductile Co phase. Existing work within the research group using supersonic laser deposition has shown that coatings are more easily deposited, than with cold spray alone. The addition of the

laser during processing which improves the ability to deposit the material, can result in undesirable cracking and delamination of the deposited coating.

A full understanding of the material failure mechanism of such a challenging nanostructured coating material, when deposited using the supersonic laser deposition process, is therefore required to demonstrate the feasibility for use in demanding commercial applications which currently rely on melt based thermal spraying deposition methods. The understanding gained from investigation of this material will be useful in evaluating deposition of other temperature sensitive nanostructured coatings with SLD.

This chapter will therefore look at the effects of the laser power on coating deposition, the bonding at the coating-substrate interface, the adhesion of the coating and the methods of failure of the coating when subjected to compression or tension using four-point bend tests.

5.2 Deposition of WC Supersonic Laser Deposition Coatings

This section investigates the deposition of WC-17Co coatings on a mild steel substrate. The aim was to look at the effect of laser power on the deposition of the coatings.

5.2.1 Deposition of WC-17Co with Cold Spray

WC-17Co is a material that has very low ductility. Due to its low ductility, a high particle velocity is required to deposit the material using cold spray. To achieve these high velocities, measured in literature to be >900 m/s, heated helium processing gas is required [178] [179]. The available cold spray system at the university is designed to work with nitrogen gas and can therefore not achieve the required velocity. The use of supersonic laser deposition however can reduce the required critical velocity, with the use of the laser, and therefore enable deposition of WC-17Co with a reduced critical velocity and the use of a lower cost gas. Low ductility WC based coatings, such as Ni60-WC have already been shown to be possible with supersonic laser deposition [180].

5.2.2 Deposition and Optimisation of Single Layer WC coatings

Initially it was necessary to determine optimal supersonic laser deposition parameters to deposit the WC-17Co powder that was used to coat a steel substrate.

Test tracks were deposited on mild steel of thickness 5 mm. Prior to deposition the substrate material was ground down using 180 grit SiC paper and water until the dark oxide layer of the as received material was removed. Any remaining grease was removed using a solvent. The initial parameters for the system were taken from a previous trial that had been done with WC-Co for a commercial partner. 6 overlapping tracks were deposited each of length 80 mm. The proportional–integral–derivative (PID)

loop was enabled and each set of tracks had an initial starting power and target temperature. The fixed starting parameters were as follows:

- PID target laser spot temperature = 1350 °C
- Step over between tracks = 2.13 mm
- Nitrogen gas temperature = 500 °C
- Traverse rate of deposition = 40 mm/s
- Powder feeder feed rate = 16000 (12RPM)
- Nitrogen gas pressure = 30 Bar
- Laser position relative to cold spray nozzle = 3 mm ahead of nozzle

In total 11 trials were done. Laser powers were observed from 1500 W to 4000 W. Due to the PID loop the output power varied along tracks and between samples as it ramped up and down to reach the target deposition site temperature recorded by the pyrometer. Results ranged from burning and ablation of the substrate above approximately 3000 W laser power to no deposition of the powder on the substrate below approximately 1800 W. These trials were done using temperature control, with target temperatures from 700 to 1500 °C. The best observed laser power for deposition was observed at approximately 2200 W. This produced tracks with a height of 0.5 mm and a track width of 3.2 mm, Figure 45. A higher laser power produces tracks of greater thickness.

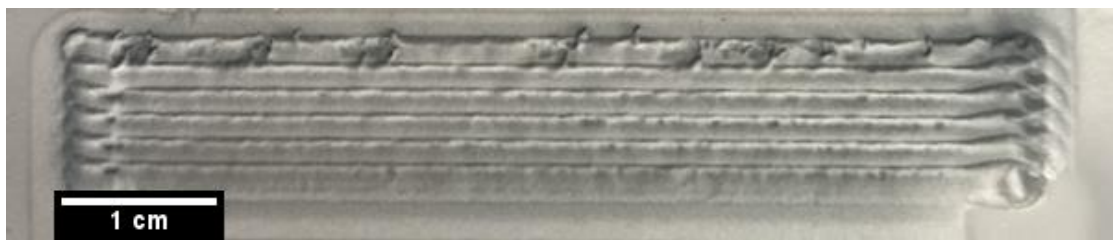


Figure 45: Six tracks of deposited WC-17Co coating on mild steel, tracks were deposited right to left starting at the top and were of thickness 0.5 mm.

Due to the variability of the recorded deposition site temperature from the pyrometer the PID loop was constantly changing the output laser power along the length of the sample. It was therefore decided to run future experiments at a fixed laser power without the PID loop. Further work could be done in future to improve the control of the PID when depositing WC-17Co, however this was beyond the scope of this work.

5.2.3 Effect of Laser Power on Deposition

This section looked to observe the effect of laser power on the deposited coating thickness. When observing the profile of the deposited track it was clear that it was not of even thickness across its

width. The centre of each track was much thicker with the thickness decreasing towards its edge. This was expected with this supersonic laser deposition system. As each deposited track had a cross section profile of a mound, the distance between each track was decreased to 2 mm to reduce the dips between the tracks and result in a flatter deposited area.

To understand the effect of increasing laser power on the coating thickness, an experiment was run to measure the thickness of coatings with different deposition laser powers. The range of laser power selected was in the area where deposition was successful, outside these areas the coating was deemed to be unsuccessful due to burning/melting or almost no deposit. From the initial testing a laser power of 1800 W and below resulted in no deposition, and a laser power of 2600 W and above resulted in melting of the substrate. Below 2300 W the coating was considered poor. The results are shown in Figure 46.

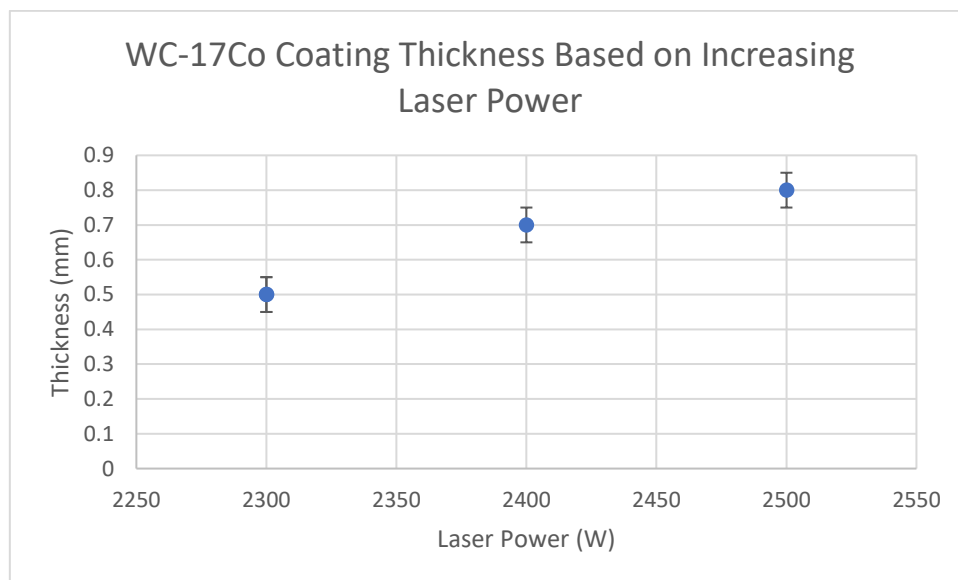


Figure 46: Graph showing how the coating thickness of a WC-17Co coating changes with increasing laser power used during deposition.

The results show that the deposition thickness of the coating can be controlled by the laser power. A change of 100 W of laser power can have an effect of up to 0.2 mm thickness change on the deposited coating. The small range of available powers to give a good coating is a very narrow range, especially given the absolute power of about 2500 W. This gives a very small range of ~10 % of the absolute value for the control of the system.

5.3 Analysis of WC-17Co Supersonic Laser Deposition Coatings

This section investigates the deposited coating and the methods by which it fails. This is done in three ways: Through cross sectioning, adhesion testing and four-point bend testing.

5.3.1 Cross Sectioning of WC-17Co Coatings

To understand the quality of the deposited coating, samples were cross sectioned, mounted and polished as described in the materials and methods chapter. Once mounted the sample could then be imaged under a white light microscope. An image of the cross section was then made; an example is shown in Figure 47. This image shows the deposited tracks well bonded onto the steel substrate with minimal porosity. It was noted that there was a dark line at the interface. When this was imaged at a higher magnification using a white light microscope, it was not clear what was occurring, Figure 48.



Figure 47: WC-17Co coating (top) on mild steel (bottom) encased in mounting resin (black). The periodic dark vertical streaks in the image are an artefact of stitching multiple images together.

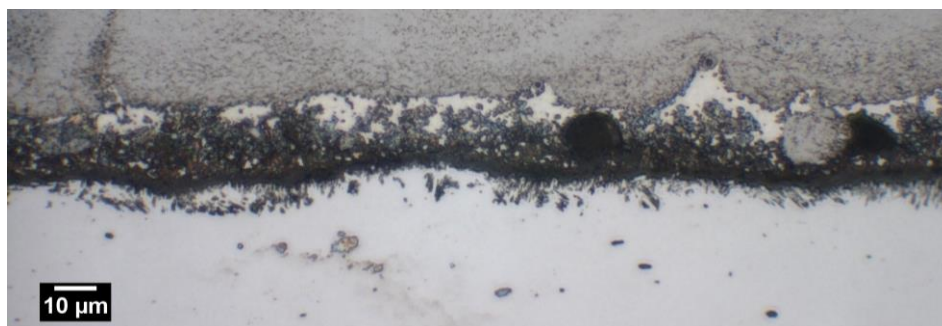


Figure 48: A magnified view of the interface of the WC-17Co coating (top) on mild steel (bottom) showing a section where there is an unidentified dark area.

Due to the uncertainty over what was being observed at the interface when seen with a white light microscope it was necessary to image the interface at greater magnification under an SEM.

A sample showing this dark area at the interface was loaded into the SEM and imaged. Some areas of the coating were well bonded with a sharp edge at the interface, Figure 49. Other areas of the coating where the dark line was most prominent shows a less clear interface, Figure 50.

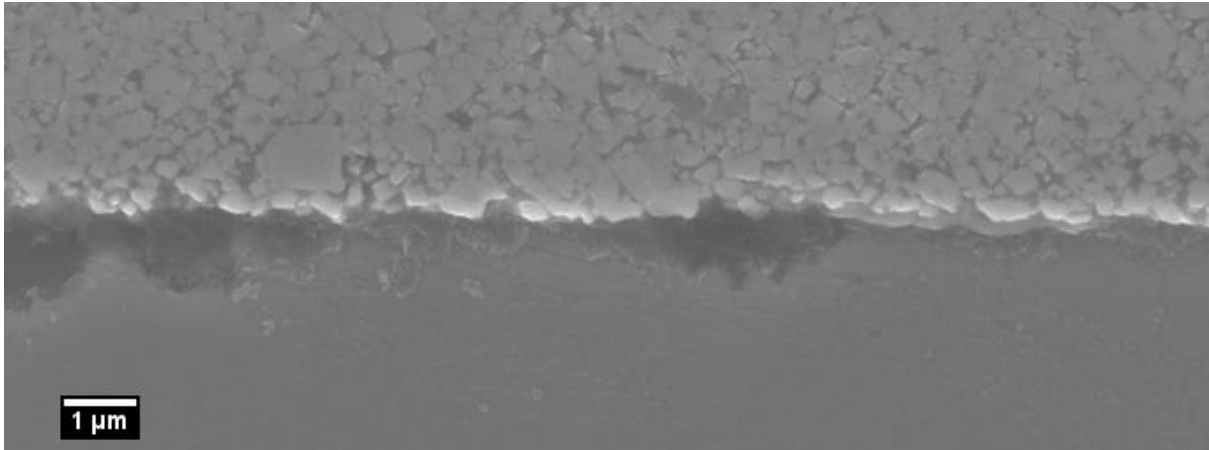


Figure 49: SEM image of the interface of WC-17Co (top) coating on mild steel (bottom). This shows a clean edge to the interface between the materials.

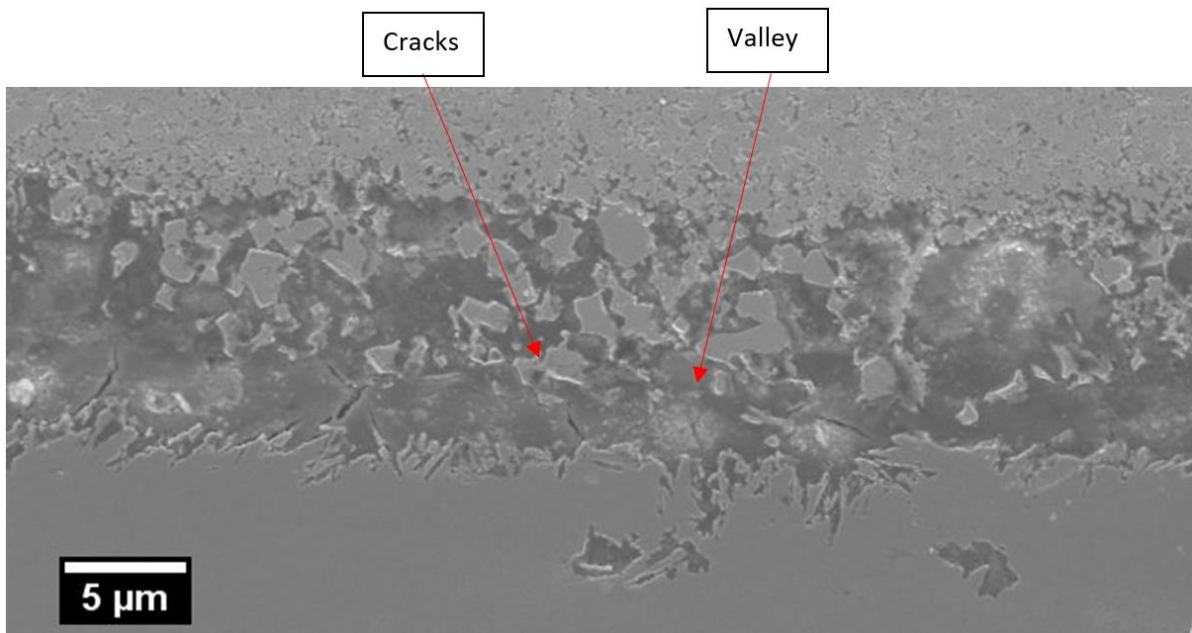


Figure 50: SEM image of the interface of WC-17Co (top) coating on mild steel (bottom). The image shows that there is a region at the interface where the two materials appear to have been changed, and not formed a clean interface as expected in supersonic laser deposition. Within this region which was slightly recessed, cracks were visible. It was suspected that some mixing had occurred of the two materials.

Having identified a clearly defined middle region at the interface, Figure 51, an EDX analysis was performed to identify the materials present and determine if any mixing had occurred.

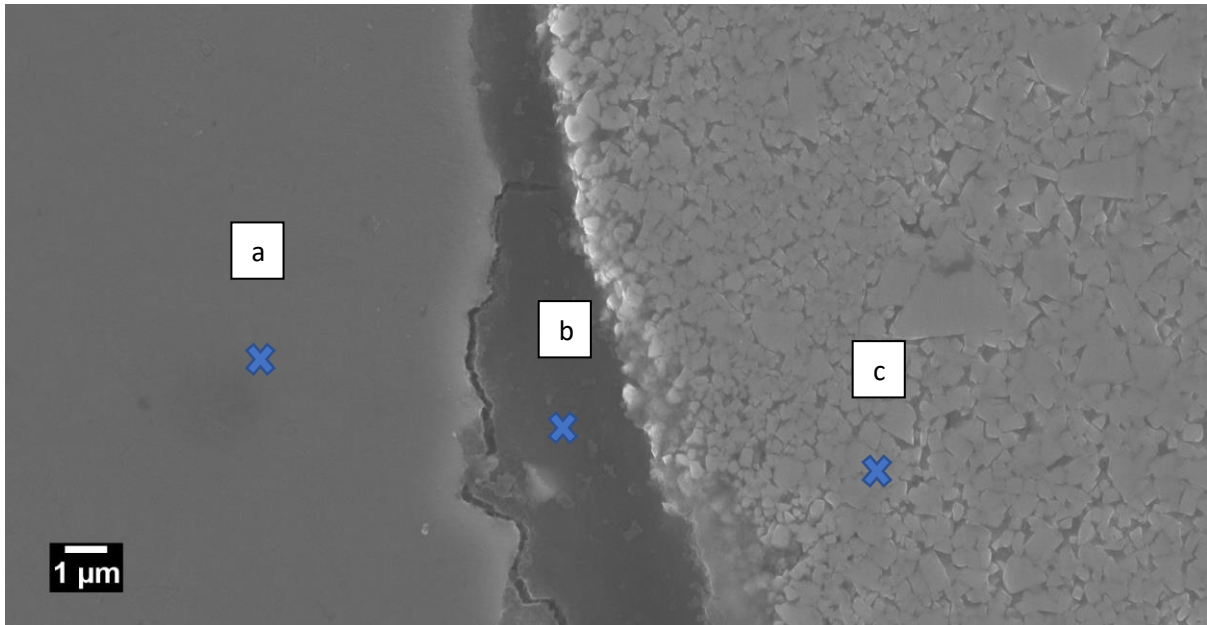


Figure 51: Image showing the location of EDX sampling. (a) within the steel substrate, (b) within the unidentified interface and (c) within the coating.

Three distinct areas were measured with EDX, (a) Within the substrate, (b) Within the unidentified interface and (c) Within the coating. The resultant spectra indicate the strong presence of oxygen, tungsten and iron at region (b). It appears that the coating and substrate have melted and oxidised to form the darker region at the interface. This is likely caused due to the heat from the laser during the deposition process. This oxidised region has potentially caused a weakness in the interlayer by making it brittle and has led to the undesirable cracking seen. An example at site a is shown in Figure 52, the full spectra along with the identified elements are shown in the appendix.

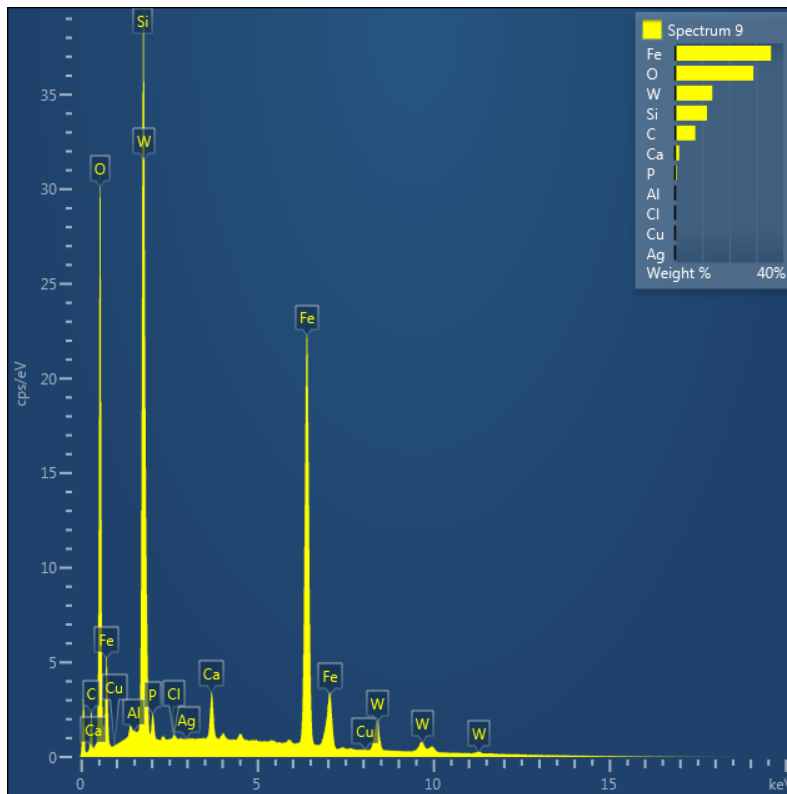


Figure 52: EDX spectrum from location (b) within the interface layer between substrate and coating.

5.3.2 Investigation of Coating Adhesion

To determine the adhesion strength of the deposited coatings, adhesion pull-off testing can be used. This section presents the results of pull off testing to determine how well the WC-17Co supersonic laser deposition coating had been adhered to the substrate during deposition.

To quantify how well bonded the coatings are to the substrate, a pull-off test was performed. The precision adhesion tester described in the materials and methods chapter was used to test an “as deposited” coating. Results for the “as deposited” coating, Figure 53, showed that the top layer of the coating pulled off with the glue. The mean force required before the top layer failed in three trials was 52.2 MPa.

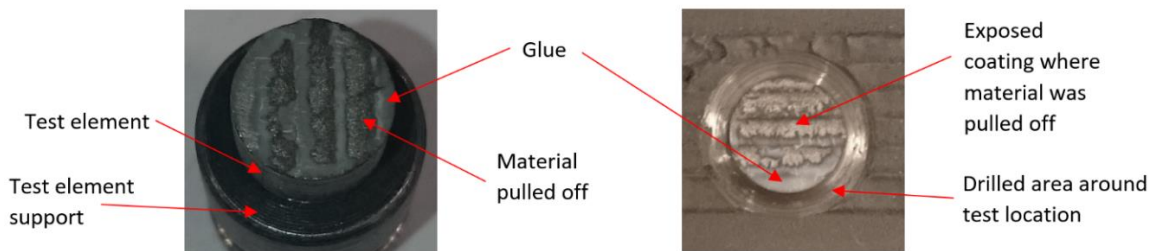


Figure 53: Example of a typical result from the pull off test on the as deposited material. The pulled off test element is on the left and the corresponding remaining substrate is on the right.

The results of this test show that the coating has failed in the top layer of deposited coating. Due to the mechanism of deposition the very top layer of each track is not fully consolidated and therefore it is failing within this weaker top layer rather than the bulk coating layer.

As it is desired to test the adhesion of the coating at the interface, the test was repeated with the top layer of the coating ground off. This ensured that the test element and glue had good bonding to the main bulk of the coating.

To remove the top surface coating layer a diamond impregnated MD Plano 220 disk with water as lubricant was used. The disk was rotated at 200 RPM and the sample was polished by hand, due to its unconventional shape for the system, until a flat surface was visible over the desired test area before the test elements were glued on. A control test sample of mild steel was also ground down using 180 SiC grit paper and water as lubricant until the darker surface layer had been removed.

A representative sample of the results from this pull off test is shown in Figure 54.

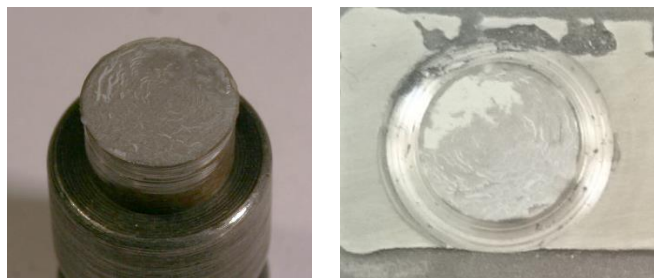


Figure 54: Example of a typical result from the pull off test on a ground down coating. The image shows that the glue failed and remains stuck to both the test element (left) and the substrate (right).

The results of the pull-off testing showed that the location of failure was within the glue rather than at the interface or within the material. The epoxy was rated to 70 MPa and the results obtained all show a failure value greater than this. This shows that the coating has both an adhesion tensile strength and internal material tensile strength of at least 70 MPa. It is not possible to obtain a higher tensile strength value for coating adhesion using this method due to bonding epoxy of much greater tensile strength not existing. The control experiment on uncoated steel showed similar results of failure of the glue.

These results are significant as they show greater adhesion than the 50 MPa shown in literature for some HVOF thermal spray coatings of WC-17Co, Staia (2000) and Siegmann (2005) [181] [182]. In more recent years increased adhesion strength of >70 MPa is now possible for HVOF which is considered sufficient for commercial use, Du et al. (2013) [183] [184]. Supersonic laser deposition of WC-17Co is therefore comparable with HVOF in this respect.

5.3.3 Investigation of the Failure Mode of Coatings

This section describes a four-point bend test that was devised to test the performance and point of failure of WC-17Co coatings under both tension and compression. This type of test is useful for these coatings as they are likely to be subjected to some tension and compression in the location of the coating during commercial use.

5.3.3.1 Four-Point Bend Testing

A four-point bend test was selected as it provides a more even distribution of the stress across the coating. This means the coating will fail along its length, rather than at the point directly below the load contact point.

To determine how and when the coating fails, a method using acoustic emission (AE) was used to monitor the sample during testing [185]. The acoustic emission sensor could detect acoustic (elastic) waves that are produced when cracks are formed in the sample. These elastic waves propagate through the sample and can be detected using the sensor on the surface of the sample.

A sample of mild steel coated with WC-17Co on one side was used. The steel was 5 mm thick and measured 25 x 250 mm. The top surface of the steel was sanded down using a mechanical sander prior to being coated to remove the dark oxide layer. The coated surface was 150 mm in length and covered the full width of the steel. The sample dimensions were selected to enable bending with the 5 kN tester and have a thick enough substrate to prevent the sample significantly bending due to the spraying of the coating. The bend tester and sample were setup in the geometry shown in a previous chapter.

Following some initial investigation, a displacement rate of 7 mm/min was chosen so that there was enough time within the test for the coating failure to be monitored with AE to show a significant increase in activity when the coating failed. For consistency, the engraved label of each bar was on the right-hand side. The AE sensor was always on the top right, positioned at the end of the bar. Load contact cylinders of diameter 1.2 mm were used. The experimental setup is shown in Figure 55.

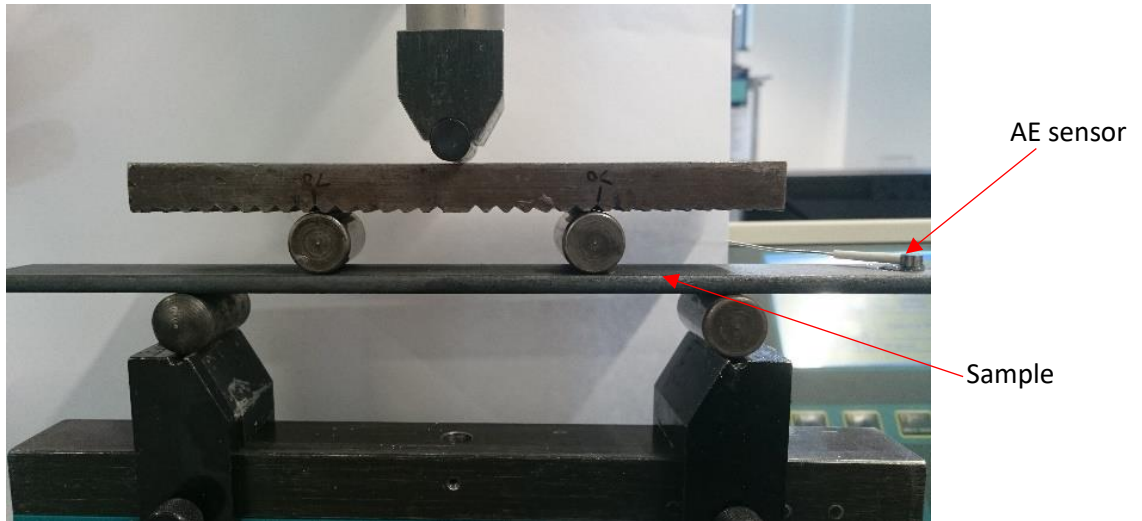


Figure 55: Image of a sample bar placed in the bend tester prior to bending. The load was applied from the top and distributed into the sample using a conversion bar, resulting in four points of contact for bending.

Samples were first tested with the coating in tension. This meant that the coating was on the underside when being tested. Three uncoated steel bars were also tested for comparison to understand the difference in the AE signal obtained with just the substrate failing.

An example of a graph of AE activity obtained is shown in Figure 56. The graph shows that above about 3000 N the AE activity increases significantly. Prior to this is a pre-cracking phase where there are a number of random events as the force on the sample is increased [186] [187].

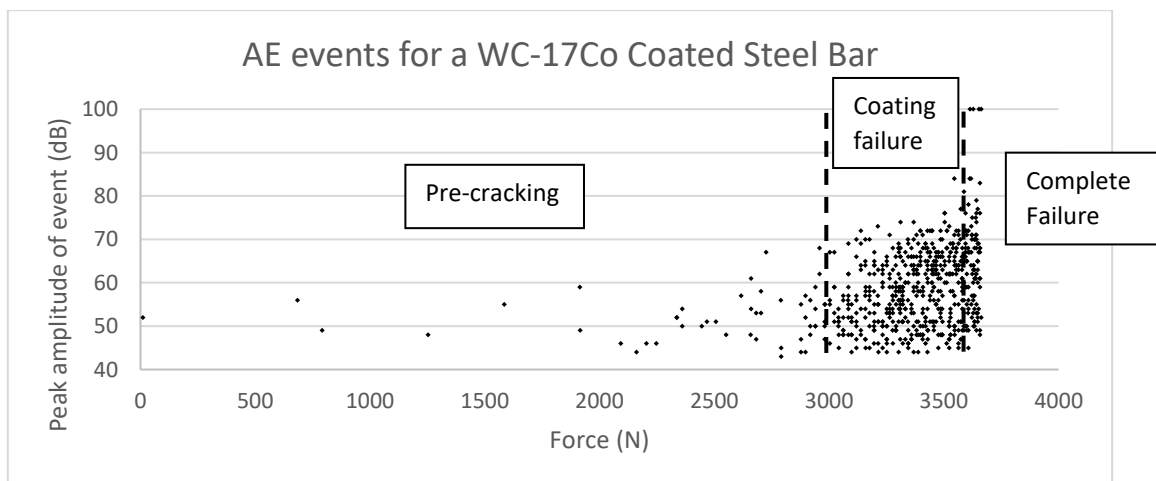


Figure 56: Graph of the AE events for a steel bar coated with WC-17Co undergoing a four-point bend test in tension. There are three phases to the signal, the first is pre-cracking where a random number of events occur. Subsequently the rate and maximum amplitude of events increases at the point of coating failure. A final increase in the peak amplitude shows the point at which complete failure occurred, this is usually accompanied by fragments of the coating being projected away.

It is interesting to compare this to the AE graph of an uncoated bar, Figure 57. This graph again shows pre-cracking, but then fails rapidly once reaching a given force.

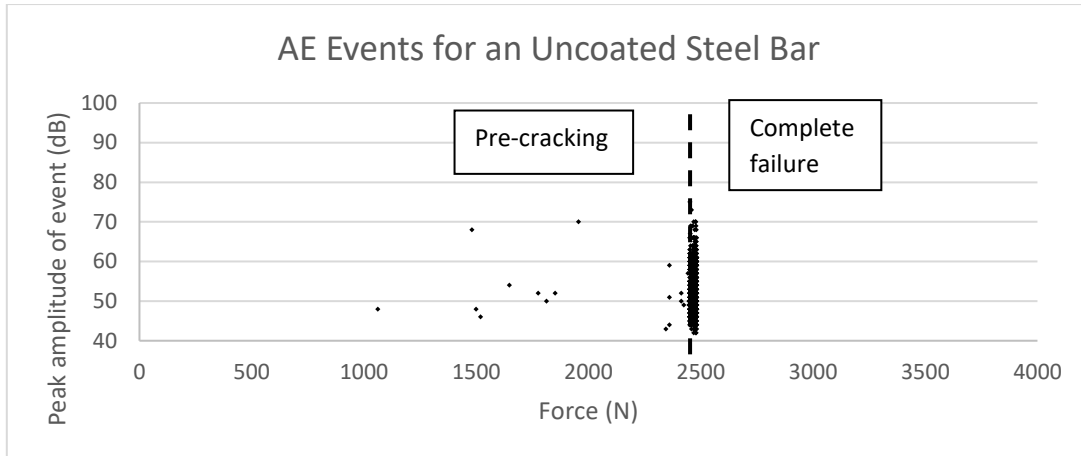


Figure 57: Graph of AE events for uncoated steel bar undergoing a four-point bend test. The graph shows two phases: The first of pre-cracking where load is taken up by the bar, the second where the bar fails catastrophically almost instantly.

For each sample, the point of failure was taken to be the point at which there was a significant increase in AE activity. This point was calculated using a histogram to visualise the increase in frequency. From this value, stress-to-fracture and strain-to-fracture have been calculated.

The stress to fracture and strain to fracture at the outer surface were calculated using the following formulae for 4-point bend tests, Equation 1 and Equation 2 [188]. F is the force applied in N, L_2 and L_1 are the outer and inner span of the apparatus in millimetres, b is the sample width, h is the thickness of the sample, and D is the deflection of the sample at mid span in millimetres.

Equation 1

$$|\text{Stress (MPa)}| = \frac{1.5F(L_2 - L_1)}{bh^2} \quad (1)$$

Equation 2

$$|\text{Strain (\%)}| = \frac{436Dh}{L_2^2} \quad (2)$$

When calculating the strain, the displacement of the centre of the bar was calculated from the displacement of the load contact points. This was done by modelling the steel bar in Matlab to calculate the difference between the contact points and ideal central point at max deflection,

assuming no failure. This is shown in Figure 58. A typical load contact point deflection at the point of failure of a coated bar was 3 mm.

The maximum deflection at the roller load contact points was calculated by

Equation 3

$$\frac{Wa^2}{6EI} (3l - 4a) \quad (3)$$

The maximum deflection at centre was calculated from

Equation 4

$$\frac{Wa}{24EI} (3l^2 - 4a^2) \quad (4)$$

W was the load on the beam, I the moment of inertia, E the modulus of elasticity [189]. The difference between these was used to correct the model for stress and strain.

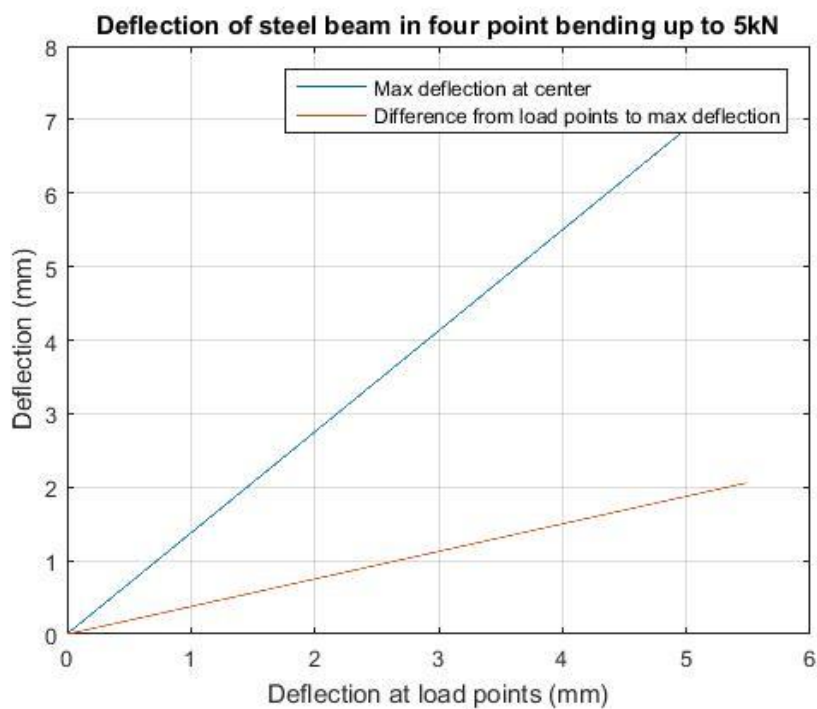


Figure 58: Plot modelling the deflection difference of the maximum displacement compared to displacement of the load points. A typical deflection at the point of failure was 3 mm.

The results for each of the samples under tension are shown below, Table 4. These values are for the outer surface of the bar. These results show that in the case of each the uncoated and coated samples, the force at failure was very similar (within 10 %). Interestingly it was observed that the coated samples failed at a higher force than the uncoated bars and therefore increased the stress in the surface layer required for failure over an uncoated bar by about 800 N or 140 MPa, a significant difference of around 25 %. The stress to fracture for the WC-17Co coated bar was similar to the 600 MPa that has been reported in literature for HVOF sprayed coatings [190].

Table 4: Results of four-point bend testing of a coating in tension for coated and uncoated samples.

Sample	Force at failure (N)	Stress to fracture (MPa)	Strain to fracture (%)
Blank 1	2380	400	0.38
Blank 2	2420	410	0.39
Blank 3	2450	410	0.40
148.4	3150	530	0.43
148.6	3350	560	0.41
148.7	3210	540	0.45
148.8	3300	550	0.43

Further to testing the coatings in tension, another series of coated samples were made, for compression testing. The same procedure as above was used, and the results are shown in Table 5. During failure, audible cracking could be heard with small flakes of coating being projected off when the coating catastrophically failed.

Table 5: Results of four-point bend testing in compression.

Sample	Force at failure (N)	Stress to fracture (MPa)	Strain to fracture (%)
167.1	3000	500	0.62
167.2	3390	570	0.54
167.3	2622	440	0.58

These results show a similar reinforcement effect, although the strain-to-fracture is greater for all samples. The force at failure is similar in value to the failure when in tension, although the spread of values is greater. These results indicate the samples were bent more than with the coating in tension but with the same force to achieve coating failure.

To ensure the reinforcement effect is not due to heat hardening from the laser and gas, another set of samples were made using steel bars sprayed using Al₂O₃, a material that does not form a coating when using the deposition parameters for WC-17Co due to its different powder properties such as

density. These samples were exposed to the same laser thermal effects as well as the peening effect from the spraying of material as the WC-17Co samples. These samples were tested using the same method as the coated samples with the “coated” side under tension, Table 6.

Table 6: Results of four-point bend testing in tension for the Al₂O₃ sprayed bar.

Sample	Force at failure (N)	Stress to fracture (MPa)	Strain to fracture (%)
180.1	2450	410	0.55
180.3	2320	390	0.41
180.4	2210	370	0.40

These results show a similar force at failure to the uncoated bars tested, indicating that the significant increase in force to failure seen from the WC-17Co coatings is not due to the thermal effects of the laser and heated gas but primarily due to the coating material. The strain however indicates that the samples bent more than the untreated bars but did not require any greater force to deform them, indicating they were slightly more malleable after treatment.

5.3.3.2 SEM Analysis

Following coating failure in tension and compression, the evidence for the type of failure during bend testing can be found from high magnification images of the fractured interfaces. To do this, coating fragments obtained during the coating failure experiments above were imaged using an SEM to view the fractured surfaces.

At low magnification, the coating appeared as though it was fractured in a sharp brittle break. At higher magnification, however it is much easier to see the fine structure of the surface, Figure 59 and Figure 60. Unlike coatings that are of a single material, the coatings seen here are made up of larger fragments of WC encased in a cobalt matrix. When looking at how the surface has been formed, the matrix that holds the WC particles in place appears to have been stretched where the larger particles have been pulled out. This would suggest that the failure was plastic in nature rather than a clean brittle fracture which would not have this distortion.

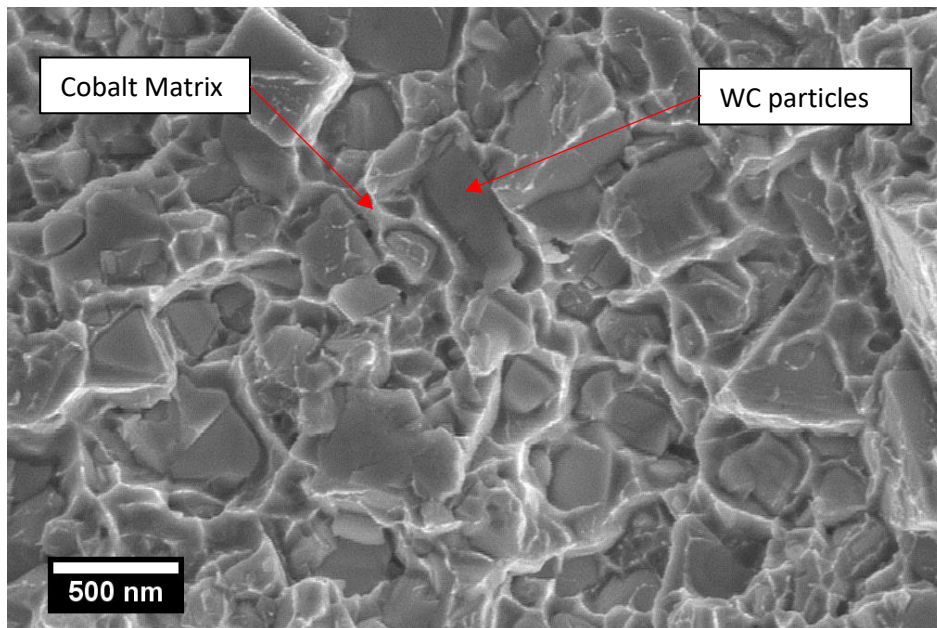


Figure 59: SEM image of the fractured surface of a WC-17Co coating in tension. The cobalt matrix has been distorted indicating a plastic deformation during failure.

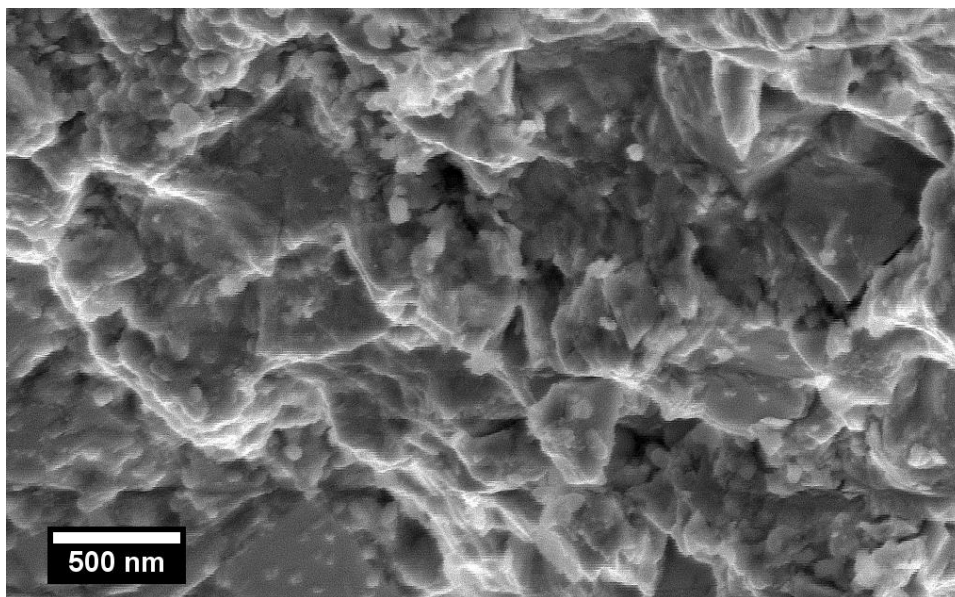


Figure 60: SEM image of a fractured WC-17Co coating under compression. The cobalt matrix has been distorted indicating a plastic deformation during failure.

On some coated samples, the coating could be chipped off using the sharp impact of a tool. This was mainly near the ends of the coating tracks where the coating was less well adhered to the substrate, due to the stage accelerating rapidly at the start of a track. To understand to what extent the failure occurred, a fragment of coating chipped off by impact was imaged at high magnification in the SEM.

In areas where the coating had fractured within itself a similar surface to that seen above was observed. However, the main reason this coating had fractured off the substrate was evident from

most of the fragment that was in contact with the substrate. As seen in Figure 61 there is significant porosity in the layer that is in contact with the substrate. Only a small proportion of the overall surface area is therefore in contact with the substrate. This means that the bulk of the coating is not well bonded to the substrate and can easily be broken off during impact.

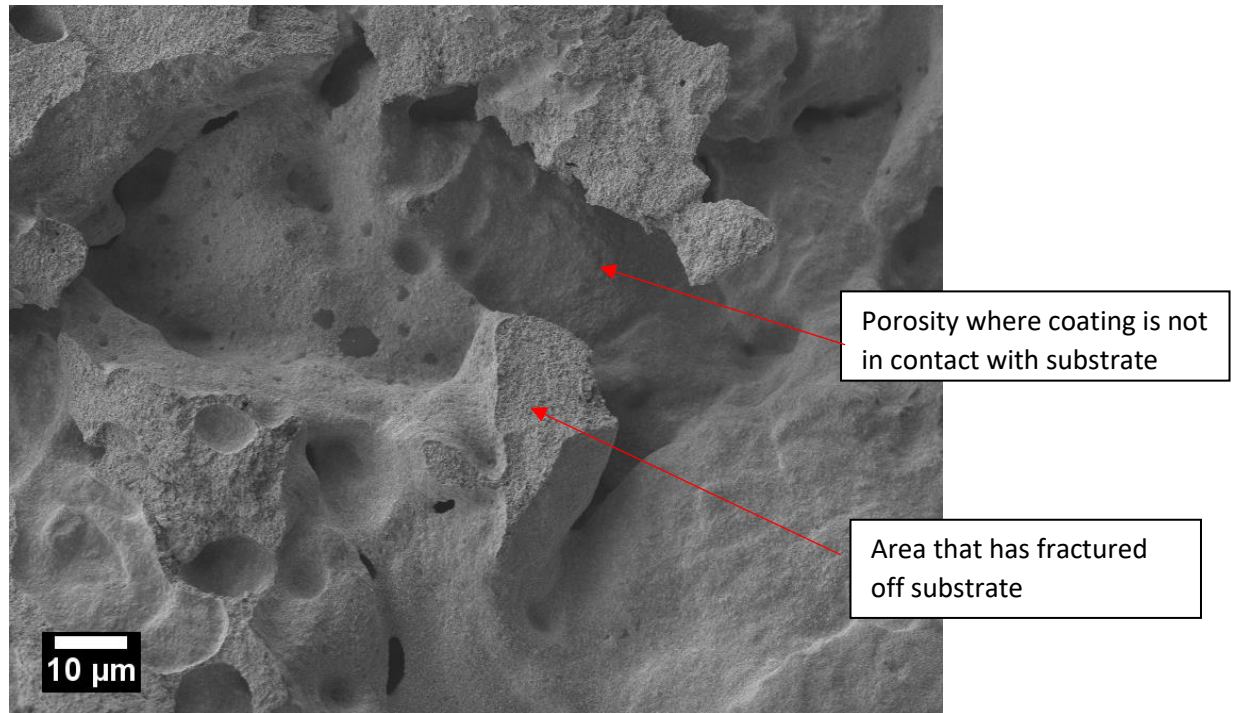


Figure 61: Fractured surface of a WC-17Co coating which was in contact with the substrate near the start of a deposited track. The image shows porosity where the coating is not in contact with the substrate, meaning there is limited surface area available for bonding to the substrate.

5.3.3.3 Failure Analysis

The results presented indicate the failure mode was plastic in nature. To further investigate the method of failure it is of interest to further look at the results from the bend testing. The graph, Figure 62, shows that the bar does not provide a constant resistive force before failure, indicating a plastic deformation. This bending of the force - time/displacement curve is significant until there is a sudden failure of the coating, often corresponding to a large section of coating being ejected from the sample with a loud crack. If the coating failed in a brittle manner, there would be a linear increase in force followed by a sudden failure of the coating.

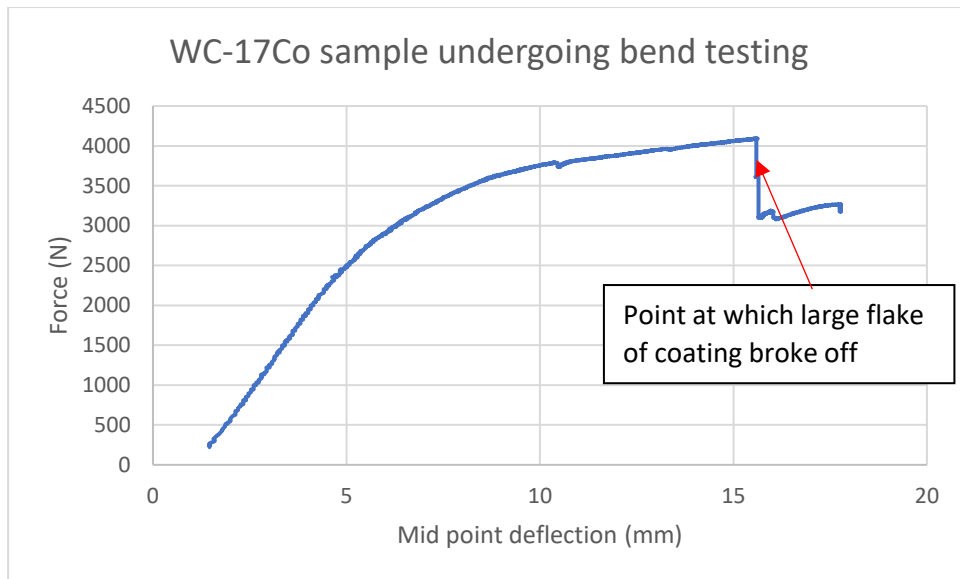


Figure 62: Graph showing the force vs. deflection profile for bending of a WC-17Co bar under compression. The increase in force is not linear indicating an amount of plastic deformation prior to complete failure at about 90 seconds.

As an illustration of how well the coatings are bonded to the substrate, it is possible to bend a metal bar almost in half. In doing this the coating fails within itself, with it barely coming detached from the substrate.



Figure 63: Image of a WC-17Co coated steel bar bent using a vice. The coating is shown to stick well to the substrate and fractures within itself in preference to breaking off.

The result indicates that as the coating failure is not sudden, it could be predicted using in situ monitoring should the need arise. The fracture tensile stress properties of Co are quoted in literature as being in the range of 295 MPa to 485 Mpa. Critical stress values are typically quoted by

manufacturers for the WC phase in the range of 350 MPa to 550 MPa. The critical strain is estimated to be 8 % for Co and 0.1 % for WC [191]. For one example of a model of an excavator bucket tooth, the estimated digging force loading can be up to 280.7 MPa and a resistive force loading of 21.1 MPa for stress. Both these values are less than the minimum stress of 440 MPa to fracture observed in these tests. It can therefore be concluded that the use of such coating in this condition would survive use and be within the elastic limit of the coating [192].

5.3.3.4 Conclusions

From the above evidence, it can be concluded that the mode of failure of the WC-17Co coatings deposited with supersonic laser deposition is plastic in nature. If the coatings are well bonded to the substrate, then they have been seen to fail within the coating before failing at the interface with the substrate. Where coatings are not well deposited and bonded to the substrate they can be chipped off due to porosity or cracking from within the layer immediately in contact with the substrate.

In conclusion, this section has demonstrated that the failure mode of supersonic laser deposition sprayed WC-17Co is plastic in nature. This has been done using four-point bend testing of the coatings in tension and compression, along with SEM analysis of the fractured surfaces. There is also the benefit in that if the component is deformed by a small amount, the coating will not catastrophically fail but deform with the substrate to a limited amount.

5.4 Powder Size Effect on Coating Quality

This section looks at the effect that the powder constituent size has on the deposition of WC-17Co coatings. During the investigation the manufacturer supplied, in error, a second powder of different specification (standard powder) from the initial one supplied (superfine powder). There were therefore two types of WC-17Co powder available to make coatings. One is known as a superfine powder and the other a standard thermal spray powder, both from Inframat, USA. The opportunity was therefore taken to compare supersonic laser deposition with each of the powders. The main powder used for the above investigation was the superfine powder.

5.4.1 Comparison of the Two Powders

Both powders investigated in this section are Inframat Infralloy S7417 83WC/17Co powder. One however is described as superfine. The particle size distribution for both powders was measured with a powder sizer. The results, Figure 64, show that both powders have a similar size distribution for the agglomerated particle size. The superfine powder is quoted as having a powder size distribution of -45 μm to +15 μm and the standard powder has a quoted size distribution of -55 μm to +15 μm . The experimental results appear to match the specification.

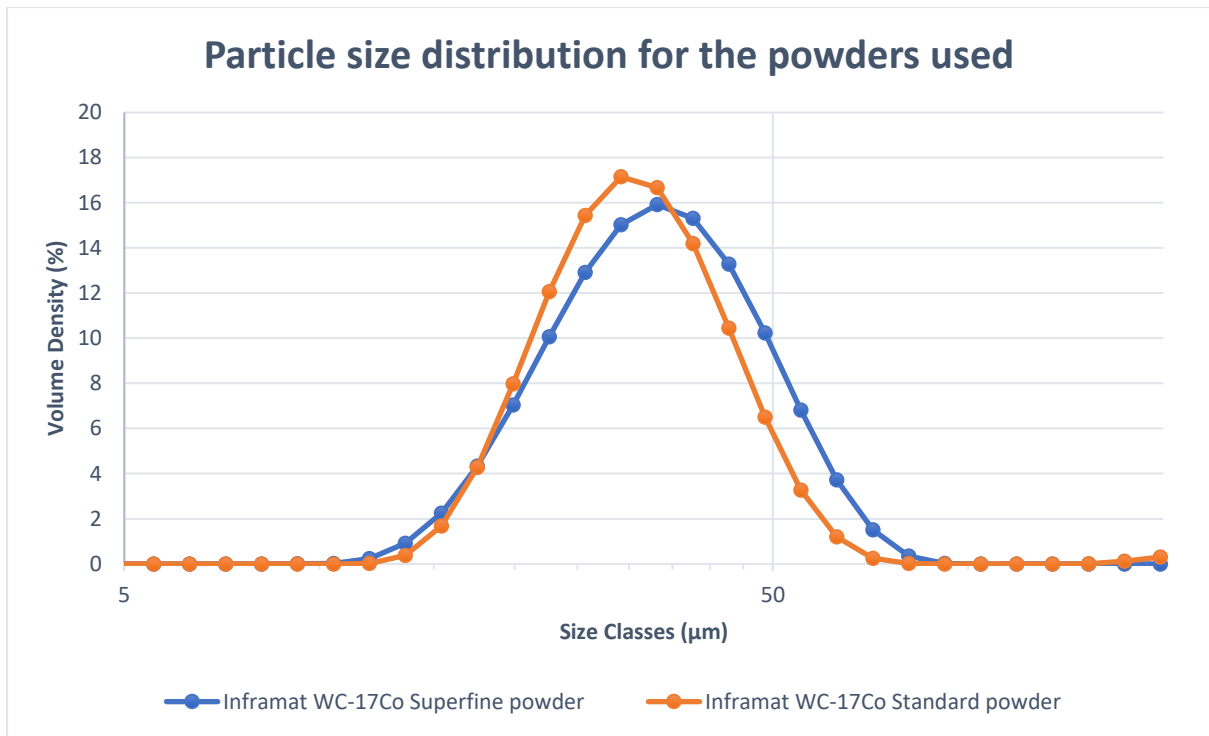


Figure 64: Powder size distribution for both WC-17 Co powders as determined using a mastersizer 3000.

The key difference between the powders is the size of the individual WC particles that make up the agglomerated WC-17Co particles measured above. The superfine powder is quoted as having WC particles <500 nm in size.

When the superfine particles were observed under a SEM, Figure 65, the typical geometry of the agglomerated particles along with the individual grains of WC in the cobalt matrix can be seen to form a densely packed sphere. In the case of the standard powder, Figure 66, the agglomerated particles can be seen to be more porous as compared to the superfine powder. The individual WC particles are also observed to be less spherical than the equivalent particles in the superfine powder. The standard powder also appears to contain a larger volume of porosity which was investigated below.

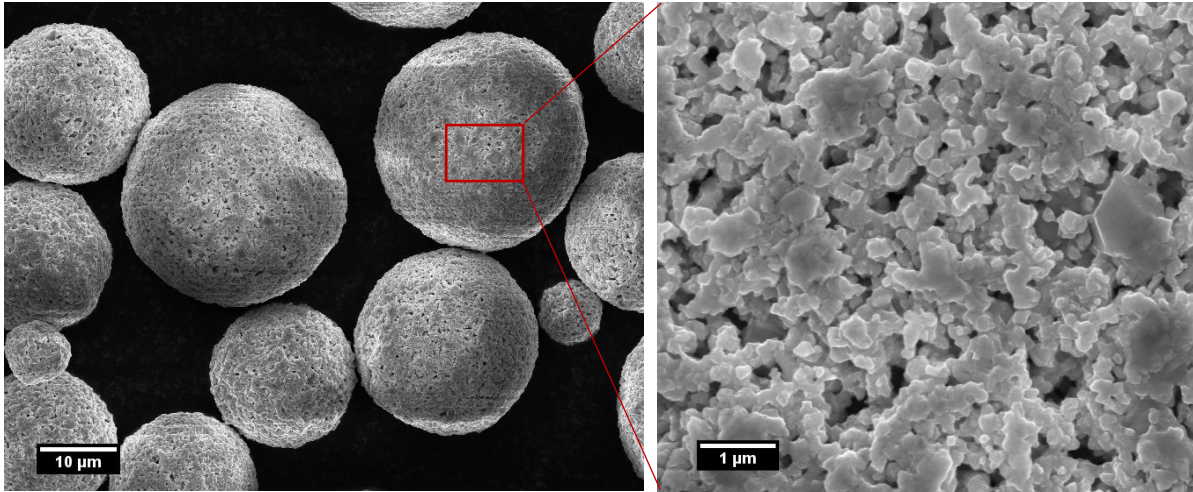


Figure 65: SEM images of the WC-17Co superfine powder used in the coatings. The images show the spherical geometry of the agglomerated particles (left) and the individual grains of WC and Co that make up the powder particles (right).

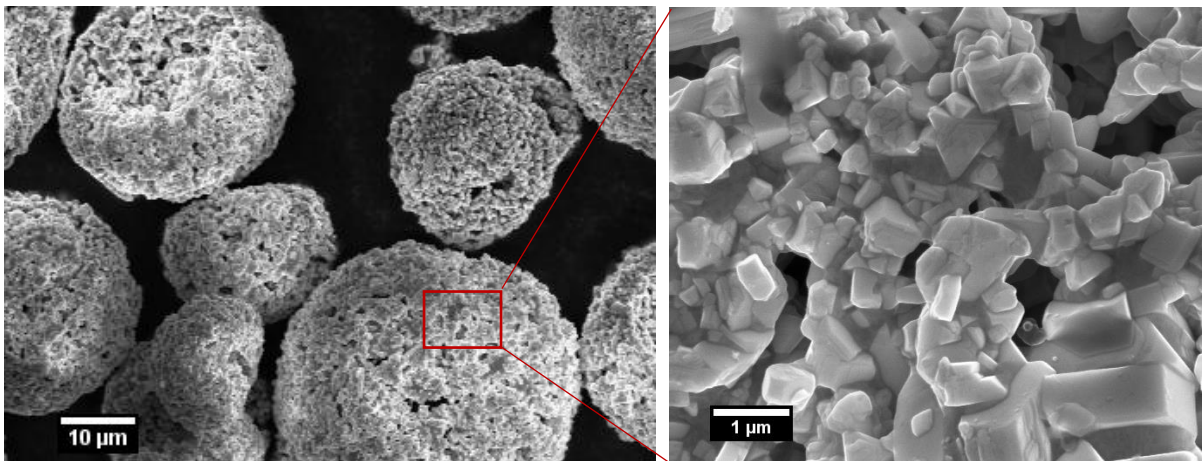


Figure 66: SEM images of the WC-17Co standard powder used in the coatings. The images show the spherical geometry of the agglomerated particles (left) and the individual grains of WC and Co that make up the powder particles (right).

To fully understand the differences in the makeup of the agglomerated particles, both powders were mounted in resin and polished to expose cross sections of the powder. These cross sections were then imaged under an SEM. A representative cross section of each powder is presented in Figure 67.

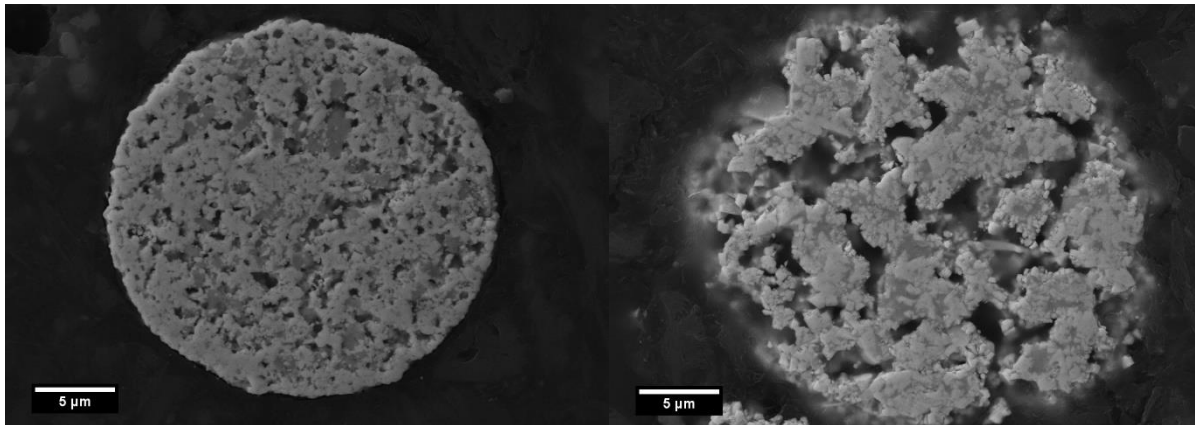


Figure 67: Cross section of the agglomerated particles of WC-17Co. The superfine powder on the left and the standard is on the right.

To determine the relative porosity of each of the powders, 10 images of agglomerated powder particle polished cross sections for each type was measured using image processing. The result, Table 7, shows that the standard powder cross section has an average of three times more porosity than the superfine powder.

Table 7: Results of the porosity of the agglomerated particles measured using image processing.

Powder	WC-17 Co superfine	WC-17Co standard
Mean porosity of agglomerated particles (%)	12	36
Standard deviation (%)	11	13
Standard error (%)	3	3

This section has shown the difference between the two powders in their makeup. This structural difference within each agglomerated particle would explain why simply replacing one powder with the other in the supersonic laser deposition system would not work, due to the volume of material being fed into the system being different in each case.

5.4.2 Comparison of Coatings with Both Powders

Coatings with both powders were deposited using the SLD process. A difference was seen in the porosity and quality of the coating with each of the powders. The superfine powder produced more dense coatings with better adhesion between the layers than the standard powder.

To see if the porosity could be reduced using different laser power, a trial was done using the standard powder. The laser power was varied from 1400 W to 2800W at 200 W intervals. The conclusions from this was that a laser power of 2400 W was the optimum power to produce the best observed coating. This is almost the same laser power that was found to work best on the superfine powder. The best

observed coating using the standard powder is shown in Figure 68. For comparison, a typical coating using the superfine powder is presented in Figure 47.



Figure 68: Cross section of a multilayer WC-17Co coating using the standard powder on a mild steel substrate. A laser power of 2400 W was used to produce this best observed coating. Large porosity can be observed in this coating.

From the results gathered it can be concluded that the size of the individual WC grains in the agglomerated particles does have a significant impact on the final coating: a smaller WC particle size resulted in a denser and less porous coating.

The impact of the size of the particles on the coating hardness was also investigated. Using a cross section of mounted coating, five points within each coating, where the coating was fully dense were measured on a Vickers hardness tester using a setting of to 10 HV (equivalent to a load of 98.07 N), a dwell time of 15 seconds and a load speed of 50 $\mu\text{m/s}$. The results are shown in Table 8, where the superfine powder is found to have a larger hardness value. This is a second advantage to using a finer powder size for the deposition process.

Table 8: Results showing average Vickers hardness for SLD coatings for each powder type.

Powder	WC-17 Co superfine	WC-17Co standard
Vickers hardness (HV)	1468	1318

5.4.3 Discussion

Within this section it has been shown that it is not just the agglomerated powder size that matters when selecting an optimal powder for supersonic laser deposition, the constituent particles must also be considered. In this study a hard WC grain forms part of the powder, for the case of more malleable materials this may be less significant, but it is theorised here that other high-performance materials for spraying that require a binder material will be affected in the same way. The results above indicate that a smaller particle size produces a denser and harder coating.

One study in literature investigated the effect of WC grain size in WC-17Co coatings, using a helium cold spray system. The results indicated that the larger WC grain size powder resulted in coatings of increased porosity, and that the WC particle size influences the formation and cohesion of the coating layer [178]. Above a certain WC gains size coating was not possible, and an increase in binder fraction would be required.

When comparing the deposition mechanism for WC-Co against more malleable materials such as copper, the adhesion mechanism is different. Whereas traditionally the incoming particle deforms the lower layers as it forms a splat, deforming a non-deformable material such as WC is not possible. For this reason, an initial layer of WC-17Co on steel is easy to deposit due to the relatively easy deformation of the steel, however subsequent layers are much harder to form, due to the reduced amount of deformable material visible to newly incoming particles. It has been observed in literature that WC grain refinement occurs when insufficient binder material is presented at the deposition surface. This may explain why the deposition efficiency of WC is low compared to more malleable materials. To alleviate this problem smaller grain sizes would be desirable. The trade-off however is that WC grains that are too small may not give the desired coating properties.

One benefit of using a supersonic laser deposition system over traditional cold spray is that the required critical velocity is reduced. This enables deposition of powders that have larger grain sizes than would otherwise be possible on traditional cold spray systems. As seen in this work, multiple layers from overlapping tracks of the coating using the larger WC grain size powder were able to be built up, whereas coatings of this thickness were not easily possible with a helium based cold spray system [178]. Supersonic laser deposition is therefore an ideal platform for depositing high performance materials where a decrease in particle grain size may not be desirable.

In conclusion, it has been shown that the WC grain size is very significant in determining whether a coating will be successfully deposited, and to what extent it has good adhesion between the layers. This is in addition to optimising the supersonic laser deposition parameters. Further work could be done to determine the optimal grain size for WC with SLD and see if the effect of particle grain size also affects other hard materials that require a binder.

5.5 Discussion of Results

This section will discuss the presented results, where deposition of WC-17Co with SLD, a high-performance material for hard facing the chapter has been introduced. The objective of this chapter was to understand the process and method of failures in the coatings.

Initially it was shown that the deposition of WC-17Co was possible using the supersonic laser deposition process. With traditional cold spray, helium is required to achieve the deposition velocities necessary, and the addition of a laser removes this requirement. It was also observed that with a powder that has larger WC particle size, deposition was achievable although the bonding at the interface had increased porosity. This is significant as trials with traditional cold spray have failed to build up multiple layers using larger grain sized powder. This would suggest that the SLD process is much more forgiving and more suited to depositing WC-17Co than traditional cold spray, as a larger

WC grain size could be used at optimal deposition parameters. This would increase flexibility in the design of the final coating properties.

Within the coating process it became clear that the existing PID loop used was not suitable for the monitoring of the deposition process in its current form to correctly set the laser power. One potential reason for this is that the deposition efficiency of WC-17Co was low, resulting in a large amount of airborne particles in the chamber and above the deposition site. This likely blocked the ability of the IR detector to successfully and reliably estimate the temperature of the deposition site. Possible solutions based on the work done here are to increase the percentage of binder or reduce the WC grain size to increase the deposition efficiency, so that there are less airborne particles at the deposition site.

Another issue encountered was that as the number of tracks/deposition time increased, a significant amount of thermal energy was imparted into the substrate. The underlying substrate then heated up and provided different initial thermal temperature for the deposition site, but having turned off the PID loop this was not compensated for. The coating at the end of a deposition run would therefore have undergone a slightly different thermal environment. It is theorised that this is the reason that occasionally the interface melted and mixing of materials occurred. The thermal effects of depositing a material with such high laser power are worth further investigation as it was observed that it can have a large impact on the success of the coating, especially as all the substrates visibly bent due to the thermal environment during the deposition. This bending also occurs with other materials but to a lesser degree, as the laser power required is usually lower.

The coatings were shown to have good adhesion up to the limit of the tester, which is comparable to recent results of competing technologies such as HVOF that are more developed and commercialised. This is significant as it illustrates that a less mature technology is already able to successfully deposit coatings with non-optimised powder and in a development system. Future work can therefore work towards increasing the performance of the coating, for the desired application.

The use of acoustic emission technique in monitoring the coating failure was successfully demonstrated. Due to the determined plastic failure mode of the coating, acoustic emission could be used for in situ monitoring of the coating to pre-empt failures in industry. The use of acoustic emission technology could also be used in the development of supersonic laser deposition, for monitoring the deposition of coatings, to greater understand the behaviour of coatings as they are being deposited in the chamber.

The reinforcement effect of WC-17Co on steel that was shown in this work could enable better design choices to be made when designing steel components that are to be coated with this material with this process. For example, less strengthening/thickness of the substrate may be required, as the coating would enhance the underlying material.

One of the key aspects to take away from this work is the make-up of the powder. The success of any one coating depends on the powder, not only on the agglomerated powder size but also the constituent grains of each powder particle, and percentage of malleable binder material to hard non-deformable material. Further work based on high performance materials using the supersonic laser deposition process should look carefully at the optimal powder makeup at the nanoscale before looking to optimise the process at the macroscale.

5.6 Conclusions

This chapter has successfully shown that WC-17Co coatings can successfully be deposited on mild steel using the supersonic laser deposition process. These coatings were found to be well bonded to the substrate when investigated using optical and SEM microscopy. Some unwanted mixing at the interface was observed. In future this could be alleviated using successful PID control of the laser power.

Adhesion testing of the coating was performed, and results showed >70 MPa adhesion, limited by the rated strength of the glue. In some cases, 100 MPa was measured before glue failure, indicating a very well bonded coating that is competitive with commercial HVOF processing.

Four-point bend testing of coatings was performed with coatings in both tension and compression. Failure was monitored using an acoustic emission technique. The results indicated that the failure mode was plastic and that the coating provided a re-enforcement effect of about 25 % over an uncoated bar.

Samples were observed to bend during deposition due to the thermal energy required for the process, even in cases where material was not deposited. This thermal aspect of the deposition requires further investigation, especially in the case here where we have a high-performance material that requires significant thermal energy for successful deposition.

6 Chapter 6 – Thermal Stresses and Coating Modification

This chapter investigates the thermal stresses in the supersonic laser deposition process. It looks at the shape change of the sample due to thermal and peening effects of the deposition process. Secondly, the effect of adding additional coating layers of a high-performance material, WC-17Co, on the final shape of the coated substrate are investigated. Thirdly, this chapter looks at two possible methods for improving WC-17Co coatings.

6.1 Motivation

The supersonic laser deposition process is both a thermal and mechanical process. Extensive work has been done on understanding the cold spray process and it is now commonly used in industrial applications. The laser processing and bending of metals is also well understood and has been widely modelled and used in manufacturing.

The combination of both the cold spray process and laser thermal processing used in the supersonic laser deposition process is not well understood. The contribution of each on the residual stress that is often seen after coating deposition, in the form of substrates that have bent from their original shape, is unclear. Deformation is seen in most substrates including those over 5 mm thick, indicating that the residual stress from the deposition process is significant. This is especially true when depositing hard coatings, such as WC-17Co. The residual stress of coatings from basic cold spray has been analysed in literature using XRD, however a greater understanding of the sources of stresses in this combined SLD process would be beneficial in designing ways to minimise unwanted stress, to prevent coating failure and delamination due to the thermal and mechanical processes during deposition, and set the direction for further research in this area.

6.2 Analysis of Thermal and Peening Effect on a Flat Substrate

This section investigates the contribution of the thermal and mechanical peening effect of the supersonic laser deposition process on flat mild steel substrates coated with WC-17Co. Following this, theoretical calculations are done to attempt to understand the magnitude of the residual stress.

6.2.1 Experimental Setup

This experiment was designed to determine the relative impact of the thermal and peening effects on the final deformation of a steel bar. This was done by processing the steel bar in three ways: with just the thermal effect from the laser, with the thermal effect of the laser and the peening effect of powder, and the thermal effect of the laser and the peening effect of the powder but with a coating being formed.

The substrate used was mild steel bar of dimensions 250 mm x 25 mm x 5 mm, which were prepared as described in the materials section.

Four mild steel bars were processed in the SLD chamber using heated gas and the laser at the power required for WC-17Co deposition, but without the powder added to the gas flow. The aim of this was to produce samples that were only stressed by the thermal processes from the heated gas and the laser scanning over the substrate.

A second set of three samples were “coated” using the same laser and gas parameters as WC-17Co, but the powder used was Al_2O_3 . This ceramic powder was chosen as it was known not to stick using the SLD process, but it would still provide the peening effect of powder hitting the substrate at the same time as the laser was passed over it. The particle size distribution of 22 to 45 μm was like that of the WC-17Co powder that it was being compared to, so that the particle impacts were comparable.

A third set of five samples were coated with a single layer of WC-17Co coating using the gas and the laser. The aim of this was to see what the total deformation on the sample would be from the complete deposition process, where material deposited.

6.2.2 Experimental Results

These three sets of samples were measured for deflection after cooling using the method described in chapter 3. An average displacement of each set of samples was then plotted and compared. The results are shown in Figure 69. It should be noted that during deposition the substrate was clamped down at each end of the bar. During deposition, the substrate was therefore constrained in position, and it was observed during removal of the clamps that there was increased force on the claps post deposition. It was only when the clamps were removed that the full deformation of the sample was achieved.

The samples that were either laser-only processed or laser processed and ceramic peened, showed the same bending. This would indicate that the thermal component of the process from the laser is responsible for almost all the residual stress and bending in the substrate. Interestingly the samples that were coated with WC-17Co bent less than the other samples, even though the recorded temperature was similar in both cases. This would indicate that the process of the coating having been deposited is working against the residual stress from thermal effects.

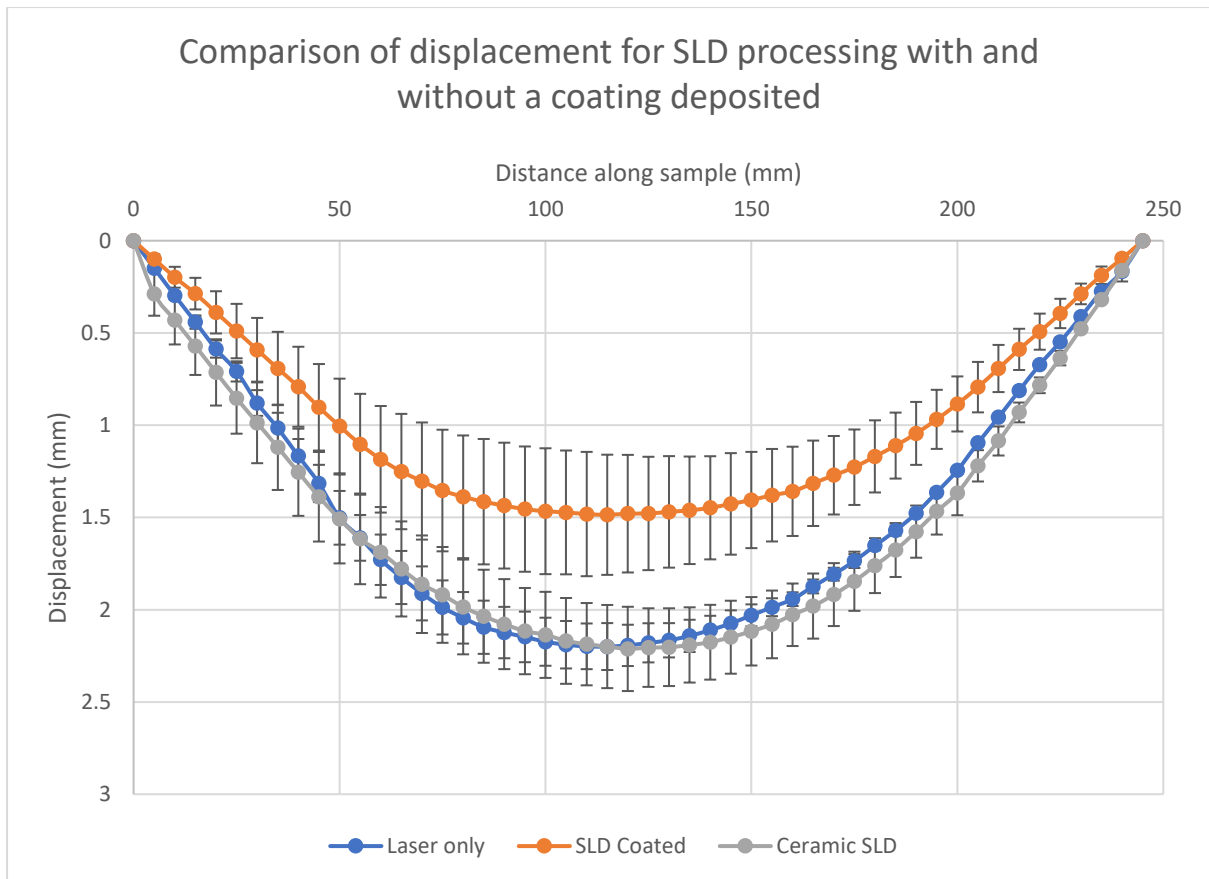


Figure 69: Graph showing the average bending of each of the sets of samples. Error bars are +/- 1 standard deviation. The samples that were coated with WC-17Co had a final deformation less than that of the uncoated samples. Samples that were processed with the laser only or with the laser and the powder for peening, were shown to have the same deformation.

6.2.3 Discussion of Experimental Results

The results indicate that the deformation of the substrate during processing appears to be dominated by a thermal effect, rather than a mechanical peening effect. A significant modification of deformation due to the peening effect on top of the thermal effect was not observed. The following discussion shall therefore focus on the thermal aspects that are thought to generate this bending.

To understand why there is an observed thermal effect, we can look at the theory for laser bending. The mechanism seen here would appear to be the temperature gradient mechanism. As the laser beam is scanning across the sample, the high intensity beam is generating a steep thermal gradient around the spot that is generating differential thermal expansion. When the flow stress of the steel is matched by the stress from the thermal expansion, compressive residual stress is generated around the heat affected zone. Upon cooling of the heated spot, the small thermal expansion of the spot becomes a large tensile residual stress that forms a bending of the substrate. This bending occurs in both axes due to the restriction of the expansion of the surrounding material. In the case of the work

here, the sample was long and thin, so the bending was more observable along the length of the sample. Thick samples of other materials produced with the SLD process on more square substrates do demonstrate this bending in both directions.

This deformation of a substrate with a laser has been shown to be the case through finite element modelling of laser beams scanned across a thin plate. Further work could be done here to model the residual stress generating the deformation of the substrate due to the laser bending using numerical simulation and finite element modelling methods, but such analysis is beyond the scope of this work.

As the initial temperature of the substrate is relatively cold, it is understood that there is a higher temperature gradient for the first track, and as more tracks are scanned, the peak temperature of the substrate increases. This would suggest that a larger portion of the residual stress is generated in the earlier tracks than the later tracks. Later tracks therefore have a smaller thermal gradient, but this can generate issues for deposition of a material and melting of the surface as seen in the previous chapter [193] [194] [195] [196].

The other aspect of bending due to thermal effects is the difference in thermal expansion coefficient between the coating and the substrate. This may work at two levels, during the deposition and post deposition. During deposition, this effect is unlikely to be significant as the coating and substrate are kept at relatively similar temperatures in a fixed position. Post deposition when the sample is cooling, the difference in thermal expansion coefficient will generate a residual stress between the coating and substrate. This residual stress may be the cause of cracking that is seen upon cooling.

6.2.4 Theoretical Estimation of the Residual Stress from the Difference in Coefficient of Thermal Expansion (CTE)

Residual stress can significantly affect the adhesion and properties of a coating once deposited. Following on from experiments depositing WC-Co, it was theorised that a proportion of the residual stress was coming from the difference in coefficient of thermal expansion between the coating and the substrate. Here the potential residual stress due to the mismatch of CTE on cooling is calculated.

Modelling thermal stresses can involve complex finite element models which are beyond the scope of this work, in this case a simple model will be used. The model will calculate the residual stress between a thin coating and a thick substrate, when cooled from the high temperature during processing to room temperature.

A simplistic estimation of residual stress can be found using Equation 5 [197]. This equation uses the assumption that the linear CTE remains constant with T. σ is thermal stress, E is the Young's modulus,

ν is Poisson's ratio, α is the CTE and d is the thickness. The coating is referred to as A and the substrate as B.

Equation 5

$$\sigma_A = \frac{1}{d_A} \cdot \left[\frac{(\alpha_B - \alpha_A) \cdot \Delta T}{\frac{1 - \nu_A}{d_A \cdot E_A} + \frac{1 - \nu_B}{d_B \cdot E_B}} \right] \quad (5)$$

The equation is based on the fact that a thin coating deposited at high temperature is thermally stressed when cooled to room temperature [198]. When a length of rod is cooled it will decrease in length based on its modulus and coefficient of thermal expansion. If the rod is constrained in space, it is unable to decrease in length and is held in tension [198]. Equating equations for both the substrate and coating, as they are attached, leads to equation 2 above.

In the case of SLD the temperature range is large and therefore this assumption that CTE remains constant at all temperatures is not valid. A modification of this equation to take account of the change of CTE with T is given in Equation 6 [197].

Equation 6

$$\sigma_A = \frac{1}{d_A} \cdot \left[\frac{1 - \nu_A}{d_A \cdot E_A} + \frac{1 - \nu_B}{d_B \cdot E_B} \right] \cdot \int_{\text{DepositionTemperature}}^{\text{RoomTemperature}} (\alpha_B(T) - \alpha_A(T)) \cdot dT \quad (6)$$

This equation can then be used to determine the residual stress due to the thermal expansion coefficients of the coating and substrate. It is assumed that the substrate is many times thicker than the coating and therefore has negligible stress.

The residual stress was determined for the case of WC-17Co on mild steel. A linear thermal expansion coefficient for mild steel of $\alpha=9.5 \times 10^{-9}T+1.04 \times 10^{-5}$ was used. Due to limited data on the bulk properties of the powder used it was assumed that the CTE of WC-17Co was constant with a YM of 200 GPa and CTE of $\alpha=7 \times 10^{-6}$ were used for WC-17Co [199]. The temperature of the substrate was assumed to be 100 °C as the gas temperature of the system decreases significantly after exiting the nozzle which heated the table and substrate in the system, although it is acknowledged that instantaneous local temperatures will have been high under the laser spot. Assumptions were that the thickness of the coating layer was 0.5 mm and the substrate thickness was 5 mm.

Compressive stress in the coating was calculated to be approximately -290 MPa. This is larger than the yield stress of mild steel of 248 MPa but less than its ultimate strength of 841 MPa. The compressive yield stress of WC-Co is approximately 5000 MPa in literature which would suggest that it is the mild steel substrate that is yielding [200] [201]. This compressive residual stress on the coating would support the theory that the coating was resisting the residual stress from the thermal effect of the laser to cause a plastic deformation that was bending the bar, but that additional stress elements must be considered.

The results here indicate that the theory is correct. It appears that the residual stress from the thermal effects of the laser are of larger magnitude and in the opposite direction than the effect of different CTE between the coating and substrate. The magnitude of the latter however is large enough that it should not be discounted for materials where the difference is significant. A proper treatment to model the effects seen here would require finite element modelling which is beyond the scope of this project but would be recommended for future work.

6.3 Analysis of Sample Deformation with Multiple Coating Layers

This section investigates if multiple coating layers are possible with this material and the effect of increasing the number of layers of coating on the final deformation and residual stress of the sample. For a coating process to be useful it is necessary to build up a thick coating, multiple coatings layers have not been achieved with this powder using traditional helium-based cold spray.

6.3.1 Experimental Setup

The deposition of two and three-layer WC-17Co coatings on a steel substrate was attempted, in the same manner as single layer coatings. Layers were built up during the same spraying session, without the sample cooling down in between layers. The laser position was reset to an offset of 1 mm in one axis between the layers, so that tracks were placed in the valleys between tracks of the underlying layer. This resulted in one less deposition track than the layer below it, like the lower layers of a pyramid shape. Three samples of two-layer coating and three samples of three-layer coating were made.

Following deposition, each of the sample's deformation was measured as described in the methods chapter.

6.3.2 Experimental Results

A study to investigate the optimal deposition power for WC-17Co on WC-17Co was first done. A two-layer coating was made with the second layer having powers from 1400 W to 2800 W. The second layer was deposited in the same spraying run as the first layer. It was found that the optimal coating

power was 2400 W for the second layer based on observations of the cross sections, Figure 70. This power was used for the following 2 and 3 later coatings.



Figure 70: Cross section of a two-layer WC-17Co coating using 2400 W power.

Two and three layers of coatings were then successfully deposited on the long steel bar substrates. The deposition was, however, not consistent between layers. Table 9 shows the average thickness of each of the layers. The second layer only added minimal thickness to the sample. This can be partially explained by the offset of the tracks, with the second layer being sprayed into the valleys between the first layer tracks. These valleys are minimal in depth and therefore do not explain the whole reason for the lack of thickness. The process of adding a third layer has not added any additional thickness to the coating. When observing the sample surface, it appears additional material was deposited over the two-layer coating. This would suggest that during the addition of the third layer, existing coating peaks were eroded away with deposition once again filling the valleys of the sample.

Table 9: Table showing the thickness of the coating layer after depositing coatings.

Coating Layers	Average coating thickness (mm)
1	0.5
2	0.6
3	0.6

As was discussed in the previous chapter about the deposition mechanism, the lack of coating build-up is likely due to the fact that there is insufficient binder material available at the surface when depositing the second and third layer. The first layer has a relatively softer material (steel) to adhere to. The second and third layers however must bond to the exposed WC particles which have minimal soft binder exposed, and do not deform. The minimal binder material at the surface can be easily eroded away, therefore for the second and third layers to stick they need to either erode away some WC particles to expose more binder, or wait for enough cobalt binder material to build up on the surface before each WC grain can embed itself. This significantly reduces the deposition efficiency. What appears to be happening to the third layer is that it is eroding the top WC grained surface away, at which point further deposition is possible.

The average deformation measured for all the samples is plotted in Figure 71. One two-layer coating bent about 5 times the other two coatings, so it was excluded from the average. The graph shows that

increasing the number of coating layers from two to three increases the maximum deflection of the sample. Moving from one to two layers however does not appear to increase the bending.

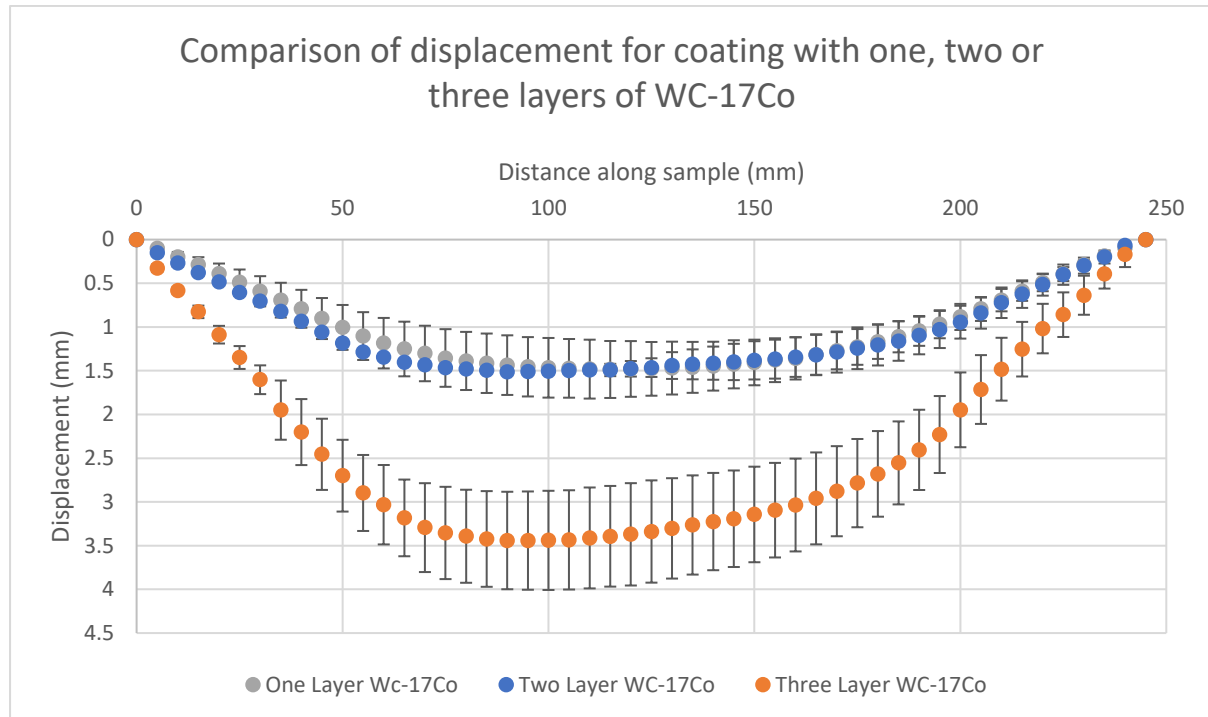


Figure 71: Graph showing the average displacement for two and three layer coatings. The data for a single layer coating is included for reference from the previous chapter. The three layer coating deformed significantly more than the single or two layer coating. Error bars are 1 standard deviation in each direction.

The increased bending of the three-layer samples could be explained by the increase in thermal energy in the sample. This would be consistent with an increased thermal component being responsible for the increased thermal bending combined with no increase in coating thickness meaning that even the resistive force from the CTE difference will not increase. Additionally, the third layer was deposited on an already heated sample. The local residual stress from the laser heating would therefore have an even greater effect than if the sample was cold, as the thermal gradient could penetrate further into the surface of the sample.

In conclusion it has been demonstrated that the thermal effect from the laser can have a dramatic effect on the deformation of the sample. The only real solution to reduce the bending of the sample is to minimise the heat into the sample. Unfortunately, the heat is required at the surface to enable the adhesion to the lower layers, to enable deposition. Without this laser heat source, as seen in other studies, it is not possible to deposit this material without helium gas. And in addition, multiple layers

do not build up with full thickness. An issue that must be addressed before it can be considered for a commercial application.

Pre-heating is a technique that is sometimes used to improve the adhesion of a coating. The reasons for this are the reduction of residual thermal stresses, and burning off grease and oil prior to deposition. Preheating can also increase the bond strength of cold sprayed coatings. It is currently not a commonly used technique but would be recommended for investigation as a method of improving these coatings [202] [203]. Another technique that could be used is to build up subsequent layers at 90 degrees to each other. This would have the effect of changing the direction of residual stress in each layer and potentially reduce the overall bending of the substrate in one direction.

6.3.3 Failure of Multilayer Coatings

The sample of the multi-layer coatings that were made were subsequently tested under tension for failure by using the four-point bending test with acoustic emission. This enabled comparison of them with single layer coatings.

To understand if the force required for the coating to fail had changed with the addition of additional coating layers, the samples from the previous section were bend tested with acoustic emission monitoring as described previously. The average force of failure for each set of samples is presented in Table 10.

Table 10: Table showing the average results from the bend testing of multi-layer coatings.

Sample ID	Layers	Force at failure (N)	Stress to fracture (MPa)	Strain to fracture (%)
190.2	2	2630	190	0.35
190.3	2	2580	440	0.39
190.4	3	2500	430	0.35
190.5	3	2300	420	0.40
190.6	3	2490	390	0.37

The results show that adding more layers decreases the force at which AE activity increases, and the coating fails, but the stress and strain to fracture are comparable. The conclusion is therefore that adding additional layers on top of the original one, using the current technique, weakens the coating and makes it more prone to failure.

6.4 Coating Modification Techniques

This section investigates two techniques for coating improvement through its modification. The first uses the addition of an interlayer of 316L between the steel substrate and WC-17Co coating to modify the overall residual stress from the CTE difference at each of the layer boundaries. The second

technique based on the earlier work on LaserForge, investigates using continuous welds, also known as laser fusing to modify the surface structure. It has been used to enhance thermally sprayed coatings to generate dense well adhered coatings with enhanced corrosion, wear resistance and decreased surface roughness.

6.4.1 Background

As shown above, the residual stress from the SLD deposition process can lead to bending of the substrate. This bending is undesired as it increases the stress at the interface. The increased stress could potentially lead to delamination of the coating from the substrate. As shown in a previous chapter, when the processing is not optimal cracking can occur along the interface, therefore minimising the stress at the interface will help to prevent the cracking propagating and leading to coating failure.

One potential option to reduce the stress at the interface is to use an interlayer material with a coefficient of thermal expansion that minimises the residual stress at each interface. Although the coefficient of thermal expansion difference is not the largest force that generates the substrate bending, it can be of an order that can counteract the bending and reduce stress. The first technique to be investigated is the use of an interlayer to alter the stresses at the interface.

Pulsed laser welding was an option outlined previously to modify the coating, this is also known as laser fusing. Laser fusing is a novel technique, that improves upon the existing practice of heat treatment for thermally sprayed coatings. Traditionally post-deposition heat treatment is done using a furnace or heat torch for annealing or re melting, this process often results in issues such as coating cracking as it relies on the skill of the operator to maintain constant heat. It is therefore usually only used on simple geometries such as cylinders. It is believed that a laser provides a more controlled heating process than gas flame fusing enabling the technique to be used on temperature sensitive substrates and larger parts [142] [143]. Lasers for example can therefore target re melting of the metal matrix while leaving the carbide reinforcement solid [144].

Laser fusing has been shown to seal coatings and reduce porosity and improve interface adhesion [142] [144]. The improvements in adhesion are due to a shift from a mechanical interface bonding to a metallurgical bond which gives a 10 times bond strength increase. Traditional pull testing as performed in the previous chapter is therefore insufficient for evaluation, due to the low tensile strength of available glue. Laser remelting was found to be beneficial for plasma and HVOF WC based coatings and therefore this section will investigate the effects of laser fusing on WC-17Co SLD coatings [204] [205] [206].

The method selected for investigation here is to use a high energy pulsed laser to make continuous overlapping welds over a large area, in the same way as is done in LaserForge. This is one option to improve the coating by reducing internal cracks and it also has the potential benefit of improving the bonding at the interface. This could also be beneficial when building up multiple layers of coatings. It is understood that laser melting could lead to WC dissociation and therefore parameters need to be carefully controlled, but literature has shown that under controlled conditions WC-Co coatings can be successfully processed to improve their performance such as increased hardness, improved wear, improved homogeneity and reduced porosity [205] [206] [204].

The two avenues of exploration were selected based on the ability to investigate them and to work towards the aims of using a pulsed laser to enhance the coatings and reduce their failure, in their current state.

6.4.2 Deposition of an Interlayer to Modify Stress at the Interface

This section investigates the possible use of materials with a different coefficient of thermal expansion (CTE), as a layer between the substrate and coating, to alter the residual stress at the interface and hence reduce the likelihood of failure.

6.4.2.1 *Experimental Trial Using Stainless 316L as an Interlayer*

The mean coefficient of thermal expansion of 316L (16×10^{-6}) is larger than mild steel (12×10^{-6}) and WC-17Co (7×10^{-6}) and therefore a good candidate to use as an interlayer to show the effect of a large CTE change at the interface [207] [199]. A material with a CTE between steel and WC-17Co was not readily available. To measure the effect of using an interlayer material on the final shape and failure of a coated sample, a trial was performed by using an interlayer of 316L between a steel substrate and a WC-17Co coating. Established 316L parameters for the system were used, along with the parameters for WC-17Co from this work. The parameters for 316L deposition were laser power: 1900 W, powder feed rate: 6000 rpm, 10 mm/s movement rate. Three samples were coated with the interlayer of 316L and then the WC-17Co. The two-layer coating was sprayed in two sessions without releasing the samples from the clamps, although the system was cooled completely between sessions. These were then compared to samples where just WC-17Co and 316L were deposited in a single layer. The average deformation of the samples is shown in Figure 72.

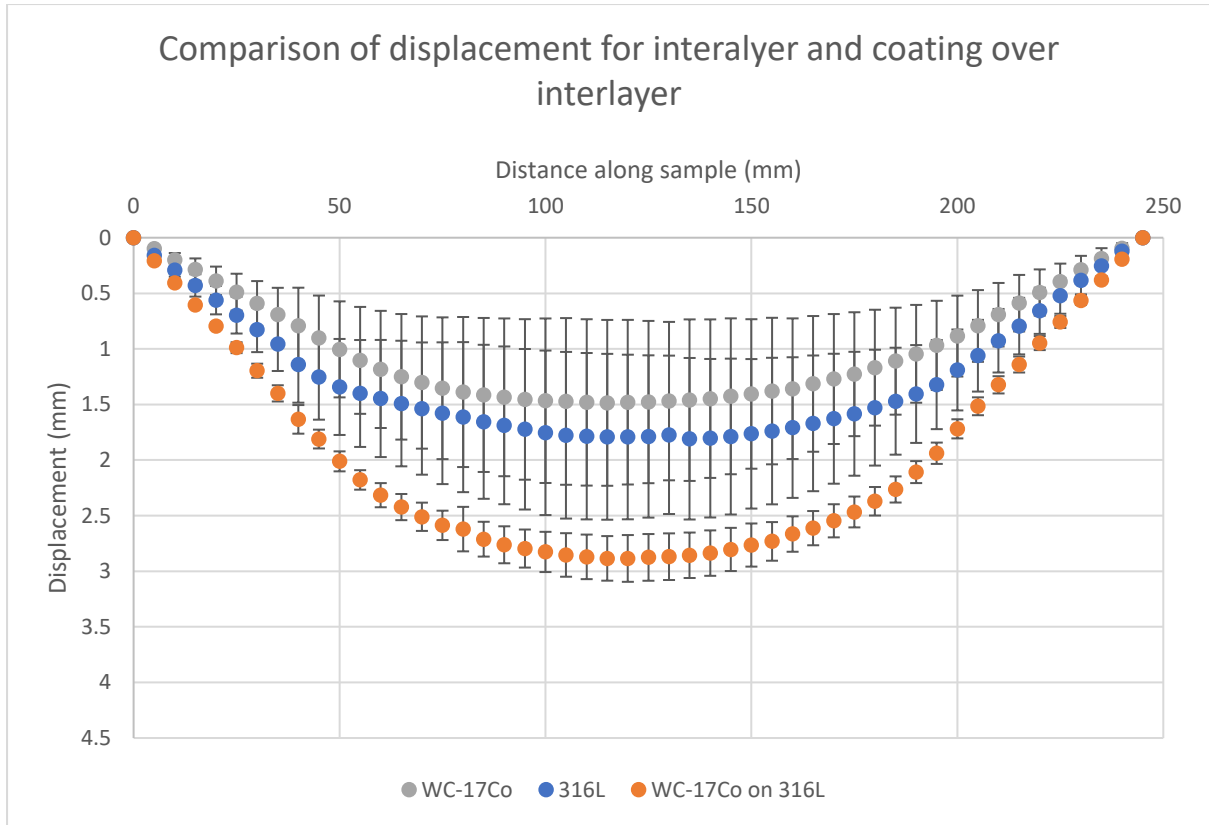


Figure 72: Graph showing the average displacement for a single layer WC-17Co coating, 316L coating and WC-17Co on 316L on steel. The data for a single layer WC-17Co coating is included for reference from the previous chapter. The samples containing the interlayer bent much more than the single layer coatings of each material. Error bars are 1 standard deviation in each direction.

The results show that the process where two coatings layers were deposited had increased bending over the single layer coatings as expected. The two-layer coating was similar in bending to the three-layer WC-17Co coating above. This would appear to agree with the previously observed results that increasing the CTE difference and thermal energy into the sample increases the bending.

6.4.2.2 Bend Testing of 316L Interlayer Samples

To understand what effect the inter layer has on the failure point of the coating, the samples were bend tested in tension with acoustic emission monitoring. The results are shown in Table 11.

Table 11: Results from bend testing of the interlayer coatings.

Sample coating	Force at failure (N)	Stress to fracture (MPa)	Strain to fracture (%)
316L	3090	520	0.60
316L	2600	440	0.43
316L	2300	390	0.42
WC-17Co on 316L	2500	420	0.53
WC-17Co on 316L	2460	410	0.37
WC-17Co on 316L	2560	430	0.42

These results show that the addition of additional layers, reduced the force with which the coatings fail. One potential explanation to why increasing the number of layers leads to lower failure values is that the additional number of interfaces increases the area over which there could be a failure and therefore the chance at which an AE signal is triggered.

6.4.3 Welding of WC-17Co SLD Coatings

Here the possibility of using laser welds as a method to alter the stresses in an SLD coating, specifically for a coating of WC-17Co, is investigated. Pulsed laser welding can also improve the contact area between the coating and the substrate. The coating here is deposited with SLD and then post processed using a pulsed laser.

Performing this method on WC17-Co is a challenge as re-melting the WC grains is undesirable as they may dissociate from the cobalt matrix. But having strategically placed welds may be beneficial for the coating on the macroscopic scale, so long as the welds do not significantly weaken the coating.

6.4.3.1 Pulsed Laser Welding on WC-17Co Coating

A single layer coating of WC-17Co was deposited on a mild steel substrate to form the coating on which the pulsed laser trials would be done.

Laser treatment of metal or MMC (carbide reinforced) coatings has been done in literature. Typically, a CO₂ laser was used in CW or pulsed mode. An example of parameters for a WC-17Co APS coating on steel used a CW CO₂ laser with an energy density of 300-2300 J/cm² and a beam shaped integrator. Processing parameters were 25 % overlap, 0.83 cm/s laser scan speed and argon shield gas [208]. Another study on FS and HVOF Ni-WC-Cr-B-Fe-Si-C coatings used a CO₂ laser with powers from 0.25 to 3 kW, spot size of 3 mm, standoff of 20 mm and overlap of 50 % and traverse rate of 500 mm/min [142].

To determine the effect of the laser parameters on the coating, two laser pulse widths were tested, 1 ms and 10 ms. These pulse widths were selected as they were at the edges of the useful operation range of the welding laser and were expected to show a clear difference in the response of the material. For each of these pulse widths the peak pulse laser power was set to be set points of 25 % (480 W), 50 % (815 W), 75 % (1210 W) and 100 % (1571 W) to give a range of laser powers. A pulsed laser snake pattern was used to weld the coating with a spacing of 0.25 mm between pulses and subsequent rows. A laser spot size of 1.4 mm was used. Nitrogen shield gas was used to reduce the effects of oxidation.



Figure 73: Illustration of the path of the laser for subsequent rows of pulses.

There was a visible mark on the coating surface for all the parameters tested. Following the laser pulse trials, the coating was cross sectioned, mounted, polished and imaged under a white light microscope. The results are shown in Figure 74.

	1 ms	10 ms
25% 480 W		
50% 815 W		
75% 1210 W		
100% 1571 W		

Figure 74: Results from the laser processing of a WC-17Co coating. The white streaks are artefacts of the image stitching.

The cross sections show that the parameter range selected resulted in the laser processing of just the surface layer all the way to welds that penetrated the substrate. The shorter pulse length shows a

porosity appearing near the surface. It also appears to generate cracking at higher energies. The longer pulse length penetrates further into the coating and reaches the substrate but also produces a significant increase in porosity due to the melting.

These results can be compared to as deposited FS coatings and laser fused coatings from literature, Figure 75. The results obtained in this here are closer to those seen in literature where insufficient laser power was used for the laser fusion. It was observed in literature that this behaviour is expected when the power is too low to generate complete fusion.

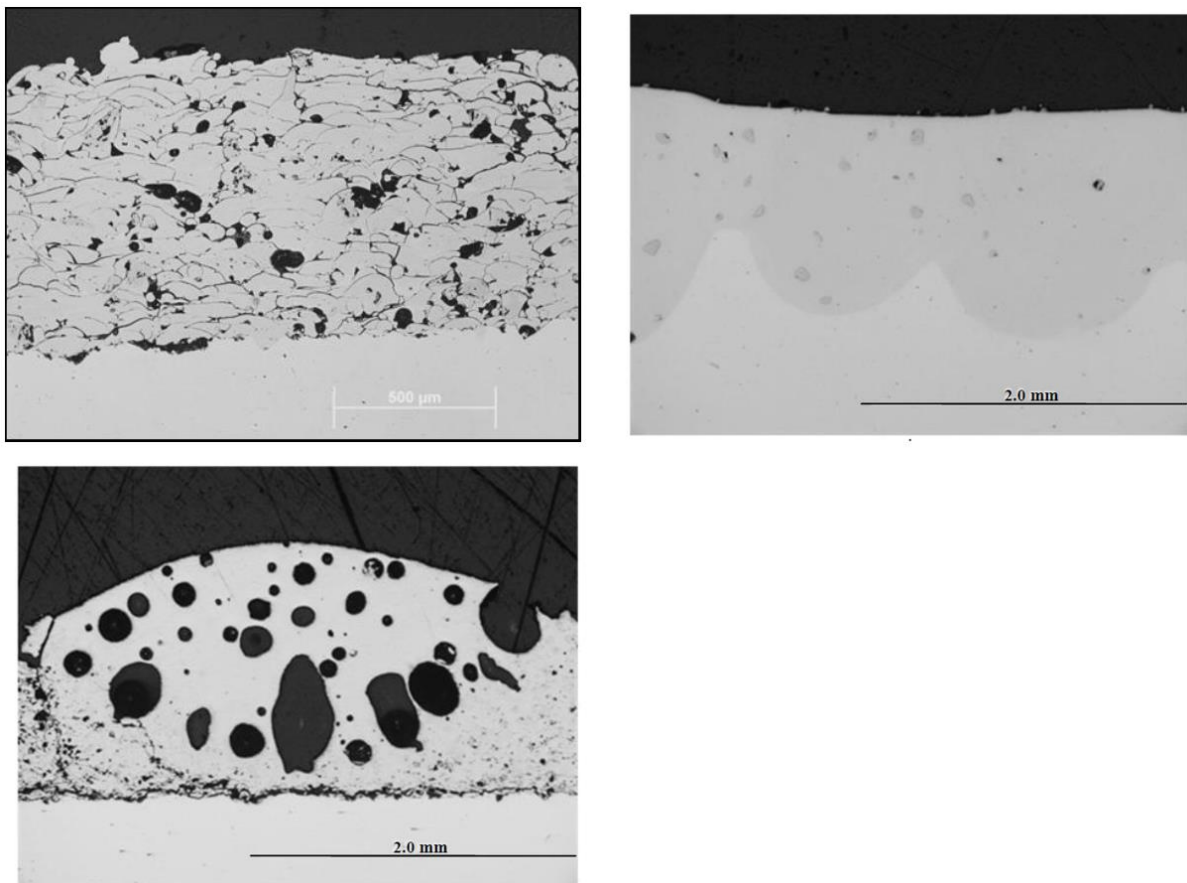


Figure 75: Results from Giacomantonio et al. showing laser fusing of a Ni-based wear and corrosion coating. (Top left) As deposited FS coating, (top right) Laser fused coating with 2.5-3 kW of laser power, (bottom left) laser fused coating at 1 kW laser power with significant porosity [142].

The significant porosity observed when using the higher energies is likely due to trapped gasses that are introduced during the welding. It is expected that increasing the power and switching to a CW laser may lead to a more uniform coating [142]. Unfortunately, the laser available was not able to generate the required higher energy to verify this.

To better understand the modified distribution of WC in the welded coating, the samples were imaged in an SEM. The laser has melted the surface layer, as seen at higher magnification in Figure 76, with

the bulk of the coating and substrate below it remaining unchanged. The WC particles are also no longer evenly distributed in the coating and significant porosity has been introduced.

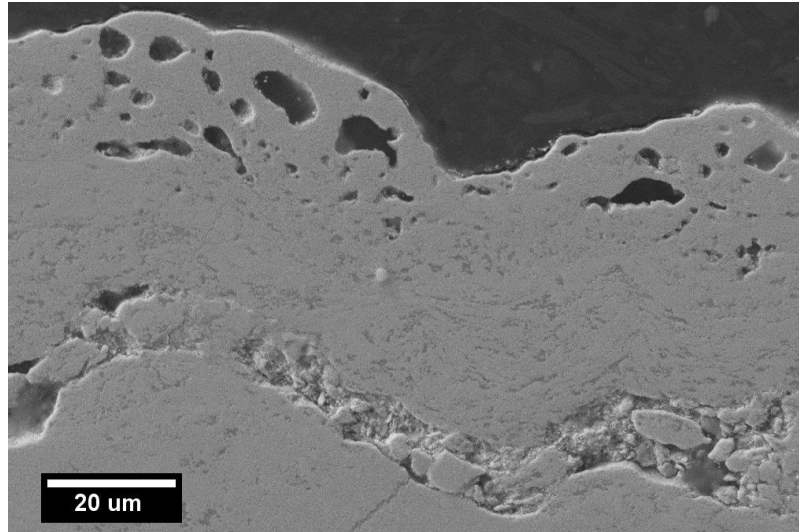


Figure 76: SEM image of laser pulsed surface with 1 ms pulse width at 25% showing melting and increase of porosity in the surface.

The introduction of porosity is undesirable in the coating, especially if this technique was to be used for reinforcement welds. In addition, with the increase of thermal energy required to get welding to the substrate, an increase of cracking is seen. This is likely due to the increase of the brittle phase of WC from the re-melted coating. Such a technique could easily be used for a material that is easy to weld, however in the case of WC-17Co welding the deposited coating makes it more susceptible to brittle failures and decreases the quality of the coating.

6.5 Discussion of Results

This section will discuss the significance of the above results, on the thermal stresses of the SLD process. The aims of this chapter were to investigate the cause of deformation of the substrate seen on the macro scale and determine the effect of depositing multiple coating layers of WC-17Co on the deformation. The multilayer coatings were additionally tested to compare their failure to single-layer coatings.

The first section investigated the contribution of the thermal and peening effect on the deformation of the substrate. The results showed that the thermal effects were significantly greater than the peening effects with respect to the deformation of the substrate. This has significant implications for SLD, as the process is built around the controlled use of a laser heat source to enable the deposition to occur.

For many materials such as copper and steel, for which low heat input is required, the thermal effects are small and the deformation minimal. The issue becomes a problem where a higher thermal input is required to deposit a material, such as WC-17Co. These are materials that require higher particle deposition velocities and may not deposit at all with nitrogen as an acceleration gas with no laser, due to it having a lower sonic velocity than helium. The need for a material to require a higher deposition velocity is usually because it does not easily deform. As shown in this work, it is expected that thermal input will cause deformation of the substrate; for a coating material that is malleable it will be able to deform along with the substrate. The low deformation and malleable material will deform to a final shape without introducing cracking. In the case of a rigid material, such as WC-17Co, it is less accommodating to small changes in shape and, with the increased deformation from the increased thermal component required, it is at a disadvantage on two accounts. The final coating is therefore more susceptible to cracking and delamination.

The solution to this problem is not obvious. There are four angles that could be investigated in future work. The first would be to minimise the required heat input. This could be done through the design of new nozzles to reduce the reliance on the laser component and increase the kinetic energy of the impacting particle. The second option would be to only spray onto thick substrates, which will deform less under the same thermal input from the laser, this however limits the applications for the coating process. A third option would be to alter the in-process conditions, so that the thermal gradient from the laser scanning the surface does not lead to thermal bending. This could be done through pre-heating of the substrate. A final option would be to post treat the deposited coatings, so that they do not fail when bent, and can resist the deformation of the substrate. Each of the angles would require a significant amount of work to investigate.

Within this first section, the effect of the coefficient of thermal expansion was investigated. From an experimental analysis, the difference in bending with and without a coating suggested that the coating was resisting the deformation. Some of this is likely to be due to the difference in CTE which results in a residual stress in the opposite direction to the bending stress, however the complex nature of the system would suggest that to gain a more precise value finite element modelling is required. There are already numerous studies in literature on modelling of cold spray, but there is a lack of literature on the modelling of the combined thermal and kinetic effects in the process, which are so important in supersonic laser deposition. The work done here emphasises the need for such models, as they will be incredibly beneficial for understanding possible optimisations to the system without the need to build multiple versions for experimentation at great cost.

The subsequent section of work investigated sample deformation using multiple coating layers. The second and third coating layers did not increase the thickness by the same amount as the first layer. The second layer added 0.1 mm in thickness, to the 0.5 mm first layer. This would confirm that the deposition mechanism was not the same between WC-17Co and the steel substrate and, WC-17Co on WC-17Co. The significant achievement here was to have an additional material layer deposited on top of the first layer, which is not possible with standard cold spray. The issue to overcome is the lack of binder material required for more adhesion of WC particles. For the first layer, less binder is required, but subsequent layers require more. Even though some material is deposited, a large fraction is not so lost.

Potential ways to alleviate this problem could be to spray an intermediate layer of the binder material to completely cover the exposed WC particles at the surface. This may have negative effects in terms of consistent coating wear, but this would then provide a fresh deformable surface at the microscale for the WC particles in the next layer to embed into, in much the same way as the first layer was able to bond to the steel substrate. A multilayer coating using a gradient of Co binder material would likely provide a more consistent final coating. Alternatively, a composite coating could be built with an interlayer of a different material, that would be designed to counteract or minimise the effect of the residual stress from the WC-17Co layer.

For the measurement of bending, even though the third layer did not increase thickness, increasing the number of layers from two to three, increased the sample bending. The two-layer coating showed the same bending as a single-layer coating. This would indicate that the thermal energy during the erosion and reapplication of the coating material did not just soften the surface but also transferred into the substrate leading to increased thermal bending.

When multi-layer coatings were tested for failure, they failed at a lower force than single layer coatings. In addition, three-layer coatings failed at a lower force than two-layer coatings. This would suggest that the addition of more layers of coating weakened the integrity of the whole coating. Therefore, in its current form, a single-layer coating is optimal. Adding a second layer only weakens it without significantly increasing its thickness. The next step in this process is to determine the optimal method for bonding an additional WC-17Co coating on top of an already coated WC-17Co coating without weakening the bulk.

The final section of work investigated two techniques that could be used to improve the coatings, the use of an interlayer material and the use of pulsed laser welding. Using an interlayer material did not have any significant impact on either the deformation of the sample or the failure. The key conclusion from this would be that it would be more beneficial to use fewer layers and minimise the heat input

into the coating from the SLD process than trying to manage the stresses from the smaller contributors.

With respect to the laser welding with WC-17Co, although laser welding was not successful in this experiment it has been shown in literature that with higher power CW lasers it is a viable option to improve the coating. This can result in reduced porosity (<0.01 %), improved interface bonding and an even WC distribution in the matrix. With other materials, lower energy welding may still be a possibility but did not form part of this work.

6.6 Conclusions

This chapter investigated the thermal effect of the laser in the supersonic laser deposition process. It has been shown that the dominant effect in the deformation of a mild steel substrate during the deposition of WC-17Co is thermal and is from the thermal effect of the laser. This effect is much larger than any deformation effect from the mechanical peening.

The effect of the difference in CTE between the materials is significant but smaller than the thermal effect of the laser during processing. To understand the full contribution further work using finite element modelling is required. This would then enable materials to be analysed before deposition to predict substrate deformation.

A significant result of depositing multiple layers of WC-17Co using supersonic laser deposition was achieved. When adding multiple coating layers, the upper layer does not deposit in significant thickness and the peaks of the lower layer is eroded due to the nature of depositing a ceramic in a metal matrix. Future work could look to add additional binder between the coating layers to improve the bonding between coating layers. This should enable full thickness coating layers to be built up.

Work was done to investigate post processing the coatings and the use of an interlayer. The benefits for the use of an interlayer were dwarfed by the need to use two spraying runs, doubling the number of laser passes required. Therefore, unless the interlayer can be applied without any thermal input, it would be more beneficial to use a single layer and work to minimise the heat input from this.

Post processing the WC-17Co coatings with a high energy pulsed laser did not benefit the coatings as expected, and instead increased the porosity and cracking within them. It is expected that if future work would be done with higher energy pulsed or CW lasers the results would be more beneficial and the increased porosity and cracking would not be observed.

In conclusion, this chapter has shown that the thermal effect from the laser is by far the largest contributor to the deformation seen in coated samples. Further work should look to model this from

a theoretical perspective and look at ways to minimise the thermal gradients during the processing, to minimise the bending of the samples such as with substrate preheating.

7 Chapter 7 - Conclusions and Further Work

This chapter presents the conclusions for each section of the work, followed by recommendations on further work.

7.1 Conclusions from Experimental Investigation of LaserForge

This work set out with the main aim of investigating the LaserForge process. This first section investigated the LaserForge coating technology. This is a commercial process that has been developed over the last 20 years. Literature on this process is very limited, consisting mainly of patent literature. It claimed to use solid state bonding to clad non metallurgically compatible materials using a high energy pulsed laser. The deposition technology underpins a system for deposition of flat-sided wires using a laser to perform solid state metallurgical bonding of a coating. In addition to available literature, the research group had access to a physical sample of the technology to help understand it, which was one of the motivators for undertaking this work. The investigation raised questions as to the nature of the technology.

Initially a laser processing system to investigate LaserForge was built. This required the setup of a new laser in a processing chamber. As part of this work 3D CAD design, metal working, and construction of electronic circuits were done.

The work investigated the parameter space for Ti-64 on aluminium identified from patent literature, with the region studied covering pulse lengths of between 1 ms and 10 ms and laser power up to 15 J per pulse. Within parameter sweeps a full range of effects were observed from keyhole welding to simple heating. The conclusion from investigating the parameter space and analysis of the known LaserForge sample was that LaserForge is a melt-based process. The process was replicated within the expected parameter range, and therefore enabled understanding of the process. Optimal parameters for the system used were found to be 10 ms pulse length, 1400 W per pulse and a 0.8 mm laser spot diameter. The process is effectively welding but with a very well controlled thermal input, that completely melts the coating layer and a very thin film of the underlying layer to form a bond. There is no special or novel mechanism in physics occurring apart from setting up the system so that there is very good thermal contact between coating and substrate.

The key knowledge gained from this work was that the LaserForge process is not using any novel physical techniques. It does however mean that welding of non-metallurgically compatible materials is possible with existing processes, so long as there is sufficient control of the thermal aspect of the process. The sample of LaserForge that was studied was determined to be of single layer thickness.

The limitations of the work were that only a small parameter range was investigated, and this was based on expected values from literature. The process was reproduced, however further parameters such as temporal pulse shaping and the system to deposit the top material was not investigated, which may increase the effectiveness of the deposition and bonding. Only one type of laser was used, from literature it was known that CO₂ lasers were used in early development and these may well give slightly different results.

Future work could investigate using this process on SLD coating to understand if they could improve the coating properties. In addition, current control techniques used in laser welding could be used to improve the control of thermal effects in supersonic laser deposition. Further post processing techniques could also be investigated such as laser peening and laser heating.

Following the result that the LaserForge process was a melt-based welding process, it was decided to change the direction of the work. The direction was changed to focus on the current issues with the SLD process, which it was hoped the LaserForge process would help with improving.

7.2 Conclusions from Failure Mechanisms in SLD

This second chapter investigated the use of WC-17Co. This material, that is commonly used in industry as a hard-facing coating, was selected as it benefits from low temperature deposition and is nanostructured. Both these things were identified in literature as being important in future cold spray development. Helium-based cold spray is the current method of deposition using cold spray for this material. This chapter investigated using a nitrogen-based supersonic laser deposition system as an alternative.

One of the key outcomes from this chapter were that WC-17Co was successfully deposited on mild steel. This material had a generally well-defined interface with minimal material mixing, although some melting and cracking was observed. This was theorised to be due to the poor thermal control of the process. The coatings were tested for adhesion and found to have an adhesion strength of >70 MPa. Acoustic emission monitoring was successfully used to detect cracking in the coatings during four-point bend testing. The outcome of this was that the WC-17Co coating was found to have a reinforcement effect of ~25 % on the coatings when compared to uncoated steel, this is larger than the expected decrease in surface stress of ~17% from simply increasing the thickness of the steel bar. The failure mode of the coating was determined to be plastic in nature. Furthermore, the properties of the powder used for the spraying were found to be critical in obtaining a low porosity coating. Smaller WC grain sizes were found to give denser agglomerated powder and lower porosity coatings.

The key contributions to knowledge were that WC-17Co coatings can successfully be deposited using supersonic laser deposition using nitrogen gas, AE technology can be used to monitor the failure of WC-17Co SLD coatings and the requirement that the individual WC grain size be < 500 nm in agglomerated particles, in addition to the agglomerated particles to be of a suitable size for the successful deposition of a low porosity coating.

The key limitation of this work is that it was not possible to use the automatic control loop for the automatic control of thermal input during deposition, due to powder blocking the pyrometer.

Further work was recommended to investigate the thermal effects of the SLD coatings, the control loop for thermal input and the ability to deposit multi-layer coatings for WC-17Co.

7.3 Conclusions from Thermal Stresses in SLD

The literature review highlighted that there was no complete theoretical model for supersonic laser deposition. There have been several theoretical studies of cold spray and laser bending separately that include theoretical modelling of stresses, but there is no complete model that has been presented to cover the supersonic laser deposition process. There is a lack of full understanding of the mechanisms used during cold spray, and therefore there is some lack of understanding in the scientific community around the mechanisms that can generate the bending seen in supersonic laser deposition of WC-17Co. This chapter aimed to investigate experimentally the potential source of post deposition sample bending seen in the previous chapter.

This work discovered that the key element generating the bending in the SLD deposition of WC-17Co is the laser. Prior to the work, it was theorised that the peening effect was also significantly contributing to the bending, but this does not appear to be the case in comparison to that of the laser. The evidence presented does not rule out that peening may have a small effect. It was also demonstrated that multiple layers of coating appeared to be deposited, although the thickness was not increased evenly between layers. These multi-layer coatings were tested for failure and it was found that increasing the number of layers decreased the force at which they fail. The effect of difference in CTE is notable, but smaller than the thermal effects. Work to investigate the use of an interlayer with different CTE showed that it modified the final shape of the substrate. Welding was investigated at 1 ms and 10 ms for four laser powers and was found to not work effectively with WC-17Co but is likely to work for other single element materials.

The key contributions to knowledge were that the dominant effect generating the sample bending was from the thermal energy of the laser, the peening effect on the substrate is negligible in

comparison, and that multiple layers of WC-17Co are possible, but further investigation is required to understand why the thickness does not increase uniformly for each layer.

The key limitations for this work were that the problem was approached from an experimental perspective. For more detailed understanding a theoretical approach is required. The material selected is also not ideal for welding, but the result confirms that such a technique requires materials that are non-nanostructured and have issues when re-melted. Additionally, the deposition of WC-17Co is not yet perfect and this may have an influence on the consistency of thermal effects observed.

Recommendations for further work are for use of a theoretical approach to understand the process and the use of alternative technologies for post processing that may be useable with WC-17Co. It would also be beneficial to do further study of multiple layer deposition, this could be done by trialling a graded coating with varying Co content or interlayers of Co binder.

7.4 Recommendations for Further Work

Following this work there are several recommendations for further work to further increase understanding in this field. It became clear early in the work that the feedback loop designed to control the laser intensity to maintain a constant deposition spot temperature was not capable of accurately enough controlling the deposition temperature. Further work should investigate ways of improving this control to more accurately control deposition site temperatures and prevent mixing at the interface.

As this work only investigated the sample deformation experimentally, there is a need for enhanced theoretical models to model the supersonic laser deposition process. Current models in literature only model the cold spray aspect or laser heating. Combining these and determining the combined effects are considered important for progress in materials that require more complex and well-defined deposition parameters.

With respect to multiple layers of WC-17Co coatings, the limiting factor was the lack of a good substrate for the second and subsequent layers, preventing much of the upper layers depositing. It is proposed that work be carried out to trial a graded coating where the Co binder fraction is greater near the substrate to enable thicker coatings and lower near the top most surface layer where increased WC exposure is desired. This is expected to enable a thicker layer of coating to be built up. It does not however solve the issue of thermal energy from the deposition leading to bending of the sample. To resolve this, it is proposed that novel laser heating techniques are considered to heat the surface of the coating without imparting significant heating into the bulk of the substrate. One experimental technique that is recommended for investigation is substrate pre-heating to minimise

thermal gradients during deposition. This technique is occasionally used for other thermal spray processes and could easily be adapted for SLD.

7.5 Bibliography

- [1] Elisabeth Weidmann, Anne Guesnier, and Brigitte Duclos, 'Metallographic preparation of thermal spray coatings'. Struers Application Notes, 2018, [Online]. Available: <https://www.struers.com/-/media/Library/Brochures/English/Application-Note-Spray-Coatings.pdf>.
- [2] E. Irissou, J.-G. Legoux, A. N. Ryabinin, B. Jodoin, and C. Moreau, 'Review on Cold Spray Process and Technology: Part I—Intellectual Property', *J. Therm. Spray Technol.*, vol. 17, no. 4, pp. 495–516, Dec. 2008, doi: 10.1007/s11666-008-9203-3.
- [3] Politecnico Di Milano, 'Final Report Summary - CORSAIR (Cold Spray Radical Solutions for Aeronautic Improved Repairs (CORSAIR))', 197923, May 2017. [Online]. Available: https://cordis.europa.eu/result/rcn/197923_en.html.
- [4] B. S. DeForce, T. J. Eden, and J. K. Potter, 'Cold Spray Al-5% Mg Coatings for the Corrosion Protection of Magnesium Alloys', *J. Therm. Spray Technol.*, vol. 20, no. 6, pp. 1352–1358, Dec. 2011, doi: 10.1007/s11666-011-9675-4.
- [5] N. M. Chavan, B. Kiran, A. Jyothirmayi, P. S. Phani, and G. Sundararajan, 'The Corrosion Behavior of Cold Sprayed Zinc Coatings on Mild Steel Substrate', *J. Therm. Spray Technol.*, vol. 22, no. 4, pp. 463–470, Apr. 2013, doi: 10.1007/s11666-013-9893-z.
- [6] S. Amin and H. Panchal, 'A Review on Thermal Spray Coating Processes', *transfer*, vol. 2, no. 4, 2016, Accessed: 23-Jul-2017. [Online]. Available: <http://www.ijctcr.com/papers/volume-2/issue-4/a-review-on-thermal-spray-coating-processes.pdf>.
- [7] K Jayakumar, T Senthil kumar, and B Shanmugarajan, 'Review study of laser cladding processes on Ferrous substrates', *Int. J. Adv. Multidiscip. Res. IJAMR*, vol. 2(6), pp. 72–87, 2015.
- [8] R. Vilar, 'Laser cladding', *J. Laser Appl.*, vol. 11, no. 2, p. 64, 1999, doi: 10.2351/1.521888.
- [9] A. Pandey and others, 'Laser Assisted Cladding-A Review.', *Int. J. Des. Manuf. Technol.*, vol. 11, no. 1, pp. 27–29, 2017.
- [10] Aravind Jonnalagadda and Siegfried Scharek, 'Short Course #4 Laser Additive Manufacturing', presented at the 30th International Congress on Applications of Lasers and Electro-Optics, Sunday, October 23.
- [11] W.-W. Liu, Z.-J. Tang, X.-Y. Liu, H.-J. Wang, and H.-C. Zhang, 'A Review on In-situ Monitoring and Adaptive Control Technology for Laser Cladding Remanufacturing', *Procedia CIRP*, vol. 61, pp. 235–240, 2017, doi: 10.1016/j.procir.2016.11.217.
- [12] S. Paul, K. Thool, R. Singh, I. Samajdar, and W. Yan, 'Experimental Characterization of Clad Microstructure and its Correlation with Residual Stresses', *Procedia Manuf.*, vol. 10, pp. 804–818, 2017, doi: 10.1016/j.promfg.2017.07.081.
- [13] Q. Lai *et al.*, 'Investigation of a novel functionally graded material for the repair of premium hypereutectoid rails using laser cladding technology', *Compos. Part B Eng.*, vol. 130, pp. 174–191, Dec. 2017, doi: 10.1016/j.compositesb.2017.07.089.
- [14] A. G. Demir, 'Micro laser metal wire deposition for additive manufacturing of thin-walled structures', *Opt. Lasers Eng.*, vol. 100, pp. 9–17, Jan. 2018, doi: 10.1016/j.optlaseng.2017.07.003.
- [15] G. Zhu *et al.*, 'The influence of the substrate-inclined angle on the section size of laser cladding layers based on robot with the inside-beam powder feeding', *Int. J. Adv. Manuf. Technol.*, vol. 88, no. 5–8, pp. 2163–2168, Feb. 2017, doi: 10.1007/s00170-016-8950-4.
- [16] H&R Technology Inc., 'LaserForge - Innovative Cold-welding and Cladding'. 03-Oct-2012.
- [17] Joshua Rabinovich, 'Laser Repair Mobile-PMD System with Flat Wire Metal Deposition', presented at the NCMS Symposium 2005, 19-Apr-2005, [Online]. Available: http://www.ncms.org/wp-content/NCMS_files/CTMA/Symposium2005/presentations/Track%201/0355%20Rabinovich.pdf.

- [18] J. E. Rabinovich, 'Low heat input laser component repair or joining with feedstock having conforming surfaces with a substrate', US 2004/0238508 A1, Dec-2004.
- [19] M. B. Frish, P. E. Nebolsine, and A. N. Pirri, 'Method for bonding using laser induced heat and pressure', US4684781A, Aug-1987.
- [20] J. Rabinovich, 'Process for energy beam solid-state metallurgical bonding of wires having two or more flat surfaces', US 2010/0155374, 2010.
- [21] J. Rabinovich, 'Rapid Manufacturing System for Metal, Metal Matrix Composite Materials and Ceramics', US006144008, 2000.
- [22] J. Rabinovich, 'Rapid prototyping system', US005578227, Nov-1996.
- [23] J. Rabinovich, 'Repair with feedstock having conforming surfaces with a substrate', US007600666, 2009.
- [24] J. E. Rabinovich, 'Repair with feedstock having conforming surfaces with a substrate', US 2004/0238508 A1, Dec-2004.
- [25] J. Rabinovich, 'Process for energy beam solid-state metallurgical bonding of wires having two or more flat surfaces', US 8,334,475, 2012.
- [26] J. R. Davis, *Handbook of Thermal Spray Technology*. ASM International, 2004.
- [27] 'Introduction to Thermal Spray Processing', in *Handbook of Thermal Spray Technology (#06994G)*, 2004.
- [28] B. Walser, 'The Importance of Thermal Spray for Current and Future Applications in Key Industries', *SPRAYTIME*, vol. 10 (No.4), pp. 1–7, 2004.
- [29] P. Fauchais, 'Understanding plasma spraying', *J. Phys. Appl. Phys.*, vol. 37, no. 9, pp. R86–R108, May 2004, doi: 10.1088/0022-3727/37/9/R02.
- [30] Herbert Herman, 'Powders for Thermal Spray Technology', *KONA Powder Part. J.*, vol. 9, pp. 187–199, Jul. 1991.
- [31] J. R. Fincke, W. D. Swank, R. L. Bewley, D. C. Haggard, M. Gevelber, and D. Wroblewski, 'Diagnostics and control in the thermal spray process', *Surf. Coat. Technol.*, vol. 146–147, pp. 537–543, Sep. 2001, doi: 10.1016/S0257-8972(01)01432-3.
- [32] R. Upadhyaya, S. Tailor, S. Shrivastava, and S. C. Modi, 'High performance thermal-sprayed WC-10Co-4Cr coatings in narrow and complex areas', *Surf. Eng.*, vol. 34, no. 5, pp. 412–421, May 2018, doi: 10.1080/02670844.2017.1375175.
- [33] W. Tillmann, E. Vogli, and B. Krebs, 'Influence of the Spray Angle on the Characteristics of Atmospheric Plasma Sprayed Hard Material Based Coatings', *J. Therm. Spray Technol.*, vol. 17, no. 5–6, pp. 948–955, Dec. 2008, doi: 10.1007/s11666-008-9261-6.
- [34] TWI, 'What are the disadvantages of plasma spraying?', *What are the disadvantages of plasma spraying?* <http://www.twi-global.com/technical-knowledge/faqs/faq-what-are-the-disadvantages-of-plasma-spraying/> (accessed Jul. 27, 2017).
- [35] G. Mauer, M. O. Jarligo, D. Marcano, S. Rezanka, D. Zhou, and R. Vaßen, 'Recent developments in plasma spray processes for applications in energy technology', *IOP Conf. Ser. Mater. Sci. Eng.*, vol. 181, p. 012001, Mar. 2017, doi: 10.1088/1757-899X/181/1/012001.
- [36] N. Markocsan, M. Gupta, S. Joshi, P. Nylén, X.-H. Li, and J. Wigren, 'Liquid Feedstock Plasma Spraying: An Emerging Process for Advanced Thermal Barrier Coatings', *J. Therm. Spray Technol.*, May 2017, doi: 10.1007/s11666-017-0555-4.
- [37] G. Mauer, K.-H. Rauwald, R. Mücke, and R. Vaßen, 'Monitoring and Improving the Reliability of Plasma Spray Processes', *J. Therm. Spray Technol.*, vol. 26, no. 5, pp. 799–810, Jun. 2017, doi: 10.1007/s11666-017-0559-0.
- [38] C. Chazelas, J. P. Trelles, I. Choquet, and A. Vardelle, 'Main Issues for a Fully Predictive Plasma Spray Torch Model and Numerical Considerations', *Plasma Chem. Plasma Process.*, vol. 37, no. 3, pp. 627–651, May 2017, doi: 10.1007/s11090-017-9808-8.
- [39] D. Zhang, L. Zheng, X. Hu, and H. Zhang, 'Numerical studies of arc plasma generation in single cathode and three-cathode plasma torch and its impact on plasma spraying', *Int. J. Heat Mass Transf.*, vol. 98, pp. 508–522, Jul. 2016, doi: 10.1016/j.ijheatmasstransfer.2016.03.038.

- [40] L. C. Kumruoglu, F. Ustel, A. Ozel, and A. Mimaroglu, 'Micro Arc Oxidation of Wire Arc Sprayed Al-Mg6, Al-Si12, Al Coatings on Low Alloyed Steel', *Engineering*, vol. 03, no. 07, pp. 680–690, 2011, doi: 10.4236/eng.2011.37081.
- [41] J. L. Margolies and S. S. Pabla, 'Wire arc spray system using composite wire for porous coating, and related method', EP 2 343 395 A1, Aug-2014.
- [42] A. Czupryński, J. Gorka, and M. Adamiak, 'Examining properties of arc sprayed nanostructured coatings', *Metalurgija*, vol. 55, no. 2, pp. 173–176, 2016.
- [43] X. Feng, M. P. Planche, S. Deng, H. Liao, H. Rabat, and D. Hong, 'Study of the particle behavior in a pulsed arc', *Surf. Coat. Technol.*, vol. 287, pp. 113–118, Feb. 2016, doi: 10.1016/j.surfcoat.2015.12.020.
- [44] J. Tikkanen *et al.*, 'Characteristics of the liquid flame spray process', *Surf. Coat. Technol.*, vol. 90, no. 3, pp. 210–216, 1997.
- [45] S. Kuroda, J. Kawakita, M. Watanabe, and H. Katanoda, 'Warm spraying—a novel coating process based on high-velocity impact of solid particles', *Sci. Technol. Adv. Mater.*, vol. 9, no. 3, p. 033002, Jul. 2008, doi: 10.1088/1468-6996/9/3/033002.
- [46] A. Vardelle *et al.*, 'The 2016 Thermal Spray Roadmap', *J. Therm. Spray Technol.*, vol. 25, no. 8, pp. 1376–1440, Dec. 2016, doi: 10.1007/s11666-016-0473-x.
- [47] E. Gozali, S. Kamnis, and S. Gu, 'Numerical investigation of combustion and liquid feedstock in high velocity suspension flame spraying process', *Surf. Coat. Technol.*, vol. 228, pp. 176–186, Aug. 2013, doi: 10.1016/j.surfcoat.2013.04.026.
- [48] Alknimov Anatoliyi R, Kodzarev Vladimir F, Nedzterovisn Nikolayi I, and Rarurin Anatoliyi N, 'Method of Producing Coatings', SU1618778 (A1), 07-Jan-1991.
- [49] Alknimov Anatoliyi R, Nedzterovisn Nikolayi I, Rarurin Anatoliyi N, Kodzarev Vladimir F, and Dznudzranov Miknail M, 'Device for Applying Coating', SU1618777 (A1), 07-Jan-1991.
- [50] A. P. Alkhimov, A. N. Papyrin, V. F. Kosarev, N. I. Nesterovich, and M. M. Shushpanov, 'Gas-dynamic spraying method for applying a coating', US5302414A, 12-Apr-1994.
- [51] V. Champagne and D. Helfritsch, 'The unique abilities of cold spray deposition', *Int. Mater. Rev.*, vol. 61, no. 7, pp. 437–455, Oct. 2016, doi: 10.1080/09506608.2016.1194948.
- [52] J. Pattison, S. Celotto, R. Morgan, M. Bray, and W. O'Neill, 'Cold gas dynamic manufacturing: A non-thermal approach to freeform fabrication', *Int. J. Mach. Tools Manuf.*, vol. 47, no. 3–4, pp. 627–634, Mar. 2007, doi: 10.1016/j.ijmachtools.2006.05.001.
- [53] R. Singh, G. Singh, and H. S. Sidhu, 'The Cold Spray Coating Process: A Future Technique in Material Deposition', *Asian J. Eng. Appl. Technol.*, vol. 5, no. 1, pp. 1–3, 2016.
- [54] V. Champagne, D. Helfritsch, P. Leyman, R. Lempicki, and S. Grendahl, 'The effects of gas and metal characteristics on sprayed metal coatings', *Model. Simul. Mater. Sci. Eng.*, vol. 13, no. 7, pp. 1119–1128, Oct. 2005, doi: 10.1088/0965-0393/13/7/008.
- [55] V. K. Champagne, S. P. Dinavahi, and P. F. Leyman, 'Prediction of Particle Velocity for the Cold Spray Process', Army Research Lab Aberdeen Proving Ground MD Weapons and Materials Research Directorate, 2011. Accessed: 03-Aug-2017. [Online]. Available: <http://www.dtic.mil/docs/citations/ADA551777>.
- [56] W.-Y. Li and C.-J. Li, 'Optimal Design of a Novel Cold Spray Gun Nozzle at a Limited Space', *J. Therm. Spray Technol.*, vol. 14, no. 3, pp. 391–396, Sep. 2005, doi: 10.1361/105996305X59404.
- [57] S. P. Pardhasaradhi, V. Venkatachalapathy, S. V. Joshi, and S. Govindan, 'Optical Diagnostics Study of Gas Particle Transport Phenomena in Cold Gas Dynamic Spraying and Comparison with Model Predictions', *J. Therm. Spray Technol.*, vol. 17, no. 4, pp. 551–563, Dec. 2008, doi: 10.1007/s11666-008-9206-0.
- [58] A.P. Alkhimov, V.F. Kosarev, and S.V. Klinkov, 'The Features of Cold Spray Nozzle Design', *J. Therm. Spray Technol.*, vol. 10(2), Jun. 2001.
- [59] M. Meyer and R. Lupoi, 'Supersonic Spray Advanced Modelling SSAM', presented at the 19th Annual Sir Bernard Crossland Symposium & Postgraduate Workshop, Queen s University

- Belfast, 2016, Accessed: 07-Aug-2017. [Online]. Available: http://www.tara.tcd.ie/bitstream/handle/2262/77888/PosterA1ssam_crossland_v1.pdf?sequence=1.
- [60] M. Grujicic, J. R. Saylor, D. E. Beasley, W. S. DeRosset, and D. Helfritsch, 'Computational analysis of the interfacial bonding between feed-powder particles and the substrate in the cold-gas dynamic-spray process', *Appl. Surf. Sci.*, vol. 219, no. 3–4, pp. 211–227, Dec. 2003, doi: 10.1016/S0169-4332(03)00643-3.
- [61] A. O. Tokarev, 'Structure of aluminum powder coatings prepared by cold gasdynamic spraying', *Met. Sci. Heat Treat.*, vol. 38, no. 3, pp. 136–139, 1996.
- [62] G. Huang, H. Wang, X. Li, and L. Xing, 'Study on the Growth of Holes in Cold Spraying via Numerical Simulation and Experimental Methods', *Coatings*, vol. 7, no. 1, p. 2, Dec. 2016, doi: 10.3390/coatings7010002.
- [63] L. Ajdelsztajn, J. M. Schoenung, B. Jodoin, and G. E. Kim, 'Cold spray deposition of nanocrystalline aluminum alloys', *Metall. Mater. Trans. A*, vol. 36, no. 3, pp. 657–666, Mar. 2005, doi: 10.1007/s11661-005-0182-4.
- [64] C.-J. Li, W.-Y. Li, and Y.-Y. Wang, 'Formation of metastable phases in cold-sprayed soft metallic deposit', *Surf. Coat. Technol.*, vol. 198, no. 1–3, pp. 469–473, Aug. 2005, doi: 10.1016/j.surfcoat.2004.10.063.
- [65] S. Bagherifard *et al.*, 'Cold Spray Deposition of Freestanding Inconel Samples and Comparative Analysis with Selective Laser Melting', *J. Therm. Spray Technol.*, vol. 26, no. 7, pp. 1517–1526, Oct. 2017, doi: 10.1007/s11666-017-0572-3.
- [66] F. Gärtner, 'Advances in cold spraying', *Surf. Eng.*, vol. 22, no. 3, pp. 161–163, Jun. 2006, doi: 10.1179/174329406X108906.
- [67] H. Koivuluoto, J. Näkki, and P. Vuoristo, 'Corrosion Properties of Cold-Sprayed Tantalum Coatings', *J. Therm. Spray Technol.*, vol. 18, no. 1, pp. 75–82, Mar. 2009, doi: 10.1007/s11666-008-9281-2.
- [68] H. Koivuluoto, A. Milanti, G. Bolelli, L. Lusvarghi, and P. Vuoristo, 'High-Pressure Cold-Sprayed Ni and Ni-Cu Coatings: Improved Structures and Corrosion Properties', *J. Therm. Spray Technol.*, vol. 23, no. 1–2, pp. 98–103, Jan. 2014, doi: 10.1007/s11666-013-0016-7.
- [69] H. Kim, C. Lee, and S. Hwang, 'Fabrication of WC-Co coatings by cold spray deposition', *Surf. Coat. Technol.*, vol. 191, no. 2–3, pp. 335–340, Feb. 2005, doi: 10.1016/j.surfcoat.2004.04.058.
- [70] X.-T. Luo, C.-X. Li, F.-L. Shang, G.-J. Yang, Y.-Y. Wang, and C.-J. Li, 'WC-Co Composite Coating Deposited by Cold Spraying of a Core-Shell-Structured WC-Co Powder', *J. Therm. Spray Technol.*, Aug. 2014, doi: 10.1007/s11666-014-0133-y.
- [71] Inovati, 'Kinetic Metallization: Coatings Once Thought Impossible', *Kinetic Metallization: Coatings Once Thought Impossible*. <https://www.inovati.com/> (accessed Aug. 08, 2017).
- [72] R. Tapphorn and H. Gabel, 'Brush-sieve powder-fluidizing apparatus for feeding nano-size and ultra-fine powders', US 7,273,075 B2, Sep-2007.
- [73] Ralph Tapphorn and Howard Gabel, 'System and process for solid-state deposition and consolidation of high velocity powder particles using thermal plastic deformation', US 6915964 B2.
- [74] V. K. Champagne and D. J. Helfritsch, 'Mainstreaming cold spray – push for applications', *Surf. Eng.*, vol. 30, no. 6, pp. 396–403, Jun. 2014, doi: 10.1179/1743294414Y.0000000277.
- [75] L. Xue, Y. Li, and S. Wang, 'Direct manufacturing of net-shape functional components/test-pieces for aerospace, automotive and other applications', *Int. Congr. Appl. Lasers Electro-Opt.*, Sep. 2010, doi: 10.2351/1.5062069.
- [76] L. Xue, S. Wang, and J. Jiang, *Cold gas dynamic spray apparatus, system and method*. Google Patents, 2015.

- [77] G. Benenati and R. Lupoi, 'Development of a Deposition Strategy in Cold Spray for Additive Manufacturing to Minimize Residual Stresses', *Procedia CIRP*, vol. 55, pp. 101–108, 2016, doi: 10.1016/j.procir.2016.08.042.
- [78] Dan Kaplowitz, 'Cold Spray for Additive Manufacturing', Open Campus, United States Army, 18-Dec-2014.
- [79] B. Prawara, H. Yara, Y. Miyagi, and T. Fukushima, 'Spark plasma sintering as a post-spray treatment for thermally-sprayed coatings', *Surf. Coat. Technol.*, vol. 162, no. 2–3, pp. 234–241, Jan. 2003, doi: 10.1016/S0257-8972(02)00564-9.
- [80] Y.-H. Shieh, J.-T. Wang, H. C. Shih, and S.-T. Wu, 'Alloying and post-heat-treatment of thermal-sprayed coatings of self-fluxing alloys', *Surf. Coat. Technol.*, vol. 58, no. 1, pp. 73–77, Jun. 1993, doi: 10.1016/0257-8972(93)90176-O.
- [81] T Stoltenhoff, H. Kreye, H.J. Richter, and H. Assadi, 'Optimisation of the cold spray process.', in *Thermal Spray 2001: New Surfaces for a New Millennium (ASM International)*, 2001, pp. 409-416 (8).
- [82] R.C. Dykhuizen and R.A. Neiser, 'Optimizing the Cold Spray Process', *Therm. Spray 2003 Adv. Sci. Appl. Technol. ASM Int.*, pp. 19-26 (8), 2003.
- [83] A. Cockburn, M. Bray, and B. O'Neill, 'The laser-assisted cold spray process', *Laser User*, no. 53, pp. 30–31, 2008.
- [84] A. Birt, V. Champagne, R. Sisson, D. Apelian, and J. Dallaraosa, 'Laser Assisted Cold Spray of Titanium', Worcester Polytechnic Institute, 24-Jun-2015.
- [85] Sathwik Reddy Toom, 'Development of Fe-Mn alloy coatings using Coaxial laser assisted cold spray process', Masters Thesis, University of Michigan- Dearborn, 2017.
- [86] Heli Koivuluoto, 'Overview of Laser-Assisted Cold-Sprayed Metallic Coatings', presented at the NACSC 2016, Edmonton, Canada, Tampere University of Technology Department of Materials Science Surface Engineering Research Team Tampere, Finland, 2016.
- [87] E. O. Olakanmi and M. Doyoyo, 'Laser-Assisted Cold-Sprayed Corrosion- and Wear-Resistant Coatings: A Review', *J. Therm. Spray Technol.*, vol. 23, no. 5, pp. 765–785, Jun. 2014, doi: 10.1007/s11666-014-0098-x.
- [88] Robert A. Sailer, Justin M. Hoey, Iskander Akhatov, Orven Swenson, Artur Lutfurakhmanov, and Michael Robinson, 'Micro cold spray direct write systems and methods for printed micro electronics', US20140370203A1.
- [89] J. Villafuerte, 'Current and future applications of cold spray technology', *Met. Finish.*, vol. 108, no. 1, pp. 37–39, 2010.
- [90] A. Moridi, S. M. Hassani-Gangaraj, M. Guagliano, and M. Dao, 'Cold spray coating: review of material systems and future perspectives', *Surf. Eng.*, vol. 30, no. 6, pp. 369–395, Jun. 2014, doi: 10.1179/1743294414Y.0000000270.
- [91] J. Vlcek, L. Gimeno, H. Huber, and E. Lugscheider, 'A Systematic Approach to Material Eligibility for the Cold-Spray Process', *J. Therm. Spray Technol.*, vol. 14, no. 1, pp. 125–133, Mar. 2005, doi: 10.1361/10599630522738.
- [92] K. Dobler, H. Kreye, and R. Schwetzke, 'Oxidation of Stainless Steel in the High Velocity Oxy-Fuel Process', *J. Therm. Spray Technol.*, vol. 9, no. 3, pp. 407–413, Sep. 2000, doi: 10.1361/105996300770349872.
- [93] A. Moridi, S. M. Hassani-Gangaraj, and M. Guagliano, 'On Fatigue Behavior of Cold Spray Coating', *MRS Proc.*, vol. 1650, 2014, doi: 10.1557/opl.2014.438.
- [94] W. R. Chen, E. Irissou, X. Wu, J.-G. Legoux, and B. R. Marple, 'The Oxidation Behavior of TBC with Cold Spray CoNiCrAlY Bond Coat', *J. Therm. Spray Technol.*, vol. 20, no. 1–2, pp. 132–138, Jan. 2011, doi: 10.1007/s11666-010-9601-1.
- [95] A. Moridi, M. Azadi, and G. H. Farrahi, 'Thermo-mechanical stress analysis of thermal barrier coating system considering thickness and roughness effects', *Surf. Coat. Technol.*, vol. 243, pp. 91–99, Mar. 2014, doi: 10.1016/j.surfcoat.2012.02.019.

- [96] H. Singh, T. S. Sidhu, S. B. S. Kalsi, and J. Karthikeyan, 'Development of cold spray from innovation to emerging future coating technology', *J. Braz. Soc. Mech. Sci. Eng.*, vol. 35, no. 3, pp. 231–245, Oct. 2013, doi: 10.1007/s40430-013-0030-1.
- [97] J. Karthikeyan, 'Development of Oxidation Resistant Coatings on GRCo-84 Substrates by Cold Spray Process', ASB Industries, Inc., Barberton, Ohio, NASA/CR—2007-214706, 2007.
- [98] V. K. Champagne, P. F. Leyman, and D. J. Helfritsch, 'Magnesium Repair by Cold Spray', U.S. Army Research Laboratory, ARL-TR-4438, 2008.
- [99] B. DeForce *et al.*, 'Application of aluminum coatings for the corrosion protection of magnesium by cold spray', US Army Research Laboratory, 2007.
- [100] P. Fauchais, G. Montavon, and G. Bertrand, 'From Powders to Thermally Sprayed Coatings', *J. Therm. Spray Technol.*, vol. 19, no. 1–2, pp. 56–80, Jan. 2010, doi: 10.1007/s11666-009-9435-x.
- [101] H. Y. Lee, Y. H. Yu, Y. C. Lee, Y. P. Hong, and K. H. Ko, 'Thin Film Coatings of WO₃ by Cold Gas Dynamic Spray: A Technical Note', *J. Therm. Spray Technol.*, vol. 14, no. 2, pp. 183–186, Jun. 2005, doi: 10.1361/105996304523791.
- [102] J.-O. Kliemann, H. Gutzmann, F. Gärtner, H. Hübner, C. Borchers, and T. Klassen, 'Formation of Cold-Sprayed Ceramic Titanium Dioxide Layers on Metal Surfaces', *J. Therm. Spray Technol.*, vol. 20, no. 1–2, pp. 292–298, Jan. 2011, doi: 10.1007/s11666-010-9563-3.
- [103] R. Lupoi and W. O'Neill, 'Deposition of metallic coatings on polymer surfaces using cold spray', *Surf. Coat. Technol.*, vol. 205, no. 7, pp. 2167–2173, Dec. 2010, doi: 10.1016/j.surfcoat.2010.08.128.
- [104] X. L. Zhou, A. F. Chen, J. C. Liu, X. K. Wu, and J. S. Zhang, 'Preparation of metallic coatings on polymer matrix composites by cold spray', *Surf. Coat. Technol.*, vol. 206, no. 1, pp. 132–136, Oct. 2011, doi: 10.1016/j.surfcoat.2011.07.005.
- [105] J. H. Lee *et al.*, 'In vitro and in vivo evaluation of the bioactivity of hydroxyapatite-coated polyetheretherketone biocomposites created by cold spray technology', *Acta Biomater.*, vol. 9, no. 4, pp. 6177–6187, Apr. 2013, doi: 10.1016/j.actbio.2012.11.030.
- [106] M. Gardon, A. Latorre, M. Torrell, S. Dosta, J. Fernández, and J. M. Guilemany, 'Cold gas spray titanium coatings onto a biocompatible polymer', *Mater. Lett.*, vol. 106, pp. 97–99, Sep. 2013, doi: 10.1016/j.matlet.2013.04.115.
- [107] Y. Xu and I. M. Hutchings, 'Cold spray deposition of thermoplastic powder', *Surf. Coat. Technol.*, vol. 201, no. 6, pp. 3044–3050, Dec. 2006, doi: 10.1016/j.surfcoat.2006.06.016.
- [108] A. S. Alhulaifi, G. A. Buck, and W. J. Arbegast, 'Numerical and Experimental Investigation of Cold Spray Gas Dynamic Effects for Polymer Coating', *J. Therm. Spray Technol.*, vol. 21, no. 5, pp. 852–862, Sep. 2012, doi: 10.1007/s11666-012-9743-4.
- [109] Jianhong He and Julie M. Schoenung, 'Nanostructured coatings', *Mater. Sci. Eng.*, pp. 274–319, 2002.
- [110] L. Ajdelsztajn, A. Zúñiga, B. Jodoin, and E. J. Lavernia, 'Cold-Spray Processing of a Nanocrystalline Al-Cu-Mg-Fe-Ni Alloy with Sc', *J. Therm. Spray Technol.*, vol. 15, no. 2, pp. 184–190, Jun. 2006, doi: 10.1361/105996306X107995.
- [111] A. C. Hall, L. N. Brewer, and T. J. Roemer, 'Preparation of Aluminum Coatings Containing Homogenous Nanocrystalline Microstructures Using the Cold Spray Process', *J. Therm. Spray Technol.*, vol. 17, no. 3, pp. 352–359, Sep. 2008, doi: 10.1007/s11666-008-9180-6.
- [112] R. Asmatulu, '14 - Nanocoatings for corrosion protection of aerospace alloys', in *Corrosion Protection and Control Using Nanomaterials*, V. S. Saji and R. Cook, Eds. Woodhead Publishing, 2012, pp. 357–374.
- [113] R. S. Lima, J. Karthikeyan, C. M. Kay, J. Lindemann, and C. C. Berndt, 'Microstructural characteristics of cold-sprayed nanostructured WC-Co coatings', *Thin Solid Films*, vol. 416, no. 1–2, pp. 129–135, Sep. 2002, doi: 10.1016/S0040-6090(02)00631-4.
- [114] P. E. Santangelo, G. Allesina, G. Bolelli, L. Lusvarghi, V. Matikainen, and P. Vuoristo, 'Infrared Thermography as a Non-destructive Testing Solution for Thermal Spray Metal Coatings', *J.*

- Therm. Spray Technol.*, vol. 26, no. 8, pp. 1982–1993, Dec. 2017, doi: 10.1007/s11666-017-0642-6.
- [115] M. A. Zavareh, B. A. Razak, and S. Kakooei, 'Fundamentals and Applications of Thermal Spray Coating', vol. 05, p. 11, 2017.
- [116] R. Kromer, S. Costil, C. Verdy, S. Gojon, and H. Liao, 'Laser surface texturing to enhance adhesion bond strength of spray coatings – Cold spraying, wire-arc spraying, and atmospheric plasma spraying', *Surf. Coat. Technol.*, May 2017, doi: 10.1016/j.surfcoat.2017.05.007.
- [117] BryCoat Inc., 'Thermal Spray Coating Technology', *Metallurgical Coating Services & Surface Engineering*. <http://www.brycoat.com/brycoat-resources/thermal-spray-coating-technology/> (accessed Jul. 15, 2018).
- [118] Sandia National Laboratories, 'Sandia's Approach to Cold Spray Research', Thermal Spray Research Laboratory, 1999, [Online]. Available: http://www.sandia.gov/coldspray/presentations/dlg_90714_csw_talk.pdf.
- [119] Sulzer Metco, 'An Introduction to Thermal Spray', https://www.upc.edu/sct/es/documents_equipment/d_324_id-804-2.pdf, Issue 4, 2013. Accessed: 15-Jul-2018. [Online]. Available: https://www.upc.edu/sct/es/documents_equipment/d_324_id-804-2.pdf.
- [120] H. Fukanuma and N. Ohno, 'A study of adhesive strength of cold spray coatings', presented at the Thermal spray 2004: advances in technology and application, Osaka, Japan, 2004, pp. 329–334.
- [121] R. Huang, W. Ma, and H. Fukanuma, 'Development of ultra-strong adhesive strength coatings using cold spray', *Surf. Coat. Technol.*, vol. 258, pp. 832–841, Nov. 2014, doi: 10.1016/j.surfcoat.2014.07.074.
- [122] Precision 3D, 'Cold Spray Rail Industry Pamphlet'. 2016.
- [123] R. N. Raelison, Ch. Verdy, and H. Liao, 'Cold gas dynamic spray additive manufacturing today: Deposit possibilities, technological solutions and viable applications', *Mater. Des.*, vol. 133, pp. 266–287, Nov. 2017, doi: 10.1016/j.matdes.2017.07.067.
- [124] A. Killinger, P. Müller, and R. Gadow, 'What Do We Know, What are the Current Limitations of Suspension HVOF Spraying?', *J. Therm. Spray Technol.*, vol. 24, no. 7, pp. 1130–1142, Oct. 2015, doi: 10.1007/s11666-015-0264-9.
- [125] A. Harir, H. Ageorges, A. Grimaud, P. Fauchais, and F. Platon, 'Low Friction Stainless Steel Coatings Graphite Doped Elaborated by Air Plasma Sprayed', *J. Mater. Eng. Perform.*, vol. 13, no. 5, pp. 557–563, Oct. 2004, doi: 10.1361/10599490419955.
- [126] N. P. Padture *et al.*, 'Towards durable thermal barrier coatings with novel microstructures deposited by solution-precursor plasma spray', *Acta Mater.*, vol. 49, no. 12, pp. 2251–2257, Jul. 2001, doi: 10.1016/S1359-6454(01)00130-6.
- [127] P. Fauchais, M. Vardelle, A. Vardelle, and S. Goutier, 'What Do We Know, What are the Current Limitations of Suspension Plasma Spraying?', *J. Therm. Spray Technol.*, vol. 24, no. 7, pp. 1120–1129, Oct. 2015, doi: 10.1007/s11666-015-0286-3.
- [128] J. D. Majumdar and I. Manna, 'Laser processing of materials', *Sadhana*, vol. 28, no. 3–4, pp. 495–562, 2003.
- [129] JS Lasertechnik, 'How tube laser cutting increases your productivity'. https://www.js-lasertechnik.com/en/laser_tube_cutting_advantages.php (accessed Mar. 22, 2019).
- [130] Dr. Edgar Willenb, 'Automated Polishing for the European Tooling Industry', Fraunhofer Institute for Laser Technology ILT, 2013. [Online]. Available: <https://cordis.europa.eu/docs/results/246001/final1-final-report-polimatic-v12.pdf>.
- [131] E. M. Breinan, C. M. Banas, and B. H. Kear, 'Processing materials with lasers', *Phys. Today*, vol. 29, no. 11, pp. 44–50, Nov. 1976, doi: 10.1063/1.3024504.
- [132] M. Naeem, 'Laser Heat-treatment', *JKLasers White Pap.*, 2009, Accessed: 25-Aug-2014. [Online]. Available: <http://www.jklasers.com/images/LaserHeatTreatment.pdf>.
- [133] W. M. Steen and J. Mazumder, *Laser Material Processing*. London: Springer London, 2010.

- [134] A. Florakis, E. Verrelli, D. Giubertoni, G. Tzortzis, and D. Tsoukalas, 'Non-melting annealing of silicon by CO₂ laser', *Thin Solid Films*, vol. 518, no. 9, pp. 2551–2554, Feb. 2010, doi: 10.1016/j.tsf.2009.09.140.
- [135] Joel De Kock, 'Laser Heat Treating', *Industrial Heating*, pp. 1–4, Oct-2001.
- [136] S. Stathopoulos, L. Tsetseris, N. Pradhan, B. Colombeau, and D. Tsoukalas, 'Millisecond non-melt laser annealing of phosphorus implanted germanium: Influence of nitrogen co-doping', *J. Appl. Phys.*, vol. 118, no. 13, p. 135710, Oct. 2015, doi: 10.1063/1.4932600.
- [137] V. Paunoiu, E. A. Squeo, F. Quadrini, C. Gheorghies, and D. Nicoara, 'Laser bending of stainless steel sheet metals', *Int. J. Mater. Form.*, vol. 1, no. 1, pp. 1371–1374, 2008.
- [138] D. Schuöcker, *Handbook of the EuroLaser Academy*. Chapman & Hall, 1998.
- [139] Y. Shi, Y. Liu, P. Yi, and J. Hu, 'Effect of different heating methods on deformation of metal plate under upsetting mechanism in laser forming', *Opt. Laser Technol.*, vol. 44, no. 2, pp. 486–491, Mar. 2012, doi: 10.1016/j.optlastec.2011.08.019.
- [140] J. Magee and L. J. De Vin, 'Process planning for laser-assisted forming', *J. Mater. Process. Technol.*, vol. 120, no. 1, pp. 322–326, 2002.
- [141] Birendra Kumar Maharana, 'Optimization of process parameters in laser sheet metal bending', National Institute of Technology Rourkela, 2011.
- [142] M. Giacomantonio, S. Gulizia, M. Jahedi, Y. Wong, R. Moore, and M. Valimberti, 'Heat treatment of thermally sprayed Ni-based wear and corrosion coatings', *Mater. Forum*, vol. 35, pp. 48–55, 2011.
- [143] Šarūnas MEŠKINIS, Judita. PUIŠO, and Algis JURAITIS, 'Effects of the High Temperature Annealing on Structure of the High Velocity Oxygen Fuel Deposited WC-Co Coatings', *Mater. Sci. MEDŽIAGOTYRA*, vol. 12, no. 3, pp. 1392–1320, 2006.
- [144] L. Pawlowski, 'Thick Laser Coatings: A Review', *J. Therm. Spray Technol.*, vol. 8, no. 2, pp. 279–295, Jun. 1999, doi: 10/c7fxjx.
- [145] G. Sundararajan, P. Sudharshan Phani, A. Jyothirmayi, and R. C. Gundakaram, 'The influence of heat treatment on the microstructural, mechanical and corrosion behaviour of cold sprayed SS 316L coatings', *J. Mater. Sci.*, vol. 44, no. 9, pp. 2320–2326, May 2009, doi: 10.1007/s10853-008-3200-2.
- [146] J. Suutala, J. Tuominen, and P. Vuoristo, 'Laser-assisted spraying and laser treatment of thermally sprayed coatings', *Surf. Coat. Technol.*, vol. 201, no. 5, pp. 1981–1987, Oct. 2006, doi: 10.1016/j.surfcoat.2006.04.042.
- [147] G. Antou, G. Montavon, F. Hlawka, A. Cornet, C. Coddet, and F. Machi, 'Modification of ceramic thermal spray deposit microstructures implementing in situ laser remelting', *Surf. Coat. Technol.*, vol. 172, no. 2–3, pp. 279–290, Jul. 2003, doi: 10.1016/S0257-8972(03)00431-6.
- [148] C. S. Montross, T. Wei, L. Ye, G. Clark, and Y.-W. Mai, 'Laser shock processing and its effects on microstructure and properties of metal alloys: a review', *Int. J. Fatigue*, vol. 24, no. 10, pp. 1021–1036, 2002.
- [149] N. C. Anderholm, 'LASER-GENERATED STRESS WAVES', *Appl. Phys. Lett.*, vol. 16, no. 3, pp. 113–115, Feb. 1970, doi: 10.1063/1.1653116.
- [150] D. W. Gregg and S. J. Thomas, 'Momentum Transfer Produced by Focused Laser Giant Pulses', *J. Appl. Phys.*, vol. 37, no. 7, pp. 2787–2789, Jun. 1966, doi: 10.1063/1.1782123.
- [151] E. D. Jones, 'Ultrafast laser-induced stress waves in solids', *Appl. Phys. Lett.*, vol. 18, no. 1, pp. 33–35, Jan. 1971, doi: 10.1063/1.1653468.
- [152] C. S. MONTROSS, V. FLOREA, and M. V. SWAIN, 'The influence of coatings on subsurface mechanical properties of laser peened 2011-T3 aluminum', *J. Mater. Sci.*, vol. 36, pp. 1801–1807, 2001.
- [153] J. N. Johnson and R. W. Rohde, 'Dynamic Deformation Twinning in Shock-Loaded Iron', *J. Appl. Phys.*, vol. 42, no. 11, pp. 4171–4182, Oct. 1971, doi: 10.1063/1.1659750.

- [154] S. H. Niehoff and F. Vollertsen, 'Laser induced shock waves in deformation processing', *Metalurgija*, vol. 11, no. 3, pp. 183–194, 2005.
- [155] C. Chen, X. Zhang, L. Han, and X. Yan, 'Effect of Laser Shock Peening on Fatigue Life of Full Scale Turbine Blades', in *ASME Turbo Expo 2017: Turbomachinery Technical Conference and Exposition*, 2017, p. V07AT31A007–V07AT31A007, Accessed: 28-Aug-2017. [Online]. Available: <http://proceedings.asmedigitalcollection.asme.org/proceeding.aspx?articleid=2650322>.
- [156] A. Kulkarni, S. Chettri, S. Prabhakaran, and S. Kalainathan, 'Effect of Laser Shock Peening Without Coating on Surface Morphology and Mechanical Properties of Nickel-200', *Mech. Mater. Sci. Eng. MMSE J. Open Access*, vol. 9, 2017, Accessed: 28-Aug-2017. [Online]. Available: <https://hal.archives-ouvertes.fr/hal-01504780/>.
- [157] 'Femtosecond laser peening of 2024 aluminum alloy without a sacrificial overlay under atmospheric conditions', *J. Laser Appl.*, vol. 29, no. 1, p. 012005, Feb. 2017, doi: 10.2351/1.4967013.
- [158] S. Xu, S. Huang, X. Meng, J. Sheng, H. Zhang, and J. Zhou, 'Thermal evolution of residual stress in IN718 alloy subjected to laser peening', *Opt. Lasers Eng.*, vol. 94, pp. 70–75, Jul. 2017, doi: 10.1016/j.optlaseng.2017.03.004.
- [159] X. Meng *et al.*, 'Residual stress relaxation and its effects on the fatigue properties of Ti6Al4V alloy strengthened by warm laser peening', *Mater. Sci. Eng. A*, vol. 680, pp. 297–304, Jan. 2017, doi: 10.1016/j.msea.2016.10.073.
- [160] S. Bagherifard, I. Fernández Pariente, R. Ghelichi, M. Guagliano, and S. Vezzù, 'Effect of Shot Peening on Residual Stresses and Surface Work-Hardening in Cold Sprayed Coatings', *Key Eng. Mater.*, vol. 417–418, pp. 397–400, Oct. 2009, doi: 10.4028/www.scientific.net/KEM.417-418.397.
- [161] G. Kelkar, 'Pulsed laser welding', *WJM Technol. Excell. Mater. Join. Cerritos CA*, vol. 90703, 2000, Accessed: 13-Apr-2015. [Online]. Available: <http://www.welding-consultant.com/PulsedLaserWelding.pdf>.
- [162] K. Colligan, 'Densification of thermal spray coatings', US7105205B2.
- [163] W. D. Pratt, 'Apparatus and method for smoothing and densifying a coating on a workpiece', 5,484,980, 16-Jan-1996.
- [164] N. Bala, H. Singh, J. Karthikeyan, and S. Prakash, 'Cold spray coating process for corrosion protection: a review', *Surf. Eng.*, vol. 30, no. 6, pp. 414–421, Jun. 2014, doi: 10.1179/1743294413Y.0000000148.
- [165] 'Nickel Alloy 625 / Inconel 625 (UNS N06625) - Aircraft Materials'. <http://www.aircraftmaterials.com/data/nickel/inconel625.html> (accessed Aug. 31, 2015).
- [166] PilotManu, 'Pilot-production of nanostructured components'. 2015, [Online]. Available: <http://diam-edil.ch/data/pdf/Pilotmanu.pdf>.
- [167] Innovnano, 'Nanostructured powders for demanding ceramic applications'. 2015, Accessed: 16-Feb-2017. [Online].
- [168] Z. Zhang, 'Processing of Nanostructured WC-Co Powders and Sintered Steels', Thesis, Materialvetenskap, 2003.
- [169] F. Luo, A. Cockburn, R. Lupoi, M. Sparkes, and W. O'Neill, 'Performance comparison of Stellite 6® deposited on steel using supersonic laser deposition and laser cladding', *Surf. Coat. Technol.*, vol. 212, pp. 119–127, Nov. 2012, doi: 10.1016/j.surfcoat.2012.09.031.
- [170] J. M. Guilemany, N. Espallargas, P. H. Suegama, A. V. Benedetti, and J. Fernández, 'Study of the Properties of WC-Co Nanostructured Coatings Sprayed by High-Velocity Oxyfuel', *J. Therm. Spray Technol.*, vol. 14, no. 3, pp. 335–341, Sep. 2005, doi: 10.1361/105996305X59350.
- [171] J. Rabinovich, 'Process for energy beam solid-state metallurgical bonding of wires having two or more flat surfaces', US 8,334,475, 2012.

- [172] M. B. Frish, P. E. Nebolsine, and A. N. Pirri, *Method for bonding using laser induced heat and pressure*. Google Patents, 1987.
- [173] R. M. White, 'Generation of Elastic Waves by Transient Surface Heating', *J. Appl. Phys.*, vol. 34, no. 12, p. 3559, 1963, doi: 10.1063/1.1729258.
- [174] C. B. Scruby, R. J. Dewhurst, D. A. Hutchins, and S. B. Palmer, 'Quantitative studies of thermally generated elastic waves in laser-irradiated metals', *J. Appl. Phys.*, vol. 51, no. 12, p. 6210, 1980, doi: 10.1063/1.327601.
- [175] A. Berezovski and M. Berezovski, 'Influence of microstructure on thermoelastic wave propagation', *Acta Mech.*, vol. 224, no. 11, pp. 2623–2633, Nov. 2013, doi: 10.1007/s00707-013-0884-4.
- [176] H. Guleryuz and H. Cimenoglu, 'Oxidation of Ti–6Al–4V alloy', *J. Alloys Compd.*, vol. 472, no. 1–2, pp. 241–246, Mar. 2009, doi: 10.1016/j.jallcom.2008.04.024.
- [177] G. E. Kim and M. Brochu, 'Thermal spray nanostructured ceramic and metal-matrix composite coatings', in *Anti-Abrasive Nanocoatings*, Elsevier, 2015, pp. 481–511.
- [178] A. S. M. Ang, C. C. Berndt, and P. Cheang, 'Deposition effects of WC particle size on cold sprayed WC–Co coatings', *Surf. Coat. Technol.*, vol. 205, no. 10, pp. 3260–3267, Feb. 2011, doi: 10.1016/j.surfcoat.2010.11.045.
- [179] P.-H. Gao, Y.-G. Li, C.-J. Li, G.-J. Yang, and C.-X. Li, 'Influence of Powder Porous Structure on the Deposition Behavior of Cold-Sprayed WC-12Co Coatings', *J. Therm. Spray Technol.*, vol. 17, no. 5–6, pp. 742–749, Dec. 2008, doi: 10.1007/s11666-008-9258-1.
- [180] F. Luo *et al.*, 'Performance characterization of Ni60-WC coating on steel processed with supersonic laser deposition', *Def. Technol.*, vol. 11, no. 1, pp. 35–47, Mar. 2015, doi: 10.1016/j.dt.2014.09.003.
- [181] M. H. Staia *et al.*, 'Effect of substrate roughness induced by grit blasting upon adhesion of WC-17% Co thermal sprayed coatings', *Thin Solid Films*, vol. 377–378, pp. 657–664, Dec. 2000, doi: 10.1016/S0040-6090(00)01447-4.
- [182] S. Siegmann, M. Dvorak, H. Gruetzner, K. Nassenstein, and A. Walter, 'Shear testing for characterizing the adhesive and cohesive coating strength without the need of adhesives', in *Proc Int Therm Spray Conf*, 2005, vol. 2005, pp. 823–9, Accessed: 04-Oct-2016. [Online]. Available: http://www.gtv-mbh.com/_old/gtv-mbh-englisch/www.gtv-mbh.de/cms/upload/publikat/Siegmann/english/2005_07_eng_Siegmann.pdf.
- [183] M. M. H. Y. C. L. C. J. L. R. S. L. G. M. Edited by Basil R. Marple, *Thermal Spray 2007: Global Coating Solutions: Proceedings of the 2007 International Thermal Spray Conference*. ASM International.
- [184] D. Du, D. Liu, B. Meng, and X. Zhang, 'Effects of pretreatment and HVOF sprayed cermet coating on fatigue properties of TC21 titanium alloy', *Sci. China Technol. Sci.*, vol. 56, no. 4, pp. 1029–1037, Apr. 2013, doi: 10.1007/s11431-013-5149-x.
- [185] C. S. Richard, G. Béranger, J. Lu, J. F. Flavenot, and T. Grégoire, 'Four-point bending tests of thermally produced WC-Co coatings', *Surf. Coat. Technol.*, vol. 78, no. 1, pp. 284–294, Jan. 1996, doi: 10.1016/0257-8972(95)02416-6.
- [186] J. Voyer and H. Kreye, 'Determination of cracking resistance of thermal spray coatings during four-point bend testing using an acoustic emission technique', *J. Therm. Spray Technol.*, vol. 12, no. 3, pp. 416–426, 2003.
- [187] L. C. Cox, 'The four-point bend test as a tool for coating characterization', *Surf. Coat. Technol.*, vol. 36, no. 3, pp. 807–815, 1988.
- [188] J. Voyer and H. Kreye, 'Determination of cracking resistance of thermal spray coatings during four-point bend testing using an acoustic emission technique', *J. Therm. Spray Technol.*, vol. 12, no. 3, pp. 416–426, 2003.
- [189] Engineers Edge, 'Beam deflection and stress formula and calculators', *Bending, Deflection and Stress Equations Calculator for Beam Supported on Both Ends Loaded Two equal Loads*.

- https://www.engineersedge.com/beam_bending/beam_bending4.htm (accessed Sep. 29, 2018).
- [190] A. Ibrahim and C. C. Berndt, 'Fatigue and deformation of HVOF sprayed WC-Co coatings and hard chrome plating', *Mater. Sci. Eng. A*, vol. 456, no. 1–2, pp. 114–119, May 2007, doi: 10/fdnn45.
- [191] S. Herd, R. J. K. Wood, J. A. Wharton, and C. F. Higgs, 'Explicit fracture modelling of cemented tungsten carbide (WC-Co) at the mesoscale', *Mater. Sci. Eng. A*, vol. 712, pp. 521–530, Jan. 2018, doi: 10/gc2s35.
- [192] S. H. Suryo, A. P. Bayuseno, J. Jamari, and A. I. Wahyudi, 'Analysis of Rake Angle Effect to Stress Distribution on Excavator Bucket Teeth Using Finite Element Method', *Civ. Eng. J.*, vol. 3, no. 12, p. 1222, Jan. 2018, doi: 10/gfzr3w.
- [193] Y. Shi, H. Shen, Z. Yao, and J. Hu, 'Temperature gradient mechanism in laser forming of thin plates', *Opt. Laser Technol.*, vol. 39, no. 4, pp. 858–863, Jun. 2007, doi: 10.1016/j.optlastec.2005.12.006.
- [194] D. Sowdari and P. Majumdar, 'Finite element analysis of laser irradiated metal heating and melting processes', *Opt. Laser Technol.*, vol. 42, no. 6, pp. 855–865, Sep. 2010, doi: 10.1016/j.optlastec.2009.11.022.
- [195] B. S. Yilbas and S. S. Akhtar, 'Laser bending of metal sheet and thermal stress analysis', *Opt. Laser Technol.*, vol. 61, pp. 34–44, Sep. 2014, doi: 10.1016/j.optlastec.2013.12.023.
- [196] O. U. Khan and B. S. Yilbas, 'Laser heating of sheet metal and thermal stress development', *J. Mater. Process. Technol.*, vol. 155–156, pp. 2045–2050, Nov. 2004, doi: 10.1016/j.jmatprotec.2004.04.229.
- [197] 'RESIDUAL STRESSES IN A MULTILAYER SYSTEM OF COATINGS', *JCPDS-Int. Cent. Diffraction Data*, 1999.
- [198] M. Ohring, *The materials science of thin films*. Boston: Academic Press, 1992.
- [199] H. Wang, T. Webb, and J. W. Bitler, 'Study of thermal expansion and thermal conductivity of cemented WC-Co composite', *Int. J. Refract. Met. Hard Mater.*, vol. 49, pp. 170–177, Mar. 2015, doi: 10/f683kv.
- [200] T. F. Juliano, M. R. VanLandingham, T. Weerasooriya, and P. Moy, 'Extracting Stress-Strain and Compressive Yield Stress Information from Spherical Indentation', p. 24.
- [201] A. F. Lisovsky, 'Properties of Cemented Carbides Alloyed by Metal Melt Treatment', *15th Int. Plansee Semin.*, vol. 2, p. 12, 2001.
- [202] R. S. C. Paredes, S. C. Amico, and A. S. C. M. d'Oliveira, 'The effect of roughness and pre-heating of the substrate on the morphology of aluminium coatings deposited by thermal spraying', *Surf. Coat. Technol.*, vol. 200, no. 9, pp. 3049–3055, Feb. 2006, doi: 10.1016/j.surfcoat.2005.02.200.
- [203] X. K. Suo, M. Yu, W. Y. Li, M. P. Planche, and H. L. Liao, 'Effect of Substrate Preheating on Bonding Strength of Cold-Sprayed Mg Coatings', *J. Therm. Spray Technol.*, vol. 21, no. 5, pp. 1091–1098, Sep. 2012, doi: 10.1007/s11666-012-9803-9.
- [204] M. Afzal, A. N. Khan, T. B. Mahmud, T. I. Khan, and M. Ajmal, 'Effect of laser melting on plasma sprayed WC-12wt.%Co coatings', *Surf. Coat. Technol.*, vol. 266, pp. 22–30, Mar. 2015, doi: 10/f68mrx.
- [205] M. Afzal, M. Ajmal, A. Nusair Khan, A. Hussain, and R. Akhter, 'Surface modification of air plasma spraying WC-12%Co cermet coating by laser melting technique', *Opt. Laser Technol.*, vol. 56, pp. 202–206, Mar. 2014, doi: 10/gfz42c.
- [206] J. Mateos, J. M. Cuetos, E. Fernández, and R. Vijande, 'Tribological behaviour of plasma-sprayed WC coatings with and without laser remelting', *Wear*, vol. 239, no. 2, pp. 274–281, Apr. 2000, doi: 10/d6tc59.
- [207] The Engineering ToolBox, 'Coefficients of Linear Thermal Expansion'. https://www.engineeringtoolbox.com/linear-expansion-coefficients-d_95.html (accessed Nov. 01, 2016).

- [208] J. Mateos, J.M. Cuetos, E. Fernandez, and M. Cadenas, 'Effect Of Laser Treatment On Tungsten Carbide Coatings', *WIT Trans. Eng. Sci.*, vol. 17, p. 8, 1997, doi: 10.2495/SURF970231.
- [209] AK Steel, '316/316L product data sheet'. AK Steel Corporation, 08-Jan-2007.

8 Chapter 8 - Appendix

8.1 Photo of the SLD Processing Chamber:

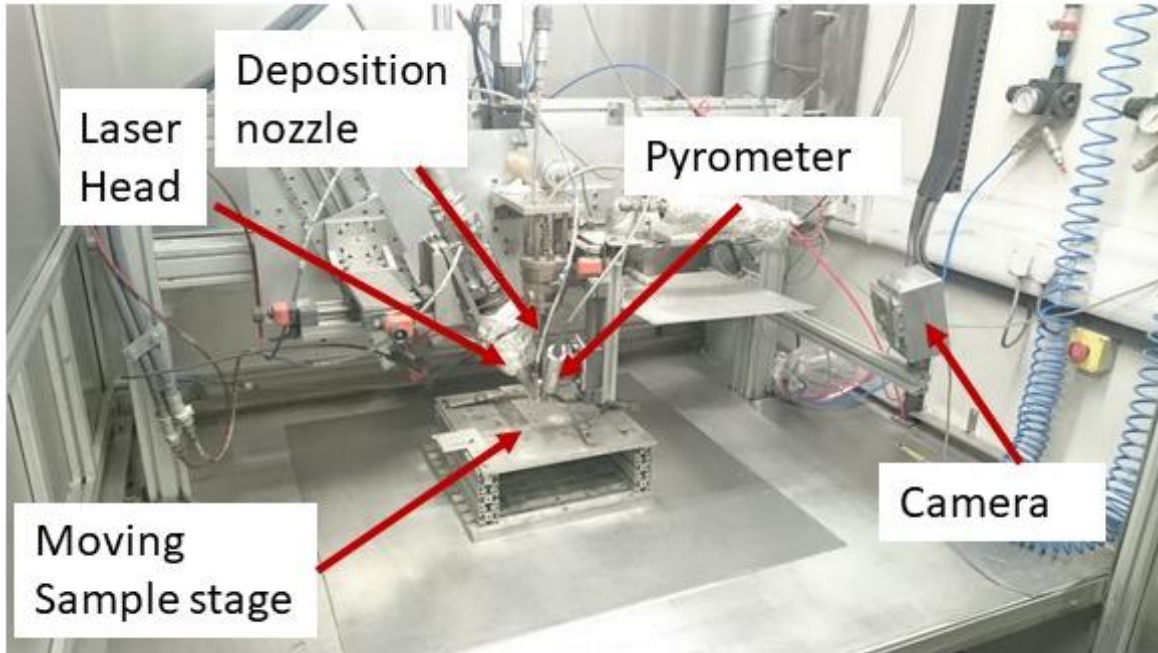


Figure 77: Image of the supersonic laser deposition chamber.

8.1.1 EDX Spectrum Graphs

8.1.1.1 Sample Location (a)

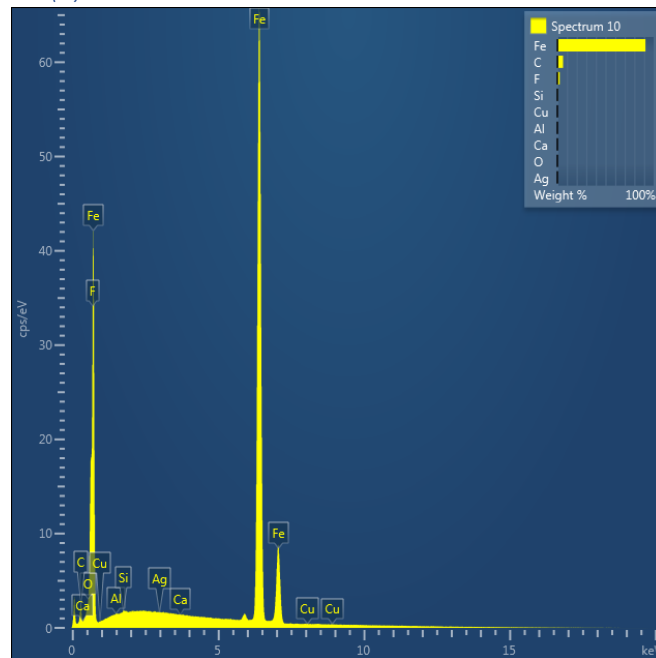


Figure 78: EDX spectrum from location (a) within the steel substrate.

8.1.1.2 Sample Location (b)

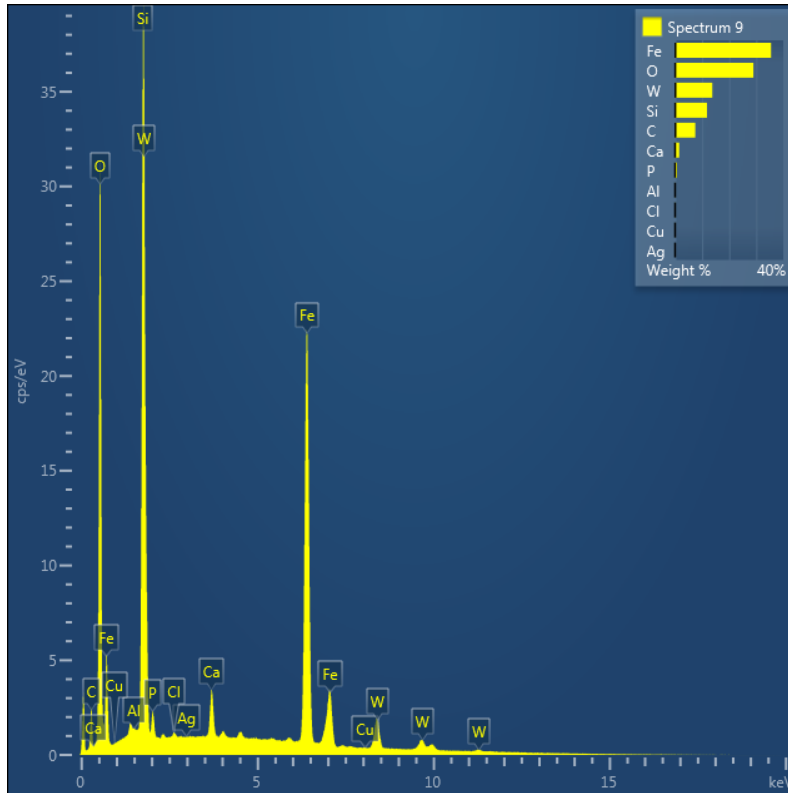


Figure 79:EDX spectrum from location (b) within the interface region.

8.1.1.3 Sample Location (c)

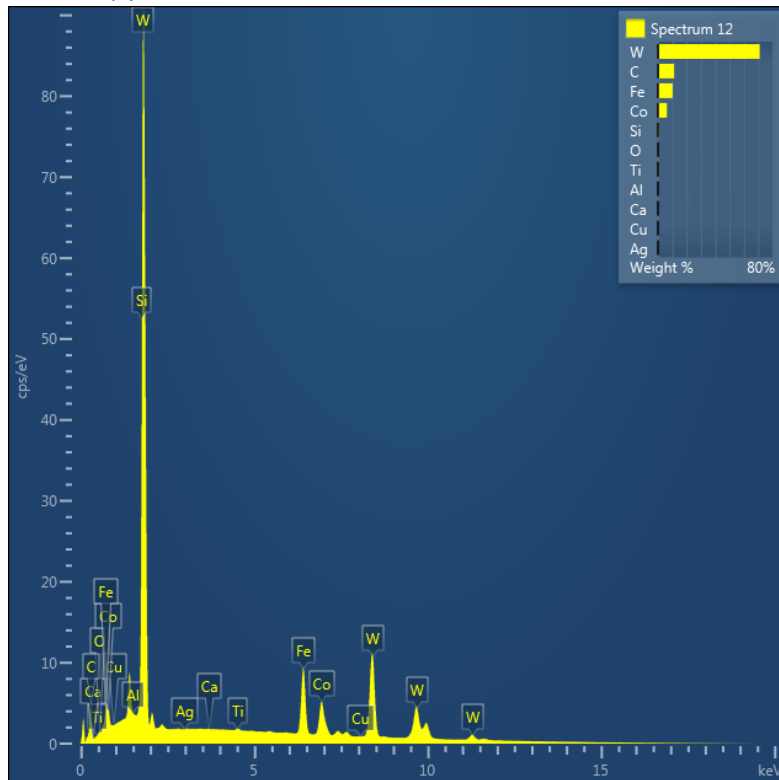








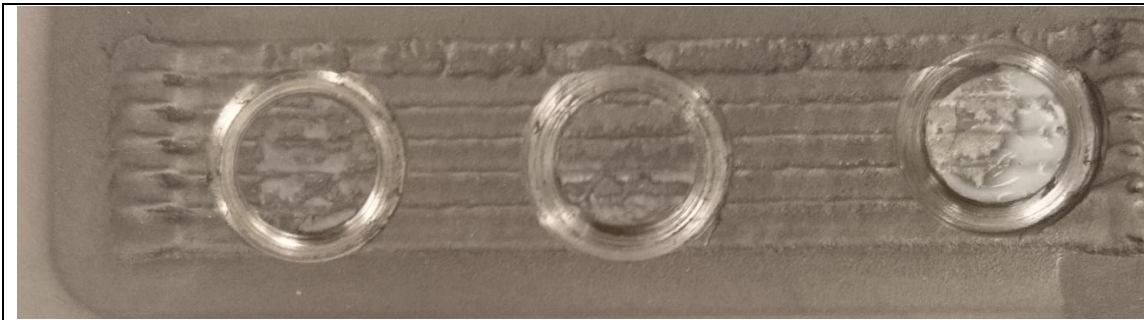
Figure 80: EDX spectrum from location (c) within the WC-17Co coating.

8.1.2 Adhesion Testing Results

Table 12: Results from a pull-off test of an as deposited coating of WC-17Co. The images show the contact surface of the test elements after failure had occurred.

<p>Sample 149.1-1</p>  <p>Failed during drilling.</p>	<p>Sample 149.1-2</p>  <p>Failure at 102.6 MPa. Top of tracks pulled off. Glue/coating interface failure.</p>	<p>Sample 149.1-3</p>  <p>Failure at 49.2 MPa Top of tracks pulled off. Glue/test element interface failure.</p>
<p>Sample 149.2-1</p>  <p>Failure at 53.4 MPa Top of tracks pulled off. Glue/glue failure in between tracks.</p>	<p>Sample 149.2-2</p>  <p>Failure at 43.2MPa Top of tracks pulled off. Glue/test element interface failure.</p>	<p>Sample 149.2-3</p>  <p>Failure at 60 MPa Top of tracks pulled off. Glue/test element interface failure.</p>

The associated substrate is shown in Figure 81 below after the test elements had been pulled off.



Sample 149.1 after pull-off testing.









Sample 149.2 after pull-off testing.

Figure 81: Images of the substrate after the test elements had been pulled off.



Figure 82: WC-17Co coatings 149.3+4 after gluing the test elements and curing in a furnace.

Table 13: Results from a pull-off test of a grounded down deposited coating of WC-17Co. The images show the contact surface of the test elements after failure had occurred.

<p>149.3-1</p>  <p>Failure at 108 MPa Failure in glue.</p>	<p>149.3-2</p>  <p>Failure at 74.4 MPa Failure in glue.</p>	<p>149.3-3</p>  <p>Failure at 84 MPa Failure in glue.</p>
<p>149.4-1</p>  <p>Failure at 73.8 MPa Failure in glue.</p>	<p>149.4-2</p>  <p>Failure at 84.6 MPa Failure in glue.</p>	<p>149.4-3</p>  <p>Failure at 90.6 MPa Failure in glue.</p>



Sample 149.3 after pull-off testing.



Sample 149.4 after pull-off testing.

Figure 83: Images of the substrate after the test elements had been pulled off.

Table 14: Results showing the test elements following the pull off testing.

Mild steel 1	Mild steel 2	Mild steel 3
		
92.4 MPa Failure in glue.	110.4 MPa Failure in glue.	82.2 MPa Failure in glue.



Figure 84: Mild steel sample after pull-off testing.

8.2 CTE Effects Data

Table 15: Mean Coefficient of Thermal Expansion for 316L [209].

Temperature range	Mean coefficient of thermal expansion (/in/°F (μm/m•K))
32 - 212°F (0 - 100°C)	8.9 x 10 ⁻⁶ (16.0)
32 - 600°F (0 - 315°C)	9.0 x 10 ⁻⁶ (16.2)
32 - 1000°F (0 - 538°C)	9.7 x 10 ⁻⁶ (17.5)
32 - 1200°F (0 - 649°C)	10.3 x 10 ⁻⁶ (18.5)
32 - 1500°F (0 - 871°C)	11.1 x 10 ⁻⁶ (19.9)